WOODHEAD PUBLISHING SERIES IN CIVIL AND STRUCTURAL ENGINEERING

Strengthening of Concrete Structures Using Fiber Reinforced Polymers (FRP)

Design, Construction and Practical Applications

Hwai-Chung Wu and Christopher D. Eamon

WP
WOODHEAD PUBLISHING

Strengthening of Concrete Structures Using Fiber Reinforced Polymers (FRP)

This page intentionally left blank

Woodhead Publishing Series in Civil and Structural Engineering

Strengthening of Concrete Structures Using Fiber Reinforced Polymers (FRP)

Design, Construction and Practical Applications

Hwai-Chung Wu

and

Christopher D. Eamon

Department of Civil & Environmental Engineering, Wayne State University, Michigan, United States of America

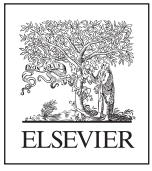

WP
WOODHEAD PUBLISHING
An imprint of Elsevier • elsevier.com

Woodhead Publishing is an imprint of Elsevier
The Officers' Mess Business Centre, Royston Road, Duxford, CB22 4QH, United Kingdom
50 Hampshire Street, 5th Floor, Cambridge, MA 02139, United States
The Boulevard, Langford Lane, Kidlington, OX5 1GB, United Kingdom

Notices
Knowledge and best practice in this field are constantly changing. As new research and experience broaden our understanding, changes in research methods, professional practices, or medical treatment may become necessary.

Practitioners and researchers must always rely on their own experience and knowledge in evaluating and using any information, methods, compounds, or experiments described herein. In using such information or methods they should be mindful of their own safety and the safety of others, including parties for whom they have a professional responsibility.

To the fullest extent of the law, neither the Publisher nor the authors, contributors, or editors, assume any liability for any injury and/or damage to persons or property as a matter of products liability, negligence or otherwise, or from any use or operation of any methods, products, instructions, or ideas contained in the material herein.

British Library Cataloguing-in-Publication Data
A catalogue record for this book is available from the British Library

Library of Congress Cataloging-in-Publication Data
A catalog record for this book is available from the Library of Congress

ISBN: 978-0-08-100636-8 (print)
ISBN: 978-0-08-100641-2 (online)

Publisher: Matthew Deans
Acquisition Editor: Gwen Jones
Editorial Project Manager: Charlotte Rowley
Production Project Manager: Poulouse Joseph
Cover Designer: Victoria Pearson

Typeset by MPS Limited, Chennai, India

Contents

Preface

This book presents guidelines for the strengthening of concrete structures using fiber-reinforced polymer (FRP) composites. This text briefly covers the basic concepts of FRP materials and composite mechanics while focusing on practical design and construction issues, including inspection and quality control. Special attention is given to the different approaches and recommendations found in a selection of international FRP design standards. Rather than a theoretical text, this book attempts to address concerns of the practitioner, and the authors hope that it will be found valuable in that regard.

If judged by the proliferation of journal articles in recent years, there is considerable interest in the engineering application of FRP. One of the fastest growing applications is the use of FRP composite sheets for strengthening deficient concrete structures, and in particular, bridges. Some of the main driving forces are the ease of installation and rapid repairs that can be made using FRP sheets in comparison to conventional rehabilitation techniques using concrete or steel jackets. Consequently, total project costs can be very competitive, despite the high initial material cost of FRP. At present, several FRP strengthening design guides from the United States, Europe, and other locations are available. These guidelines are often inconsistent and, individually, do not adequately cover all important design, construction, and inspection issues to a desirable level of detail. Consequently, this book first provides a review and comparison of the provisions found in a selection of these existing guidelines, and then suggests design, installation, inspection, quality control, and maintenance activities for best practice. By doing so, this text aims to fill a significant gap in the available strengthening guides and might serve as a resource for engineers, architects, academics, and students interested in FRP materials and their structural applications.

The authors wish to acknowledge the work of Sasan Siavashi, Abdel Aziz Makkay, and Abdulkareem Kuaryouti, who spent many hours collecting information from existing guidelines as well as prepared numerous figures and tables. We are also grateful to Gwen Jones of Woodhead/Elsevier. Her support and encouragement has made this book possible. Finally, we wish to thank our wives, Shiow-Hwa Gau (HCW) and Marie Chris Eamon (CDE). The completion of this text would not be possible without their love, patience, and understanding.

Hwai-Chung Wu and Christopher D. Eamon
Wayne State University, Detroit, MI, United States

This page intentionally left blank

Introduction

1

1.1 Overview

Various causes contribute to the deterioration of the civil infrastructure. Although bridges are generally expected to have a service life of 50−100 years, many are showing signs of distress much earlier. Extreme temperatures in the summer and winter, including many cycles of freeze thaw, and the use of deicing salts, are significant factors that contribute to the progressive damage of bridge structural members (Staton and Knauff, 2007). Other factors include heavy traffic loading, lack of adequate maintenance, and collision damage.

In the United States, State Departments of Transportation (DOT) conduct regular inspections of transportation structures such as bridges. Bridge inspection and reporting by DOTs are part of the larger, federally mandated National Bridge Inspection Standards (NBIS) administered by the Department of Transportation (USDOT) Federal Highway Administration (FHWA) (USDOT-FHWA, 2004). According to FHWA data, in 2009, 5% of bridges on the National Highway System were structurally deficient, 17% were functionally obsolete, and about 35% had superstructures rated less than in "good" condition. Unsurprisingly, older bridges are more likely to have problems. Considering all bridges, for example, the proportion of structurally deficient and functionally obsolete bridges exceeds 40% for structures 51−75 years old, and from 54 to 65% of the structures older than 75 years are deficient or obsolete (FHWA, 2010).

Depending on the nature and severity of the deficiency, different corrective actions may be required. Traditional methods of strengthening and rehabilitating steel bridges include the replacement of damaged structural members, repair of corroded beam ends, addition of stiffeners, and application of protective coatings (Wipf et al., 2003). For concrete bridges, traditional rehabilitation measures may include sealing hairline cracks using epoxy injection, spot-patching damaged areas, waterproofing, jacketing structural members to restore or increase their load carrying capacity, and cathodic protection against reinforcement corrosion. However, traditional methods have inherent limitations. For example, spot-patching methods can mend corrosion-induced spalls, but typically do not retard chloride-induced corrosion; corrosion rates have been observed to be higher at the perimeter of a patch and are independent of the type of patch material used (Tabatabai et al., 2005). Moreover, these traditional repairs are often expensive and disruptive to traffic, particularly for bridges. As such, an alternative that is growing in popularity is to utilize fiber-reinforced polymer (FRP) composite materials.

Strengthening of Concrete Structures Using Fiber Reinforced Polymers (FRP).
DOI: http://dx.doi.org/10.1016/B978-0-08-100636-8.00001-6

FRP has been used for strengthening applications in various industries. However, common applications for bridge components involve externally bonded (EB) composite fabrics or jackets on beams, columns, and bridge decks, where significant improvements in compressive, shear, and flexural performance has been obtained (Nanni et al., 1992; Karbhari et al., 1993; Saadatmanesh et al., 1994; Chajes et al., 1995; Labossiere et al., 1995; Seible et al., 1997; Nanni, 2000; Mo et al., 2004; Nanni, 2004; Ludovico et al., 2005; Walker and Karbhari, 2006; Mertz and Gillespie, 1996; Miller et al., 2001; Tavakkolizadeh and Saadatmanesh, 2003; Rizkalla et al., 2008; Elarbi, 2011).

Advantages of FRP include a high strength-to-weight ratio, light weight, excellent corrosion resistance, and ease of installation. Because of their light weight, FRP composites are cheaper to transport, require no formwork and less or no scaffolding to install, and minimally add to a structure's dead load. Due to the strength of FRP composites, often only thin layers are needed to rehabilitate beams and columns, minimally altering original dimensions. In some cases, this may become important to maintain vehicular clearance and other tolerances within acceptable limits. Corrosion resistance is a principal advantage, as steel reinforcement corrosion has long been recognized as a significant and costly maintenance problem.

In general, for the external application of FRP sheets, a layer of dry fiber sheet (usually unidirectional tape) is placed on top of a coat of polymer resin that hardens to bond the fiber sheet to the concrete structure. However, wet lay-up, precured, and nearsurface mounted construction techniques have been used in practice. When needed, multiple layers of fiber sheets can be sequentially added by repeating the application procedure. The resulting properties and potential failure modes of the FRP composite member are a function of the properties of the original member, the FRP, and their interfaces. The interface between the FRP sheet and the structural member, usually concrete, is particularly important, since composite action requires a solid bond. Final failure is often caused by the debonding of the FRP sheet from the concrete substrate (Meier, 1995; Buyukozturk and Hearing, 1998). The degradation of a constituent in FRP over time affects various composite properties, and may even change the order of governing failure modes (Wu and Yan, 2013). This is a particularly important concern, as a FRP-bonded structure could fail abruptly due to a change in dominant failure mode.

1.2 FRP strengthening systems

Early fiber composite applications have mainly been limited to aerospace, chemical and shipbuilding due to cost and research limitations (Emmons, 1998). However, modern composites can be found in various forms from underground storage tanks to boat hulls and jet fighters. Carbon FRP (CFRP) strip bonding for structural repair and strengthening applications was first introduced in Switzerland by Meier in 1984 (Barton, 1997). Later, the California Department of Transportation, Caltrans, pioneered the use of FRP in the United States during the

early 1990s by seismically upgrading bridge columns in California with Glass FRP (GFRP) fabrics (Sika Corp., 2012).

FRP is available in a variety of forms of interest to structural engineers such as bars, grids, sheets, and prestress tendons. Some of these components, such as those in bar and tendon form, are primarily used in place of steel reinforcement when new concrete members are cast. For existing concrete components, modern rehabilitation methods include the use of FRP composite sheets in the form of beam wrapping to strengthen flexural or shear capacity, column wrapping to enhance compressive and seismic performance, bonded FRP flange plates to increase bending capacity, and epoxying FRP rods in grooves cut into the substrate to increase member strength (Khan, 2010). One of the most flexible strengthening options is the use of EB FRP systems. Commercially available FRP systems are offered by suppliers such as Sika, Fyfe, and QuakeWrap. Systems are offered in either unidirectional or bidirectional fiber orientation. These systems are made of carbon fibers, glass fibers, or, for some bidirectional systems, carbon fibers in one direction and glass fibers in the other. Depending on the application, epoxy adhesives are an integral part of the system and can be formulated to provide a range of application characteristics and mechanical properties when cured. Epoxy formulation provides the bond between the reinforcing plies (laminate) and the concrete base, the bond between different plies, and a protective coat to shield the laminate from the elements during service life. Tables 1.1 and 1.2 present the physical and mechanical properties of a typical selection of unidirectional and bidirectional FRP strengthening systems offered by Sika and Fyfe.

1.3 Composite interfacial debonding

A critical concern of EB FRP reinforced structures is delamination, or debonding. Although detailed weather-induced bond deterioration is not fully understood, the results of debonding and its related failure phenomenon are well known. The quality of interfacial bonding has a strong influence on structural performance, as this significantly affects the composite action required for many applications, and ultimate failure of the strengthened component is often caused by debonding of the FRP sheet from the concrete substrate (Meier, 1995; Buyukozturk and Hearing, 1998).

1.4 FRP design standards and guides

Various documents have been developed in the last two decades describing FRP strengthening systems and provide guidelines for design assumptions and calculations. The most widely known guide in the United States is ACI 440.2R, *Guide for the Design and Construction of Externally Bonded FRP Systems for Strengthening Concrete Structures* (2008). A number of reports issued by the National

Table 1.1 Properties of FRP systems from Sika and Fyfe

Physical and mechanical properties of unidirectional FRP strengthening systems by Sika and Fyfe								
	Sika unidirectional (0°)				Fyfe unidirectional (0°)			
	Unit	Sikawrap Hex 103C	Sikawrap Hex 117C	Sikawrap Hex 230C	Tyfo SCH-41	Tyfo SCH-41-0.5X	Tyfo SCH-41-2X	Tyfo SCH-41H
Fiber properties								
Tensile strength	psi	550,000	55,000	500,000	550,000	550,000	550,000	675,000
	MPa	3793	3793	3450	3790	3790	3790	4650
Tensile modulus	psi	33,000,000	34,000,000	33,400,000	33,400,000	33,400,000	33,400,000	42,000,000
	GPa	228,000	234,000	230,000	230,000	230,000	230,000	289,000
Ult. elongation	%	1.50	1.50	1.50	1.70	1.70	1.70	1.70
Density	lbs/in.^{3}	0.065	0.065	0.065	0.063	0.063	0.063	0.065
	g/cc	1.8	1.8	1.8	1.74	1.74	1.74	1.8

Laminate physical properties								
Fiber type		Carbon	Carbon	Carbon	Carbon	Carbon	Carbon	Carbon
Color		Black	Black	Black	Black	Black	Black	Black
Weight	OZ/Y^2	18	9	6.7	19	9.5	40	24
	g/m^2	618	309	230	644	322	1424	814
Ply thickness	in.	0.04	0.02	0.015	0.04	0.024	0.08	0.04
	mm	1.016	0.51	0.381	1.0	0.6	2.0	1.0

Cured laminate mechanical properties														
		Test	Design	Design	Test	Design	Test	Design	Test	Design	Test	Design	Test	Design
Tensile strength	psi	123,000	104,000	105,000	129,800	104,000	143,000	121,000	137,000	116,000	143,000	121,000	200,000	170,000
	MPa	849	717	724	894	715	986	834	944.6	799.8	986	834	1380	1.170
Tensile modulus	psi	10,239,800	9,446,600	8,200,000	9,492,300	8,855,000	13,900,000	11,900,000	14,500,000	12,3000,000	13,900,000	11,9000,000	15,500,000	13,100,000
	MPa	70,552	65,087	56,500	65,402	61,012	95,800	82,000	99,900	84,800	95,800	82,000	106,800	90,300
Tensile elongation	%	1.12	0.98	1.0	1.33	1.09	1.00	0.85	0.95	0.80	1.00	0.85	1.30	1.10
Tensile strength per inch width	lbs	4928	4160	2100	1947	1560	5720	4840	3288	2784	11,440	9680	8000	6800
	kN	21.9	18.5	9.3	8.7	6.9	25.4	21.5	14.6	12.4	50.9	43.1	35.6	30.2

Table 1.2 Bidirectional laminate selection offered by Sika

		Sika bidirectional (0°/90°)	
		Sikawrap Hex 113C	**Sikawrap Hex 115C**
Fiber properties			
Tensile strength	psi	500,000	550,000
	MPa	3450	3793
Tensile modulus	psi	33,400,000	33,000,000
	GPa	230,000	234,500
Ult. elongation	%	1.50	4.00
Density	lbs/in.^{3}	0.065	0.065
	g/cc	1.8	1.8

Laminate physical properties			
Fiber type		Carbon	Carbon
Color		Black	Black
Weight	OZ/Y^2	5.7	18.7
	g/m^2	196	638
Ply thickness	in	0.01	0.04
	mm	0.25	1.00

Cured laminate mechanical properties (with Sikadur Hex 300 epoxy)				
		Design	**Test**	**Design**
Tensile strength	psi	66,000	83,980	70,870
	MPa	456	579	489
Tensile modulus	psi	6,000,000	7,017,555	6,149,730
	MPa	41,400	48,351	42,468
Tensile elongation	%	1.20	1.14	0.98
Tensile strength per inch width	lbs	660	3359	2835
	kN	2.90	14.9	12.6

Cooperative Highway Research Program (NCHRP) are design/construction guides for FRP systems and include:

- NCHRP Report 678, *Design of FRP Systems for Strengthening Concrete Girders in Shear* (Belarbi et al., 2011).
- NCHRP Report 655, *Recommended Guide Specification for the Design of Externally Bonded FRP Systems for Repair Strengthening of Concrete Bridge Elements* (Zureick et al., 2010).
- NCHRP Report 564, *Field Inspection of In-Service Bridge Decks* (Telang et al., 2006), which contains a manual for the in-service inspection of FRP bridge decks.
- NCHRP Report 514, *Bonded Repair and Retrofit of Concrete Structures Using FRP Composites* (Mirmiran et al., 2004), which describes recommended construction specifications and a control process for FRP strengthening including material preparation,

application, a QA/QC plan, as well as training, qualification, inspection, and maintenance recommendations.

Other US and international guides include:

- AASHTO (2013), *Guide Specifications for Design of Bonded FRP Systems for Repair and Strengthening of Concrete Bridge Elements*.
- AC125 (2012), *Acceptance Criteria for Concrete and Reinforced and Unreinforced Masonry Strengthening Using Externally Bonded Fiber-Reinforced Polymer (FRP) Composite Systems.* AC125 is issued by ICC Evaluation Service to establish minimum requirements for the issuance of evaluation reports on FRP composite systems under the 2012, 2009, and 2006 *International Building Code* (IBC) and the 1997 *Uniform Building Code* (UBC).
- ACI 440.3R (2004), *Guide Test Methods for Fiber-Reinforced Polymers (FRPs) for Reinforcing or Strengthening Concrete Structures.*
- ACI 440R (2007), *Report on Fiber-Reinforced Polymer (FRP) Reinforcement for Concrete Structures.*
- ACI SP-215 (2003), *Field Applications of FRP Reinforcement: Case Studies.*
- ISIS (2008), *Design Manual No. 4, FRP Rehabilitation of Reinforced Concrete Structures*, issued by the Canadian Network of Centers of Excellence on Intelligent Sensing for Innovative Structures.
- CEB-FEB (2001), Bulletin No. 14, *Externally Bonded FRP Reinforcement for RC Structures*, contains design guidelines for the use of FRP reinforcement in accordance with the design format of the CEB-FIP Model Code and Eurocode2.
- CNR-DT 200 (2004), *Guide for the Design and Construction of Externally Bonded FRP Systems.*
- Japanese Society of Civil Engineers (1997), *Recommendations for Design and Construction of Concrete Structures Using Continuous Fiber Reinforcing Materials.*
- Japan Concrete Institute (1997), *State of the Art Report on Retrofitting with CFRM, Guidelines for Design, Construction and Testing.*
- TCS (2000), *Design Guidance for Strengthening Concrete Structures Using Fiber Composite Materials*, Technical Report 55, United Kingdom.

1.5 Designing with FRP reinforcement

In the civil infrastructure, FRP is typically used to strengthen reinforced concrete bridge elements. A reinforced concrete element strengthened with FRP is a member consisting of three materials: concrete, steel, and FRP, where the FRP supplements the existing steel reinforcement. The application of FRP requires engineers to address the interaction of these three materials, with each material having different material properties and statistical variation. This latter issue is critical to address for a design guide that falls within a modern, probabilistically calibrated load and resistance factor design format. To account for uncertainties in material properties, design formulations addressing each material's contribution to the overall strength (R_n) of the element can be based on individual reduction factors applied separately to each of the materials constituting the composite (concrete, steel, and FRP); a combined reduction factor applied to the entire composite; or a combination of the two where both individual and combined reduction factors are applied to the

system (Sika, 2012). For example, ACI 440.2R-08 recommends the use of ACI-318 (steel) reinforced concrete resistance (ϕ) factors applied to the overall element strength, in combination with an additional FRP reduction factor ψ, which takes into account the effects of FRP material property variation.

1.5.1 Flexural strengthening

To account for the complex behavior and various possible failure mechanisms of FRP-bonded structures, extensive experimental investigations were carried out by numerous researchers (Seible et al., 1997; Mo et al., 2004; Nanni, 2004; Ludovico et al., 2005; Walker and Karbhari, 2006, among many others). For FRP bonded flexural beams, several failure modes were generally observed:

1. Crushing of the concrete in the compression zone before rupture of the FRP sheet or yielding of the reinforcing steel (brittle failure).
2. Yielding of the tension steel before concrete crushing or rupture of FRP sheet (ductile failure).
3. Yielding of the compression steel reinforcement of a doubly reinforced section (relatively ductile failure).
4. Rupture of the FRP sheet before steel yield and the compressive strain in the concrete is below its ultimate strain (the most brittle failure).
5. Anchorage failure (delamination) in the bond zone of the FRP sheet (often a ductile failure).
6. Peeling or shear/tension failure of the concrete substrate near the FRP sheet's cut off zone (brittle failure).

These six failure modes were classified into two types by Thomsen (2004). Type one includes modes exhibiting composite action up to failure, either due to concrete crushing, FRP rupture, or lack of shear resistance. Type two consists of failures by loss of composite action due to debonding of the FRP sheet, or by end peeling, where the concrete cover near the support regions peels off. To avoid detachment failure at the FRP/concrete interface, existing guidelines often attempt to curtail the allowable interface strain. For example, ACI 440.2R (2008) introduces a bond reduction factor (k_m) to limit the strain permitted in the FRP system. According to ACI 440.2R, k_m is taken as a value not greater than 0.9, which reduces the usable strength of the FRP below its ultimate rupture strain. Even so, FRP rupture or delamination might occur if the FRP or bond strength later deteriorates. However, provided that the bond remains sufficiently strong to avoid failure, four failure modes are assumed possible, two corresponding to failure of the concrete in compression and two corresponding to failure of the FRP sheet (Choi et al., 2008): concrete crushing after steel yields, concrete crushing before steel yields, steel yield followed by FRP rupture, and debonding of the FRP at the FRP/concrete interface.

For illustration, in the ACI approach, which is similar to other provisions, the nominal moment capacity of a tension-reinforced section M_n can be obtained from Eq. (1.1), where the first term is the moment capacity generated from the

tension steel force and the second term is the moment capacity generated from the FRP sheet. Design capacity ϕM_n is then determined by reducing the nominal moment capacity by the appropriate resistance factor ϕ:

$$M_n = A_s f_s \left(d - \frac{\beta_1 c}{2} \right) + \psi A_f f_{fe} \left(h - \frac{\beta_1 c}{2} \right) \tag{1.1}$$

Parameter ψ represents a factor used to reduce the contribution of the FRP sheet, while other parameters in Eq. (1.1) are similar to those used in typical reinforced concrete flexural capacity analysis (representing areas of steel and FRP tension material, A_s and A_f, respectively; their stresses at section capacity, f_s and f_{fe}; and their lever arms to the compression zone of the concrete, d-$\beta_1 c$/2 and h-$\beta_1 c$/2). Here it is assumed that the external sheet is bonded to the tension side of a beam of height h. In a recent study (Elarbi and Wu, 2012), Eq. (1.1) was found to typically underestimate experimental results by 20−60%. However, a greater concern is the possibility of over-estimating capacity by not properly accounting for loss of FRP or bond strength over time. It was observed that more reliable strength reduction coefficients need to be developed to represent the long-term use of FRP exposed to the environmental and service parameters specific to a local region. To better develop design standards and construction guides, PennDOT commissioned a research program by selecting candidate bridges for nondestructive testing before and after the application of EB FRP for beam strengthening. Results from finite element analysis and test data were used to develop draft PennDOT design standards and construction specifications, and to apply lessons learned to the design and constructability of nearly 1000 concrete T-beam bridges in Pennsylvania (Davalos et al., 2012).

1.5.2 Shear strengthening

The additional shear strength that can be provided by the FRP is based on several factors, including the geometry of the beam or column, the wrapping technique, and the quality of the existing surface of the concrete. There are three typical types of FRP wrapping schemes, depending on the number of sides wrapped (4, 3, or 2). The four-sided wrapping scheme is most efficient. However, this is often impossible for bridge members, such as in the case of a T-beam integral with a deck slab above. In such situations, shear strength can also be improved by wrapping three sides (U-wrap) or bonding to two sides of the member, though the latter is the least effective (ACI, 2007).

FRP sheets have been shown to significantly increase the shear strength of existing concrete beams and columns when used to wrap members (Chajes et al., 1995; Labossiere et al., 1995; Seible et al., 1997; Mo et al., 2004). The nominal shear strength of an FRP strengthened concrete member V_n can be determined by adding the contribution of the FRP reinforcing (V_f) to the contribution of the steel shear reinforcement (V_s) and the concrete (V_c), as per Eq. (1.2), which presents the ACI

approach. The total design strength is then found by reducing V_n by the appropriate shear resistance factor ϕ.

$$V_n = (V_c + V_s + \psi V_f) \tag{1.2}$$

The contribution of the FRP sheet to shear strength is based on fiber orientation and the assumed shear crack pattern. The shear strength provided by the FRP reinforcement can be determined by calculating the force resulting from the tensile stress in the FRP across an assumed crack, in a similar fashion to the process used for design with steel stirrups. As given by ACI 440 (2007), the shear strength contribution from FRP is

$$V_f = \frac{A_f f_{fe}(\sin\alpha + \cos\alpha)d_f}{s_f} \tag{1.3}$$

where A_f is the cross-sectional area of the FRP sheet, f_{fe} is the tensile stress in the FRP reinforcement, d_f is the effective beam height, α is the orientation angle of the FRP, and S_f is the spacing between adjacent FRP strips. To avoid delamination failure, mechanical anchorage can be used. However, the effective strain in FRP is limited (for example, to 0.004 per ACI 440), and the total shear reinforcement allowed is often limited as well. For example, FRP shear reinforcement in ACI is limited to the same criteria for steel alone per ACI-318 (2011), given as $V_s + V_f \leq 8\sqrt{f_c'}b_w d$.

1.6 Numerical modeling

Numerous researchers have developed numerical models of FRP strengthened concrete elements (Ouyang and Wan, 2006; Ibrahim and Mahmood, 2009; Obaidat et al., 2010, etc.). For example, Pesic and Pilakoutas (2003) conducted a finite element analysis to address concrete cover delamination and plate end failure of concrete beams with bonded flexural FRP reinforcement, while Elarbi (2011) developed refined models using finite element analysis to predict the deformation and failure of concrete beams strengthened with carbon FRP sheets applied to the bottom surface. Some of these models can become very involved, and can provide valuable predictions for FRP strengthened member behavior beyond that found in simplified code procedures. For illustration, Elarbi (2011) developed refined models in recent research using the finite element analysis code ABAQUS, to predict the deformation and failure of concrete beams strengthened with carbon FRP sheets applied to the bottom surface. This approach explicitly modeled the concrete and FRP materials with independent elements and nonlinear time-dependent material properties to account for deterioration. The two types of expected failure modes have been correctly predicted by the model: FRP rupture and FRP delamination. Two groups of beams were examined: one group with perfectly bonded FRP

reinforcement and another group of aged beams with deteriorated FRP reinforcement bond. For the healthy FRP bonded beams in the study, the dominant failure mode was FRP rupture, where the concrete first began to crack on the midpoint of the tension side and propagated approximately one-third of the section height upwards, followed by rupture of the FRP sheet. For the aged (bond deteriorated) FRP bonded beams, the dominant failure mode was delamination. FRP delamination began at the midpoint of the beam and then spread toward the beam ends. These two failure modes predicted from the model well-matched the observed experimental failure sequences.

1.7 Installation of EB FRP systems

While installation is usually straightforward, it is well recognized that even minor deviation from the prescribed procedures may dramatically affect final system performance, impact adhesion quality, and cause premature delamination at the concrete/FRP reinforcement interface. If the concrete is not properly prepared prior to wrapping, the FRP composite may not adhere adequately to the concrete surface. Surface preparation includes removal of all contaminants such as organic growth, old bituminous products, surface coats, oil and dirt, by high pressure water cleaning and/or sand blasting (TRCF, 1998). Moreover, dry, open-pore concrete allows the epoxy primer to be drawn into the substrate to create a substantial mechanical anchoring bond. A simple test can be done by sprinkling water on the substrate and checking for beading; the water should be absorbed immediately if the desired open-pore structure exists.

Manufacturers of EB FRP products emphasize the importance of proper installation. Some offer extensive training modules for contractors, while others allow installation only through certified applicators. NCHRP 514 (2004) recommends that a DOT prequalify suppliers for a particular FRP system, after reviewing product data sheets, testing data, and existence of a comprehensive hands-on training program that can be taken by the FRP installer. It further recommends that the contractor is left responsible for the quality control of all materials and procedures in the project, and should submit a quality control and quality assurance (QC/QA) plan for approval. This plan should include specific procedures for: personnel safety, tracking and inspecting FRP components prior to installation, inspecting the prepared concrete surfaces to receive FRP, inspection of the work in progress to ensure conformity with specifications, evaluation of FRP QA samples, and inspection of all completed work. A proper installation plan includes adequate specification of: safety procedures, equipment and materials preparation and procurement, surface preparation, precutting fabric, how the correct fabric to resin ratio is maintained, epoxy mixing and saturation of FRP sheets, application of the sheets to the structural member, and application of specified coatings (Mirmiran et al., 2004). The above discussion represents a brief introduction to some of the topics that will be addressed in this book.

Fiber-reinforced polymer composites

2

Fiber-reinforced polymer (FRP) has been used for numerous strengthening applications in various industries. However, common applications for bridge components involve externally bonded composite fabrics or jackets on beams, columns, and bridge decks. A significant number of general guidelines exist for the design and construction of FRP systems. However, the combination of complex environmental and mechanical loading for bridges complicates the durability assessment of FRP composites (Wu et al., 2006a; Hollaway and Head, 2001; Helbling et al., 2006).

2.1 FRP constituents

2.1.1 Fibers

FRP composites consist of two main constituents: a load bearing constituent, mainly fibers, and a polymeric matrix that serves as a binder and protector of the fibers. The matrix facilitates load transfer among fibers and ensures that embedded fibers maintain their orientation and directional stability (Ansley et al., 2009). As multiphase materials, composites are generally anisotropic in nature exhibiting differing mechanical properties in three orthogonal directions. Properties of FRP composites have some variation depending on the manufacturing and fabrication processes employed (Elarbi, 2011). Three types of reinforcing fibers are commonly used: glass, aramid, and carbon. Recently, basalt fibers have become commercially available. Basalt fibers are produced from volcanic basalt rocks and have excellent thermal and chemical resistance. Although applications are still in infancy, basalt fibers have shown great potential to replace carbon fibers due to their much lower cost. Regardless of the type of fiber used, each is available with different grades and varying properties. In general, carbon fibers have the highest modulus of elasticity while glass fibers have the lowest. All fiber types exhibit linear elastic behavior when tested.

The mechanical and physical properties of a representation of commercially available fibers are given in Table 2.1. Values in the table are adapted from Mallick (2007). Note that the negative thermal expansion coefficient of aramid and carbon fibers indicates that shrinkage occurs when these materials are heated.

Glass fiber became commercially available in 1939 with the start-up of an Owens Corning production facility. Glass FRP (GFRP) composites have relatively low stiffness, high elongation, and moderate strength and weight. Glass is by far the most widely used fiber, because of the combination of low cost and reasonable performance. Glass fibers are classified into three types: E-glass, S-glass, and alkali

Strengthening of Concrete Structures Using Fiber Reinforced Polymers (FRP).
DOI: http://dx.doi.org/10.1016/B978-0-08-100636-8.00002-8

Table 2.1 Typical reinforcing fiber material properties

Fiber type	Fiber identification	Density (lbs/ft.^{3})	Tensile modulus (ksi)	Tensile strength (ksi)	Failure strain (%)	Thermal expansion coefficient ($\times 10^{-6}$/°F)	Poisson's ratio
Basalt		168	13,050	435	3.2	8.0	
Glass	E-Glass	159	10,500	500	4.80	8.99	0.20
	S-Glass	155	12,600	625	5.00	5.22	0.22
Aramid	Kevlar 49	91	19,000	525	2.80	−3.60	0.35
	Technora	88	10,100	435	4.60	−10.79	0.35
Carbon	T-300	110	33,500	530	1.40	−1.08	0.20
	P-100	134	10,000	350	0.32	−2.61	0.20
	AS-4	112	36,000	590	1.65	−1.08	0.20
	IM-7	111	43,500	770	1.81	−1.35	0.20

resistant AR-glass fibers. GFRP has a potential creep rupture problem when constantly loaded more than about 20% of their ultimate strength. However, when used in a passive fashion, such as wrapping a deficient structural component to enhance live load carrying capability, creep rupture is much less likely to occur. Carbon fibers have been commercially available since 1959. They are durable and perform very well under fatigue loading as well as in hot and moist environments. Aramid fibers were also produced in the late 1950s, appearing first under the trade name Nomex by DuPont. Aramid fibers are mainly used for aerospace and military applications, such as in ballistic rated body armor and as an asbestos substitute. Unlike, carbon, aramid fibers are sensitive to high heat and moisture.

Theoretically, carbon fibers could obtain a tensile strength of 15,000 ksi and a modulus of elasticity of 145,000 ksi. Such values assume that the crystal structure could be optimally oriented and packed. However, if polymer chains are folded in the crystalline state, a typical occurrence, neither the theoretical strength nor modulus can be fully developed. Carbon fiber composites are ideally suited for applications where strength, lower weight, and outstanding fatigue characteristics are critical requirements. As such, carbon FRP (CFRP) sheets and strips have been used to strengthen concrete structures such as beams, columns, slabs, piles, and decks (Elarbi, 2011).

2.1.2 Matrix

The most commonly used matrix for structural composites is thermosetting polymer. Polyester, vinyl ester, and epoxy are the most common polymeric matrix materials used with high-performance reinforcing fibers. They are all thermosetting polymers with good process ability and chemical resistance. Epoxies are more expensive than polyesters and vinyl-esters, but have in general better mechanical properties and outstanding durability. Thermoset polymers, including epoxy, are

Table 2.2 Mechanical properties of commonly used FRP epoxies

Epoxy type	Sikadur 300 (psi)	Tyfo S epoxy (psi)
Tensile strength	8000	10,500
Tensile modulus	250,000	461,000
Tensile elongation	3%	5%
Flexural strength	11,500	17,900
Flexural modulus	500,000	452,000

cured by chemical reactions, and the process of curing is irreversible. Table 2.2 contains the mechanical properties of two commercially available epoxies widely used in FRP composites.

2.1.3 Interface

One of the important functions of the matrix is to transfer stresses. Interface bonding between fiber and matrix is critical to the success of advanced composites. When the matrix is degraded due to environmental exposure or mechanical loads, often the fiber/matrix interface is weakened. The degradation of GFRP in hot water is found to be caused by the absorption of water by matrix resin and the dissolution of the fiber/matrix interface (Hamada et al., 1996; Nguyen et al., 1998). The dissolution of the interface results in debonding between fibers and matrix.

2.2 Composite interfacial adhesion and debonding

The quality of the adhesive bond at the interfaces between plies and between concrete and the strengthening FRP layers is critical to the utilization of the composite constituents. Adhesive bond at the interface is achieved primarily by attaching the surfaces within a layer of molecular dimensions, that is, on the order of 0.1−0.5 nm.

The term “adhesion” is associated with intermolecular forces acting across an interface and involves a consideration of surface energies and interfacial tensions. As a liquid, adhesives flow over and into the irregularities of a solid surface, coming into contact with it and as a result, interacting with its molecular forces. The adhesive then solidifies to form the “joint.” The basic requirements for good adhesion are thus intimate contact between the adhesive and the substrates, and an absence of weak layers or contamination at the interface. Adhesive bonding therefore involves a liquid “wetting” a solid surface, which implies the formation of a thin film spreading uniformly without breaking into droplets. Fundamentally, the surface tension of the adhesive should be lower than the surface energy of the solids involved, in this case, the treated surface of FRP and the exposed constituents of concrete. Because of the similarity in epoxy adhesive and composite matrix composition, values of surface tension and surface energy are similar. Both compositions contain polar

molecular groups which are mutually attractive and chemically compatible. Thus good adhesion can be achieved, provided that contamination is removed by adequate surface preparation. The quality of the adhesive bond at the interface has the potential to impact the failure mode of an FRP composite structure. The interface between the FRP sheet and the concrete is particularly important, since composite action requires a well-developed bond. Final failure is often caused by the debonding of the FRP sheet from the concrete substrate (Meier, 1995; Buyukozturk and Hearing, 1998; Mikami et al., 2015). The degradation of a constituent in FRP over time affects various composite properties, and may even change the order of governing failure modes which may be matrix, fiber, or interface-dominated (Wu and Yan, 2013). This is a particularly important concern, as a FRP-bonded structure could fail abruptly due to a change in dominant failure mode.

Debonding can be considered as the propagation of an interfacial crack with residual shear stress acting along the interface (Taljsten, 1996; Leung and Tung, 2006). In the case of FRP bonded to flat concrete members, debonding may occur at the end of the FRP sheet or initiate at an interior location where a stress concentration is present. Once debonding initiates, however, it may initially remain stable depending on how adjacent cracks interact, potentially allowing for further increases in load (Niu and Wu, 1990; Chen et al., 2007).

To model debonding, an interfacial shear-slip relation is generally needed. Most interfacial relation models are based on two similar assumptions. First, the initiation of interfacial debonding begins when the interfacial stress has reached the prescribed interfacial strength (τ_s). Second, in the debonded zone, the residual shear stress (τ) softens linearly with the interfacial sliding (s), such as given by (Leung and Tung, 2006): $\tau = \tau_0 - ks$, where τ_0 and k are the interfacial material parameters defining the initial residual shear stress and the shear softening rate after debonding. Based on this equation, the distribution of tensile stress (σ_p) along the debonded portion of FRP is calculated from

$$\frac{d^2\sigma_P}{dx^2} + \alpha^2\sigma_P = 0 \tag{2.1}$$

Finally, in the elastic zone where debonding has not yet occurred, σ_p is given by

$$\frac{d^2\sigma_P}{dx^2} - \beta^2\sigma_P = 0 \tag{2.2}$$

where α and β are parameters describing the structural configuration and material properties.

Solving the above equations with appropriate boundary conditions provides the tensile stresses along the FRP sheet as well as interfacial shear stresses. Such an analytic approach can simulate the debonding process in great detail, permitting comparisons with experiments. However, such analytical solutions are available for simple cases only.

Another popular approach to model debonding is to use finite element analysis. By using suitable interface elements, very good results have been obtained (Wu et al., 2004; Mu et al., 2006; Elarbi and Wu, 2012). This approach allows simulations of rather complex loading and geometrical configurations, but does not provide a detailed description of the delamination process. Therefore both approaches may need to be considered to properly characterize delamination behavior.

It is also important to be able to monitor bond quality over time. Hence, several evaluation techniques have been developed. For example, Hong and Harichandran (2005) detected the debonding of CFRP from concrete beams using electrochemical impedance spectroscopy sensing technology. Alternatively, Wu and Warnemuende (2002) proposed an innovative active modulation approach, Nonlinear Active Wave Modulation Spectroscopy (NAWMS), to detect weak bond between the FRP sheet and concrete substrate. In this procedure, a probe acoustic wave is passed through the system. Simultaneously, a second, modulating wave is applied to the system. Using 3-in. thick concrete slabs, they prepared several FRP-bonded samples with artificial flaws (1-in. square) designed into the interface. The sender was on one side of the flaw and the receiver on the other. While, maintaining the separation of the pair of transducers, a complete scan was carried out. The resulting frequency modulations were analyzed and well correlated to the presence of the flaws.

2.3 FRP durability

Under everyday service conditions, FRP-bonded bridges are subjected not only to heavy traffic loads but also to a wide range of temperature and moisture changes. Freeze and freeze/thaw exposures lead to material level degradation through matrix cracking and fiber-matrix debonding, increased brittleness, and substantial changes in damage mechanisms from those commonly observed under ambient conditions (Lord and Dutta, 1988; Dutta and Hui, 1996; Dutta, 1998; Karbhari and Pope, 1994; Karbhari et al., 2000). Chu et al. (2004) used accelerated weathering test data to predict long-term properties of pultruded E-glass/vinyl ester composites, and the predictions correlated well with their experimental results. Karbhari (2002) and Karbhari et al. (2002) adopted a semi-empirical approach to predict the long-term modulus and strength of unidirectional carbon/vinyl ester composites subject to freeze−thaw cycling. Their study indicated that typical analytical predictions are somewhat conservative for strength, and freeze/thaw cycling does not have an appreciable effect on modulus. It was also shown that freeze−thaw cycling between 4.4°C and −17.8°C alone caused very insignificant changes in flexural strength, storage modulus, and loss factor for the E-glass/vinyl ester specimens conditioned in distilled water and saltwater (Wu et al., 2006b). Furthermore, Wu et al. (2006a) concluded that (1) small reductions in modulus were observed after 250 freeze−thaw cycles in water when the specimens were loaded to 25% of their ultimate strain while undergoing freeze/thaw cycles; (2) no deterioration was observed for the specimens prestrained and freeze−thaw cycled in dry air conditions, and;

(3) constant freezing at −17.8°C resulted in a minor increase in flexural strength and storage modulus over time.

The degradation of a constituent in FRP over time affects various composite properties, and, as noted above, may change the order of governing failure modes which may be matrix, fiber, or interface-dominated. This is an important concern, as an FRP-bonded structure could fail abruptly due to a change in dominant failure mode. In most cases, however, the FRP-concrete bond line is the critical component to the effectiveness of most FRP structural strengthening applications, as this is the location where the transfer of stresses from the concrete to the FRP occurs. An exception to this is a structural element that uses FRP for confinement, such as a wrapped column. Regardless, field experience has shown that the bond between the FRP composite and concrete cannot always be assured. The bond can degrade over time, eventually causing the system to become ineffective. Bond quality is influenced by the condition of the existing concrete, surface preparation of the concrete substrate, quality of the composite system application, quality of the composite, and the durability of the epoxy primer and resin. A large number of additional parameters affect bond strength, including exposure to ultra-violet radiation, chemical activity, temperature, moisture, and stress level, as well as other factors (Karbhari, 1997; Mikami et al., 2015). As FRP composites for bridges have been in service for a relatively short period of time, there are few long-term data available to define environmental effects and the resulting degradation rate.

Most FRP durability information has been gathered from laboratory simulations of harsh environments (Dutta and Hui, 1996; Toutanji and Balaguru, 1999; Karbhari et al., 2003). Karbhari (2004) found that low-temperature thermal cycling appears to have a greater deteriorative effect on FRP than constant immersion at below-freezing temperatures, due in part to interface-level degradation. Here, microcracking at lower temperatures results in an increase of water absorption during warmer periods, followed by increased resin plasticization and hydrolysis. The expansion of frozen water collected in cracks results in debonding and transverse microcrack growth (Rivera and Karbhari, 2002). Various other researchers have found that such freeze/thaw exposures can lead to significant material degradation through matrix cracking and fiber-matrix debonding, as well as increased brittleness, resulting in a substantial change in the damage mechanisms commonly observed under ambient conditions (Dutta, 1989, 1992; Lord and Dutta, 1988; Haramis, 2003; Karbhari et al., 1994, 2000, 2002). For glass and carbon-wrapped columns, however, freeze−thaw cycles alone appear to have insignificant effect on compressive strength. It was also found that, using accelerated corrosion experiments, column wrapping significantly reduced reinforcing bar corrosion (Harichandran and Baiyasi, 2000).

Wu et al. (2006, 2006a) completed a comprehensive study on the combined effects of low-temperature thermal cycling, cycling frequency, sustained loads, and presence of salinity on FRP. It was found that sustained loads significantly accelerated degradation in all cases; that the significance of salinity depended on the cycling frequency; and that a high-humidity environment produced most damage. Moreover, when FRP materials were conditioned at higher temperatures, water

absorption was increased under sustained loads (Gibson, 1994; Kulkarni and Gibson, 2003). Elarbi and Wu (2012) recently found that high-temperature and high-humidity environments have a very detrimental effect on the strength and stiffness of FRP materials, as well as the bonding between FRP and concrete. Although experimental data on bond deterioration due to natural weathering are unavailable, under accelerated laboratory environments, a large reduction (more than 80%) in bond strength between FRP and concrete in a high-temperature environment has been reported, primarily due to the deterioration of the FRP material (Bank et al., 1998; Katz et al., 1999; Galati et al., 2006).

At present, there is no standardized durability test procedure for FRP materials for infrastructure applications. However, an accelerated test procedure to simulate the effects of natural weathering on FRP has been developed by Wu et al. (2006a, 2006b). This procedure, modified from ASTM C666 (2008), the standard freeze/thaw durability test for concrete, incorporates the combined effects of temperature, medium (i.e., immersion environment), and sustained load into a complete test program. Using this test procedure, it was found that failure modes of FRP composites most likely to be affected by environmental conditions are those associated with the polymer matrix material (Wu et al., 2006b). It was also found that after 250 freeze/thaw cycles with less than 25% sustained load applied, flexural strength of an FRP-bonded concrete specimen experienced significant reductions if exposed to moisture (Wu et al., 2006b).

Using tests similar to the above, degradation rates can be fundamentally calculated from change in strength or stiffness versus time plots. However, to reduce experimental time, an accelerated test method uses one or several accelerating mechanisms to increase the rate of degradation. The rate of degradation under the accelerated condition is then related to the degradation rate under field service conditions by an acceleration factor, which is defined as the ratio of the degradation rate in the accelerated environment (i.e., laboratory) to that in the actual service environment. Acceleration factors for various environments may be determined using the framework outlined in ASTM E632 (1996). With appropriate acceleration factors known, short-term, relatively inexpensive laboratory experiments or finite element simulations can be used to accurately simulate durability performance over real time (Yan, 2005). Currently, however, appropriate acceleration factors for FRP-bonded concrete members for specific climatic regions are unknown.

Elarbi (2011) conditioned a series of concrete beams strengthened with CFRP to simulate the aging effect that weather-exposed components are expected to experience, and was conducted using various accelerated hygrothermal conditions. For the control specimens exposed to indoor conditions only, it was found that the ACI-based predictions of capacity significantly underestimated the failure load, whereas in contrast, the numerical models were reported to agree well with the experimental results. Using a different set of specimens, which were exposed to accelerated weathering cycles, it was found that bond strength deteriorated and led to delamination, a failure which is not currently considered in ACI 440, but was predicted in the numerical simulations.

This page intentionally left blank

Composite mechanics

3

3.1 Introduction

Fiber-reinforced polymers (FRPs) (or advanced fiber composites) have been successfully utilized over a long period of time by the aerospace and aircraft industries. Composites are currently gaining a rapid momentum in finding their way into civil engineering structural applications. The earliest reported application with plate bonding is from South Africa in the end of the 1960s where a concrete beam in an office building was strengthened with steel plates. Since then numerous strengthening applications have been reported, both with steel plates and in the last decade with various FRP systems. As compared with steel plates, FRP systems have many advantages. In addition to their resistance to corrosion which allows the possibility of extended service life or perhaps limited required maintenance, FRP laminates and fabric come in great lengths, which can be cut to suitable sizes in the field. Also, the light weight of FRP provides considerable cost savings in terms of labor: a worker can handle the FRP material, whereas a crane would be required for its steel equivalent.

FRP strengthening can be applied to mitigate several failure modes. For flexural strengthening of beams, slabs, or girders, FRP plates can be applied to the tensile face of the concrete. Shear and torsion strengthening can be accomplished by placing FRP on the sides of beams. Columns are typically strengthened by wrapping the FRP around the column in the hoop direction, thus increasing the confinement of the concrete core. This can be accomplished with wet lay-up or prefabricated cylindrical jackets.

Installation of FRP plates includes two possibilities: precured and cured-in-place laminates (manual lay-up). For the latter, a surface primer is often applied first to the concrete surface. After the primer is cured, a layer of putty is applied to level uneven spots and fill surface cavities. The recommended resin is then mixed and applied to the concrete surface in a thin uniform layer using a roller. A fiber sheet (preimpregnated or dry) is cut to the desired length and width and pressed to the concrete using a "bubble roller." This act eliminates the entrapped air between the fibers and resin and ensures the full impregnation of the FRP sheet. Attention should be paid to the alignment of the fiber orientation when installing the FRP sheet since a poor orientation of the fibers generally reduces the strength of the FRP. Precured FRP systems consist of a wide variety of composite shapes manufactured in the system supplier's facility and shipped to the job site. Typically, an adhesive is used to bond the precured sheets or plates to the concrete surface or

Strengthening of Concrete Structures Using Fiber Reinforced Polymers (FRP).
DOI: http://dx.doi.org/10.1016/B978-0-08-100636-8.00003-X

they are inserted into slots cut into the substrate. The system manufacturer must specify the adhesive used to bond the precured system to the concrete surface.

3.2 Laminate

Thin sheet constructions, known as laminates, are an important class of composite. They are made by stacking together usually unidirectional layers (also called single ply or lamina) in predetermined directions and thicknesses to give the desired stiffness and strength properties. The skins of airplane wings and tails, the hull sides and decking of ships, and the sides and bottom of water tanks are typical examples. Even cylindrical components, such as filament wound tanks, can be treated as laminates, provided the radius-to-thickness ratio is sufficiently large (say >50). Laminates typically consist of between 4 and 40 plies, and each ply is around 0.125 mm thick if it is carbon or glass fiber/epoxy. Typical lay-ups (the arrangement of fiber orientations) are cross-ply, angle-ply, and quasi-isotropic. When making a laminate, one must decide on the order in which the plies are placed through the thickness (known as the stacking sequence). This has an important influence on the flexural performance of the laminate. There is an established convention for denoting both the lay-up and stacking sequence of a laminate. For example, a cross-ply laminate, which has ply fiber orientations in the sequence 0, 90, and 0 degrees from the upper to the lower surface, would be denoted (0/90 degree)s. The suffix "s" means that the stacking sequence is symmetric about the mid-thickness of the laminate. Laminates denoted by (0/45/90 degree)s and (45/90/0 degree)s have the same lay-up but different stacking sequences.

3.2.1 Unidirectional ply

Based on the mechanical properties of fiber and matrix materials, the actual tensile strength and tensile modulus of the composite materials in the fiber direction can be calculated according to the following equations (Jones, 1999):

$$\sigma_{com} = \sigma_f v_f + \sigma_m v_m \tag{3.1}$$

$$E_{com} = E_f v_f + E_m v_m \tag{3.2}$$

In the transverse direction, the tensile strength and tensile modulus of the composite materials are given as

$$\sigma_{com} = \sigma_m \tag{3.3}$$

$$E_{com} = \frac{1}{\frac{V_f}{E_f} + \frac{V_m}{E_m}} \tag{3.4}$$

where σ_{com} is the tensile strength of the cured laminate composite, σ_f represents the tensile strength of dry fiber, σ_m is the tensile strength of matrix material, v_f is the volume fraction of fiber, and v_m represents the volume fraction of matrix, the tensile modulus, E of the fiber (subscript f), of the matrix (subscript m), and of the FRP composite (subscript com).

$$v_f = w_f \frac{\rho_c}{\rho_f} \tag{3.5}$$

$$v_m = w_m \frac{\rho_c}{\rho_m} \tag{3.6}$$

where w_f is the weight or mass fraction of fiber, w_m represents the weight or mass fraction of matrix, ρ_c, ρ_f, and $\rho_m$are the weight density (or mass density) of composites, fiber, and matrix, respectively.

$$w_f = \frac{W_f}{W_c} \tag{3.7}$$

$$w_m = \frac{W_m}{W_c} \tag{3.8}$$

W_f, W_m, and W_c is the weight (or mass) of the fiber, matrix, and composites, respectively.

The density of the composite (fiber + matrix) can be found by this equation:

$$\rho_c = v_f \rho_f + v_m \rho_m = \frac{1}{\left[\frac{w_f}{\rho_f} + \frac{w_m}{\rho_m}\right]} \tag{3.9}$$

$$v_f + v_m = 1 \tag{3.10}$$

$$w_f + w_m = 1 \tag{3.11}$$

3.2.2 Classical laminate theory

A laminate composite material is different from an isotropic material in two ways: it is a layered material built up from stacked plies, and, in addition, each ply is not isotropic but has directional properties with a higher strength/stiffness in the direction of the fibers, which can change from ply to ply. In a more complicated case, a composite plate can consist of a light weight core material sandwiched between two laminates.

To predict the laminate properties, the stress−strain relations are required for loading a lamina at an angle θ to the fiber direction (Jones, 1999; Matthews and Rawlings, 1994). The modulus, E_x, of a ply loaded at an angle θ to the fiber direction is given by

$$\frac{1}{E_x} = \frac{1}{E_1}\cos^4\theta + \left(\frac{1}{G_{12}} - \frac{2\nu_{12}}{E_1}\right)\sin^2\theta\,\mathrm{con}^2\theta + \frac{1}{E_2}\sin^4\theta \tag{3.12}$$

where E_1 and E_2 are the modulus of the composite lamina parallel to the fibers (Eq. (3.2)) and perpendicular to the fibers (Eq. (3.4)), ν_{12} is the principal Poisson's ratio of the lamina (typically 0.3) and G_{12} is the in-plane shear modulus of the lamina. Unlike isotropic materials, which require two elastic constants to define their elastic stress−strain relationships, the anisotropy of a composite lamina (which is an orthotropic material, i.e., it has three mutually perpendicular planes of material symmetry) needs four elastic constants to be known in order to predict its in-plane behavior (Jones, 1999).

Ply orientations in a laminate are taken with reference to a particular loading direction, usually taken to be the direction of the maximum applied load, which, more often than not, coincides with the fiber direction to sustain the maximum load, and this is defined as the 0 degree direction. In design it is usual to choose balanced symmetric laminates. A balanced laminate is one in which there are equal numbers of $+\theta$ and $-\theta$ plies; a symmetric laminate is one in which the plies are symmetric in terms of geometry and properties with respect to the laminate mid-plane. Hence a laminate with a stacking sequence $0/90/+45/-45/-45/+45/90/0$, which is written $(0/90/\pm 45)$s is both balanced and symmetric. Balanced symmetric laminates have a simple response. In contrast, an unbalanced asymmetric laminate will, in general, shear, bend, and twist under a simple axial loading (Ogin, 2000).

In most lay-ups the thickness is small compared with the other dimensions of the structure so that it forms a plate type structure. It is generally assumed that the strains through the thickness of the plate vary linearly in the local through-thickness (z) direction. Since the material properties vary from layer to layer, the stress variation through the thickness of the composite is much more complicated than that of the strains. In general, there will be discontinuous changes of stress from ply to ply. This means that a simple material stiffness cannot be used for a laminated material. Instead the stress−strain relationships for a laminate can be predicted using laminate theory, which sums the contributions from each layer in an appropriate way for both in-plane and out-of-plane loading. Laminate theory gives good agreement with measured laminate elastic properties for all types of composite material fabricated from continuous unidirectional prepreg layers (UD). Predicting laminate strengths, on the other hand, is much less reliable, except in some simple cases, and is still the subject of ongoing research. Because composite structures are usually designed to strains below the onset of the first type of visible damage in the structure (i.e., to design strains of about 0.3−0.4%), the lack of ability to predict the ultimate strength accurately is rarely a disadvantage.

"Classical Laminate Theory" is an extension of the theory for bending of homogeneous plates, but with an allowance for in-plane tractions in addition to bending moments, and for the varying stiffness of each ply in the analysis. In general cases, the determination of the tractions and moments at a given location will require a solution of the general equations for equilibrium and displacement compatibility of plates. This theory is treated in a number of standard texts (Timoshenko and Woinowsky-Krieger, 1959), and will not be discussed here.

We begin by assuming a knowledge of the tractions N and moments M applied to a plate at a position x, y:

$$N = \begin{Bmatrix} N_x \\ N_y \\ N_{xy} \end{Bmatrix} \tag{3.13}$$

$$M = \begin{Bmatrix} M_x \\ M_y \\ M_{xy} \end{Bmatrix} \tag{3.14}$$

The stresses are integrated through the thickness of the plate. The average values of the stress give the in-plane loads N and the linear variation gives the couples M. The end loads and moments are shown in Fig. 3.1 (note $N_{xx} = N_x, N_{yy} = N_y$). Using the elasticity properties of each ply, rotated to the fiber directions, the end loads and

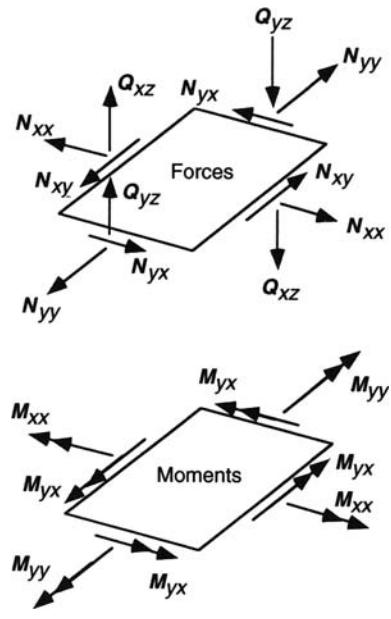

Figure 3.1 Mid-plane forces and moments.

moments can be related to the mid-plane strains ε^o and curvatures κ to give the laminate stiffness properties as

$$\begin{bmatrix} N \\ M \end{bmatrix} = \begin{bmatrix} A & B \\ B & D \end{bmatrix} \begin{bmatrix} \varepsilon^o \\ k \end{bmatrix} \tag{3.15}$$

where A are in-plane stiffness propitiates, D are the bending stiffness propitiates, and B is the coupling that arises between the bending and membrane actions.

3.3 Textile fabric

Instead of using unidirectional fiber plies, textile fabric sheets can be used. Textile-reinforced composites have been in service in engineering applications for many years, e.g., woven glass reinforced polymer hulls for minesweepers. This is because textile-reinforced composite materials show potential for reduced manufacturing costs and enhanced processability, with more than adequate, or in some cases improved, mechanical properties. Those economic entities within which composite materials have been well developed, notably the European community (with about 30% of global composite usage), the United States (with about 30%) and Japan (with about 10%) have seen a growing interest in textile reinforcement in the 1990s, with China, Taiwan, Russia, South Korea, India, Israel, and Australia being additional major contributors (Ogin, 2000). In the last years of the 20th century, conferences devoted to composite materials had burgeoning sessions on textile reinforcement.

Of the available textile reinforcements (woven, braided, knitted, stitched), woven fabric reinforcement for polymer matrices is the most used. Several textile techniques are likely to be combined for some applications. For example, a combination of braiding and knitting can be used to produce an I-shaped structure (Nakai et al., 1997).

For structural applications, the properties which are usually considered must include stiffness, strength, and resistance to damage/crack growth. The range of textiles under development for composite reinforcement is indicated in the schematic diagram shown in Fig. 3.2 from Ramakrishna (1997).

Compared to unidirectional fiber tapes, textile fabrics possess better bonding to concrete or steel surface due to the additional anchorages formed by resins through the weaveness of the textile fabrics. Note that the size of the openings, formed by two adjacent warp and weft yarns, not only control the strength and stiffness of the fabric structure, but also provide access points for concrete to form anchorage.

3.3.1 Mechanics

Because of the design flexibility and the wide availability of manufacturing capacity in the fiber and textile industry, suitable textile includes weave, knitted, and

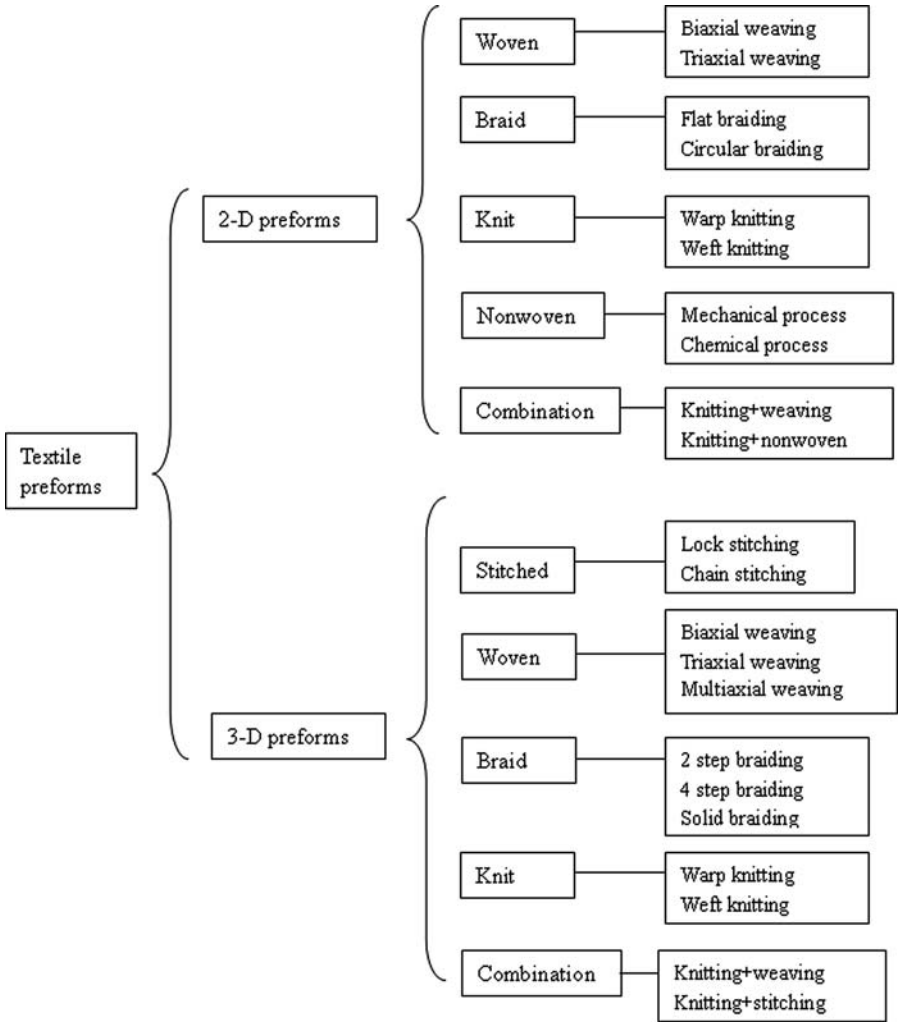

Figure 3.2 Textile techniques under development for composite materials.
Source: After Ramakrishna, S., 1997. Characterization and modeling of the tensile properties of plain weft-knit fabric reinforced composites. Compos. Sci. Technol. 57, 1−22.

braided fabrics. By judicious selection of fiber materials and fiber architecture for the weave or braided structures, the load-deformation behavior of these fibrous fabrics could be tailored.

When continuous carbon fibers are processed into 1-D or 2-D fabrics, the rupture strain remains similar to that of carbon fibers (typically 1−1.5%). Cox et al. (1992, 1994) investigated 3-D woven carbon/epoxy composites, which consisted of two sets of nominally straight tows forming 0/90 degree array (stuffers and fillers) and a relatively low volume fraction of interlock tows (warp weavers) providing

continuous reinforcement in the through-thickness direction. They showed that these 3-D composites possess an ultimate strain in the range of 2.5−4%. Such a significant increase in composite ductility is associated with individual tow rupture. All stuffers have failed well before the peak load prior to the load sharp drop has been reached; such load transfer is believed to occur via a lock-up mechanism involving tow waviness (Cox et al., 1996). Therefore the much enhanced rupture strain of the 3-D woven fabric could lead to a much improved ductility of the reinforced composite over that of a 2-D fabric reinforced composite. The post peak behavior of the 3-D woven composites is also greatly improved due to stuffers pull-out following the rupture of individual yarns (Cox et al., 1994).

Weave and braided structures are the primary fiber architectures in the textile industry and their manufacturing technology is well established (Ko, 1989). The analysis of a complex fabric structure is very challenging, mainly due to the complexity of the structural configuration.

Harris et al. (1998) and Somboonsong et al. (1998) developed a design process for braided structures by analytically formulating the stress−strain relationship as a function of various manufacturing parameters, such as the core and sleeve modulus, fiber volume fractions, crimp size, and braiding angle.

In the case of weave structures, especially the plain weave for which the warp and weft are aligned so that they form a simple crisscross pattern, the mechanics model that was previously developed by Wu (1992, 1993) and Wu et al. (1995) could be used.

Yang and Chou (1987) have shown the effects of different fiber architectures on the change in the moduli, E_x and E_y, of a carbon fiber-reinforced epoxy laminate (Fig. 3.3). These laminates have the same fiber volume fraction of 60%. The cross-ply composite has E_x and E_y moduli of about 75 GPa. In the biaxial weaves of the eight-harness satin and the plain weave, the moduli both fall to about 58 and 50 GPa, respectively. These reductions mainly come from the crimps in the interlaced woven structure. More crimps per unit length in the plain weave hence result in a smaller modulus. The triaxial fabric, with three sets of yarns interlaced at 60 degree angles, behaves similarly to a (0 ± 60)s angle-ply laminate. The triaxial fabric is quasi-isotropic under in-plane loading; it has the same Young's modulus for any direction in the plane of the laminate. The triaxial fabric shows a further reduction in E_x and E_y (about 42 GPa), but this fabric benefits from a higher in-plane shear modulus (which is not shown in the diagram) than the biaxial fabrics. The anticipated range of properties for a multiaxial warp-knit fabric (or multilayer multidirectional warp-knit fabric) reinforced composite is also shown, lying somewhere between the triaxial fabric and above the cross-ply laminate (at least for the modulus E_x), depending on the precise geometry. Here warp, weft, and bias yarns (usually ± 45) are held together by "through-the-thickness" chain or tricot stitching. Finally, a three dimensional braided composite is shown, with braiding angles in the range of 15−35 degree. This type of fiber architecture gives very anisotropic elastic properties as shown by the very high E_x moduli (which are fiber dominated) and the low E_y moduli (which are matrix dominated).

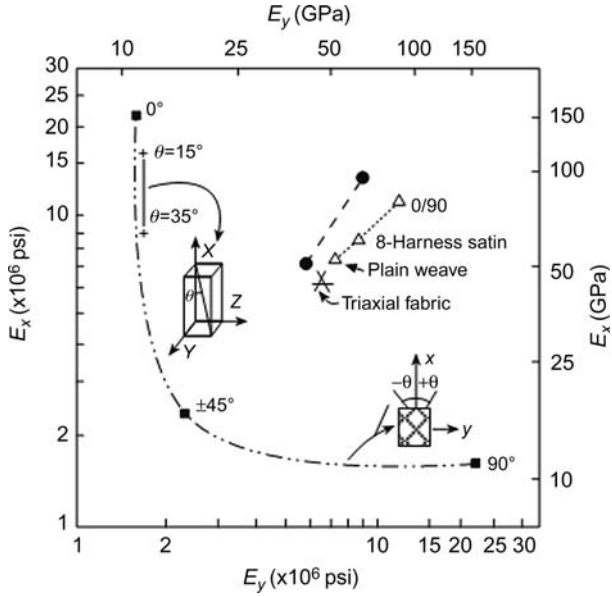

Figure 3.3 Predicted E_x and E_y moduli for a range of reinforcement architectures; $\pm\theta$ angle-ply (for $\theta = 0$ to $\pm 45-90$), cross-ply (0/90), eight-harness satin and plain woven, triaxial woven fabric, braided ($\theta = 35-15$ degree) and multiaxial warp knit (•--•), for the same fiber volume fraction of 60%.
Source: Reprinted, with minor changes, from Yang, J.-M., Chou, T.-W., 1987. Performance maps of textiles structural composites. In: Matthews, F.L., Buskell, N.C.R., Hodgkinson, J. M., Morton, J. (Eds.), Proceedings of Sixth International Conference on Composite Materials and Second European Conference on Composite Materials (ICCM6/ECCM2). Elsevier, London, 5579−5588.

3.4 Durability and failure modes

The prediction of long-term strength of FRP laminates subject to environmental exposure is much more difficult than that of the modulus (Gibson, 1994; Wu and Yan, 2011). As to be discussed, there are a few different failure criteria that must be considered in the design of FRP laminate plates.

At the material level, FRP composites are typically composed of two distinct constituents, namely fiber and matrix. The properties and failure modes of a composite therefore depend on the properties of each individual constituent, i.e., fiber, matrix, and their interfaces. Any constituent degradation over time affects various composite properties to different extents and even changes the order of significance of failure modes since there are quite a few failure modes operative simultaneously at any given time. Each failure mode can be attributed to be matrix dominated, fiber dominated, or interface dominated. The long-term performance of a FRP composite may not simply degrade over time; abrupt failure might occur due to a change in the dominant failure mode.

In infrastructural applications, FRP strengthening design is typically stiffness-critical; the environmentally induced failure modes of major interest should be those having the greatest effect on the material's stiffness and strength of the matrix resins, since the properties of the fibers are generally not affected. Furthermore, those failure modes of the composite laminates which are most likely to be affected by environmental conditions are the failure modes mainly associated with the polymer matrix materials. A laminate has a laminated construction with individual plies stacked at different fiber orientations, but the longitudinal plies have the greatest influence on the stiffness. The stiffness of longitudinal plies under tension is fiber dominated, and environmentally induced degradation of the polymer matrix would have a small affect on tensile stiffness for reasonable fiber volume fractions. However, the microbuckling failure of longitudinal plies under longitudinal compression is strongly influenced by the stiffness of the polymer matrix and would therefore be most affected by environmental conditions.

3.4.1 Failure modes and strength prediction

The ultimate strength of a FRP laminate depends on which failure mode prevails at the time of the failure. Possible failure modes include delamination between plies or between the laminate and concrete substrate, ply rupture, and ply buckling. The order of significance may change over time as a result of the various deterioration rates of the constituents. FRP composites always experience some degree of delamination, broken fibers and cracked matrices, but any of these is only significant if the damage grows substantially so that the composite starts to lose its integrity. There are three dominant failures would be considered: first-ply failure, interface shear failure, and local buckling.

3.4.1.1 First-ply failure

It is assumed that the initial failure of any ply of a laminate causes laminate failure, which is referred to as the first-ply failure criterion. The first-ply failure load is usually conservative, since a failure in the form of matrix cracks may not lead to immediate laminate failure. It has been long recognized that the failure loads of materials subject to a multiaxial stress state may well differ from those when they are only loaded by an uni-axial stress. For composite laminates, there are a few common failure criteria such as Tsai-Hill, Hoffman, and Tsai-Wu criteria (Jones, 1999). These interactive criteria are formulated in such a way that they take account of stress interactions. The Tsai-Hill criterion, which has been proven to be successful under a wide variety of circumstances (Tsai, 1988), is shown as

$$I_{fpf} = \left(\frac{\sigma_1}{S_L^2}\right)^2 \frac{\sigma_1\sigma_2}{S_L^2} + \left(\frac{\sigma_2}{S_T^2}\right)^2 + \left(\frac{\tau_{12}}{S_{LT}^2}\right)^2 \geq 1 \tag{3.16}$$

where I_{fpf} is the first-ply failure index, '1' is in the fiber's longitudinal direction, '2' is transverse to the fiber's axis. The values of the strength used in this equation

are chosen depending on the direction of σ_1 and σ_2. For example, if σ_1 is tensile S_L^+ is used, and if σ_2 is compressive S_T^- would be used. Subscript "L" represents longitudinal direction and "T" transverse direction. Superscript "+" represents tension and "−" denotes compression. S_{LT} is in-plane shear strength.

3.4.1.2 Shear failure

There are two possible ways of delamination. The first one is the delamination between plies of the laminate. The other is the delamination between the laminate and the substrate of the bonded structure. Therefore the shear stresses at these interfaces must be carefully examined to prevent from shear failure (leading to delamination).

By employing the quadratic delamination failure criterion proposed by Brewer and Lagace (1988), delamination is predicted to occur based on the out-of-plane stresses. Failure occurs as (Senne et al., 2000):

$$\left(\frac{\tau_{xz}}{S_{XZ}}\right)^2 + \left(\frac{\sigma_z}{S_Z^+}\right)^2 \geq 1 \tag{3.17}$$

where τ_{xz} and σ_z are the out-of-plane interlaminar stresses; interlaminar shear strength S_{XZ} and interlaminar tensile strength S_Z^+. Usually the second term in Eq. (3.17) is negligible, the shear delamination criterion takes on the simplified form

$$I_{sf} = \left(\frac{\tau_{xz}}{S_{xz}}\right)^2 \text{or} \left(\frac{\tau_{yz}}{S_{yz}}\right)^2 \tag{3.18}$$

where I_{sf} is shear failure index and S_{yz}, S_{xz} are interlaminar shear strengths.

3.4.1.3 Local buckling

Buckling of laminate plates is characterized by excessive transverse deflections under in-plane compressive forces. Buckling is a critical strength limit state and must be prevented in the design. The thickness of a laminate is normally much smaller than other dimensions of the laminate, hence a laminate is a thin-walled structure. Local buckling is only needed to be considered when the laminate is subjected to very high compressive stresses.

In practice, finite element analysis can be conveniently carried out. In ABAQUS, buckling can be predicted by using the *BUCKLE step. In each step, a nominal load is applied. The magnitude of the load is not of significance, since such eigenvalue buckling is a linear perturbation procedure: the stiffness matrix and the stress matrix are evaluated at the beginning of the step without any of this load applied. The *BUCKLE step calculates the eigenvalues. The buckling load then equals the eigenvalue multiplied by the applied load plus any "base state" load. The eigenvectors associated with the eigenvalues are also obtained.

3.5 Finite Element Analysis (FEA)

Since the early years of the mathematical modeling of problems in continuum mechanics, numerous examples have shown that the exact solution to some of the controlling differential equations hardly ever exists, and even if it did, it is frequently hard to accustom for common use.

Analytical solutions can be found for certain simplified situations. For problems concerning complex material properties and boundary conditions, numerical methods are typically used that give approximate and suitable solutions. In the numerical methods, the solution more commonly capitulates approximate values of unidentified quantities only at a finite number of points in the structure. The way of choosing only a certain number of discrete points in the body of the structure can be described as "discretization." One of the ways of discretizing a body or a structure is to split it into an equivalent system of smaller bodies or structures. These bodies are then assembled to represent the solution for the original body, and inside this combination, the bodies are assumed to be connected to each other at separate points called nodes. These nodes define the geometry of the small bodies used in the discretization, which are referred to as "elements." The elements of consideration in an FEA framework have an actual, or finite, dimension, rather than a differential length as considered in classical analytical approaches which integrate throughout the entire field of the structure to develop equations that describe load-displacement relationships.

The finite element method started as an extension of the matrix method and its application to trusses and frames of directly connected members by matching the nodal displacements without consideration for interelement continuity. Since that time, finite element method has expanded to cover fields beyond structural mechanics such as heat flow, fluid flow, seepage of water, and others.

The formulation of the finite element method has often made use of two principles. The first is the principle of minimum potential energy, which is concerned with satisfying the continuity conditions within the structure and the kinematic boundary conditions, but no requirements that the equilibrium between stress and boundary conditions be satisfied (displacement or stiffness model); the second is the principle of minimum complementary energy, which is concerned with the stress fields that satisfy the conditions of equilibrium, but not necessarily the requirements of compatibility (stress or flexibility model).

In general, two types of analysis are commonly used in finite element to model structures, 2-D modeling and 3-D modeling. Although 2-D modeling has the advantage of simplicity and allows for computationally efficient models, it may not provide the accuracy available in 3-D modeling. Although 3-D modeling has the potential to produce more accurate results, complex 3-D models sacrifice the ability to run on all but the fastest computers effectively. Within each of these modeling systems, linear or nonlinear analyses are possible. Nonlinear analyses are typically needed when large strains or large deformations are considered, as well as phenomenon beyond the linear or elastic range of a material such as cracking and plastic behavior. Nonlinear solution methods are also generally needed to model contact and some instabilities.

The nodal grid of elements into which a structure is discretized is commonly called a mesh. Elements within the mesh contain the load-displacement relationships between nodes that define the behavior of the structure. The load-displacement relationship for an element is generally defined by a constitutive (stress-strain) as well as a strain-displacement relationship. The former depends on the material model and associated properties input by the analyst, where the latter is a function of the type of element chosen and how it was derived.

Due to the many choices available in the FEA approach, such as the element type, mesh density, load and boundary condition idealization, material model and solution procedure used, the accuracy of an FEA model relies heavily on the expertise of the analyst. Typically, nodal displacements are the most accurately predicted quantity in an FEA model, then strains and stresses within the element. Moreover, the accuracy of the FEA procedure generally increases as mesh density increases and element size correspondingly decreases. Thus, there is often a desire to use a high density mesh. However, such a choice may be costly, as computational effort can be thought to be roughly proportional to the square of the number of active degrees of freedom (number of active nodes multiplied by the degrees of freedom per node, which depends on the element type chosen) in the problem. The simplified relationship given above is not exactly true for a modern solver, but does provide a rough indication of how computational effort is expected to dramatically change as problem size increases. To minimize this problem, element size and nodal density can be changed throughout the mesh. For example, in areas of interest, such as those of high stress, high stress gradients, or expected failure or fracture points, which may occur at fillets, corners, and other geometric complexities, a high density mesh could be used. Away from these points, a much more coarse mesh, which is only needed to correctly capture nodal displacements, could be specified to reduce computational effort.

3.5.1 Finite element simulation

In general, the major, general-purpose commercial finite element software packages (often called FEA 'codes') are similar in capability. Although ABAQUS is mentioned in this chapter, it was only used to illustrate the design examples. Most commercial codes provide a reasonably simple, consistent interface for creating, submitting, monitoring, and evaluating FEA results. These codes are often divided into modules, where each module defines a logical aspect of the modeling process; for example, defining the geometry, defining material properties, and generating a mesh. As one moves from module to module, the analyst can build the model from which the FEA program generates an input file which is then submitted to the solver for solution. The solver then sends solution information to the user to allow solution progress monitoring, and generates an output database which is sent to a post-processor for results reporting and visualization. At a minimum, the analysis model requires the following information:

- Discretized geometry.
- Element section properties.

Table 3.1 Concrete material properties

Young's modulus	4.23×10^6 psi
Compressive strength	5502 psi
Poisson's ratio	0.18
Density	0.0867 lbs/in.^{3}

Figure 3.4 Contact surfaces between concrete beam and FRP strengthening sheet.

- Material data.
- Loads and boundary conditions.
- Analysis type.
- Output requests.

As an example, a numerical analysis was performed to simulate the flexural behavior and failure of a rectangular concrete beam strengthened by a FRP sheet applied on the tension side of the beam. The model was constructed and solved using the ABAQUS−CAE extended finite element program. The modeling space was chosen as 2-D planar and divided into two parts. Part 1 represented the rectangular concrete beam model where all geometries and properties were input. The element was considered as an elastic-isotropic material. The material behavior was selected to be "Maxps Damage," and the concrete properties are given in Table 3.1.

Part 2 represented the FRP strengthening sheet. Parts 1 and 2 were connected by a "Tie" interface element and a surface-to-surface contact was assumed. The concrete beam was designated as the master surface, and the FRP was the slave surface (see Fig. 3.4).

The load was applied as a static concentrated load, while one support was considered as a pin and the other a roller (see Fig. 3.5).

3.5.2 Numerical modeling of FRP-strengthened concrete beams

Two types of material properties were input to ABAQUS−CAE. The first set of material properties was for concrete (first part), while the mechanical properties of the FRP composite (second part) were used based on the data provided by the manufacturer. The two parts of 2-D simulation were meshed by specifying an element size; the total number of nodes was 451.

Under increasing loads, the concrete cracked first from the tension side of the concrete beam at the center and the crack propagated upward until approximately one-third of the beam's height (Fig. 3.6), then the FRP ruptured (Fig. 3.7). Therefore, the mode of final failure was FRP rupture. The failure load was predicted

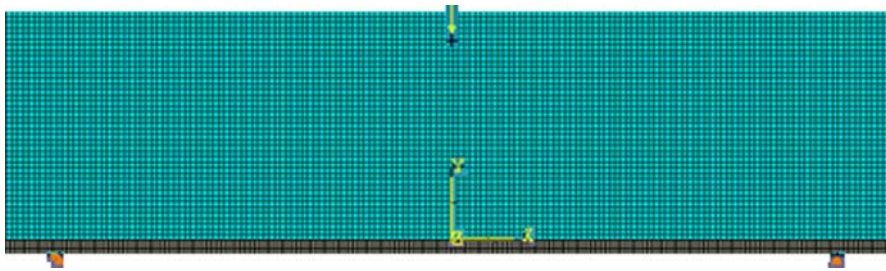

Figure 3.5 Load and boundary conditions of FRP-strengthened beam model.

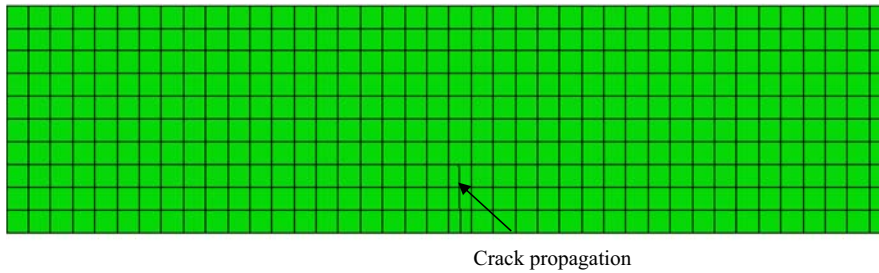

Figure 3.6 Crack propagation of strengthened concrete beam model.

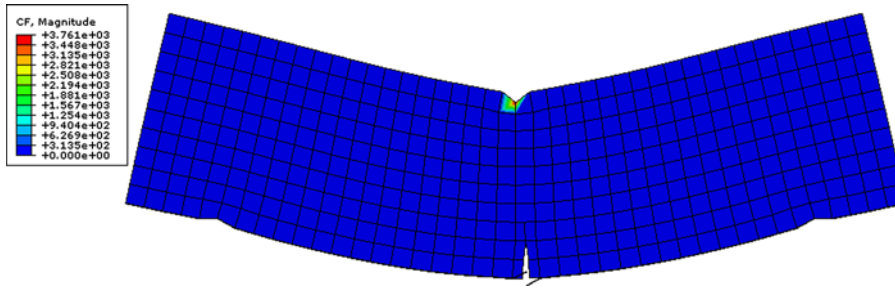

Figure 3.7 FRP rupture of strengthened concrete beam.

to be 3761 lbs and the mid-span deflection at the maximum failure load was 0.00226 in. Fig. 3.8 shows the mid-span deflection at the maximum flexural load.

When FRP-strengthened concrete beams are aged under natural weathering or accelerated laboratory testing, the dominant failure mode often found is delamination between the FRP and concrete. Such phenomenon have been successfully simulated (e.g., see Elarbi, 2011). Again, after the concrete cracked, delamination started from the bottom of the concrete crack and then spreaded to both beam ends (see Fig. 3.9A and B). The simulation results of FRP delamination agree very well with the experimental tests.

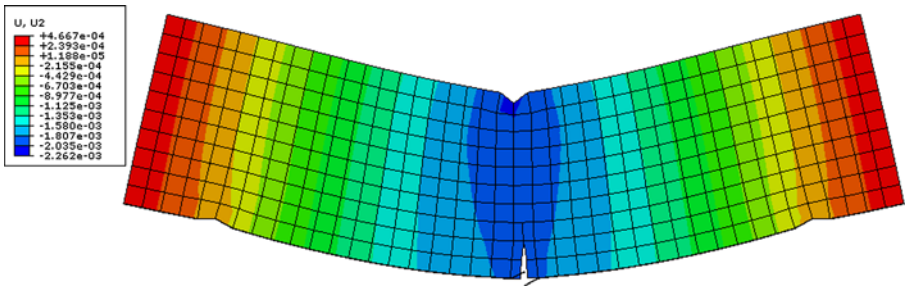

Figure 3.8 Maximum displacement of strengthened concrete beam.

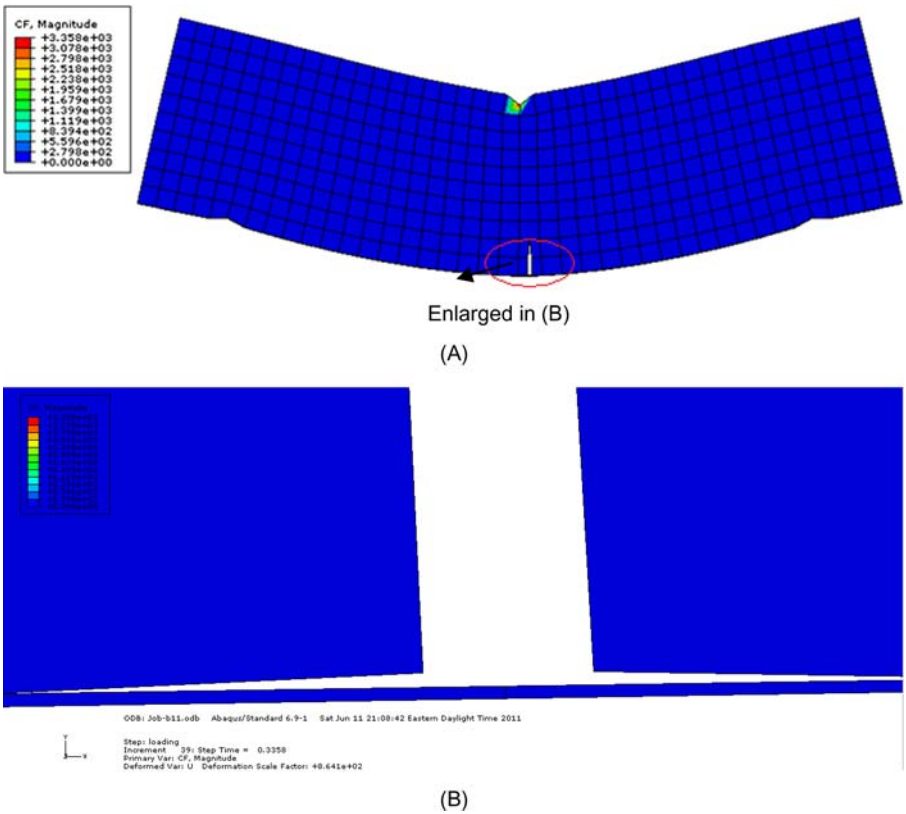

Figure 3.9 FRP delamination of strengthened concrete beam. (A) overall view, (B) enlarged view from the circled area in (A).

Design provisions

4

4.1 Introduction

In this chapter, six international design guidelines representative of the use of externally applied fiber-reinforced polymer (FRP) for strengthening reinforced concrete bridge members are reviewed. These guidelines are taken from North America, Europe, and Japan and are as follows:

1. ACI 440.2R-08—*Guide for the Design and Construction of Externally Bonded FRP Systems for Strengthening Concrete Structures* (ACI 440.2R, 2008).
2. ISIS—*Design Manual 4-FRP Rehabilitation of Reinforced Concrete Structures* (ISIS Design Manual 4, Version 2, 2008).
3. AASHTO—*Guide Specification for the Design of Bonded FRP Systems for Repair and Strengthening of Concrete Bridge Elements* (AASHTO FRP Guide, 2012).
4. *JSCE Recommendations for Upgrading of Concrete Structures with use of Continuous Fiber Sheets* (JSCE Recommendations, 2001).
5. TR55—*Design guidance for strengthening concrete structures using fibre composite materials* (TR55, 2000).
6. CNR-DT 200/2004—*Guide for the Design and Construction of Externally Bonded FRP Systems* (CNR-DT 200, 2004).

The review concerns analysis and design procedures for flexural strengthening, shear strengthening, and confinement. Section 4.2 covers flexural strengthening, where the effect of concrete strength, FRP strength, existing steel reinforcement ratio, and other parameters are considered. Section 4.3 covers shear strengthening, where continuous and spaced U-wrap, complete wrap, and two-sided strips are considered. Finally, Section 4.4 covers confinement, with consideration given to circular and square columns.

4.2 Flexural FRP strengthening of RC/PC bridge members

4.2.1 Introduction

The items considered for review and comparison in this section are based on the organization presented in ACI 440.2R-08, as it one of the most complete overviews of flexural strengthening. These specific items include:

- Strengthening limits
- Environmental reduction factors
- FRP strain limits
- Strength reduction factors

Strengthening of Concrete Structures Using Fiber Reinforced Polymers (FRP).
DOI: http://dx.doi.org/10.1016/B978-0-08-100636-8.00004-1

- Serviceability and service load limits
- Creep rupture and fatigue limits
- FRP end peeling and development length
- Flexural design approach and assumptions
- Nominal moment analysis and design procedure

The use of FRP strengthening systems can substantially enhance flexural strength. It has been documented that an increase in flexural strength from 10 to 160% can be obtained from FRP strengthening (Meier and Kaiser, 1991; Ritchie et al., 1991; Sharif et al., 1994). However, taking into account code-specified strengthening and ductility limits, strength increases of 40% are more reasonable.

4.2.2 Strengthening limits

AASHTO, ACI, and ISIS set strengthening limits to qualify a structural member for strengthening. The limits ensure the member's ability to support a specified amount of service dead and live loads in the case of loss of strengthening due to construction error, severe environmental damage, vandalism, or fire (ACI 440.2R, 2008). Other guides emphasize the need for a thorough inspection of the existing structure, and a review of plans and specifications, the as-built plans, as well as any repair/maintenance documentation of the structure. Unlike AASHTO, ACI, and ISIS, other guides leave the decision to strengthen a structure to the responsible agency on a case by case basis. The following paragraphs present strengthening limits specified by AASHTO, ACI, and ISIS.

4.2.2.1 AASHTO

The provisions of AASHTO are limited to concrete members with a specified compressive strength $f_c^{'}$ not exceeding 8 ksi and apply to bridge elements for which the factored resistance satisfies the following requirement (*AASHTO LRFD Bridge Specifications, 5th Edition*):

$$R_r \geq \eta_i[(DC + DW) + (LL + IM)] \tag{4.1}$$

where R_r = factored resistance; DC = load effect due to component and attachments; DW = load effect due to wearing surfaces and utilities; LL = live load effect; IM = force effect due to dynamic load allowance; η_i = load modifier calculated using the following expression:

$$\eta_i = \eta_D \eta_R \eta_I \geq 0.95 \tag{4.2}$$

where

η_D = a factor relating to ductility;
≥1.05 for nonductile components and connections;
=1.00 for conventional designs and details complying with the AASHTO LRFD Specifications;

≥0.95 for components and connections for which additional ductility-enhancing measures have been specified beyond those required;
For all other limit states: $\eta_D = 1.00$.
η_R = a factor relating to redundancy;
≥1.05 for nonredundant members;
=1.00 for conventional levels of redundancy;
≥0.95 for exceptional levels of redundancy;
For all other limit states: $\eta_R = 1.00$.
η_I = a factor relating to operational classification;
≥1.05 for critical or essential bridges;
=1.00 for typical bridges;
≥0.95 for relatively less important bridges;
For all other limit states: $\eta_I = 1.00$.

Note that the resistance of components and connections is determined, in many cases, on the basis of inelastic behavior (i.e., ultimate strength), although the force effects are determined by using elastic analysis. This inconsistency is common to many specifications, and allows for substantial simplification of the structural analysis and thus design process.

4.2.2.2 ACI 440.2R-08

Similar to AASHTO, ACI sets limits to qualify a structure for strengthening. Here, two conditions must be met. The first condition is expressed by Eq. (4.3) (ACI Eq. 9.1) to ensure the structure's ability to sustain a minimum specified load after loss of strengthening. Eq. (4.3) states that the existing structural design capacity must equal or exceed the new service dead load by at least 10%, and must have the ability to support at least 75% of the new service live loads. For cases where the live load is likely to be sustained on the structure over a significant period time, such as in library stacks or other heavy storage areas, the structure should be capable of supporting 100% of the live load, per Eq. (4.4).

$$(\phi R_n)_{\text{existing}} \geq (1.1S_{DL} + 0.75S_{LL})_{\text{new}} \qquad (4.3 - \text{ACI Eq. 9.1})$$

$$(\phi R_n)_{\text{existing}} \geq (1.1S_{DL} + 1.00S_{LL})_{\text{new}} \qquad (4.4)$$

To be considered for strengthening a structural member must also meet the condition expressed by Eq. (4.5) (ACI Eq. 9.2), which ensures the structure is able to sustain load for the duration of its fire rating in the case of fire. The quantity $R_{n\theta}$ represents the nominal strength at elevated temperature in accordance with the guidelines of ACI 216R (ACI 216R-1989) or through testing. Fire scenarios considered should be in accordance with ASTM E119 (ASTM E119). The $R_{n\theta}$ value is to be computed for the structure's fire rating without considering the strength contribution from FRP. Fig. 4.1 shows the required minimum relationship between $R_{n\theta}$ and the desired service live load, for various levels of existing dead load.

$$(R_{n\theta})_{\text{existing}} \geq S_{DL} + S_{LL} \qquad (4.5 - \text{ACI Eq. 9.2})$$

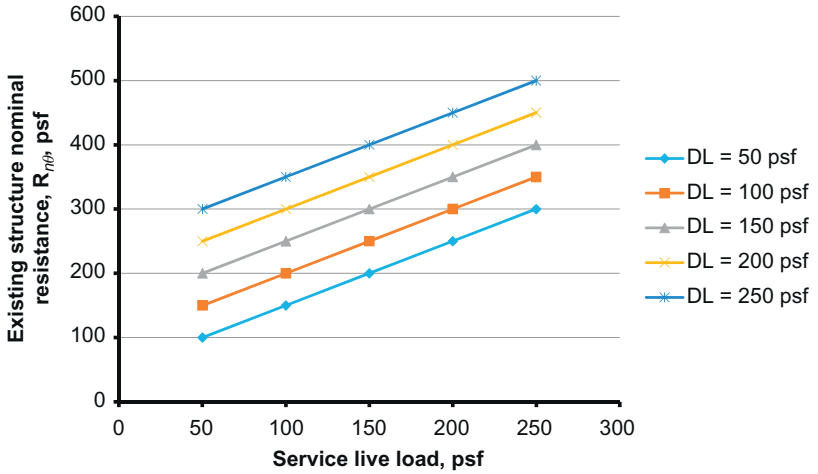

Figure 4.1 ACI strengthening limits at elevated temperatures.

4.2.2.3 ISIS

ISIS Design Manual 4 (Canada) recommends that an existing structure have the capacity to support dead loads and at least 50% of its live loads to qualify for strengthening (note although ISIS describes the requirement, it does not provide an explicit expression). The ISIS condition for strengthening may be expressed in a manner similar to that of ACI, as presented by Eq. (4.6).

$$(\phi R_n)_{\text{existing}} \geq (1.0\, S_{DL} + 0.5\, S_{LL})_{\text{new}} \tag{4.6}$$

The ISIS condition given above is specific to the S6-06 Canadian bridge code (CSA-S6-06, 2006). The live load factor of 0.5 serves as a minimum limit, but ISIS notes that it is subject to increase.

4.2.2.4 Other codes

The UK Concrete Society Standard TR55 offers no specific quantitative expression as a set criterion to qualify a structure for strengthening. However, it states that the decision to strengthen should be guided by a careful assessment process that is independent of structure type and based on rigorous criteria and sound engineering judgment. TR55 refers to TR54—*Diagnosis of deterioration in concrete structures* (TR54, 2000) and the Institution of Structural Engineers' *Appraisal of Existing Structures* (1996) for assistance in evaluating the condition of the structure.

Italy's CNR presents factors to consider that insure the durability of the member to be strengthened, while JSCE offers no specific quantitative expression or condition to serve as set criterion to qualify a structure for strengthening.

4.2.2.5 Summary

To illustrate the difference between the above strengthening limits, consider a case where the new service dead load (S_{DL}) is to be 50 psf and the new service live load (S_{LL}) is to be 140 psf. In this case, ACI limits strengthening to members that can support a minimum existing capacity of 160 psf, and, if fire is considered, the member must be able to sustain 190 psf. In contrast the ISIS minimum load capacity is 120 psf.

Fig. 4.2 presents a comparison of ACI, AASHTO, and ISIS strengthening limits. Note that ACI offers two scenarios, one for sustained live loads (generally not applicable to most bridges), and another for a typical transient live load. From the graph, it can be seen that AASHTO and ACI adopt similar limits for strengthening while ISIS is less conservative. The ACI fire endurance limit appears similar to the exiting strengthening limit provided by of AASHTO. Therefore no special fire endurance condition appears needed and AASHTO provisions are recommended for use.

In summary, AASHTO and ACI have similar strengthening limits, where ISIS allows strengthening at a lower threshold of existing structure strength. As the LL/DL ratio increases, with differences increasing significantly while the remaining codes do not quantify strengthening limits.

4.2.3 Environmental reduction factors

Environmental factors are applied to FRP material properties to account for degradation in exposure conditions, as a function of exposure as well as FRP material and application.

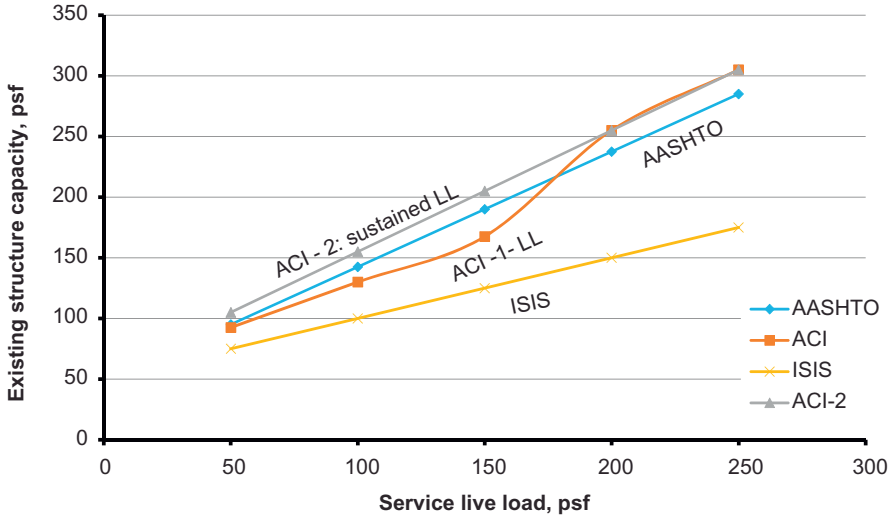

Figure 4.2 FRP strengthening limits for different codes (with fixed dead load of 50 psf).

4.2.3.1 ACI

ACI indicates that the values presented in Table 4.1 (ACI Table 9.1) are conservative and based on the relative durability of each fiber type.

4.2.3.2 CNR

The CNR code (Italy) recommends an environmental conversion factor η_a with values identical to those presented in the ACI standards above. The factor η_a is used to determine the maximum FRP design strain, ε_{fd}, which is also a function of the characteristic rupture strain of the FRP reinforcement (ε_{fk}), the maximum strain of the FRP before debonding (ε_{fdd}), and a partial safety factor for FRP rupture (γ_f).

$$\varepsilon_{fd} = \min\left\{\eta_a \frac{\varepsilon_{fk}}{\gamma_f}, \varepsilon_{fdd}\right\} \tag{4.7}$$

Generally, ε_{fdd} is the minimum governing value. Therefore the environment factor usually does not govern the design. See Table 4.2 for values of η_a (CNR Table 3.4).

Table 4.1 Environmental reduction factors

Exposure conditions	Fiber type	Environmental reduction factor, C_E
Interior exposure	Carbon	0.95
	Glass	0.75
	Aramid	0.85
Exterior exposure (bridges, piers, and unenclosed parking garages)	Carbon	0.85
	Glass	0.65
	Aramid	0.75
Aggressive environment (chemical and wastewater treatment plants)	Carbon	0.85
	Glass	0.50
	Aramid	0.70

Table 4.2 Environmental conversion factor, η_a

Exposure conditions	Type of fiber/resin	η_a
Internal	Glass/epoxy	0.75
	Aramid/epoxy	0.85
	Carbon/epoxy	0.95
External	Glass/epoxy	0.65
	Aramid/epoxy	0.75
	Carbon/epoxy	0.85
Aggressive environment	Glass/epoxy	0.50
	Aramid/epoxy	0.70
	Carbon/epoxy	0.85

4.2.3.3 ISIS

ISIS does not directly specify an environmental reduction factor. Rather, ISIS considers "material resistance factors," which include an environmental reduction factor along with other partial safety factors combined in a single factor. ISIS presents two sets of factors depending on the code used; one for bridges and another for buildings. In this document, greater consideration is given to the Canadian bridge code S6-06 (CSA-S6-06, 2006) recommendations. Factors are developed based of several criteria including type of material, type of manufacturing process, and other durability and environmental considerations, as shown in Table 4.3 (ISIS Table 4.3.4). Note that the reduction factor specific to pultruded carbon fiber-reinforced plastic (CFRP) (hand applied wet lay-up) is 0.56, which is considerably conservative compared to AASHTO's 0.85 reduction factor.

4.2.3.4 TR55

The TR55 gives no explicit environmental factors. However, additional safety factors are used for FRP depending on the type and manufacturing process; these are discussed under the strength reduction factors section in this chapter.

4.2.3.5 JSCE

JSCE recommends using suitable reduction factors for environmental effects, and refers to several Japanese standards for further reference, including, *The Standard Specifications for Design and Construction of Concrete Structures* (1996), Proposed Specification for Durability Design of Concrete Structures, 1995 (limited to new construction), and *Guidelines for Maintenance of Concrete Structures* (1995). However, these guides were not available in English translation at the time of preparing this book.

Table 4.3 Material resistance factors

Material (installation process)	Bridges	Buildings
Pultruded aramid FRP (NSMR)	$\phi_{FRP} = 0.60$	–
Pultruded aramid FRP (externally bonded plate)	$\phi_{FRP} = 0.50$	$\phi_{FRP} = 0.75$
Aramid FRP sheet (hand applied wet lay-up)	$\phi_{FRP} = 0.38$	$\phi_{FRP} = 0.75$
Pultruded carbon FRP	$\phi_{FRP} = 0.75$	$\phi_{FRP} = 0.75$
Carbon FRP sheet (hand applied wet lay-up)	$\phi_{FRP} = 0.56$	$\phi_{FRP} = 0.75$
Pultruded glass FRP	$\phi_{FRP} = 0.65$	$\phi_{FRP} = 0.75$
Glass FRP sheet (hand applied wet lay-up)	$\phi_{FRP} = 0.49$	$\phi_{FRP} = 0.75$
Concrete	$\phi_C = 0.75$	$\phi_C = 0.60$
Steel (passive reinforcement)	$\phi_S = 0.95$	$\phi_S = 0.85$
Steel (prestressing tendons)	$\phi_P = 0.95$	$\phi_P = 0.90$

4.2.3.6 AASHTO

AASHTO CFRP Standards (AASHTO FRP Guide, 2012) have no consideration for dedicated environmental reduction factors. However, *AASHTO LRFD Bridge specifications for GFRP-Reinforced Concrete Bridge Decks and Traffic Railings* (2009) recommends environmental reduction factors for GFRP bars. The recommended factors for embedded GFRP bars are applicable when concrete is exposed to earth and weather (see Table 4.4).

4.2.3.7 Summary

In summary, ACI offers the most comprehensive coverage of environmental factors presented in Table 4.1 (ACI Table 9.1). CNR offers identical factors to ACI, but they are rarely incorporated in design since the condition to apply them (ε_{fd}) does not usually govern the design. Fig. 4.3 presents a comparison of environmental reduction factors for ACI, CNR, and AASHTO (GFRP).

4.2.4 FRP strain limits

4.2.4.1 ACI

ACI sets limits to FRP strain in a strengthened section to prevent debonding cracks from developing. Eqs. (4.8) and (4.9) (ACI Eq. 10.2) below limit FRP strain at 90% of ε_{fu} or lower. The expressions are modifications of the work by

Table 4.4 AASHTO environmental reduction factors for GFRP bars

Exposure condition	Environmental reduction factor, C_E
Concrete not exposed to earth and weather Concrete exposed to earth and weather	0.80 0.70

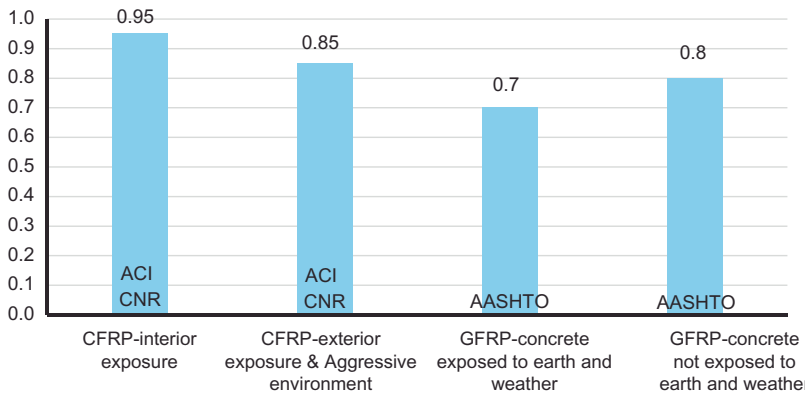

Figure 4.3 Comparison of environmental reduction factors.

Teng et al. (2001, 2004) and are based on measured FRP strain at debonding cracks of flexural test samples.

$$\varepsilon_{fd} = 0.083\sqrt{\frac{f'_c}{nE_f t_f}} \le 0.9\varepsilon_{fu} \text{ in. in. - lb units} \qquad (4.8 - \text{ACI Eq. } 10.2)$$

$$\varepsilon_{fd} = 0.41\sqrt{\frac{f'_c}{nE_f t_f}} \le 0.9\varepsilon_{fu} \text{ in. SI units} \qquad (4.9 - \text{ACI Eq. } 10.2)$$

The ACI code notes that transverse clamping of flexural samples has shown to improve bond behavior relative to that predicted by Eq. (4.8) (ACI Eq. 10.2). Provision of transverse clamping FRP U-wraps along the length of flexural FRP reinforcement has been observed to increase FRP debonding strain by up to 30% (CECS-146, 2003) prior to debonding failure.

To illustrate the condition expressed in Eq. (4.8), assume a 4000 psi concrete beam strengthened with three plies of BASF MBRACE CF130 CFRP, where the thickness per ply is 0.0065 in. Further assuming tensile properties are: ultimate tensile strength, $f^*_{fu} = 550$ ksi; tensile modulus, $E_f = 33{,}000$ ksi; ultimate rupture strain, $\varepsilon^*_{fu} = 1.67\%$; nominal thickness, $t_f = 0.0065$ in./sheet. The application of Eq. (4.8) (ACI Eq. 10.2) results in FRP strain ε_{fd} being limited to 0.0065 in./in., which is 46% of the ultimate FRP strain ε_{fu} value of 0.0142 in./in (0.0167 reduced by the environmental factor of 0.85).

4.2.4.2 ISIS

ISIS considers debonding and anchorage failures as premature tension failures that require evaluation to reduce ε_{FRP} on a case by case basis through testing. However, the Code specifies a maximum value of $\varepsilon_{\text{FRP}} = 0.006$ as specified by the building code S806-02 (CAN/CSA S806-02, 2002).

4.2.4.3 AASHTO

AASHTO requires that the strain developed in the FRP reinforcement at the ultimate limit state shall be equal to or greater than 2.5 times the strain in the FRP reinforcement at the point where the steel tension reinforcement yields (Eq. (4.10)). This limitation is present to ensure that the tension steel reinforcement yields before the point of incipient debonding of the externally bonded FRP reinforcement, thereby enabling the development of a ductile mode of flexural failure.

$$\frac{\varepsilon^u_{frp}}{\varepsilon^y_{frp}} \ge 2.5 \qquad (4.10)$$

With a maximum useable strain of 0.005 at the FRP reinforcement/concrete interface, the maximum strain developed in the FRP reinforcement is (Eq. (4.11)):

$$\varepsilon = 0.005 - \varepsilon_{bo} \tag{4.11}$$

where ε_{bo} is the initial tensile strain at the bottom concrete surface as a result of the moment due to dead load (the existing tensile strain prior to FRP installation).

4.2.4.4 TR55

For strain limits, TR55 refers to Neubauer and Rostasy (1997), who suggest an ultimate limit of $0.5\varepsilon_y$ or half the ultimate plate strain, which for the materials tested was 0.75%. TR55 further suggests that other research has suggested somewhat lower limits, in the order of 0.6% for sagging moments and 0.4% for hogging moments. However, practical experience in the United Kingdom suggests that the higher strain limits are more reasonable. On this basis, TR55 recommends that, to avoid debonding failure, the strain in the FRP should not exceed 0.8% when the applied loading is uniformly distributed, and 0.6% if combined high shear forces and bending moments are present, such as where the load is concentrated at a point and at hogging regions close to supports.

4.2.4.5 CNR

Within CNR the maximum FRP tensile strain, ε_{fd}, is calculated as follows:

$$\varepsilon_{fd} = \min\left\{\eta_a.\frac{\varepsilon_{fk}}{\gamma_f}, \varepsilon_{fdd}\right\} \tag{4.12}$$

where ε_{fk} = characteristic value of the adopted strengthening system; η_a = environmental factor; γ_f = partial factor for FRP rupture; ε_{fdd} = maximum strain due to intermediate debonding.

The above definitions are further explained in the CNR code.

4.2.4.6 JSCE

JSCE does not provide maximum FRP strain limit recommendations. In this context, JSCE cites the work to establish criteria of peeling of continuous fiber sheets by Wu and Niu (2000). The code describes the work as ongoing research and does not explicitly present research findings. JSCE uses Eq. (4.35) (JSCE Eq. 6.4.1) to set the FRP stress limit σ_f as a function of interfacial fracture energy G_f, which is determined from bond strength tests of FRP sheets to concrete. Refer to Eq. (4.35) under Article 4.2.7.6 of this chapter for further description.

4.2.4.7 Summary

In summary, three standard guidelines have fixed strain limit values, AASHTO has a limit of 0.005 at the concrete/FRP interface, ISIS has a value of 0.006 (for bridges), and the TR55 strain value is 0.008 for uniform load application and 0.006 for combined high shear/bending applications. The effect of f'_c and the number of FRP plies are evaluated on these code limits, as presented in Fig. 4.4. Here, f'_c was varied from 3 to 8 ksi while the area of FRP plies is kept at 0.3315 in.^{2} (three plies of BASF MBrace CF130). In Fig. 4.5 the number of plies is varied from 1 to 5

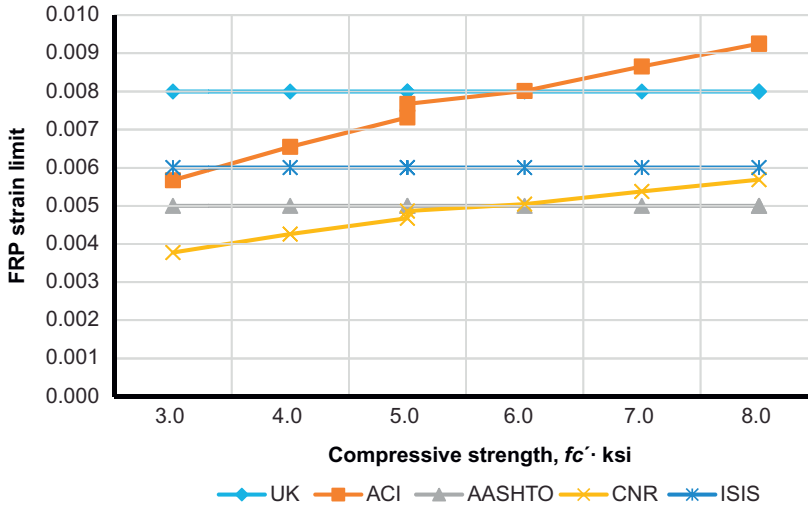

Figure 4.4 Effect of concrete compressive strength f'_C on FRP strain limits (number of FRP layers = 3, area = 0.33 in.^{2}).

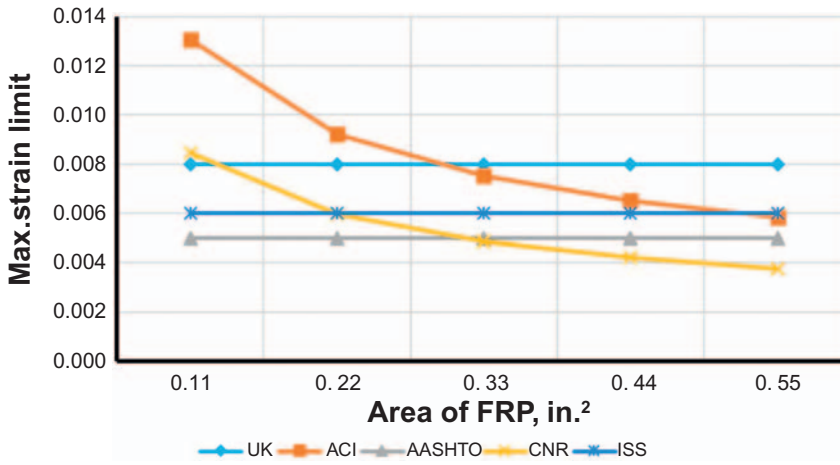

Figure 4.5 Effect of amount of FRP strengthening on FRP strain limits, f'_c = 5.5 ksi.

(area changes from 0.11 to 0.55 in.^{2}) while maintaining f'_c at 5500 psi. Figs. 4.4 and 4.5 show the effect of these changes for various codes. From the graphs, it can be seen that the codes with fixed FRP strain limits are independent of changes of f'_c or the amount of FRP strengthening used. Only ACI and CNR exhibit an increase in the strain limit with an increase in f'_c, and a reduction in strain limit when increasing the amount of FRP used. ACI appears to allow a maximum strain in excess of 0.009 at $f'_c = 8$ ksi. While this may appear less conservative, other factors such as environmental and strength reduction factors are used in combination with this limit. Note that ACI and CNR limits increase approximately linearly as f'_c increases while the limits decrease nonlinearly as FRP area increases.

The two graphs above (Figs. 4.4 and 4.5) show that AASHTO's approach is relatively conservative and is similar to the results of ISIS, which is also relatively conservative (note that both of these codes are bridge codes, while the other codes are generally applicable). At 1 and 2 FRP plies, ACI reaches a relatively high strain limit value of 0.013. As FRP area increases, most guides converge between 0.004 and 0.006, except for the TR55 limit of 0.008. In general, ACI maximum strain limits are relatively unconservative at lower levels of FRP strengthening as well as at higher values of f'_c.

4.2.5 Strength reduction factors

4.2.5.1 ACI

ACI follows the approach of ACI 318-05 philosophy in evaluating the strength reduction factor ϕ to promote ductile behavior. According to ACI 318-05 the strength reduction factor ϕ is applicable for steel grades with yield stress up to 60 ksi. The factor is a general factor applied to concrete, steel, and FRP equally. A maximum value of 0.9 is used when steel strain $\varepsilon_t \geq 0.005$ at ultimate capacity (i.e., when concrete has a strain value of 0.003 in compression), which represents a tension controlled failure characterized by ductile behavior. A minimum value of 0.65 is used when $\varepsilon_t \leq \varepsilon_{sy}$, signifying a compression controlled failure (nonductile behavior). ϕ values follow a linear transition between the two extremes (see Eq. (4.13)). ϕ is applied to all moment components equally; it is considered a global factor.

$$\phi = \begin{cases} 0.90 & \text{for } \varepsilon_t \geq 0.005 \\ 0.65 + \dfrac{0.25(\varepsilon_t - \varepsilon_{sy})}{0.005 - \varepsilon_{sy}} & \text{for } \varepsilon_{sy} < \varepsilon_t < 0.005 \\ 0.65 & \text{for } \varepsilon_t \leq \varepsilon_{sy} \end{cases} \qquad (4.13 - \text{ACI Eq.10.5})$$

As observed, the values for ϕ depend on the steel strain level. Another recommended reduction factor specific to the FRP moment contribution is ψ_f, with a value of 0.85. The combined reduction factor for the FRP moment contribution is $\phi \times \psi_f$. ψ_f is a reduction factor to account for the uncertainty in the FRP-generated moment strength. Uncertainty is attributed to variation in material properties, section

dimensions, and possible different failure modes observed for FRP-strengthened members (delamination of FRP reinforcement). The reduction factor is determined based on a statistical evaluation of variability in mechanical properties, predicted versus full-scale test results, and field applications. The FRP-related reduction factors are calibrated to produce nominal reliability indices (β) typically above 3.5. However, reliability indices between 3.0 and 3.5 can be encountered as well (Nowak and Szerszen, 2003; Szerszen and Nowak, 2003).

Research conducted by Okeil et al. (2007) presents the development of a resistance model for reinforced concrete bridge girders flexurally strengthened with externally bonded CFRP laminates. The resistance model was used to calculate the reliability index of CFRP strengthened cross-sections, and it was found that the reliability index for CFRP strengthened sections is greater than that for RC sections. This is primarily attributed to the low coefficient of variation for CFRP ultimate strength, which is lower than the coefficient of variation of the strength of steel or concrete. However, although reliability index improves with addition of CFRP, the flexural resistance of RC members strengthened with FRP is recommended to be reduced by 0.85 over a similar nonstrengthened member. This recommendation is based on the recognition of the brittle nature of CFRP behavior.

4.2.5.2 ISIS

As noted earlier, ISIS combines various factors into "material resistance factors" which serve to account for resistance uncertainties as well as environmental reduction factors. ISIS presents two sets of factors, one for bridges and another for buildings. The factors provided are also classified by the FRP installation process, as shown in Table 4.3 (ISIS Table 3.4). The table presents material resistance factors for concrete, steel, and several FRP schemes. The ISIS ϕ factors are applied separately to different materials.

The ISIS reduction value for carbon sheets using a wet lay-up is 0.56 for bridge applications and 0.75 for building applications. The ISIS low values are partially due to the fact that they represent the multiplication of three equivalent factors in ACI, namely C_E, ψ, and ϕ. ISIS refers to clauses in the S6-06 bridge code (Clauses 16.5.3 and 8.4.6) (CSA-S6-06, 2006) for further reference.

Table 4.5 compares the resulting CFRP factor for a hand applied wet lay-up between ACI and ISIS, the latter of which results in a more conservative value.

Table 4.5 ISIS and ACI reduction factor comparison

Type	ACI	ISIS
Environmental exterior exposure, C_E	0.85	
Additional reduction factor, ψ	0.85	
ϕ	0.90	
Equivalent factor	0.65	0.56

4.2.5.3 AASHTO

AASHTO uses a fixed-value strength reduction factor ϕ_{frp} with a value of 0.85, for externally applied FRP. Note that the AASHTO strain limit is 0.005 for FRP, which limits the use of FRP to flexural members which will have relatively ductile failure conditions. In contrast, for comparison, in the case of internal GFRP bars used to reinforce bridges, AASHTO specifies the following values for ϕ (Fig. 4.6):

$$\phi = \begin{cases} 0.55 & \text{for } p_f \le p_{fb} \\ 0.3 + .025\dfrac{p_f}{p_{fb}} & \text{for } p_{fb} < p_f < 1.4p_{fb} \\ 0.65 & \text{for } p_{fb} \ge 1.4p_{fb} \end{cases} \tag{4.14}$$

In which

$$\rho_{fb} = 0.85\beta_1 \frac{f'_c}{f_{fd}} \frac{E_f \varepsilon_{cu}}{E_f \varepsilon_{cu} + f_{fd}} \tag{4.15}$$

where ρ_f = GFRP reinforcement ratio = A_f/bd; β_1 = factor taken as 0.85 for concrete strength not exceeding 4 ksi. For concrete strengths exceeding 4 ksi, β_1 is reduced at a rate of 0.05 for each 1 ksi of strength in excess of 4 ksi, except that β_1 is not be taken less than 0.65; f'_c = specified compressive strength of concrete, ksi; f_{fd} = design tensile strength of GFRP bars considering reduction for service environment, ksi; E_f = modulus of elasticity of GFRP reinforcement, ksi; ε_{cu} = ultimate strain in concrete; ρ_{fb} = GFRP reinforcement ratio producing balanced strain conditions.

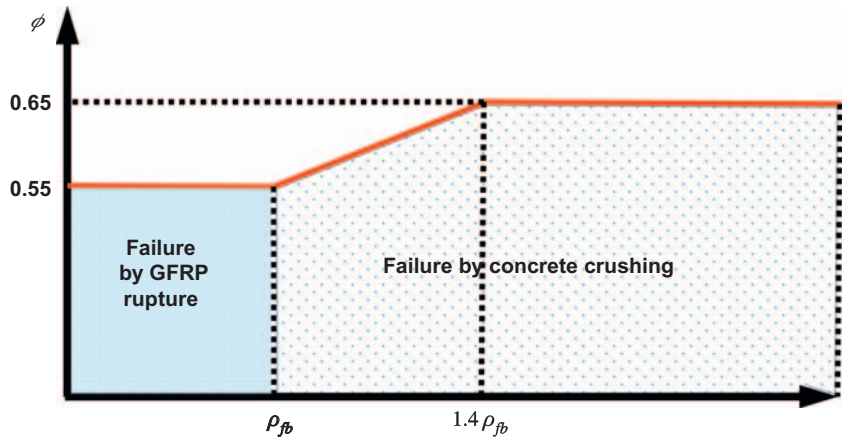

Figure 4.6 Strength reduction factor for GFRP.
Adapted from: AASHTO GFRP manual.

In ASSHTO GRRP, resistance factors ϕ for shear are to be taken as 0.75. If concrete strength is higher than specified, the member can fail due to GFRP rupture. To find a transition between two values of ϕ, a section controlled by concrete crushing is defined as a section in which $\rho_f \geq 1.4\ \rho_{fb}$, and a section controlled by GFRP rupture is defined as one in which $\rho_f \leq \rho_{fb}$.

4.2.5.4 TR55

In TR55 (UK) the characteristic material properties are divided by appropriate partial safety factors (γ_{mf}, γ_{mm}, γ_{mE}) to determine the appropriate design values. γ_{mf} is a factor based on the type of material used; γ_{mm} relates to the strengthening system and method of application, and γ_{mE} addresses the effect of material stiffness deterioration with time. The product of the three factors, (γ_{mf}, γ_{mm}, γ_{mE}), determines the final safety factor. Thus

$$f_{mfd} = \frac{f_{fk}}{\gamma_{mf} \cdot \gamma_{mm} \cdot \gamma_{mE}} \qquad (4.16 - \text{TR55 Eq. 5.2})$$

where the values of (γ_{mf}, γ_{mm}, γ_{mE}) are determined from Tables 4.6–4.8 (TR55 Tables 5.2, 5.3, and 5.4).

The product ($\gamma_{mf} \cdot \gamma_{mm}$), labeled γ_{mF}, is a partial safety factor applied to the characteristic mechanical properties of the FRP system (Eq. (4.17)). The partial safety factor γ_{mF} is a function of the type of FRP material (γ_{mf}), and the manufacturing process (γ_{mm}).

$$\gamma_{mF} = \gamma_{mf} \cdot \gamma_{mm} \qquad (4.17 - \text{TR55 Eq. 5.3})$$

The guide provides examples of how Eq. (4.17) (TR55 Eq. 5.3) is applied using the above tables. For example, for a carbon fiber pultruded plate, strength measured on the plate, $\gamma_{mF} = 1.4 \times 1.1 = 1.54$; for an aramid sheet, strength measured on in situ specimens, $\gamma_{mF} = 1.5 \times 1.4 = 2.1$; for a glass prefabricated shell, made by hand lay-up, $\gamma_{mF} = 3.5 \times 1.4 = 4.9$.

In order to facilitate comparison of TR55 partial safety factors to strength reduction factors of other codes, the reciprocal values, ($1/x$), for TR55 are considered as an equivalent reduction factors. Fig. 4.7 presents the equivalent reduction factors corresponding to γ_{mf} values in Table 4.6. Fig. 4.8 presents equivalent reduction

Table 4.6 Example partial safety factors for strength at ultimate limit state (TR55 Table 5.2)

Material	Partial safety factor, γ_{mf}
Carbon FRP	1.4
Aramid FRP	1.5
Glass FRP	3.5

Table 4.7 Recommended partial safety factors for manufactured composites (TR55 Table 5.3)

Type of system (and method of application or manufacture)	Additional partial safety factor, γ_{mm}
Plates	
Pultruded	1.1
Prepreg	1.1
Performed	1.2
Sheets or tapes	
Machine-controlled application	1.1
Vacuum infusion	1.2
Wet lay-up	1.4
Prefabricated (factory-made) shell	
Filament winding	1.1
Resin transfer molding	1.2
Hand lay-up	1.4
Hand-held spray application	2.2

Table 4.8 Partial safety factor for modulus of elasticity at ultimate (TR55 Table 5.4)

Material	Factor of safety, γ_{mE}
Carbon FRP	1.1
Aramid FRP	1.1
Glass FRP	1.8

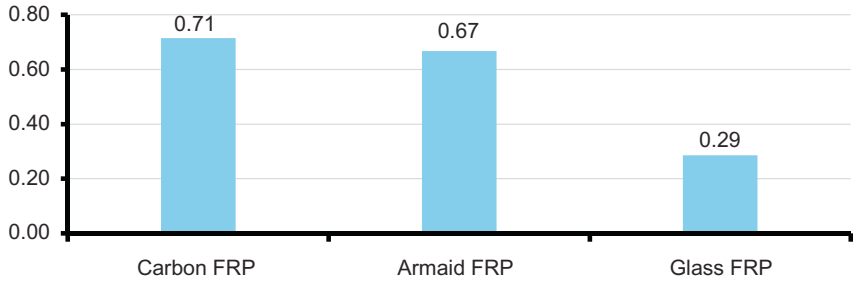

Figure 4.7 Equivalent reduction factors corresponding to material partial safety factors, γ_{mf}, for ultimate strength limit state.

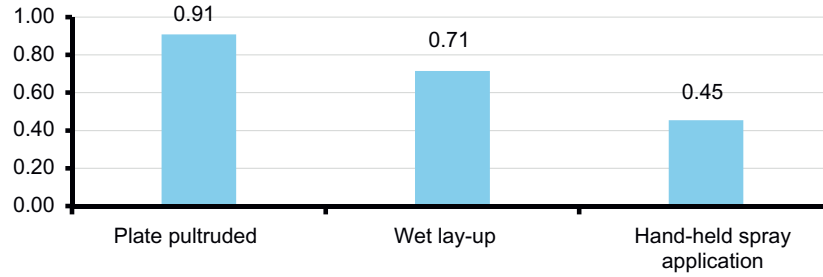

Figure 4.8 Equivalent reduction factors corresponding to manufacturing process partial safety factors, γ_{mm}, for select processes.

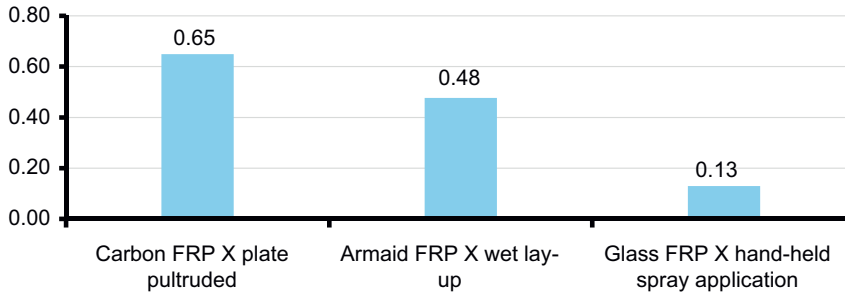

Figure 4.9 Equivalent reduction factors corresponding to γ_{mF} of select materials and manufacturing processes.

factor values corresponding to γ_{mm} of three select manufacturing processes from Table 4.7. Fig. 4.9 presents equivalent reduction factors corresponding to γ_{mF} calculated values discussed in the previous paragraph.

4.2.5.5 CNR

CNR specifies a partial safety factor, γ_{Rd}, that depends on the resistance model; either bending, shear, or confinement. These factors are applicable to ultimate limit states as presented in Table 4.9 (CNR Table 3-3).

Other partial factors include materials and products factors γ_m with values that depend on failure mode; either FRP rupture or FRP debonding. Values of γ_m are depending of application type; type A or type B. Type A applies to certified strengthening systems, while type B applies to uncertified strengthening systems. Certification of a strengthening system must be in accordance with CNR acceptance criteria stipulated in section 2.5 of the code (CNR-DT 200, 2004). Values of γ_m are presented in Table 4.10.

In the case of FRP wet lay-up systems, CNR considers the coefficients α_{fE} and α_{ff}. α_{fE} is a reduction factor for stiffness, while α_{ff} is a reduction factor for

Table 4.9 CNR partial safety factor, γ_{Rd}

Resistance model	γ_{Rd}
Bending/combined bending and axial load	1.0
Shear/torsion	1.2
Confinement	1.1

Table 4.10 CNR partial factor for materials and products, γ_m

Failure mode	Partial factor	Type-A application	Type-B application
FRP rupture	γ_f	1.10	1.25
FRP debonding	$\gamma_{f,d}$	1.20	1.50

FRP tensile strength which should not exceed 0.90. In design applications, CNR considers partial safety factors of 1.15, 1.60, and 1.20 for steel, concrete, and FRP, respectively. The reciprocals of the partial safety factors are considered equivalent reduction factors for steel, concrete, and FRP:

Steel equivalent reduction factor = 0.87
Concrete equivalent reduction factor = 0.63
FRP equivalent reduction factor = 0.83

4.2.5.6 Summary

FRP strength reduction factor values are near 0.85 for the majority of codes. Certain codes offer separate factors depending of the material and manufacturing process used as in the cases of ISIS (Canada) and TR55 (UK). Depending on the manufacturing process the factors considered by ISIS and TR55 are more conservative when compared to the fixed FRP reduction factor value for ASSHTO (0.85), and values considered by ACI. The multiplicative factors specified by TR55 and CNR can result in relatively large reductions in strength. The ACI resistance factor varies with the mode of failure and ductility. Depending on the application, ACI provides a more conservative strength reduction factor when compared with the fixed AASHTO factor of 0.85, but AASHTO is more restrictive with maximum FRP design strain. Table 4.11 summarizes the FRP reduction factors specified by various codes. Table 4.12 summarizes commonly used reduction factors of concrete, steel, and CFRP. Blank rows in the tables indicate nonapplicable cases for the code considered.

Table 4.11 Strength reduction factors with and without environmental factor

Code	Application	Reduction factor including environmental factor	Reduction factor excluding environmental factor
ACI	Interior exposure includes C_E and ψ	0.81	0.85
	Exterior exposure includes C_E, ψ, and ϕ	0.72	
ISIS	CFRP sheet-wet lay-up	0.56	
	CFRP plate-wet lay-up	0.75	
AASHTO	Fixed value for FRP		0.85
TR55	CFRP wet lay-up sheets (equiv.)		0.65
	CFRP wet lay-up pultruded plates (equiv.)		0.83
CNR	Fixed value for FRP		0.83

Table 4.12 Reduction factor values for concrete, steel, and CFRP

	ACI	AASHTO	ISIS	UK	CNR
Steel	$0.9 \geq \phi \geq 0.65$	$1.0 \geq \phi \geq 0.65$	0.90 nonprestressed 0.95 prestressed	0.87	0.87
Concrete			0.75	0.67	0.80
CFRP	0.85	0.85	0.56 sheet-hand applied 0.75 pultruded	0.65	0.83

4.2.6 Serviceability and service load limits

4.2.6.1 ACI

For nonprestressed concrete members, ACI restricts stresses in reinforcing steel and concrete under service loads to avoid the development of inelastic deformation, especially when structures are subject to cyclic loading. The service limits for steel as well as concrete stresses are provided in Eqs. (4.18) and (4.19).

$$f_{s,s} \leq 0.80 f_y \qquad (4.18 - \text{ACI Eq. } 10.6)$$

$$f_{c,s} \leq 0.45 f'_c \qquad (4.19 - \text{ACI Eq. } 10.7)$$

Under service loads, the stress in steel can be computed using Eq. (4.20) (ACI Eq. 10.14), and the stress in the FRP strengthening system can be computed using Eq. (4.21) (ACI Eq. 10.15). The values calculated are compared to the service

stress limits found in Eqs. (4.18) and (4.19) (ACI Eqs. 10.6 and 10.7) to verify if serviceability conditions are met.

$$f_{s,s} = \frac{\left[M_s + \varepsilon_{bi} A_f E_f \left(d_f - \left(\frac{k_d}{3}\right)\right)\right](d - k_d)E_s}{A_s E_s \left(d - \left(\frac{k_d}{3}\right)\right)(d - k_d) + A_f E_f \left(d_f - \left(\frac{k_d}{3}\right)\right)(d_f - k_d)} \qquad (4.20 - \text{ACI Eq. } 10.14)$$

$$f_{f,s} = f_{s,s}\left(\frac{E_f}{E_S}\right)\frac{(d_f - k_d)}{(d - k_d)}\varepsilon_{bi} E_f \qquad (4.21 - \text{ACI Eq. } 10.15)$$

ACI does not provide references for Eqs. (4.18) and (4.19) (ACI Eqs. 10.6 and 10.7).

4.2.6.2 AASHTO

AASHTO references *AASHTO LRFD Bridge Design Specifications*, 2010, for more detail on the load combinations specific to different limit states including serviceability, strength, extreme events and fatigue. Recommended values for AASHTO service stress limits are provided in Table 4.13.

4.2.6.3 ISIS

ISIS specifies no limits on concrete stresses under service loads, but stipulates that the stress in steel reinforcement under service loads may not exceed 80% of the yield stress, which is similar to ACI limit.

4.2.6.4 TR55

TR55 references BS 8110, part 2, 1985, or BS 5400, Part 4, 1990, for crack width limits not to be exceeded under service loads. A procedure to calculate crack width is referenced to Part 2—section 3 of BS 8110, 1985. To avoid excessive deformations in bridges, the stresses in the steel reinforcement and concrete at working loads should not normally exceed $0.8f_y$ and $0.6f_{cu}$ (or 0.6 times the worst credible strength), respectively.

Table 4.13 Summary of service limit state

	ACI	AASHTO	ISIS	UK	CNR
Steel	$0.80\,f_y$	$0.80\,f_y$	$0.80\,f_y$	$0.80\,f_y$	
Concrete	$0.45\,f'_c$	$0.36\,f'_c$		$0.60\,f_{cu}$	
CFRP	$0.55\,f_{fu}$	$0.80\,f_{fu}$		0.65	$0.80\,f_{fu}$

4.2.6.5 CNR

CNR specifies that when investigating a service limit state, stresses in the FRP system shall satisfy the limitation of

$$\sigma_f \leq \eta\ f_{fk} \tag{4.22}$$

where f_{fk} = the FRP characteristic strength at failure; η = a factor for environmental effects, long-term effects, impact and explosive loadings and vandalism.

CNR also specifies that the service stress in concrete and steel must be in accordance with limits stated in the current building code (CNR-DT 200, 2004).

4.2.6.6 JSCE

According to JSCE, cracks in FRP-strengthened members are relatively more dispersed than in unstrengthened members, and accordingly, the individual crack width is reduced. In pull-out tensile strength tests of members strengthened with CFRP sheets, the crack width is proportional to the average strain of the sheet and reinforcement, and is almost independent of the concrete cover, the steel rebar diameter, the rigidity of the continuous fiber sheets, and the compressive strength of concrete. At the level just before the steel yield point, the crack width is approximately 0.3−0.7 times the width of cracks in members not bonded with FRP.

For structures with large dead loads, JSCE recommends that crack width be calculated using Eq. (7.4.1) of the *Standard Specifications for Design and Construction of Concrete Structures (Design)*, 1996. The equation proposed is identical to Eq. (4.23), but without the (0.7) multiplier.

For the specific case of large dead load, and the absence of concrete cracking prior to the application of FRP, or for structures governed by live loads, the flexural crack width may be calculated using Eq. (4.23) (JSCE Eq. C6.5.1), in which the crack width is taken as 70% of the width calculated from Eq. (7.4.1).

$$w = 0.7k[4c + 0.7(C_s - \phi)]\left[\frac{\sigma_{se}}{E_s}\left(or\ \frac{\sigma_{pe}}{E_p}\right) + \varepsilon'_{cs}\right] \qquad (4.23 - \text{JSCE Eq. C6.5.1})$$

4.2.6.7 Summary

The service stress limits for different codes are summarized in Table 4.13. The same steel limit is shared by all standards except JSCE and CNR codes. AASHTO and CNR allow the highest FRP limits, while ACI specifies the lowest.

4.2.7 Creep rupture and fatigue stress limits

4.2.7.1 ACI

According to ACI, of the available fiber types, CFRP is least affected by creep rupture. After 500,000 h which ACI roughly equates to "about 50" years (actually 57), CFRP is predicted to maintain 90% of its initial ultimate stress (Yamaguchi et al., 1997; Malvar, 1998). The values for GFRP and AFRP are 30 and 50% of the CFRP limit, respectively. Taking 0.6 as a safety factor (ACI 440.2R), the limit values for GFRP, AFRP, and CFRP are 20, 30, and 55% as shown in Table 4.14.

The tabulated limits in Table 4.14 represent fiber stress limits under service conditions $f_{f,s}$. An evaluation of $f_{f,s}$ using Eq. (4.21) must be less or equal the tabulated limit in Table 4.14.

4.2.7.2 ISIS

ISIS provisions to guard against fatigue failure include limits on the difference between maximum and minimum stresses in the steel bars to 125 MPa (CAN/CSA S6-06 bridge code, 2006). ISIS imposes limits on the service stresses providing different limits for bridges and buildings to protect against creep rupture. Table 4.15 (ISIS Table 5.1) presents these limits for AFRP, CFRP, and GFRP. ISIS limits are slightly higher than those provided by ACI since they are specific to creep rupture protection only, while the ACI limits include cyclic service loads.

4.2.7.3 AASHTO

AASHTO imposes an FRP strain limit of 0.005 and at ultimate capacity, a maximum allowable FRP strain level of 2.5 times the FRP strain at steel yield. Subjected to the fatigue load combination of the AASHTO LRFD Bridge Design

Table 4.14 ACI sustained plus cyclic service load stress limit in FRP reinforcement

Fiber type		
GFRP	**AFRP**	**CFRP**
$0.20f_{fu}$	$0.30f_{fu}$	$0.55f_{fu}$

Table 4.15 ISIS maximum stress level against creep rupture

Material	Bridges	Buildings
Aramid FRP	0.35 f_{FRPU}	0.38 f_{FRPU}
Carbon FRP	0.65 f_{FRPU}	0.60 f_{FRPU}
Glass FRP	0.25 f_{FRPU}	0.25 f_{FRPU}

Specifications, the maximum compression strain in the concrete, ε_c, the strain in the steel reinforcement, ε_s, and the strain in the FRP reinforcement, ε_{frp}, are given as:

$$\varepsilon_c \leq 0.36\frac{f'_c}{E_c} \tag{4.24}$$

$$\varepsilon_s \leq 0.8\varepsilon_y \tag{4.25}$$

$$\varepsilon_{frp} \leq \eta\varepsilon^u_{frp} \tag{4.26}$$

where ε^u_{frp} = the characteristic value of the tensile failure of FRP reinforcement.

By limiting the maximum strain in the concrete to the above value, the stress range in the concrete is kept less than $0.40f'_c$. Limiting the steel reinforcement strain under service load to 80% of yield strain is equivalent to the recommendation of ACI Committee 440, where the stress in the reinforcing steel under service load is limited to 80% of yield stress (Eq. (4.18)). This recommendation is based on the work of El-Tawil et al. (2001), Shahawy and Beitelman (1999, 2000), and Barnes and Mays (2000). It was found that concrete strengthened with CFRP and subjected to cyclic fatigue leads to stress results similar to those obtained for static creep, and limiting the service load stress of steel bars in reinforced concrete beams strengthened with CFRP to $0.8f_y$ is adequate.

Strain limits on the FRP reinforcement are also specified to avoid creep rupture. AASHTO suggests that the creep rupture reduction factor, η should be based on experimental data and in the absence of such data, a value of $\eta = 0.8$, 0.5, and 0.3 shall be used for carbon, aramid, and glass fiber, respectively. However, FRP strains investigated under the service load combination are usually sufficiently low that creep rupture of the FRP is typically not of concern. Note that AASHTO, FIB 14 (Swiss code), and ACI base the selection of η values on the work of Yamaguchi et al. (1997) and Malvar (1998), although ACI recommends using 0.9 rather than 0.8 for carbon.

Per AASHTO, the investigation of material strain limits can be done as follows. If the section cracking moment M_{cr} is less than the moment caused by the fatigue load combination, the portion of the concrete in tension is neglected and a transformed section of the cracked, FRP and steel-reinforced section is developed. The cracking moment can then be evaluated per Eq. (4.27).

$$M_{cr} = f_r\frac{I_g}{t} \tag{4.27}$$

where

$$f_r = 0.24\sqrt{f'_c} \tag{4.28}$$

From the FRP reinforcement load-strain data, E_{frp} can be evaluated.

$$E_{frp} = \frac{f_{frp}}{\varepsilon_{frp}} = \frac{N_b/t_{frp}}{\varepsilon_{frp}} \tag{4.29}$$

$$\text{Modular ratio for concrete:} \quad n_c = \frac{E_c}{E_{frp}} \tag{4.30}$$

$$\text{Modular ratio for steel} \quad n_s = \frac{E_s}{E_{frp}} \tag{4.31}$$

Once the transformed section is developed and the neutral axis location (z) is identified, strains in the concrete, steel reinforcement and FRP due to fatigue can then be calculated using Eqs. (4.32)−(4.34).

$$\varepsilon_c = \frac{M_f z}{I_T E_{frp}} \tag{4.32}$$

$$\varepsilon_s = \frac{M_f (d - z)}{I_T E_{frp}} \tag{4.33}$$

$$\varepsilon_{frp} = \frac{M_f (h + t_{frp} - z)}{I_T E_{frp}} \tag{4.34}$$

4.2.7.4 CNR

CNR expresses the effect of fatigue, cyclic loading and continuous (creep) stress by use of a conversion factor for long term effects, η_1. Values for η_1 are provided in Table 4.16 for several FRP systems.

4.2.7.5 TR55

TR55 recommends that checks for fatigue should be carried out in accordance with the recommendations in Clause 4.7 of BS 5400, *Steel, Concrete, and Composite Bridges-Part 4, 1990*, and the stress range in the FRP should be limited to the appropriate values given in Table 4.17 (TR55 Table 6.1).

Table 4.16 Conversion factor for long term effects for several FRP systems for service limit states

Loading mode	Type of fiber/resin	η_1
Continuous (creep and relaxation)	Glass/epoxy	0.30
	Aramid/epoxy	0.50
	Carbon/epoxy	0.80
Cyclic (fatigue)	All	0.50

Table 4.17 Maximum stress range as a percentage of the design ultimate strength

Material	Stress range (%)
Carbon FRP	80
Aramid FRP	70
Glass FRP	30

Table 4.18 Maximum stress range under service loads to avoid stress rupture for different materials

Material	Maximum range (%)
Carbon FRP	65
Aramid FRP	40
Glass FRP	55

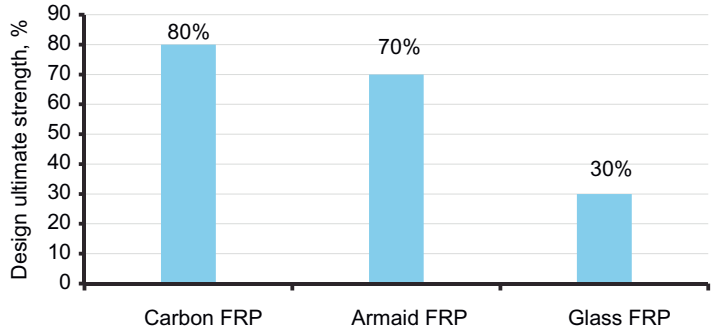

Figure 4.10 TR55 maximum stress range as a proportion of the design ultimate strength.

TR55 stipulates that a stress rupture of the FRP may occur under sustained service loads. The code recommends that the maximum stress in the FRP at service loads, as a proportion of the design strength, should not exceed the values given in Table 4.18 (TR55 Table 6.2).

Figs. 4.10 and 4.11 are visual representations of Tables 4.17 and 4.18, respectively. Fig. 4.10 presents the permitted maximum service stress range as a percentage of the ultimate strength of the FRP material to protect against fatigue failure for bridges exposed to repeated live loads. Fig. 4.11 presents the maximum service stress to protect against stress rupture. From the data, carbon fibers perform best under fatigue loads and to resist creep rupture. Aramid fiber, while performs well under fatigue load conditions, it performs poorly to protect against creep rupture. Glass fiber performs poorly under fatigue loading, but moderately resists creep rupture.

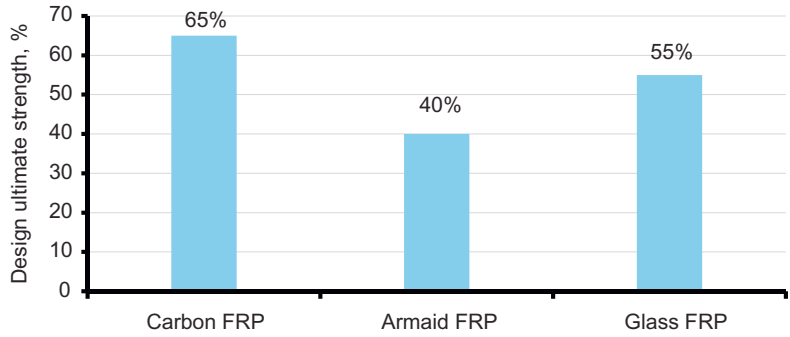

Figure 4.11 TR55 maximum stress range under service loads to avoid stress rupture.

4.2.7.6 JSCE

According to JSCE the design flexural fatigue resistance of members strengthened with FRP reinforcements shall be calculated considering the flexural fatigue characteristics of existing sections, the fatigue characteristics of the continuous fiber sheet and the characteristics of interfacial peeling fatigue failure between the continuous fiber sheet and the concrete. The code indicates that methods for accurate calculation of flexural capacity fatigue resistance have not yet been established. One recommended test method for performing tensile fatigue strength of continuous fiber sheets (JSCE-E 546, 2000).

To set a fatigue limit, JSCE uses its limit to avoid peeling failure using an interfacial fracture energy approach (Eq. (4.35), JSCE Eq. 6.4.1). Eq. (4.36) is modified to consider interfacial peeling fatigue failure for continuous fiber sheets and concrete substrate (Eq. (4.36), JSCE Eq. C6.4.11). A reduction factor, μ, is introduced to limit the value of tensile fiber stress, σ_f, instead of being set for peeling failure limit to further accommodate fatigue loading.

$$\sigma_f \leq \sqrt{\frac{2G_f E_f}{n_f \cdot t_f}} \qquad (4.35 - \text{JSCE Eq. } 6.4.1)$$

where n_f = number of plies of continuous fiber sheets; E_f = modulus of elasticity for continuous fiber sheet (N/mm^2); t_f = thickness of one layer of continuous fiber sheet (mm); G_f = interfacial fracture energy between continuous fiber sheet and concrete (N/mm).

$$\sigma_f \leq \sqrt{\frac{2\mu G_f E_f}{n_f . t_f}} \qquad (4.36 - \text{JSCE Eq. C}6.4.11)$$

where μ = reduction factor resulting from the influence of fatigue load on the interfacial fracture energy relating to the bond of continuous fiber sheets to concrete. In general, this value may be set to 0.7.

4.2.7.7 Summary

The factors for creep rupture and fatigue effects vary significantly. CNR and TR55 set fixed values for creep rupture and fatigue limits, while ACI and ISIS express this limit as a function of FRP strength. AASHTO provides the most elaborate checks for creep rupture and fatigue, providing strain (or stress) limits for concrete, steel and FRP. These limits are presented in Tables 4.19. Refer to Table 4.12 for recommended reduction factors for steel, concrete and FRP.

Fig. 4.12 summarizes reduction factors for carbon, aramid, and glass fiber to guard against creep rupture and fatigue. In general, ACI, AASHTO, and ISIS factors are similar, while ACI and AASHTO generally provide the most conservative factors.

Table 4.19 FRP limits due to creep rupture and cyclic loading

Code	Formula/description	Limit
AASHTO	$\varepsilon_c = \dfrac{M_f z}{I_T E_{frp}}$ $\varepsilon_s = \dfrac{M_f (d-z)}{I_T E_{frp}}$ $\varepsilon_{frp} = \dfrac{M_f (h + t_{frp} - z)}{I_T E_{frp}}$	$\leq 0.36 \dfrac{f'_c}{E_c}$ $\leq 0.8 \varepsilon_y$ $\leq \eta \varepsilon^u_{frp}$ Note: η for CFRP is taken as 0.80
TR55	Stress range as a proportion of the design ultimate strength	80%
ACI	Sustained plus cyclic stress limit	0.55 f_{fu}
ISIS	Maximum stress level for creep	0.65 f^u_{FRP}
CNR	Partial factor for creep rupture and fatigue	0.8 for creep and relaxation 0.5 for fatigue
JSCE	σ_f	$\sigma_f \leq \sqrt{\dfrac{2\mu G_f E_f}{n_f . t_f}}$

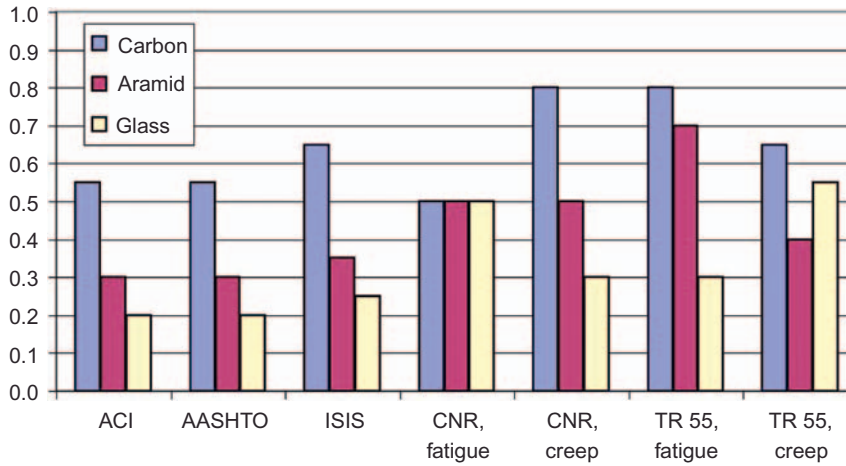

Figure 4.12 Summary of FRP fatigue/creep rupture coefficients.

4.2.8 End peeling

4.2.8.1 ACI

An end peeling failure frequently occurs due to a high stress at the FRP termination point causing a splitting away of the concrete cover at plane of the steel reinforcement. In ACI, to prevent this failure, the FRP reinforcement requires anchorage if the factored shear V_u at the termination point is greater than 2/3 of the concrete shear strength V_c, or

$$V_u > 0.67\ V_c \tag{4.37}$$

where

$$V_c = 2\lambda\sqrt{f'_c}\ b_w \cdot d \qquad (4.38 - \text{ACI 318, Eq. 11-3})$$

The anchoring is generally done using a transverse FRP U-wrap with an area A_f.

4.2.8.2 AASHTO

The peel stress at the point of end termination of externally bonded reinforcement is required to meet following limit:

$$f_{\text{peel}} \leq 0.065\sqrt{f'_c} \tag{4.39}$$

In which

$$f_{\text{peel}} = \tau_{av}\left[\left(\frac{3E_a}{E_{frp}}\right)\frac{t_{frp}}{t_a}\right]^{1/4} \tag{4.40}$$

where

$$E_a = 2G_a(1 + \upsilon_a) \tag{4.41}$$

υ_a = Poisson's ratio of the adhesive, and is taken as 0.35.

$$\tau_{av} = \left[V_u + \left(\frac{G_a}{E_{frp}t_{frp}t_a}\right)^{1/2} M_u\right]\frac{t_{frp}(h-y)}{I_T} \tag{4.42}$$

τ_{av} = the characteristic value of the limiting shear stress in the adhesive (ksi). In the absence of experimental data a value of 5.0 can be used.

AASHTO discusses three possible modes of debonding at the termination point of an externally bonded FRP reinforcing system when the structure is subjected to shear and flexure. One possibility is critical diagonal crack debonding with or without

concrete cover separation and plate-end interfacial debonding. In this case, if the FRP termination point is in a zone of high shear and the amount of steel reinforcement is insufficient, critical diagonal cracking may occur. In such cases a critical diagonal shear crack forms and intersects the FRP, then propagates toward the end of the member. A second possibility occurs in beams with higher amounts of existing steel shear reinforcement, instead of a single critical diagonal crack, multiple diagonal cracks of smaller width may occur. In this case, concrete cover separation is generally the controlling debonding failure mode. Here, failure of the concrete cover is initiated by a crack near the FRP termination point. The crack then propagates to and then along the level of the steel tension reinforcement. This mode of failure has been demonstrated experimentally for beams with externally bonded steel plates and FRP reinforcement, and is the mode of failure discussed in Section 4.2.8.1.

A third possibility occurs when high interfacial shear and normal stresses near the end of the FRP exceed the strength of the weakest element, generally the concrete, and plate-end interfacial debonding is initiated. Debonding in this case propagates from the FRP termination point toward the middle of the structural member, near the FRP−concrete interface. Note that this failure mode is only likely to occur when the FRP is significantly narrower than the beam section. AASHTO does not quantify a threshold for a ratio at which debonding initiates and propagates.

Although a wide range of predictive models that include numerical, fracture mechanics, data-fitting, and strength of material-based methods have been developed to address end peeling failures (Yao, 2004), AASHTO recommends a simplified equation based on the approximate analysis of Roberts (1989). At present, AASHTO does not specify a standard test method for determining the peel strength of an FRP reinforcement system from the concrete surface. However, AASHTO recommends for this purpose the use of ASTM Standard Test Method D 3167, *Standard Test Method for Floating Roller Peel Resistance of Adhesives* (2010). The ASTM method can be used for determining the peel resistance of adhesive bonds between rigid and flexible surfaces adhered together. For cases in which the peeling occurs within the concrete layer, AASHTO recommends that the peeling strength be limited to $0.065\sqrt{f'_c}$ and if the peeling stress exceeds $0.065\sqrt{f'_c}$, mechanical anchors at the FRP termination point must be used.

4.2.8.3 TR55

TR55 refers to early research on FRP separation failure and suggests a number of possible approaches for combating this problem, including: the use of plate-end anchorage devices, flexible adhesives, and imposing limits on the plate aspect (i.e., breadth/thickness) ratio. Bolted systems, bonded angle sections and composite straps bonded across the soffit plate are examples of plate-end anchorage devices that have been proposed as possible methods of preventing FRP separation failure. Generally, TR55 states that end plate separation failure can be avoided by meeting two criteria: (1) limiting the longitudinal shear stress between the FRP and the substrate, and (2) anchoring the FRP by extending it beyond the point at which it is theoretically no longer required.

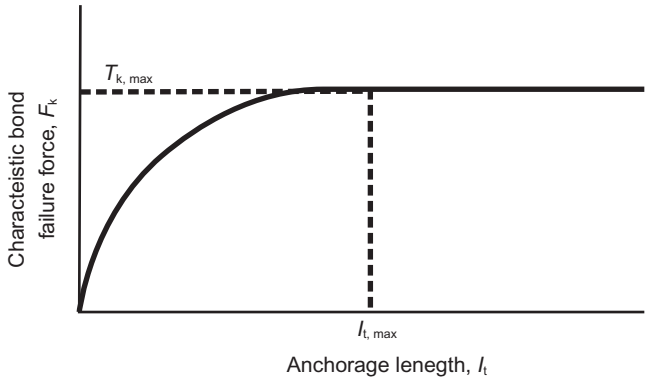

Figure 4.13 Characteristic bond failure force vs. anchorage length (TR55).

To meet the first criterion, TR55 notes that field experience indicates that limiting the longitudinal shear stress at the ultimate limit state to a value no greater than 0.8 N/mm^2, premature peeling failure can be avoided. TR55 also presents a procedure to calculate the minimum anchorage length as it relates to the maximum ultimate bond force. The longitudinal shear stress, τ, can be calculated using the following expression (Eq. (4.43)):

$$\tau = V\alpha_f \alpha A_f (h - x)/I_{cs} b_a \tag{4.43}$$

The relationship between the bond force,T_k, and the corresponding anchorage length, l_t is presented in Fig. 4.13. It is further recommended that a minimum anchorage length of 500 mm should be provided. In situations where it is not possible to provide the maximum allowable anchorage length, the bond force should be less than the following:

$$T_k = \left(\frac{T_{k,\max} l_t}{l_{t,\max}}\right)\left[\frac{2 - l_t}{l_{t,\max}}\right] \tag{4.44}$$

Additionally, TR55 considers using an anchorage device, provided its capacity has been verified by testing.

4.2.8.4 JSCE

JSCE does not clearly specify design equations other than the following limiting peeling stress expression:

$$\sigma_f \leq \sqrt{\frac{2G_f E_f}{n_f . t_f}} \tag{4.45}$$

JSCE notes how the interfacial fracture energy factor G_f varies with the strengthening system, the number of plies, and the anchoring system used, and states that this value should be determined through testing. When testing cannot be performed, JSCE recommends using a G_f value of 4 lb/in. (0.7 N/mm).

4.2.8.5 CNR

The following equation is used to limit the peeling stress in CNR:

$$\tau_{b,e} \leq f_{bd} \tag{4.46}$$

Per Eq. (4.46), to prevent peeling failure, the equivalent shear stress $\tau_{b,e}$ should be less than the design bond strength (f_{bd}). If the shear stress is higher, an anchorage device must be used. The equivalent shear stress is given by Eq. (4.47):

$$\tau_{b,e} = k_{id} \cdot \tau_m \tag{4.47}$$

where k_{id} = a coefficient (≥ 1) accounting for shear and normal stresses close to the anchorage ends, assumed to be 1.0.

$$\tau_m = \frac{V_{(z=a)} \cdot t_f \cdot (h - x_e)}{I_c / n_f} \tag{4.48}$$

τ_m = average shear stress; $V_{(z=a)}$ = shear force acting on the section where FRP strengthening ends; t_f = fiber thickness; n_f = modular ratio, E_f/E_c; x_e = distance from the extreme compression fiber to the neutral axis; I_c = moment of inertia of the transformed section.

$$f_{bd} = k_b . \frac{f_{ctk}}{\gamma_b} \tag{4.49}$$

f_{bd} = design bond strength, a function of the characteristic tensile strength of the concrete, f_{ctk}.
γ_b = 1.0 for rare loading combinations;
= 1.2 for frequent loading combinations.

The peeling stress is then given as

$$f_{\text{peel}} = \tau_{av} \left[\left(\frac{3E_a}{E_{frp}} \right) \frac{t_{frp}}{t_a} \right]^{1/4} \tag{4.50}$$

where

$$\tau_{av} = \left[V_u + \left(\frac{G_a}{E_{frp} t_{frp} t_a} \right)^{1/2} M_u \right] \frac{t_{frp}(h - y)}{I_T} \tag{4.51}$$

References are not provided for the basis of the safety factors γ_b. Environmental factors are not accounted for. A value of 116 psi (0.8 N/mm^2) is recommended for use as an upper limit to avoid premature peeling failure.

4.2.8.6 Anchorage methods for FRP

For cases of high peeling or shear stress an anchorage system may be required to avoid debonding failure. In these cases an anchorage system might allow the use of a FRP strengthening plan that otherwise would not meet design code provisions. For example, anchorage may allow greater strengthening or the use of a wider range of possible FRP geometries and material properties. A drawback of the use of many anchorage systems is the added cost and complexity of installation.

NCHRP 678 (Belarbi et al., 2011) describes several anchorage systems, including the near-surface mounted system, where the end of the FRP wrap or preformed plate is bent and embedded into a groove cut into the concrete, then secured with epoxy. Another system available involves anchoring the FRP to the concrete with a spike made from a bundle of fibers. In this process, half of the spike length is covered with resin and allowed to harden. The precured spike end is then inserted into a resin-filled hole that is drilled into the concrete, and the dry fibers on the other end of the spike are spread apart on the surface of the FRP layer to be anchored, and then saturated with resin. Yet other types of anchorage systems involve embedding nails or rods into the concrete to secure steel plates on top of the FRP layer to be anchored.

ISIS also describes several common anchorage systems, including bonding an additional FRP strip along the edges of the applied FRP; anchoring FRP shear stirrups into the bottom of the slab in T-beam applications; and clamping the FRP strips with plates and bolts, as later illustrated in Section 4.3.2.3.

4.2.8.7 Summary

A summary of peeling limits and procedures are given in Table 4.20.

Table 4.20 Peeling summary

Code	Quantity	Formula	Limit
ACI 440.2R	V_u	$A_{f_{\text{anchor}}} = \dfrac{(A_f f_{fu})_{\text{longitudinal}}}{(E_f \kappa_v \varepsilon_{fu})_{\text{anchor}}}$	$V_u \geq 0.67\, V_c$
AASHTO	f_{peel}	$f_{\text{peel}} = \tau_{av}\left[\left(\dfrac{3E_a}{E_{frp}}\right)\dfrac{t_{frp}}{t_a}\right]^{1/4}$	$f_{\text{peel}} \leq 0.065\sqrt{f'_c}$
CNR-DT 200	Bond shear strength	$\tau_{b,e} \leq f_{bd}$	$f_{bd} = k_b.\dfrac{f_{ctk}}{\gamma_b}$
TR55	Shear stress	$V_u \leq 116$ psi $(0.8\ N/\text{mm}^2)$	116 psi (0.8 N/mm^2)
JSCE	Shear stress	$\Delta\sigma_f = \sqrt{\dfrac{2G_f E_f}{n_f.t_f}}$	$\sqrt{\dfrac{2G_f E_f}{n_f.t_f}}$

As shown in the table, different methods are used to evaluate peeling for the various codes. ACI uses a peeling limit evaluating the shear capacity of concrete at the FRP termination point, expressed as a function of $\sqrt{f'_c}$ and section shear capacity and demand ($V_u \geq 0.67\ V_c$). AASHTO and CNR limits are similar, and are a function of f'_c and $\sqrt{f'_c}$ respectively, while JSCE expresses the limit in terms of FRP-related quantities. To compare code expressions a rectangular concrete beam of $h = 30$ in and $b = 18$ in is considered as an example. The beam is assumed to have the following properties: factored shear force at the reinforcement end termination = 100 kips; factored moment at the reinforcement termination = 500 kip-in; materials properties of Mbrace Saturant and Mbrace CF130 wrap are used, such that fiber thickness (one ply) = 0.0065 in.; fiber modulus of elasticity = 33,000 ksi; adhesive thickness = 0.0022 in.; adhesive modulus of elasticity = 440 ksi; Poisson ratio of adhesive = 0.40; $\gamma_b = 1.2$ (assumes a frequent load combination (for CNR)). Peeling stresses and limits are evaluated as a function of the amount of FRP strengthening (Fig. 4.14), and concrete compressive strength f'_c (Fig. 4.15).

Two notable observations are that: (1) for the example beam, the peeling stress exceeds the peeling limit in all cases, and end anchorage is required; and (2) peeling stresses significantly increase as f'_c increases, and marginally increases as the amount of FRP strengthening increases. However, peeling limits are independent of the amount of FRP strengthening, but vary with the increase in f'_c. AASHTO and CNR are similar in the treatment of peeling stresses and peeling limits, although AASHTO peeling limits are slightly more conservative than those of CNR.

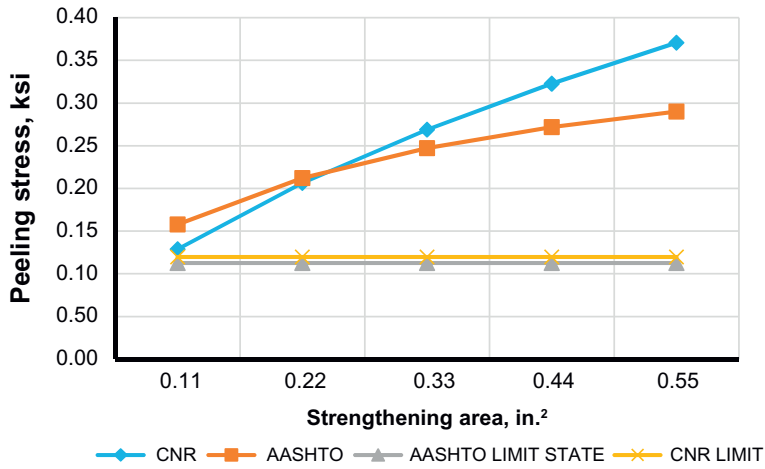

Figure 4.14 Peeling stress versus FRP strengthening area.

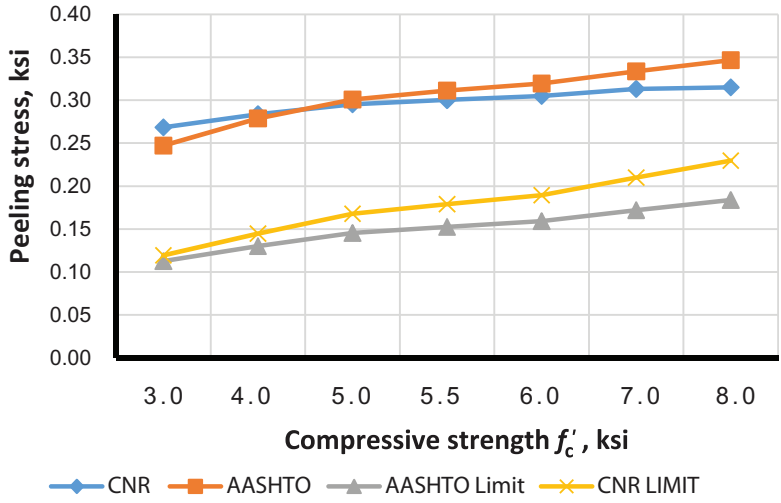

Figure 4.15 Peeling stress versus f_c'.

4.2.9 Development length

4.2.9.1 AASHTO

In AASHTO the tension development length, L_d, is taken as

$$L_d \geq \frac{T_{frp}}{\tau_{int} b_{frp}} \tag{4.52}$$

where T_{frp} = tensile force in the FRP reinforcement corresponding to an FRP strain of 0.005; τ_{int} = interface shear transfer = 0.065 $\sqrt{f_c'}$.

The specified development length is required to allow the full tension strength of the FRP to be developed in the region of maximum moment.

As will be shown below, the AASHTO development length calculations produce more conservative values as FRP area increases. It was also found that AASHTO development length values are most conservative at lower values of f_c', producing values as well as trends that are significantly different from the other codes studied (see Figs. 4.16 and 4.17). Other code results appear to be independent of the changes in FRP area as well as f_c' (ISIS and TR55) or slightly dependent on these factors (ACI and CNR). To understand the reasons for these discrepancies, the basis of AASHTO's development length methodology is reviewed.

The interface shear transfer strength (τ_{int}) given in AASHTO is based on the recommendation of Naaman and Lopez (1999), who conducted tests on uncracked and precracked reinforced concrete beams externally bonded with FRP reinforcement and subjected to accelerated freeze−thaw cycles. This shear limit represents a lower bound of the experimental data found from short-term direct tension tests of FRP reinforcement bonded to concrete surfaces (Haynes, 1997; Bizindavyi and Neale, 1999).

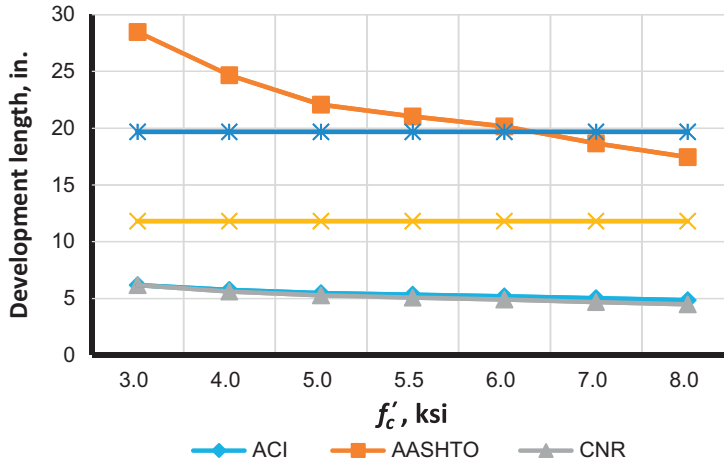

Figure 4.16 Development length as a function of f'_c, ksi.

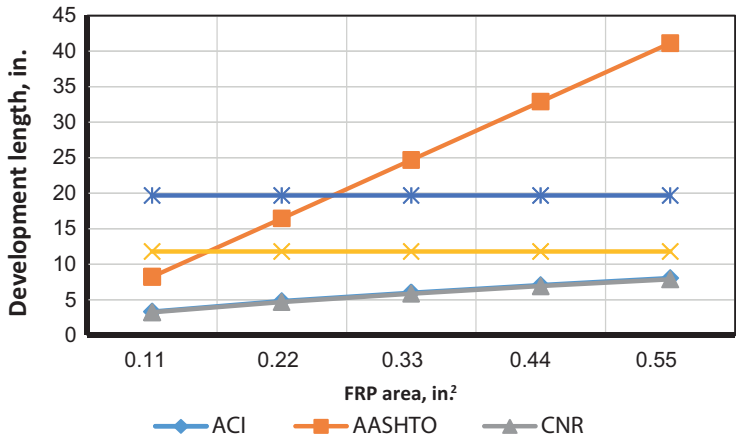

Figure 4.17 Development length as a function of FRP area, in.^{2}.

This research was conducted for MDOT and is detailed in Report RC-1372, "Repair and strengthening of reinforced concrete beams using CFRP laminates, behavior of beams subjected to freeze-thaw cycles."

In the experimental program, reinforced concrete beams were subjected to a maximum of 300 freeze−thaw cycles according to ASTM C666. The parameters investigated were two different adhesive systems, the Tonen CFRP sheet system (MBrace), and the Sika CFRP system (Carbodur); as well as the degree of cracking prior to strengthening. It was found that freeze−thaw cycles influenced the behavior of reinforced concrete beams with glued-on CFRP laminates, and the recommended value of interface shear transfer strength (τ_{int}) represents the lower bound of the test results.

4.2.9.2 ACI

In ACI the bond capacity of FRP is developed over a critical length l_{df}. To develop the effective FRP stress at a given section, the available anchorage length of FRP should exceed the value given in the equation below:

$$l_{df} = 0.057\sqrt{\frac{nE_f t_f}{\sqrt{f'_c}}} \quad \text{in.-lb units} \tag{4.53}$$

$$l_{df} = \sqrt{\frac{nE_f t_f}{\sqrt{f'_c}}} \quad \text{SI units} \tag{4.54}$$

4.2.9.3 ISIS

ISIS specifies the minimum required anchorage length for the externally bonded FRP beyond the point where no strengthening is required, l_a. According to the S6-06 bridge code, l_a may be evaluated as follows:

$$l_a = 0.5\sqrt{E_{\text{FRP}} t_{\text{FRP}}} \geq 11.81 \text{ in. } (300 \text{ mm}) \qquad (4.55 - \text{ISIS Eq. } 5.29)$$

Anchorage lengths longer than l_a must be provided if required by the manufacturer's installation procedure. For cases where l_a is not provided, suitable anchorage mechanisms must be used.

4.2.9.4 CNR

The optimal bonded length l_e may be estimated as follows:

$$l_e = \sqrt{\frac{E_f t_f}{2\sqrt{f_{ctm}}}} \qquad (4.56 - \text{CNR Eq. } 4.1)$$

where l_e is in mm; the value from Eq. (4.56) should be multiplied by 0.03937 to obtain l_e in inches.

4.2.9.5 TR55

TR55 specifies a threshold anchorage length, $l_{t,\max}$, above which no increase in the bond failure force is possible. The maximum anchorage length, $l_{t,\max}$, needed to activate this bond force is calculated using the following expressions:

$$l_{t,\max} = 0.7\sqrt{E_{fd} t_f / f_{ctm}} \geq 19.69 \text{ in. } (500 \text{ mm}) \qquad (4.57 - \text{TR55 Eq. } 6.19)$$

where

$$f_{ctm} = 0.18(f_{cu})^{2/3} \qquad (4.58 - \text{TR55 Eq. 6.22})$$

4.2.9.6 Summary

Generally, all expressions (with the exception of ISIS), express development length as a function of tension in the FRP and concrete compressive strength f'_c. The ISIS formula f'_c sets a minimum limit of 11.81 in. (300 mm), while TR55 sets the development length minimum value at 19.69 in. (500 mm). A comparative evaluation of development length is given in Figs. 4.16 and 4.17 (note that to evaluate CNR, f_{ctm} is assumed to be 0.3 $(f'_c)^{2/3}$ in accordance with the Eurocode, since CNR does not provide an expression for the value). Two scenarios are considered; the first (Fig. 4.16) varies f'_c, while the second (Fig. 4.17) varies FRP area from one to five plies of BASF MBrace CF130 CFRP wrap (see article 4.2.8.7 in this book for example beam properties and other relevant data).

It can be seen from the figures that a significant variation in development length requirements exist. For ISIS and TR55 the lower limits specified generally controlled. For AASHTO, development length is independent of FRP modulus, while all other codes have expressions for development length as a function of FRP modulus. The AASHTO expression is also significantly more sensitive to FRP area. As discussed above, AASHTO recommendations differ significantly from the other codes and generally provide conservative results. However, the values considered by AASHTO were specifically based on testing conducted for MDOT at the University of Michigan that included freeze−thaw conditioning relevant to Michigan.

4.2.10 Flexural design approach and assumptions

4.2.10.1 AASHTO

In AASHTO the calculation of the flexural strength of reinforced concrete members externally reinforced with FRP materials assumes perfect bond between the reinforcing steel, FRP reinforcement and the concrete; that the contribution of tension stress in the concrete to flexural strength is neglected; the stress−strain behavior for FRP reinforcement is linear-elastic until failure; the stress−strain behavior of steel reinforcement is bilinear, with elastic behavior up to yielding and perfectly plastic behavior thereafter; the maximum usable compression strain in the concrete is equal to 0.003; and the maximum usable strain at the FRP/concrete interface is 0.005.

When concrete compressive strain is less than 0.003, the concrete compression stress distribution is to be modeled with a parabolic shape according to the following equation:

$$f_c = \frac{2(0.9f'_c)(\varepsilon_c/\varepsilon_0)}{1 + (\varepsilon_c/\varepsilon_0)^2} \qquad (4.59)$$

where

$$\varepsilon_0 = 1.71\frac{f'_c}{E_c} \tag{4.60}$$

ε_0 is the concrete strain corresponding to the maximum stress on the concrete stress−strain curve.

The factored resistance, *Mr*, of a steel-reinforced concrete rectangular section strengthened with FRP externally bonded to the beam tension surface is be taken as

$$Mr = 0.9[A_s f_s(d_s - k_{2c}) + A'_s f'_s(k_{2c} - d'_s)] + \phi_{\text{FRP}} T_{\text{FRP}}(h - k_{2c}) \tag{4.61}$$

where ϕ_{FRP} = resistance factor = 0.85.

$$T_{\text{FRP}} = nb_{\text{FRP}} N_b \tag{4.62}$$

n = number of FRP reinforcement plates; N_b = FRP reinforcement strength per unit width, corresponding to 0.5% strain in the FRP reinforcement when subjected to tension in accordance with ASTM D3039; assumed to be 1.07.

4.2.10.2 JSCE

JSCE considers carbon and aramid fibers. It employs five partial safety factors: material, load, member, structure, and analysis. However, JSCE does not include explicit design equations for flexure. Due to the lack of a clear procedural description of flexural capacity evaluation, JSCE was not further considered for moment capacity analysis and comparison.

4.2.10.3 CNR

Similar to JSCE, CNR also provides no explicit capacity expression, but the flexural failure mode and capacity can be determined from strain compatibility, section equilibrium, and the required material strength limits. In CNR the concrete stress block is not specified, so the FIB 14 procedure (2001) is used, where the coefficient representing the resultant of the compressive stress can be expressed as follows:

ψ = 0.8 for $f'_c < 7.3$ ksi (50 MPa);
= 0.8—(f'_c-50)/400 for $f'_c > 7.3$ ksi (eq. in MPa).
λ = coefficient representing the extreme compression fiber;
= 0.40 (from FIB 14, as no value is given in CNR).
K_b = geometric coefficient, ≥ 1.0.

Finally the maximum strain in FRP is to be calculated as follows:

$$\varepsilon_{fd} = \min\left\{\eta_a . \frac{\varepsilon_{fk}}{\gamma_f}, \varepsilon_{fdd}\right\} \tag{4.12}$$

For comparison to other codes (as applicable in Figs. 4.18–4.35) the following assumptions are used in CNR flexural calculations: steel yield strength is reduced by the specified partial safety factor of $\gamma_s = 1.15$ such that $f_{yd} = f_y/\gamma_s$; the mean value of concrete tensile strength $f_{ctm} = 0.3\left(\sqrt{f'_c}\right)^{2/3}$ (not explicitly defined in CNR, but taken from Eurocode; concrete compressive strength is taken as $f_{cd} = 0.85(f'_c/\gamma_c)$, with the partial safety factor taken as $\gamma_s = f_{ctm} = (\sqrt{f'_c})^{2/3} f_{cd} = (f'_c/\gamma_c)\gamma_c = 1.6$.

4.2.10.4 ACI

ACI assumes that the maximum concrete compressive strain is 0.003. The FRP strain limit is imposed using Eq. (4.8) as shown below:

$$\varepsilon_{fd} = 0.083\sqrt{\frac{f'_c}{nE_f t_f}} \le 0.9\varepsilon_{fu} \text{ in in.-lb units} \tag{4.8 – ACI Eq. 10.2}$$

$$\varepsilon_{fd} = 0.41\sqrt{\frac{f'_c}{nE_f t_f}} \le 0.9\varepsilon_{fu} \text{ in SI units} \tag{4.9}$$

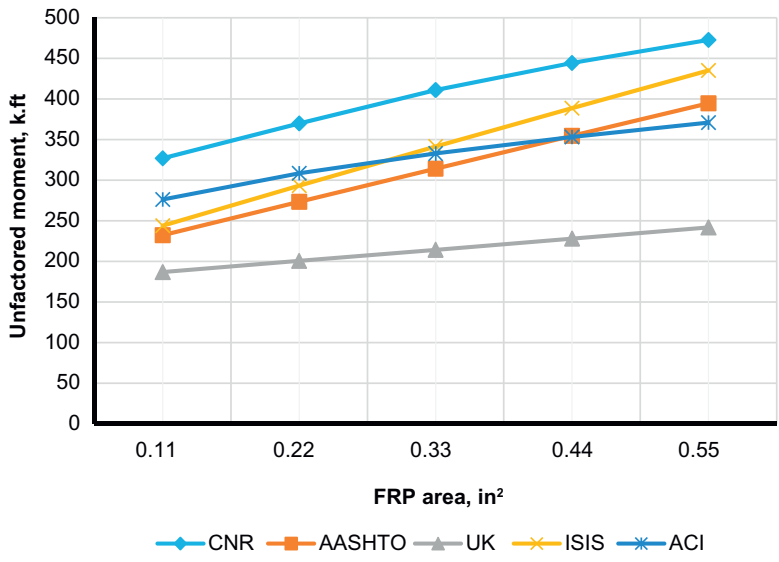

Figure 4.18 Effect of amount of FRP flexural strengthening on unfactored moment ($\rho = 0.0033$).

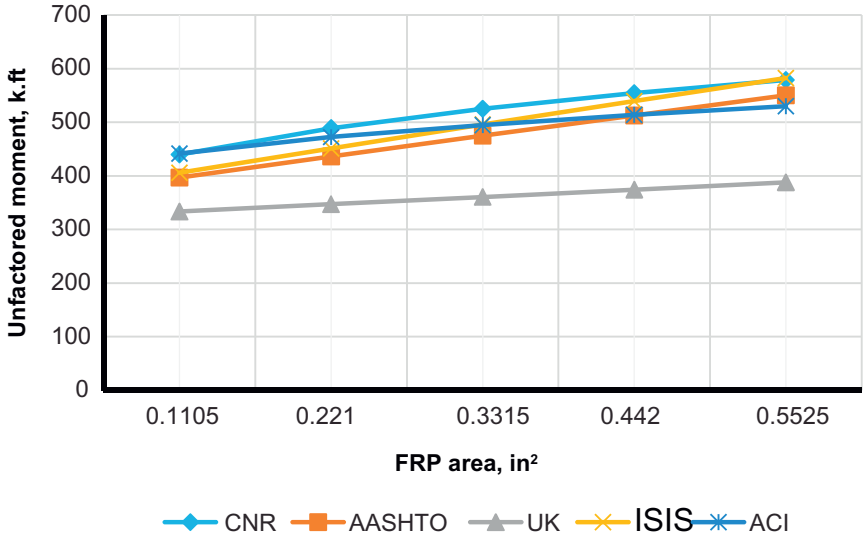

Figure 4.19 Effect of amount of FRP flexural strengthening on unfactored moment ($\rho = 0.0064$).

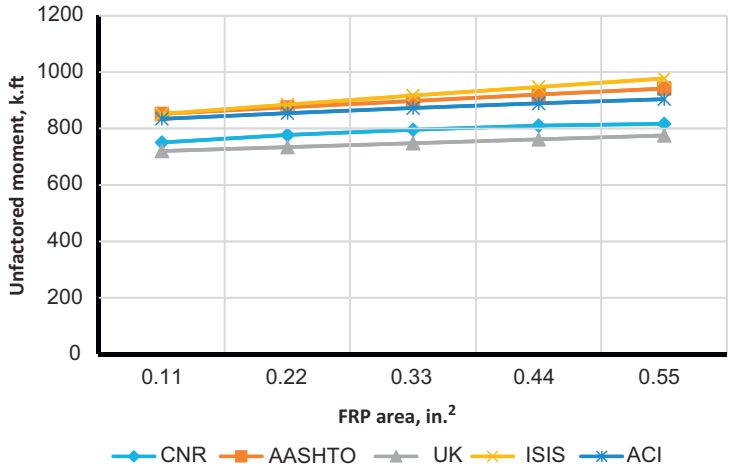

Figure 4.20 Effect of amount of FRP flexural strengthening on unfactored moment ($\rho = 0.0171$).

Eq. (4.63) (ACI Eq. 10.13) is typically used to evaluate the nominal moment capacity of the section:

$$M_n = A_s f_s \left[d - \left(\frac{\beta_{1c}}{2} \right) \right] + \phi A_f f_{fe} \left[h - \left(\frac{\beta_{1c}}{2} \right) \right] \qquad (4.63 - \text{ACI Eq. } 10.13)$$

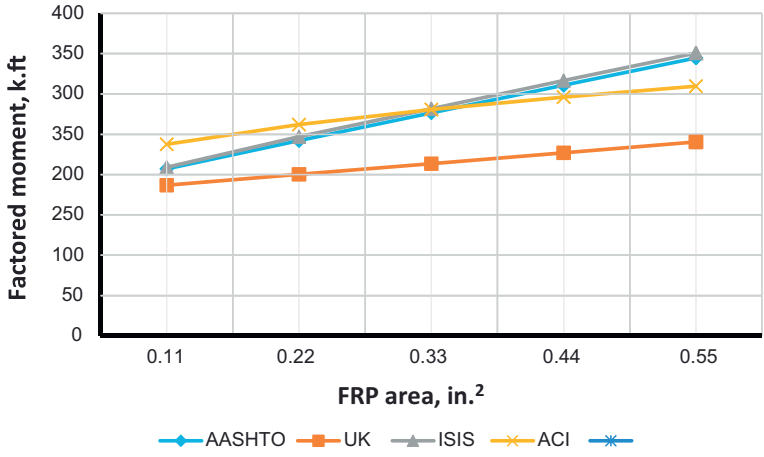

Figure 4.21 Effect of amount of FRP flexural strengthening on factored moment ($\rho = 0.0033$).

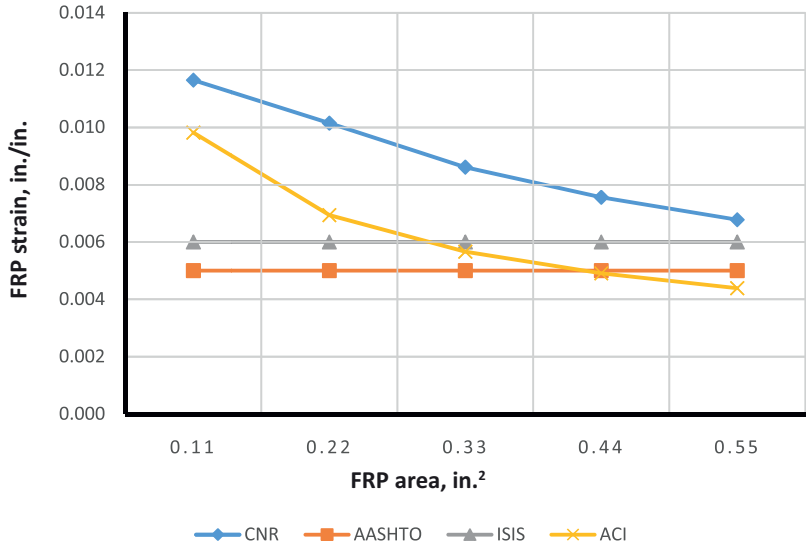

Figure 4.22 Effect of amount of FRP flexural strengthening on FRP strain ($\rho = 0.0033$).

For the special case when ε_c is smaller than 0.003, values for β_1 and α_1 are evaluated as follows:

$$\beta_1 = \frac{4\varepsilon_c' - \varepsilon_c}{6\varepsilon_c' - 2\varepsilon_c} \tag{4.64}$$

$$\alpha_1 = \frac{3\varepsilon_c'\varepsilon_c - \varepsilon_c^2}{3\beta_1\varepsilon_c'^2} \tag{4.65}$$

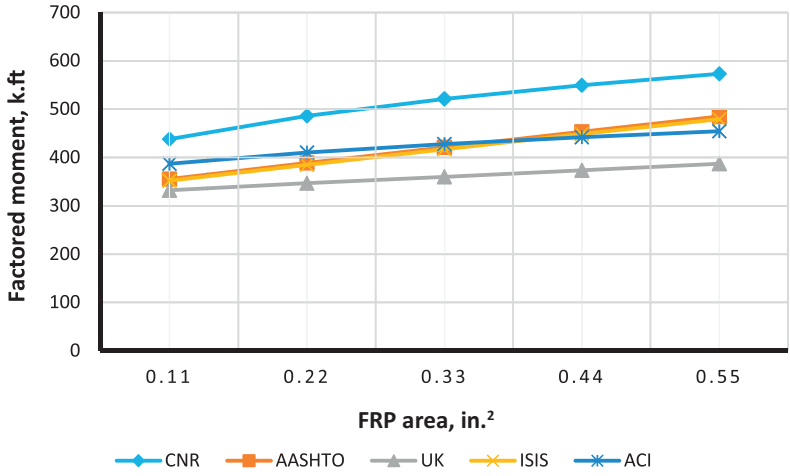

Figure 4.23 Effect of amount of FRP flexural strengthening on factored moment ($\rho = 0.0064$).

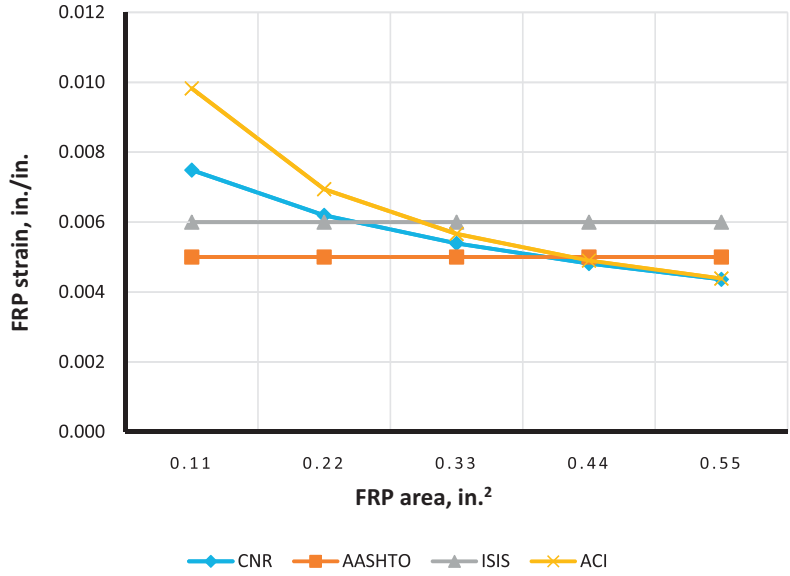

Figure 4.24 Effect of amount of FRP flexural strengthening on FRP strain ($\rho = 0.0064$). Note: As steel reinforcement ratio increases and FRP strain decreases, failure mode changes from compression to tension failure. Also, with increasing f'_c, the mode of failure changes from compression to tension failure.

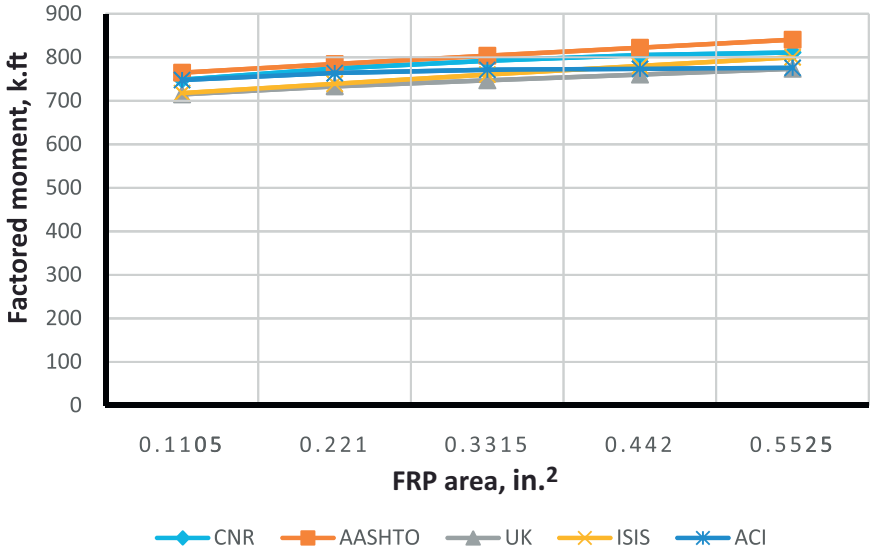

Figure 4.25 Effect of amount of FRP flexural strengthening on factored moment ($\rho = 0.0171$).

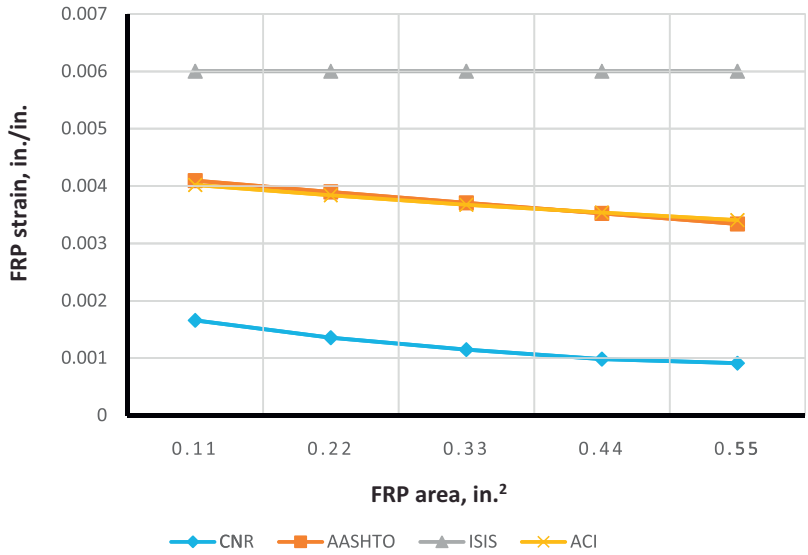

Figure 4.26 Effect of amount of FRP flexural strengthening on FRP strain ($\rho = 0.0171$).

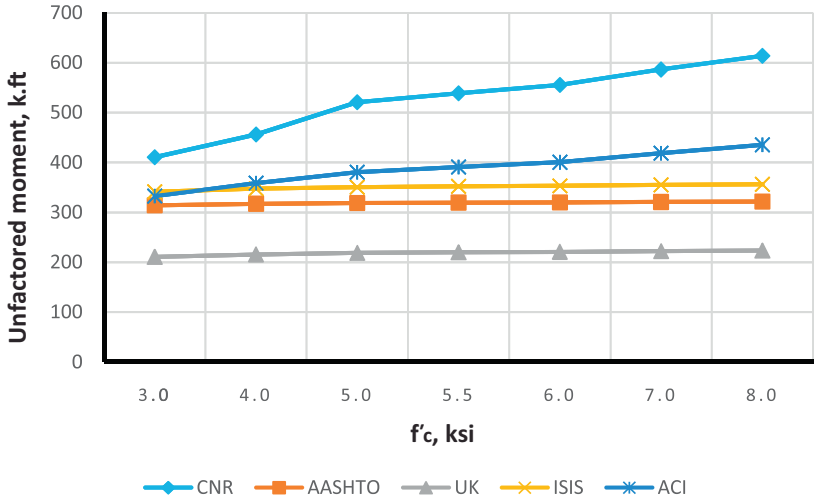

Figure 4.27 Effect of f'_c on unfactored moment ($\rho = 0.0033$).

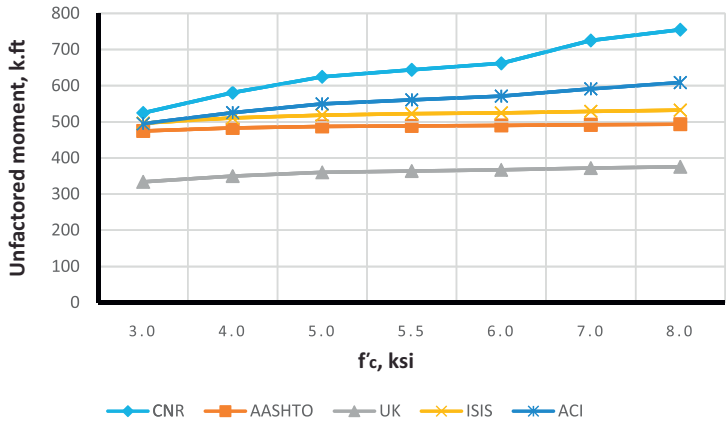

Figure 4.28 Effect of f'_c on unfactored moment ($\rho = 0.0064$).

Using $\beta_1$and α_1 the neutral axis location can be evaluated from Eq. (4.66).

$$c = \frac{A_s f_y + A_f f_{fe}}{\alpha_1 f'_c \beta_1 b} \tag{4.66}$$

Steel and FRP service stresses are calculated using Eqs. (4.20) and (4.21) to ensure compliance with serviceability requirements.

$$f_{s,s} = \frac{\left[M_s + \varepsilon_{bi} A_f E_f \left(d_f - \left(\frac{k_d}{3}\right)\right)\right](d - k_d) E_s}{A_s E_s \left(d - \left(\frac{k_d}{3}\right)\right)(d - k_d) + A_f E_f \left(d_f - \left(\frac{k_d}{3}\right)\right)(d_f - k_d)} \quad (4.20 - \text{ACI Eq. } 10.14)$$

$$f_{f,s} = f_{s,s} \left(\frac{E_f}{E_S}\right) \frac{(d_f - k_d)}{(d - k_d)} \varepsilon_{bi} E_f \quad (4.21 - \text{ACI Eq. } 10.15)$$

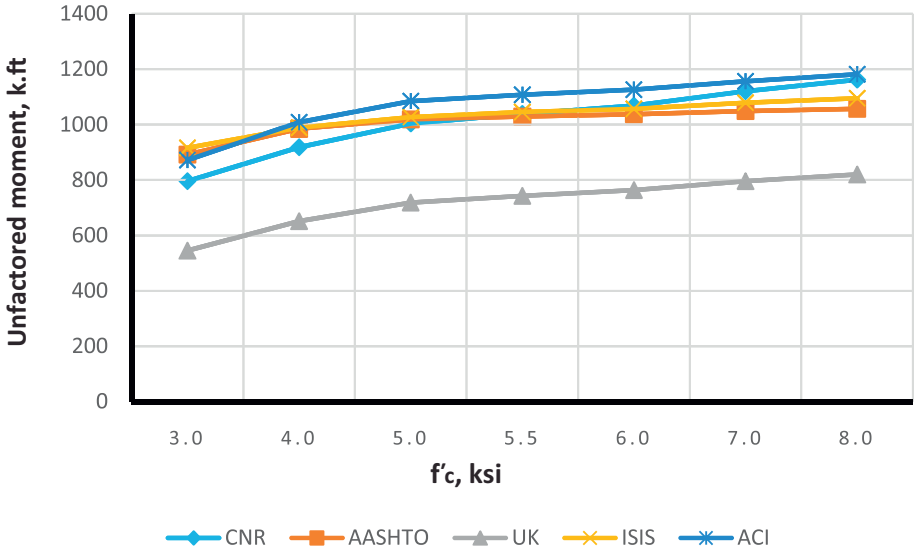

Figure 4.29 Effect of f'_c on unfactored moment ($\rho = 0.0171$).

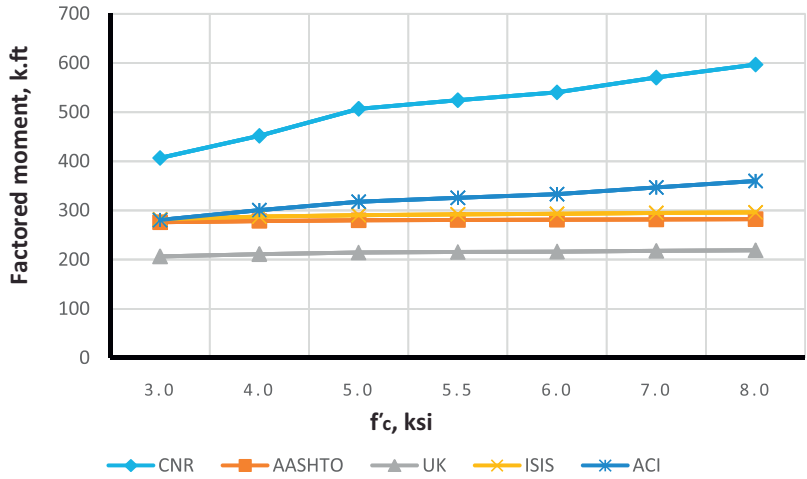

Figure 4.30 Effect of f'_c on factored moment ($\rho = 0.0033$).

An environmental reduction factor C_E (taken as 0.85 assuming exterior exposure) and the additional reduction factor ψ specific to FRP are considered in the factored moment calculations.

4.2.10.5 ISIS

The ISIS design procedure is straightforward with the assumptions given in the code. The neutral axis is determined using strain compatibility and section balance. In ISIS, it is assumed that concrete maximum compressive strain is ≤ 0.0035; the

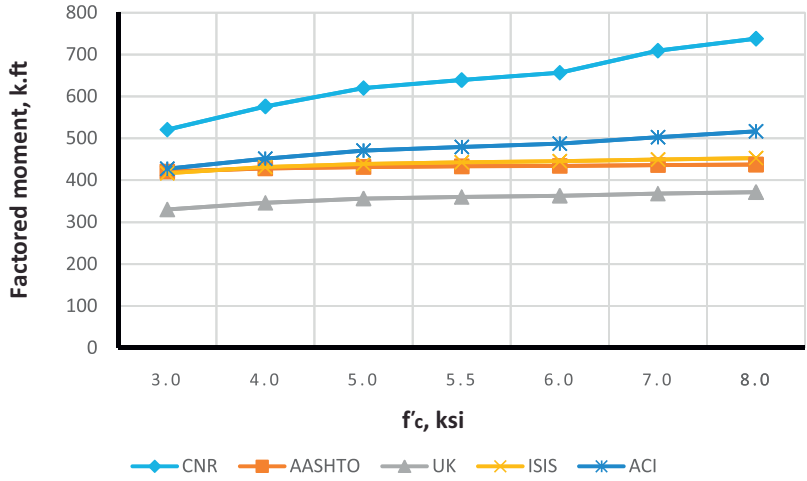

Figure 4.31 Effect of f'_c on factored moment ($\rho = 0.0064$).

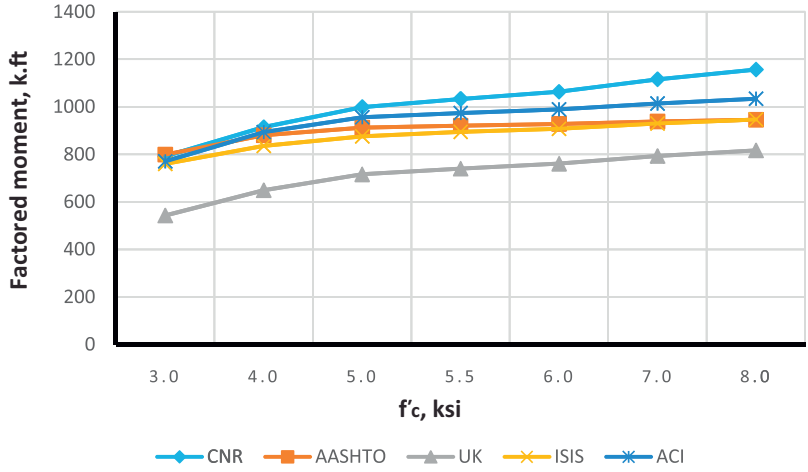

Figure 4.32 Effect of f'_c on factored moment ($\rho = 0.0171$).

maximum FRP strain (per the bridge code) = 0.006; and, the appropriate reduction factors are used as specified earlier in this chapter.

4.2.10.6 TR55

TR55 is similar to the other codes in its assumptions of the applicability of basic engineering mechanics to establish section capacity. Specific to TR55 are the following recommendations for flexural capacity: the FRP strain limit to prevent

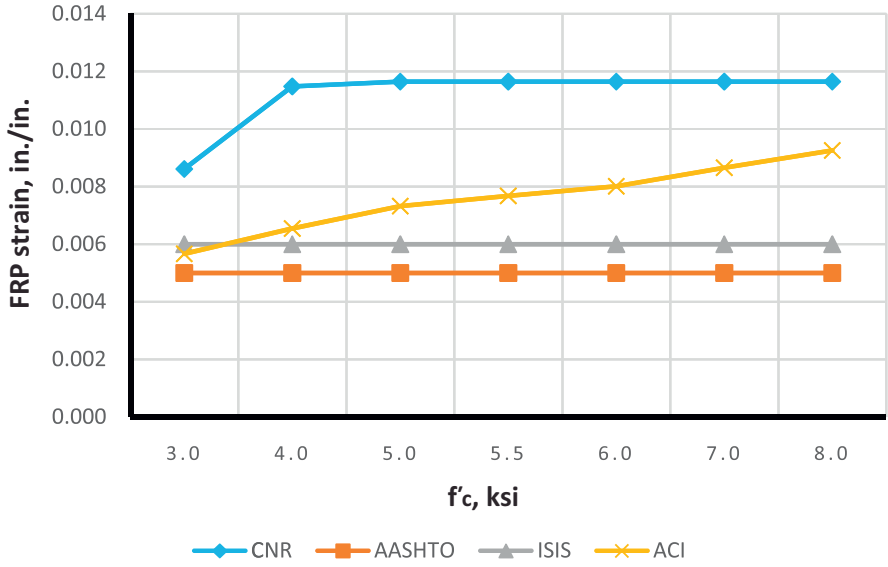

Figure 4.33 Effect of f'_c on FRP strain ($\rho = 0.0033$).

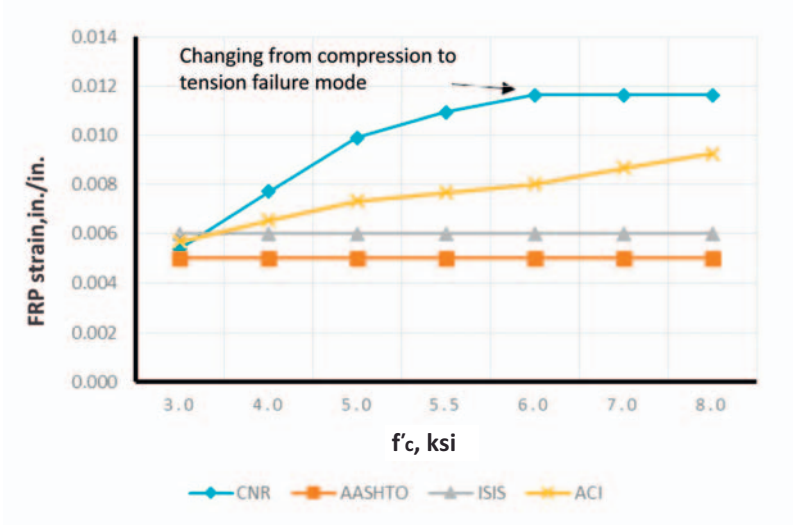

Figure 4.34 Effect of f'_c on FRP strain ($\rho = 0.0064$).

debonding is taken as 0.008 for uniformly distributed loads and 0.006 for load effects of simultaneous high shear and moment; and the ultimate compressive strain in concrete $\varepsilon_{cu} = 0.0035$.

Unique to In TR55, an additional moment capacity, M_{add}, representing the FRP contribution, is added to the original section nominal moment capacity. Assuming a

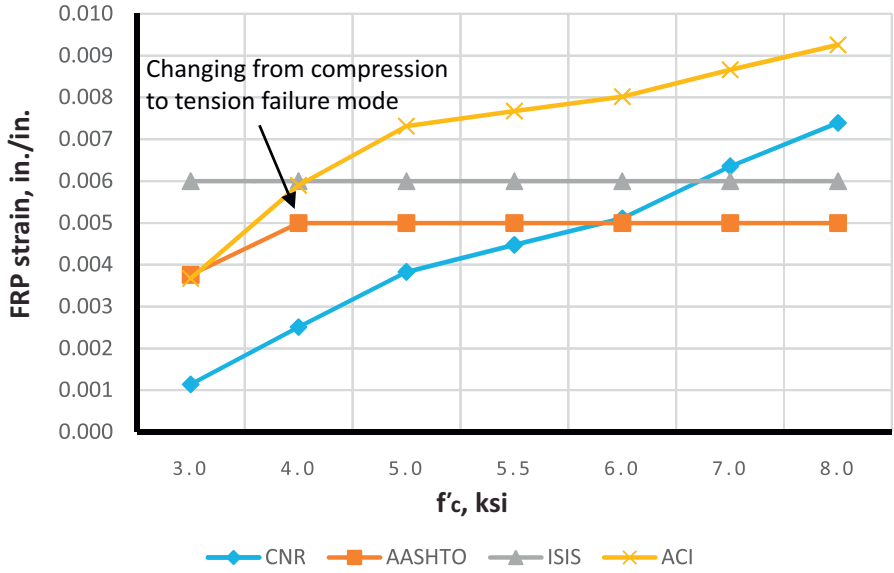

Figure 4.35 Effect of f'_c on FRP strain ($\rho = 0.0171$).

flexural section is to be strengthened to carry a larger moment M than its current capacity, with a singly-reinforced section, the nominal moment is evaluated as follows:

$$M_r = F_s z + F_f[z + (h - d)] \qquad (4.67 - \text{UK Eq. } 6.14)$$

where

$$M_r = M \text{ and } F_s = \left(\frac{f_y}{\gamma_{ms}}\right) \cdot A_s$$

4.2.10.7 Summary

For comparison of different code results a rectangular reinforced concrete beam with $b = 18$ in and $h = 30$ in is considered for strengthening with MBrace CF130 CFRP. Figs. 4.18–4.26 illustrate how moment capacity changes as a function of FRP area and initial steel reinforcement ratio. It was found that, as expected, an increase in moment capacity accompanies an increase in FRP area. An exception is observed for ACI with a steel ratio of 0.0171 (Fig. 4.25—factored moment case). This exception occurs because the steel reinforcement strain falls in the transition zone between a tension and compression controlled failure, causing a reduction in the value of ϕ and thus reducing the factored moment as FRP area increases. It was also found that as steel reinforcing ratio increases, a compression failure is observed in some codes but not in others. For example, AASHTO and CNR develop

compression failures at a steel reinforcement ratio of 0.0171 for all values of FRP strengthening. It is important to note that the compression failures were obtained for the relatively low f'_c chosen for the evaluation beam of 3000 psi. This low value was specifically chosen such that the behavior of different code procedures considering different beam failure modes (i.e., tension and compression controlled) could be compared. In most cases, where f'_c is greater that 3000 psi, the likelihood of developing a compression failure is reduced for the same amount of FRP reinforcement.

It was also found that due to the need to maintain section equilibrium, when FRP area increases, FRP strain is reduced. However, when the code-specified FRP strain limits are imposed (for example, ISIS enforces a maximum FRP strain of 0.006), FRP rupture sometimes becomes the only possible mode of failure. Moreover, ACI exhibits a higher FRP strain at lower values for FRP area, relative to other codes. This can be attributed to one of the two ACI strain limit expressions, where the strain limit is inversely propotional to FRP area (Eq. (4.8)).

$$\varepsilon_{fd} = 0.083\sqrt{\frac{f'_c}{nE_f t_f}} \le 0.9\varepsilon_{fu} \text{ in in.} - \text{lb units} \qquad (4.8 - \text{ACI Eq. } 10.2)$$

$$\varepsilon_{fd} = 0.41\sqrt{\frac{f'_c}{nE_f t_f}} \le 0.9\varepsilon_{fu} \text{ in SI units} \qquad (4.9)$$

Although predicted FRP strains differ, AASHTO and ISIS, both bridge-specific codes, generally produce similar moment capacity values for the different cases investigated. ACI, AASHTO, and ISIS are also reasonably consistent with flexural capacity prediction. ACI has greatest capacity for lower FRP area and higher f'_c, while AASHTO and ISIS have greatest capacity for higher FRP areas. TR55 is more sensitive when there is a change in concrete compressive strength and is less affected by change in FRP area. It is the most conservative for almost all cases. Despite its largest FRP strain limit of 0.008, it produces the least capacity due to its conservative (nonadjustment of the neutral axis) flexural capacity calculation method. In most cases, FRP rupture was found to be the mode of failure.

Figs. 4.27–4.35 illustrate the effect of changing f'_c on moment capacity, as a function of several other parameters. For this comparison, FRP area was fixed at three plies of 17 in. wide of MBrace CF130 CFRP. As expected, higher FRP strains result in higher the moment capacities. It was also found that ACI results in higher values for FRP strain as well as factored and unfactored moments when compared to other codes. For lower steel reinforcement ratios ($\rho = 0.0033$ and 0.0064), tension failure is the dominant mode of failure, though the higher value for ρ(0.0171), when combined with the FRP, results in possible compression failures (for example, AASHTO and CNR transition from tension failure into compression failure at the 0.0171 steel reinforcement ratio).

4.3 Shear FRP strengthening of RC/PC bridge members

4.3.1 Introduction

A review and analysis of the shear strengthening provisions for concrete bridge members with FRP is presented in this section for the six reviewed guidelines. The organization of this section is based on the framework presented in ACI 440.2R-08 since it offers the most complete coverage of the subject. The specific items for analysis and comparison include:

- Wrapping schemes
- Strength reduction factors
- Reinforcement and spacing limits
- FRP strain limits
- Shear design approach and assumptions
- Shear analysis procedure and results

4.3.2 Wrapping schemes

Three types of wrapping schemes are generally used to increase the shear strength of rectangular beams: four-sided (complete or "closed") wrap, three-sided (U-wrap), and two-sided wrap, as shown in Fig. 4.37. Each standard mentions these three types, and some offer recommendations and comments, which are summarized below.

4.3.2.1 ACI

ACI notes that the completely wrapped scheme is the most efficient, followed by the three-sided U-wrap, although complete wrap is more common in columns. In all wrapping schemes the FRP system can be installed continuously along the span of a member or placed as discrete strips (Fig. 4.36). However, the use of continuous FRP that completely encases a member is discouraged since it potentially prevents migration of trapped moisture.

4.3.2.2 AASHTO

Similar to ACI, AASHTO notes that the two-sided wrap is least effective, as it is subject to premature debonding under high shear loads. Similarly, U-wrap schemes may debond prior to a complete wrap scheme, but U-wrap is popular in practice because of its wide applicability and ease of installation. U-wrap, or U-jacketing, can be combined with anchorage to increase the effectiveness of the FRP by anchoring the fibers, preferably, in the compression zone. Properly design anchors can result in the fibers reaching their tensile capacity prior to debonding, permitting the jacket to behave as if it were completely wrapped.

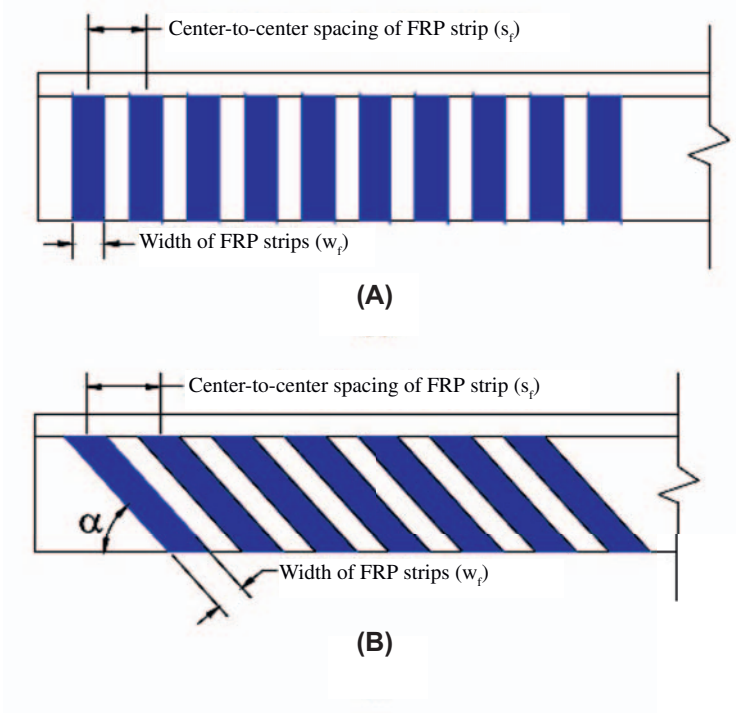

Figure 4.36 (A) Fibers at 90 degree direction, (B) fibers at inclined direction (AASHTO).

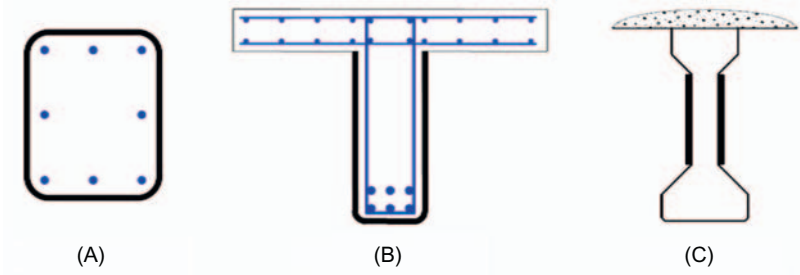

Figure 4.37 Recommended application of wrapping schemes in ISIS. (A) Closed wrapping; (B) U-shaped stirrups; (C) Side bonding.

4.3.2.3 ISIS

As with ACI and AASHTO, ISIS recommends the use of closed wrapping in beams whenever possible as this approach is most effective. U-shaped stirrups are recommended when access to the full perimeter of the beam is not possible, as in the case of a T-beam. In the case of AASHTO-type beams (Fig. 4.37) or shear walls, side bonding is the only form of strengthening possible. ISIS notes that

two- and three-sided schemes are bond critical and, depending on shear value (discussed in ISIS section 7.4.2), may require anchorage. Fig. 4.38 illustrates the typical anchoring systems described in ISIS.

4.3.2.4 CNR

CNR notes that, for U-wrap schemes, delamination of the ends of the FRP reinforcement can be avoided by using anchors in the form of laminates/sheets and/or bars installed in the direction of the member longitudinal axis. In such cases, the behavior of the U-wrap can be considered equivalent to that of a completely wrapped member.

4.3.2.5 TR55

TR55 recommends that the FRP is placed such that the principal fiber orientation is either 45 or 90 degrees to the longitudinal axis of the member.

4.3.2.6 Wrapping schemes—summary

In summary, there is little difference in the wrapping schemes presented and recommended by the different codes. Essentially, completely wrapped sections, three-sided wrap, and two-sided wrap are considered, where the wrapping can be continuous or in parallel strips either at 90 degrees to the member direction or at an inclined angle. Detailed provisions to determine the strength of such schemes differs somewhat among codes and is discussed in Section 4.3.6.

4.3.3 Strength reduction factors

FRP shear strength reduction factors are summarized in Fig. 4.39 for the different codes. The largest reduction value (most conservative) is adopted by ISIS (0.56) and the smallest value (least conservative) is adopted by AASHTO (0.85). It is noted that AASHTO uses other limits such as restricting the maximum FRP stirrup spacing, depending on the total shear value. Similar to flexure, the highly conservative reduction factor for shear given by ISIS is attributed to the fact that the ISIS factor incorporates environmental and material reduction factors as well.

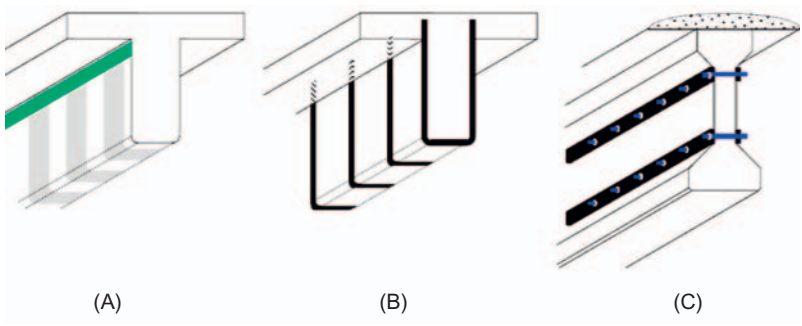

Figure 4.38 Typical anchoring systems for FRP shear reinforcement described in ISIS. (A) Longitudinal strips; (B) In-slab bonding; (C) Clamping plates.

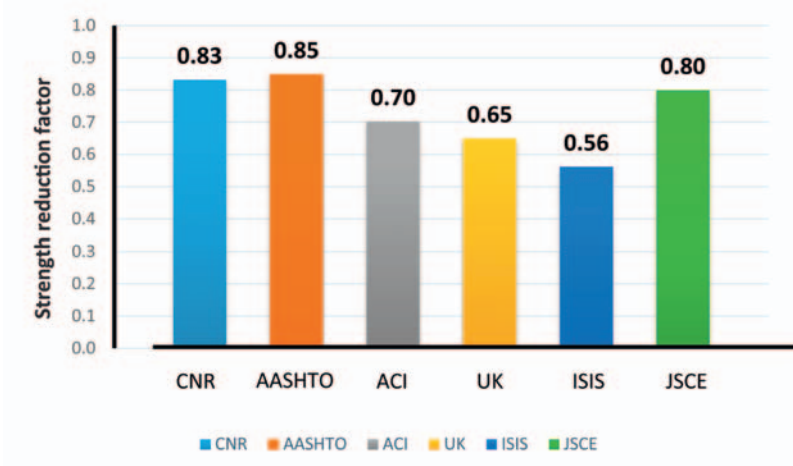

Figure 4.39 FRP strength reduction factor.

4.3.4 Reinforcement limits and spacing limits

4.3.4.1 ACI

Shear strengthening limits

The sum of the shear strengths provided by the FRP and existing shear reinforcement are to be limited to the criteria given for steel alone, as given in ACI 318. This limit is given in terms of four times the nominal shear strength of the concrete ($2\sqrt{f'_c}b_w d$), and is expressed as

$$V_s + V_f \leq 8\sqrt{f'_c}\, b_w d \quad \text{in.-lb units} \qquad (4.68 - \text{ACI Eq. } 11.11)$$

$$V_s + V_f \leq 0.66\sqrt{f'_c}\, b_w d \quad \text{SI units} \qquad (4.69)$$

Spacing of FRP strips

For external FRP shear strengthening in the form of discrete strips, ACI specifies limits in articles 11.1 and 11.4.2. Article 11.1 stipulates that the center-to-center spacing between the strips should not exceed the sum of *d*/4 plus the width of the strip. Moreover, Article 11.4.2 states that spacing limits should follow those given in ACI 318, which are as follows (Eqs. (4.70) and (4.71)):

$$\text{For } V_s + V_f \leq 4\sqrt{f'_c}\, b_w\, d \quad S_{\max} = \frac{d}{2} \leq 24 \text{ in.} \qquad (4.70)$$

$$\text{For } V_s + V_f > 4\sqrt{f'_c}\, b_w\, d \quad S_{\max} = \frac{d}{4} \leq 12 \text{ in.} \qquad (4.71)$$

4.3.4.2 AASHTO

Maximum FRP shear reinforcement

In AASHTO the amount of FRP used cannot result in a section with nominal shear strength exceeding the limit given in Eq. (4.72):

$$V_n = 0.25 f'_c b_v d_v + V_p \qquad (4.72 - \text{AASHTO Eq. 5.8.3.3-2})$$

where

$$V_n = V_c + V_s + V_{frp} \qquad (4.73)$$

The factored shear strength, V_r, is defined as

$$V_r = \phi(V_c + V_s + V_p) + \phi_{frp} V_{frp} \qquad (4.74 - \text{AASHTO Eq. 4.3.1-1})$$

where V_c = the nominal shear strength provided by the concrete in accordance with Article 5.8.3.3 of the AASHTO *LRFD Bridge Design Specifications*

$$= 0.0316\beta\sqrt{f'_c} b_v d_y \qquad (4.75 - \text{AASHTO Eq. 5.8.3.3-3})$$

V_s = the nominal shear strength provided by the transverse steel reinforcement in accordance with Article 5.8.3.3 of the AASHTO LRFD Bridge Design Specifications

$$= \frac{A_v f_{yt}.d_v(\cot\theta + \cot\alpha \sin\alpha)}{S_v} \qquad (4.76 - \text{LRFD Eq. 5.8.3.3-4})$$

where

$$d_v = \max(d_{v1}, d_{v2}, d_{v3}) \qquad (4.77)$$

$$d_{v1} = d - \frac{a}{2}, d_{v2} = 0.9d, d_{v3} = 0.72h_T$$

V_p = component of the effective prestressing force in the direction of applied shear as specified in Article 5.8.3.3 of the AASHTO *LRFD Bridge Design Specifications*; V_{frp} = the nominal shear strength provided by the externally bonded FRP system in accordance with AASHTO Article 4.3; $\phi = 0.9$; ϕ_{frp} = FRP resistance factor = 0.85.

4.3.4.3 Summary

Table 4.21 summarizes expressions for shear reinforcement limits by different codes, while Table 4.22 summarizes spacing limits.

As shown in Table 4.21 the maximum combined shear contribution is a fixed value for a given section. For this reason the amount of allowable FRP shear reinforcement depends upon the amount of steel shear reinforcement present in the

Table 4.21 Maximum shear resistance allowed

Code	Limit	Equation
AASHTO	Maximum total allowable shear	$V_n = 0.25 f'_c b_v d_v + V_p$ where $V_n = V_c + V_s + V_f$
CNR	Maximum total allowable shear	$V_{Rd,\max} = 0.3 f_{cd} bd$
ACI	Max. shear by steel and FRP	$V_s + V_f \le 8\sqrt{f'_c}\, b_w d$ in-lbs units $V_s + V_f \le 0.66\sqrt{f'_c}\, b_w d$ SI units
UK	Maximum permissible shear stress	$0.8\sqrt{f_{cu}}$ or 675 psi (5 N/mm^2)
ISIS	Max. strengthening (bridge code)	$V_c + V_s + V_{FRP} \le 0.25 \phi_c f'_c b_v d_v$

Table 4.22 Maximum spacing of FRP shear reinforcement

Code	Equation
AASHTO	For $v_u < 0.125 f'_c$, use $S_{\max} = 0.8 d_v \le 24$ in. For $v_u > 0.125 f'_c$, use $S_{\max} = 0.4 d_v \le 12$ in.
CNR	2 in (50 mm) $\le w_f \le$ 10 in. (250 mm), and $w_f \le p_f \le \min\{0.5d, 3\, w_f, w_f + 8$ in. (200) mm$\}$
ACI	$S_{FRP} \le w_{FRP} + \dfrac{d_{FRP}}{4}$ For $V_s + V_f \le 4\sqrt{f'_c}\, b_w\, d$, use $S_{\max} = \dfrac{d}{2} \le 24$ in. For $V_s + V_f > 4\sqrt{f'_c}\, b_w\, d$, use $S_{\max} = \dfrac{d}{4} \le 12$ in.
ISIS	Bridge code S6-06: $S_{FRP} \le w_{FRP} + \dfrac{d_{FRP}}{4}$ Building code: $s \le 0.75\, d_v \le 24$ in. (600 mm) for $\dfrac{V_f - V_p}{b_v d_v} < 0.1 \phi_c f'_c$ $s \le 0.33\, d_v \le 12$ in. (300 mm) for $\dfrac{V_f - V_p}{b_v d_v} \ge 0.1 \phi_c f'_c$

section (and associated shear capacity of the steel stirrups V_s). The effect of the existing level of V_s on the allowed FRP shear capacity (V_f) is shown in Fig. 4.40, for different ratios of V_s/V_c and values of f'_c. An obvious observation is the increase in allowed FRP shear strengthening with an increase of f'_c. It is also seen that ACI is most restrictive, while CNR allows the most strengthening, while AASHTO and ISIS fall between these bounds. Notice that for ACI, with a V_s/V_c ratio of 4.0, no FRP shear strengthening is allowed (Fig. 4.40) (Fig. 4.41).

The effect of the FRP strip width on spacing limits for different codes is evaluated for different beam depth using beam dimensions provided in Section 4.3.6.7 of this book. Beam depths considered are 12, 24, 36, 48, and 60 in. Figs. 4.41–4.45 present the maximum spacing limits as a function of strip width for different codes.

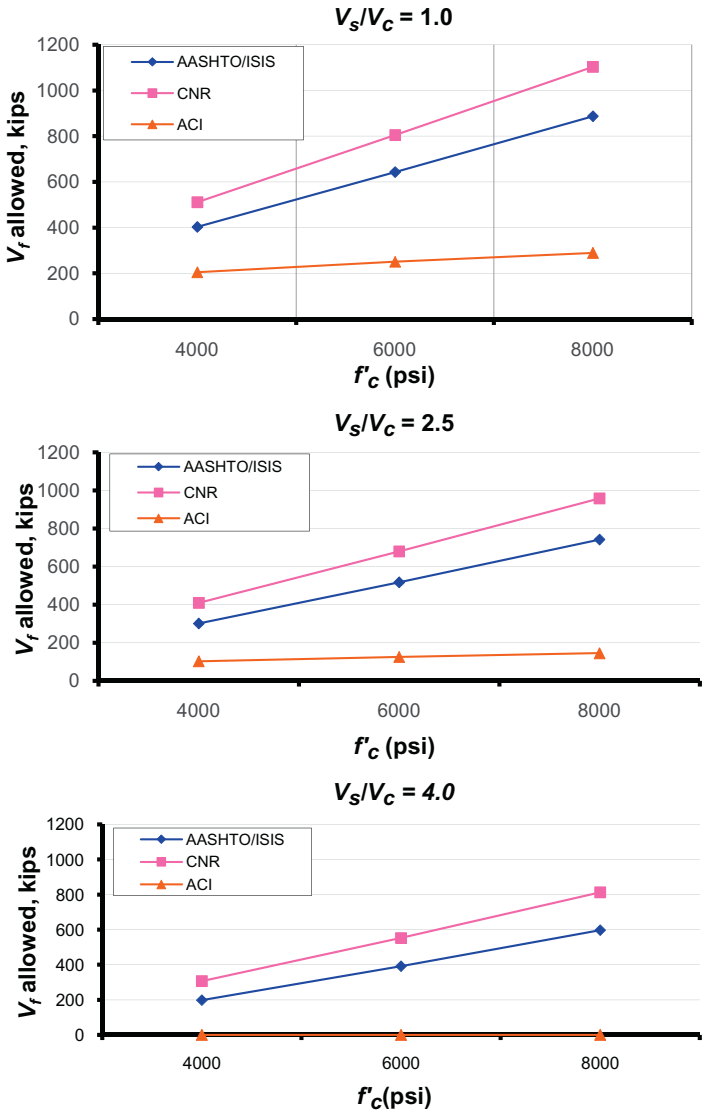

Figure 4.40 Effect of V_s/V_c on allowed V_f.

Except for CNR and ISIS, codes have different maximum spacing limits depending the applied shear value. For most codes, spacing limits for low shear values fall between 10 in. and 20 in., while for high shear values, limits fall between 5 in. and 10 in. Limits are generally expressed as a function of concrete compressive strength. However, the ISIS S6-06 bridge code spacing limit is independent of concrete compressive strength f'_c and is a function of the depth d_{FRP} and strip width w_{FRP}.

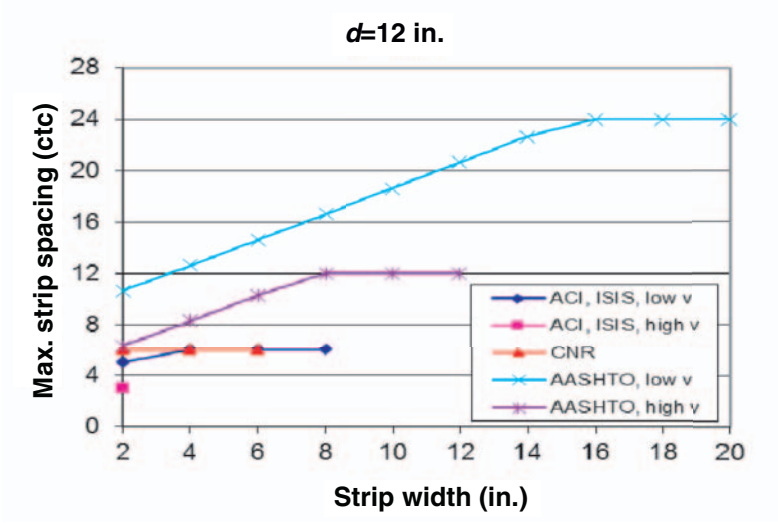

Figure 4.41 Effect of strip width on maximum strip spacing, $d = 12$ in.

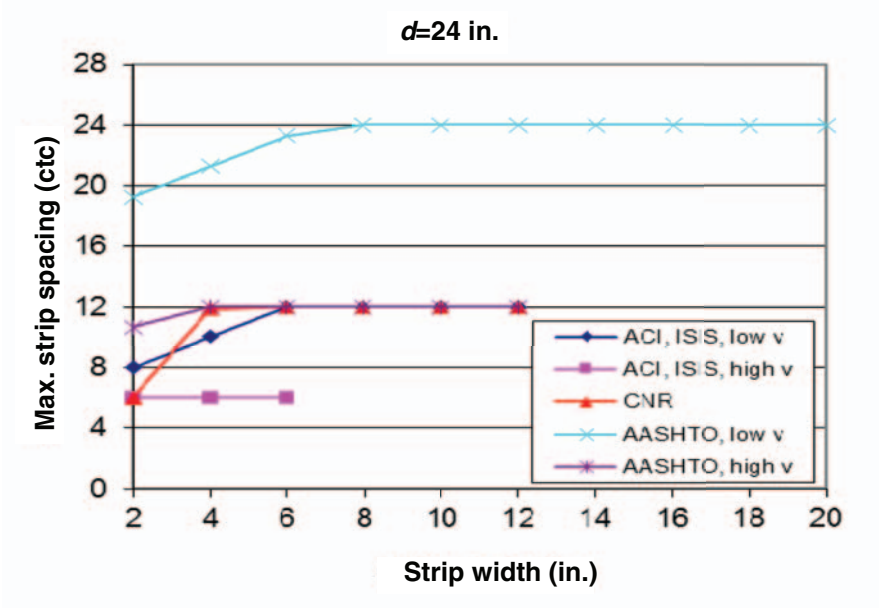

Figure 4.42 Effect of strip width on maximum strip spacing, $d = 24$ in.

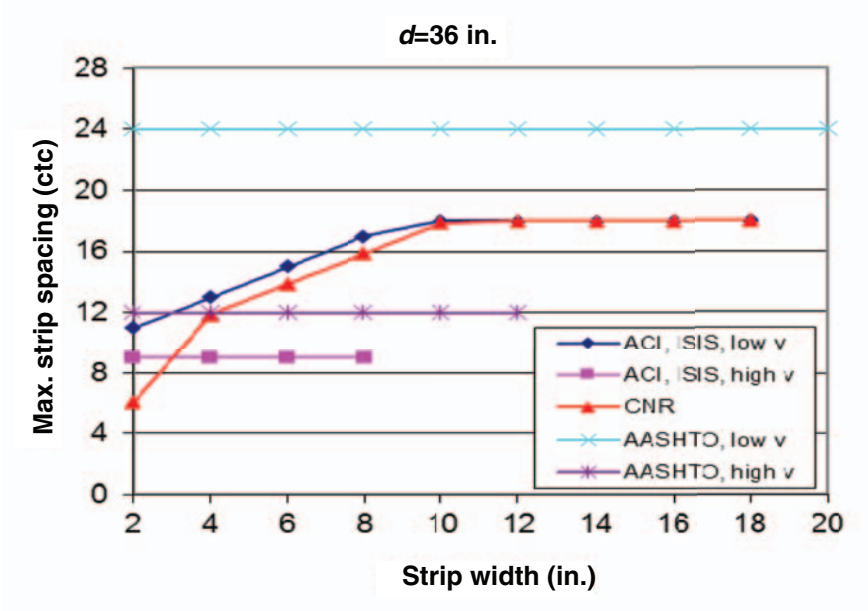

Figure 4.43 Effect of strip width on maximum strip spacing, $d = 36$ in.

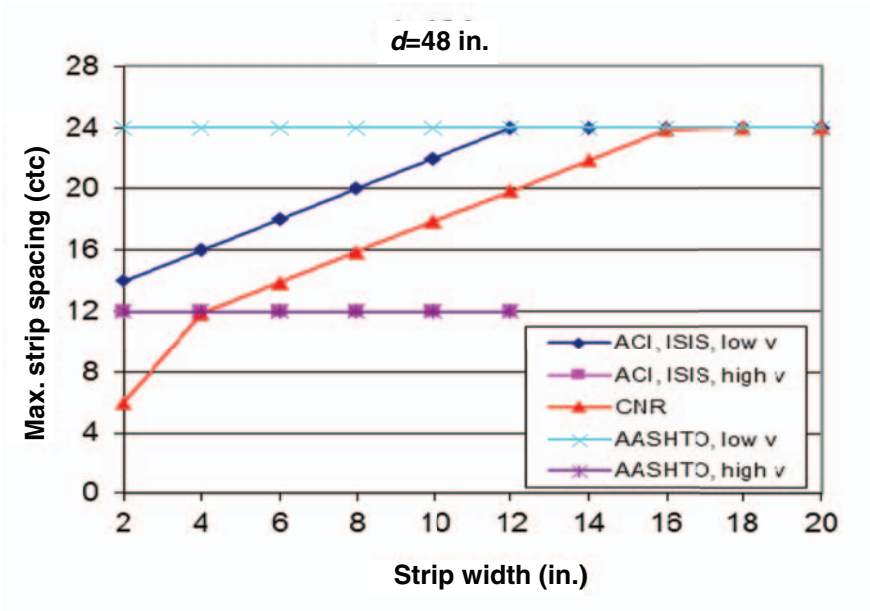

Figure 4.44 Effect of strip width on maximum strip spacing, $d = 48$ in.

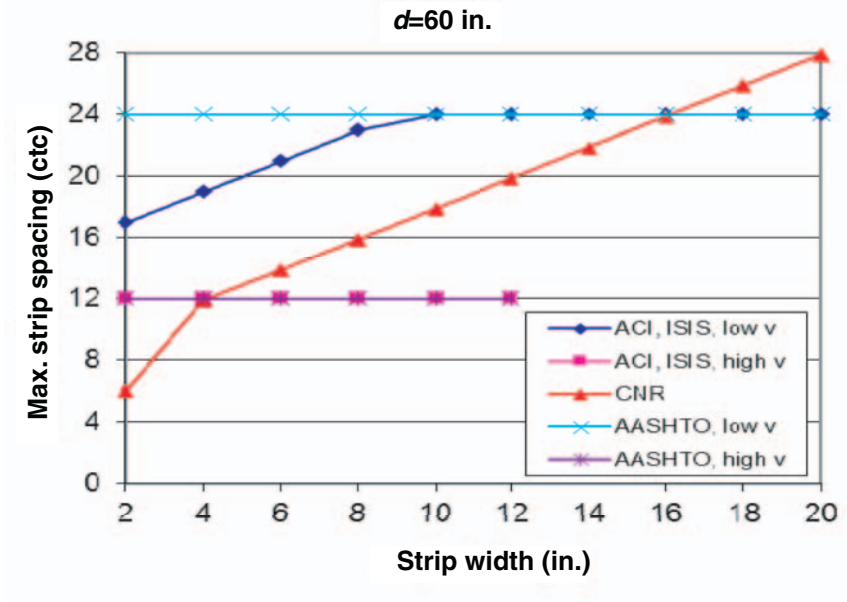

Figure 4.45 Effect of strip width on maximum strip spacing, $d = 60$ in.

4.3.5 FRP design strain limits

4.3.5.1 ACI

For completely wrapped members with FRP, ACI sets the following FRP strain limit to prevent wide cracks from forming that could cause a loss of aggregate interlock in the concrete (Eq. (4.78), ACI Eq. 11-6a):

$$\varepsilon_{fe} = 0.004 \leq 0.75\varepsilon_{fu} \qquad (4.78 - \text{ACI Eq. 11-6a})$$

For U-wrap and two-sided wrap schemes, aggregate interlock is preceded by FRP delamination. Therefore setting strain limits to prevent delamination failure is the control criterion. The following strain limit equation incorporates a bond-reduction coefficient κ_v applicable to shear (Eq. (4.79), ACI Eq. 11.6b):

$$\varepsilon_{fe} = \kappa_v \varepsilon_{fu} \leq 0.004 \qquad (4.79 - \text{ACI Eq. 11.6b})$$

where

$$\kappa_v = \frac{k_1 k_2 L_e}{468\varepsilon_{fu}} \leq 0.75 \quad \text{(in.-lb units)} \qquad (4.80 - \text{ACI Eq. 11.7})$$

$$\kappa_v = \frac{k_1 k_2 L_e}{11900\varepsilon_{fu}} \le 0.75 \quad \text{(SI units)}$$

$$L_e = \frac{2500}{(n_f t_f E_f)^{058}} \quad \text{(in.-lb units)} \qquad (4.81 - \text{ACI Eq. } 11.8)$$

$$L_e = \frac{23300}{(n_f t_f E_f)^{058}} \quad \text{(SI units)}$$

$$k_1 = \left(\frac{f'_c}{4000}\right)^{2/3} \quad \text{(in.-lb units)} \qquad (4.82 - \text{ACI Eq. } 11.9)$$

$$k_1 = \left(\frac{f'_c}{27}\right)^{2/3} \quad \text{(SI units)}$$

$$k_2 = \begin{cases} \dfrac{d_{fv} - L_e}{d_{fv}} & \text{for U-wraps} \\ \dfrac{d_{fv} - 2L_e}{d_{fv}} & \text{for two sides bonded} \end{cases} \qquad (4.83 - \text{ACI Eq. } 11.10)$$

4.3.5.2 AASHTO

AASHTO specifies the effective FRP strain, ε_{fe}, which represents the average strain experienced by the FRP at shear failure of the strengthened member. When the FRP is fully anchored, as in the case of complete wrap or for U-wrap with anchors, FRP rupture is the expected mode of failure. The strain limit to prevent such a failure is expressed as follows:

$$\varepsilon_{fe} = R_f \varepsilon_{fu} \qquad (4.84)$$

where

$$R_f = 0.088 \le 4(\rho_f E_f)^{-0.67} \le 1.0 \qquad (4.85)$$

In the case of side bonding or U-wrap with other anchorage causing nonrupture failures to be the more likely mode of failure, the expression for strain limit is as follows:

$$\varepsilon_{fe} = R_f \varepsilon_{fu} \le 0.004 \qquad (4.86)$$

where

$$R_f = 0.06 \leq 3(\rho_f E_f)^{-0.67} \leq 1.0 \tag{4.87}$$

The reduction factor, R_f, is to be found from tests in which the load is applied at a distance from the support sufficient to assume that plane sections before deformation remain plane after deformation, i.e., slender beam behavior. Thus these provisions are only applicable to beams with a shear span-to-depth ratio greater than 2.5.

4.3.5.3 ISIS

The reviewed ISIS procedure to establish strain limits is taken from the S6-06 bridge code. Strain limits are specified in Eqs. (4.88)–(4.90) (7.3) with limits for FRP strength given by Eq. (4.88) (7.3a), aggregate interlock by Eq. (4.89) (7.3b), and bond critical applications such as U-shaped FRP stirrups by Eq. (4.90) (7.3c).

$$\varepsilon_{FRPe} \leq 0.75\varepsilon_{FRPu} \quad \text{FRP strength} \qquad (4.88 - \text{ISIS Eq. 7-3a})$$

$$\varepsilon_{FRPe} \leq 0.004 \quad \text{aggregate interlock} \qquad (4.89 - \text{ISIS Eq. 7-3b})$$

$$\varepsilon_{FRPe} \leq k_v\varepsilon_{FRPu} \quad \text{bond capacity (U-wrap only)} \qquad (4.90 - \text{ISIS Eq. 7-3c})$$

Eq. (4.90) requires the evaluation of the bond-reduction coefficient κ_v. The steps for calculating κ_v are identical to those described for ACI, above.

4.3.5.4 Summary

Table 4.23 summarizes the shear strengthening strain limits. UK and CNR have fixed strain limits of 0.004 for U-wrap and side wrap, while CNR has a limit of 0.005 for a completely wrapped system.

4.3.6 Shear design approach and assumptions

4.3.6.1 ACI

The goal of the analytical procedure described in ACI is to evaluate FRP shear resistance V_f while applying applicable strain limits necessary to meet strength, aggregate interlock, and bond requirements. The following are the steps needed for FRP shear calculation.

Step 1: Evaluate the bond reduction coefficient κ_v (provided in the strain limits section above).

Table 4.23 Specified maximum FRP strain for different codes

Code	Application	Equation
AASHTO	U-wrap and two sided	$\varepsilon_{fe} = R_f \varepsilon_{fu} \le 0.004$ where $R_f = 0.06 \le 3(\rho_f E_f)^{-0.67} \le 1.0$
	Completely wrapped	$\varepsilon_{fe} = R_f \varepsilon_{fu}$ where $R_f = 0.088 \le 4(\rho_f E_f)^{-0.67} \le 1.0$
CNR	Completely wrapped	ε_f, max = 0.005
	U-wrap and two sided	0.004
UK	U-wrap	0.004
ACI	Completely wrapped	$\varepsilon_{fe} = 0.004 \le 0.75\varepsilon_{fu}$
	U-wrap and two sided	$\varepsilon_{fe} = K_v \varepsilon_{fu} \le 0.004$
ISIS	All wrapping cases	$\varepsilon_{\mathrm{FRP}e} \le 0.75\varepsilon_{\mathrm{FRP}u}$ $\varepsilon_{\mathrm{FRP}e} \le 0.004$
	U-shaped FRP stirrups only	$\varepsilon_{\mathrm{FRP}e} \le K_v \varepsilon_{\mathrm{FRP}u}$

$$\kappa_v = \frac{k_1 k_2 L_e}{468\varepsilon_{fu}} \le 0.75 \quad \text{(in.-lb units)} \qquad (4.80 - \text{ACI Eq. 11-7})$$

$$\kappa_v = \frac{k_1 k_2 L_e}{11900\varepsilon_{fu}} \le 0.75 \quad \text{(SI units)}$$

Step 2: Evaluate ε_{fe} for U-wrap case using the strain limit equation:

$$\varepsilon_{fe} = \kappa_v \varepsilon_{fu} \le 0.004 \qquad (4.79 - \text{ACI Eq. 11-6b})$$

Step 3: Calculate the effective stress of FRP, f_{fe}:

$$f_{fe} = E_f \varepsilon_{fe} \qquad (4.91 - \text{ACI Eq. 11-5})$$

Step 4: Calculate FRP shear area, A_{fv}:

$$A_{fv} = 2nt_f w_f \qquad (4.92 - \text{ACI Eq. 11-4})$$

Step 5: Calculate shear resistance for FRP, V_f:

$$V_f = \frac{A_{fv} f_{fe} (\sin\alpha + \cos\alpha) d_{fv}}{S_f} \qquad (4.93 - \text{ACI Eq. 11-3})$$

For a 90 degree angle (i.e., vertically placed strips), $(\sin\alpha + \cos\alpha) = 1$, as per the assumption in Eq. (4.95).

Step 6: Calculate shear resistance by concrete and steel:

$$V_c = 2\lambda\sqrt{f'_c}b_w d \tag{4.94}$$

$$V_s = \frac{A_v f_y d}{s} \tag{4.95}$$

Step 7: Calculate nominal and factored shear by concrete, steel, and FRP:

$$V_n = V_c + V_s + V_f$$

$$\phi V_n = \phi(V_c + V_s + V_f)$$

4.3.6.2 ISIS

The ISIS procedure to calculate the shear resistance of FRP is as follows:

Step 1: Evaluate d_{FRP}:

d_{FRP} = The greater of $0.72h$ or $0.9d$

Step 2: Choose the smallest FRP strain value from the following conditions (ISIS Eq. 7.3):

$\varepsilon_{\text{FRP}e} \leq 0.75\varepsilon_{\text{FRP}u}$ FRP strength (4.88 – ISIS Eq. 7-3a)

$\varepsilon_{\text{FRP}e} \leq 0.004$ aggregate interlock (4.89 – ISIS Eq. 7-3b)

$\varepsilon_{\text{FRP}e} \leq \kappa_v\varepsilon_{\text{FRP}u}$ bond capacity (U-wrap only) (4.90 – ISIS Eq. 7-3c)

Step 3: Use Eq. (4.32) to evaluate V_{FRP}:

$$V_{\text{FRP}} = \frac{\phi_{\text{FRP}}E_{\text{FRP}}\varepsilon_{\text{FRP}}A_{\text{FRP}}d_{\text{FRP}}(\cot\theta + \cot\beta)\sin\beta}{S_{\text{FRP}}} \tag{4.96 – ISIS Eq. 7-3c}$$

Step 4: Calculate the shear resistance of concrete and steel (building code):

$V_c = 0.2\lambda\phi_c\sqrt{f'_c}b_v d$ for beams (4.97 – ISIS Eq. 7-22a)

$V_c = 0.2\lambda\phi_c\sqrt{f'_c}0.8\,A_g$ for columns (4.98 – ISIS Eq. 7-22b)

$V_c = 0.2\lambda\phi_c\sqrt{f'_c}0.8\,b_v L$ for walls (4.99 – ISIS Eq. 7-22c)

$$V_s = \frac{\phi_s f_y A_v d}{s} \qquad (4.100 - \text{ISIS Eq. } 7.21)$$

Step 6: Calculate the total shear capacity of the concrete, steel, and FRP:

$$V_r = V_c + V_s + V_{\text{FRP}}$$

Note: When computing the unfactored total shear, the reduction factors ϕ_c, ϕ_s, and ϕ_{FRP} are dropped from the equations for V_c, V_s, and V_{FRP}.

4.3.6.3 AASHTO

The AASHTO procedure is as follows:

Step 1: Evaluate the nominal shear resistance of the concrete:

$$V_c = 0.0316\beta\sqrt{f'_c}\, b_v\, d_v \qquad (4.101)$$

Assuming $\beta = 2$ and $\theta = 45^\circ$ (simplified procedure), $d = \text{Max}\,(d - \frac{a}{2}, 0.9d, 0.72h_T)$

Step 2: Evaluate the nominal shear resistance of the steel:

$$V_s = \frac{A_v f_y d_v(\cot\theta + \cot\alpha)\sin\alpha}{S} \qquad (4.102)$$

where $S =$ internal shear reinforcement spacing; $A_v =$ area of internal shear reinforcement.

Step 3: Evaluate the nominal shear resistance of the FRP:

$$V_{frp} = \rho_f E_f \varepsilon_{fe} b_v d_f(\sin\alpha_f + \cos\alpha_f) \qquad (4.103 - \text{AASHTO Eq. } 4.3.2\text{-}1)$$

where $\rho_f =$ reinforcement ratio of FRP.

$$\text{for discrete strips,}\quad \rho_f = \frac{2n_f t_f w_f}{b_v s_f} \qquad (4.104)$$

$$\text{for continuous sheets,}\quad \rho_f = \frac{2n_f t_f}{b_v} \qquad (4.105)$$

$t_f =$ FRP reinforcement thickness; $w_f =$ width of the strip; $s_f =$ center-to-center spacing of FRP; $b_v =$ effective web width taken as the minimum web width within the effective depth (d_f); $f_{fe} =$ effective stress of FRP; $d_f =$ effective depth of FRP measured from the top of FRP reinforcement to the centroid of the longitudinal reinforcement; $\alpha_f =$ angle of inclination of FRP with respect to the longitudinal axis of the member; $E_f =$ modulus of elasticity of FRP; $\varepsilon_{fe} =$ effective strain of FRP (refer to Eqs. (4.84)−(4.87)).

Step 4: Evaluate the nominal shear resistance of the member:

$$V_n = V_c + V_s + V_{\text{FRP}}$$

AASHTO GFRP

The steps to calculate shear resistance for AASHTO GFRP are as follows:

Step 1: Evaluate the nominal shear resistance provided by the concrete:

$$V_c = 0.16\sqrt{f'_c}\, b_w\, c \le 0.32\sqrt{f'_c}\, b_o\, c \tag{4.106}$$

where

c = distance from extreme compression fiber to neutral axis, in.
$= kd$
k = ratio of depth of neutral axis to reinforcement depth

$$k = \sqrt{2\rho_f n_f + (\rho_f n_f)^2} - \rho_f n_f \tag{4.107 – AGFRP Eq. 2.7.3-4}$$

b_w = width of web, in.; d = distance from extreme compression fiber to centroid of tension reinforcement, in.; b_o = perimeter of critical section computed at $d/2$ away from the concentrated load (in.).

Note: the shape of the critical section is taken as the same shape of the concentrated load.

Step 2: Evaluate design tensile strength for shear:

$$f_{fv} = 0.004E_f \le f_{fb} \tag{4.108}$$

where

$$f_{fb} = \left(0.005\frac{r_b}{d_b} + 0.3\right) f_{fd} \le f_{fd} \tag{4.109}$$

E_f = modulus of elasticity of GFRP reinforcement, ksi; f_{fb} = strength of the bent portion of a GFRP bar, ksi; r_b = internal radius of the bent GFRP bar, in.; d_b = GFRP bar diameter, in.; f_{fd} = design tensile strength of GFRP bars considering reduction for service environment, ksi.

Step 3: Evaluate the nominal shear resistance by the shear reinforcement, V_f.

$$V_f = \frac{A_{fv} f_{fv} d}{S} \tag{4.110}$$

Step 4: Evaluate the nominal shear resistance, V_n:

$$V_n = V_c + V_f \tag{4.111}$$

4.3.6.4 CNR

The CNR procedure is as follows (see Fig. 4.46):

Step 1: Evaluate the shear resistance of concrete:

$$V_{Rd,ct} = 0.6 f_{ctd} b d \delta \tag{4.112}$$

where

$$\delta = 1$$

$$f_{ctd} = 0.7 \frac{f_{ctm}}{\gamma_c} \tag{4.113}$$

$$f_{ctm} = 0.3 f_c'^{0.67} \tag{4.114}$$

$$\gamma_c = 1.6$$

Step 2: Evaluate the shear resistance of steel:

$$V_{Rd,s} = \frac{A_{sw}}{s} \cdot f_{ywd} \cdot 0.9d \tag{4.115}$$

where A_{sw}, s, and f_{ywd} represent area, spacing, and steel stirrups yield strength, respectively.

Step 3: Evaluate the effective FRP design strength:

For a U-wrap configuration:

$$f_{fed} = f_{fdd} \cdot \left[1 - \frac{1}{3} \cdot \frac{l_e \cdot \sin\beta}{\min\{0.9 \cdot d, h_w\}}\right] \tag{4.116}$$

For completely wrapped members having rectangular cross-sections:

$$f_{fed} = f_{fdd} \cdot \left[1 - \frac{1}{6} \cdot \frac{l_e \cdot \sin\beta}{\min\{0.9 \cdot d, h_w\}}\right] + \frac{1}{2}(\phi_R f_{fd} - f_{fdd}) \cdot \left[1 - \frac{l_e \cdot \sin\beta}{\min\{0.9 \cdot d, h_w\}}\right] \tag{4.117}$$

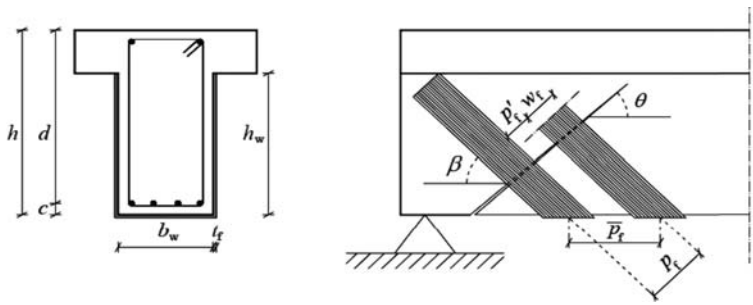

Figure 4.46 CNR shear strengthening notation (CNR).

where f_{fd} = design strength of FRP reinforcements.

$$\phi_R = 0.2 + 1.6\frac{r_c}{b_w}, \quad \text{and} \quad 0 \le \frac{r_c}{b_w} \le 0.5 \tag{4.118}$$

Step 4: Evaluate the FRP contribution to the shear capacity:
For a rectangular cross-section and FRP side bonding configuration:

$$V_{Rd,f} = \frac{1}{\gamma_{Rd}} \min\{0.9d, h_w\} f_{fed} 2t_f \frac{\sin\beta}{\sin\theta} \frac{w_f}{p_f} \tag{4.119}$$

For U-wrapped or completely wrapped configurations:

$$V_{Rd,f} = \frac{1}{\gamma_{Rd}} 0.9d f_{fed} 2t_f (\cot\theta + \cot\beta) \frac{w_f}{p_f} \tag{4.120}$$

Step 5: Evaluate the total shear capacity:

$$V_{Rd} = \min\{V_{Rd,ct} + V_{Rd,s} + V_{Rd,f}, V_{Rd,\max}\} \qquad (4.121 - \text{CNR Eq. 4.24})$$

where

$$V_{Rd,\max} = 0.3 f_{cd} bd \qquad (4.122 - \text{CNR Eq. 10.14})$$

$\gamma_{Rd} = 1.20$; d = member effective depth; h_w = stem depth; f_{fed} = effective FRP design strength; t_f = thickness of the adopted FRP system; w_f = FRP width; p_f = FRP spacing.

4.3.6.5 JSCE

The JSCE procedure is as follows:
Step 1: Evaluate the shear resistance of concrete:

$$V_{cd} = \beta_d \beta_p \beta_n f_{vcd} b_w \frac{d}{\gamma_b} \qquad (4.123 - \text{JSCE Eq. 6.4.4})$$

where

$$f_{vcd} = 0.2\sqrt[3]{f'_{cd}}(\text{N/mm}^2) \le 0.72(\text{N/mm}^2) \qquad (4.124 - \text{JSCE Eq. 6.4.5})$$

$$\beta_d = \sqrt[4]{1/d}(d\text{:m}), 1.5 \quad \text{when} \quad \beta_d > 1.5$$

$$\beta_p = \sqrt[3]{100 p_w}(d\text{:m}), 1.5 \quad \text{when} \quad \beta_p > 1.5$$

$$\begin{aligned} \beta_n &= 1 + M_0/M_d (N'_d \ge 0), \quad \text{when } \beta_n > 2 \\ &= 1 + 2M_0/M_d (N'_d \ge 0), \quad \text{when } \beta_n > 0 \end{aligned}$$

N'_d = design axial compressive force; M_d = design bending moment; M_0 = decompression moment; b_w = web width; d = effective depth; $p_w = A_s/(b_w \times d)$;

A_s = cross-sectional area of reinforcing bars in tension side; f'_{cd} = design compressive strength of concrete (N/mm^2); γ_b = member factor (in general, may be set to 1.3).

Step 2: Evaluate the shear resistance of steel:

$$V_{sd} = [A_w f_{wyd}(\sin \alpha_s + \cos \alpha_s)/S_s]Z/\gamma_b \qquad (4.125 - \text{JSCE Eq. 6.4.6})$$

where A_w = total cross-sectional area of shear reinforcement in spacing S_s; f_{wyd} = design tension yield strength of shear reinforcement [58 ksi max. (400 N/mm^2)]; α_s = angle formed by shear reinforcement about the member axis; s_s = spacing of shear reinforcement; z = lever arm length (generally may be set to d/1.15); γ_b = member factor (generally may be set to 1.15).

Step 3: Evaluate the effective FRP design strength:

$$V_{fd} = K[A_f f_{fud}(\sin \alpha_f + \cos \alpha_f)/S_f]Z/\gamma_b \qquad (4.126 - \text{JSCE Eq. 6.4.7})$$

where K = shear reinforcing efficiency of continuous fiber sheets according to Eq. (4.127) (JSCE Eq. 6.4.8).

$$K = 1.68 - 0.67R, \quad \text{however,} \quad 0.4 \le K \le 0.8 \qquad (4.127 - \text{JSCE Eq.6.4.8})$$

$$R = (\rho_f E_f)^{1/4} \left(\frac{f_{fud}}{E_f}\right)^{2/3} \left(\frac{1}{f'_{cd}}\right)^{1/3}, \quad \text{however,} \quad 0.5 \le R \le 2.0$$

$$\rho_f = A_f/(b_w s_f)$$

Step 4: Evaluate the total shear capacity:

$$V_{fyd} = V_{cd} + V_{sd} + V_{fd} \qquad (4.128 - \text{JSCE Eq. 6.4.3})$$

4.3.6.6 UK

The maximum allowable design shear force due to ultimate loads, $V_{R,\max}$ at any cross-section, is obtained from:

$$V_{R,\max} = v_{\max} \cdot b \cdot d \qquad (4.129 - \text{UK TR55 Eq. 7.1})$$

where $v_{\max}$ = maximum permissible shear stress; b = width of section; d = effective depth of section; $V_{R,\max}$ = min $\{0.8(f_{cu})^{0.5}, 5\ \text{N/mm}^2\}$.

Step 1: Evaluate the shear resistance of concrete (per BS 8110):

$$v_c = \frac{0.79}{\gamma_m}\left\{\frac{100A_s}{(b_v d\}}\right\}^{1/3}\left(\frac{400}{d}\right)^{1/4} \text{N/mm}^2 \qquad (4.130)$$

Step 2: Evaluate the shear resistance of steel (BS 8110):

$$V_s = \frac{0.87A_{sv}f_{yv}d}{s_v} \qquad (4.131)$$

Step 3: Evaluate the effective FRP design strength.

The amount of FRP required can be calculated using the same principles as in conventional reinforced concrete design. The shear resistance of the FRP is given by

$$V_{Rf} = \left(\frac{1}{\gamma_{mf}}\right) A_{fs}(E_{fd}\varepsilon_{fe})\sin\beta\,(1+\cot\beta)(d_f/s_f) \qquad (4.132 - \text{UK TR55 Eq. 7.3})$$

where A_{fs} = area of FRP shear reinforcement and $= 2t_f\, w_{fe}$ assuming that the FRP is placed on both sides of the member; w_{fe} = effective width of FRP, which is a function of shear crack angle and FRP strengthening configuration, equal to $(d_f - L_e)$ where FRP is in the form of a U-jacket and $(d_f - 2L_e)$, where FRP is bonded to side faces; L_e = effective bond length = $461.3/(t_f . E_{fd})^{0.58}$; ε_{fe} = design strain in the FRP; β = angle between FRP and the longitudinal axis of the member = 45° or 90°; d_f = effective depth of FRP shear reinforcement, usually equal to d for rectangular sections and $(d$ - slab thickness) for T-sections; s_f = spacing between the center line of FRP plates (see Section 4.7.3). Note that for continuous sheet reinforcement $s_f = w_{fe}$; γ_{mf} = partial safety factor for FRP.

Step 4: Evaluate the total shear capacity. Add the concrete, steel, and FRP shear components:

$$V_T = V_c + V_s + V_{Rf}$$

4.3.6.7 Summary

To identify the effect of different parameters on the shear capacity of beams according to the different code procedures, an example singly-reinforced rectangular beam section was examined. The example beam has a $f'_c = 4$ ksi, and grade 60 longitudinal steel with area $A_s = 3$ in.^{2}, and 3 stirrups spaced at 12 in. ($A_v = 0.22$ in.^{2}). The analysis includes the use of a single CFRP ply of BASF MBrace CF130 to strengthen the beam in shear with a U-wrap scheme. The critical variables explored include the width of the FRP shear strengthening strip and the spacing between strips.

All applicable code reduction factors are removed when calculating unfactored FRP shear results, which are presented in Figs. 4.47–4.50 for FRP stirrups. As shown in the figures, unfactored shear resistance values are very close for the different codes. As expected the FRP shear capacities increase as FRP spacing decreases. Strip width has a minimal impact on capacity.

When code reduction factors are applied, some significant differences in capacity are observed, as shown in Figs. 4.51–4.54 for FRP strips. Here, AASHTO and ACI consistently provide the largest design capacity values for FRP. Factored shear values for CNR, UK, and ISIS result in nearly identical values as well, but significantly lower than AASHTO and ACI, with shear resistance values approximately 30–40% higher than those provided by CNR, UK, and ISIS. Note that some code values do not appear on the graphs; this is due to a maximum strip spacing

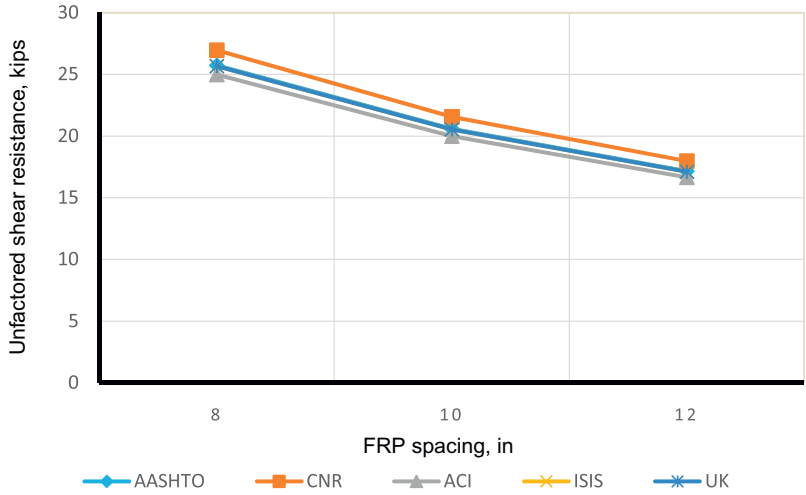

Figure 4.47 Unfactored fiber shear resistance versus FRP spacing, width = 6 in., U-wrap.

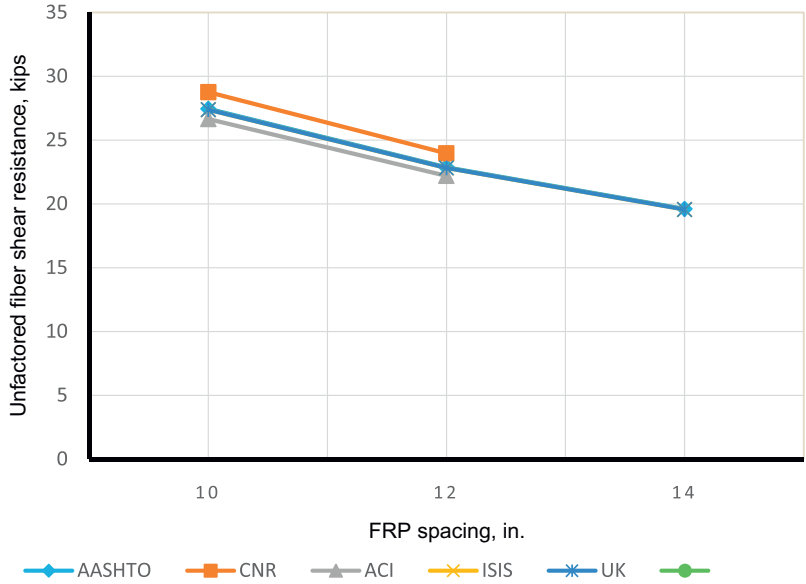

Figure 4.48 Unfactored fiber shear resistance versus FRP spacing, width = 8 in., U-wrap.

restriction. This is particularly apparent for ACI, which has relatively strict spacing requirements.

Figs. 4.55 and 4.56 illustrate the FRP shear resistance for continuous U-wrap. As shown in Fig. 4.55, results are similar for all codes. However, large differences emerge when reduction factors are applied, as shown in Fig. 4.56. Similar to the

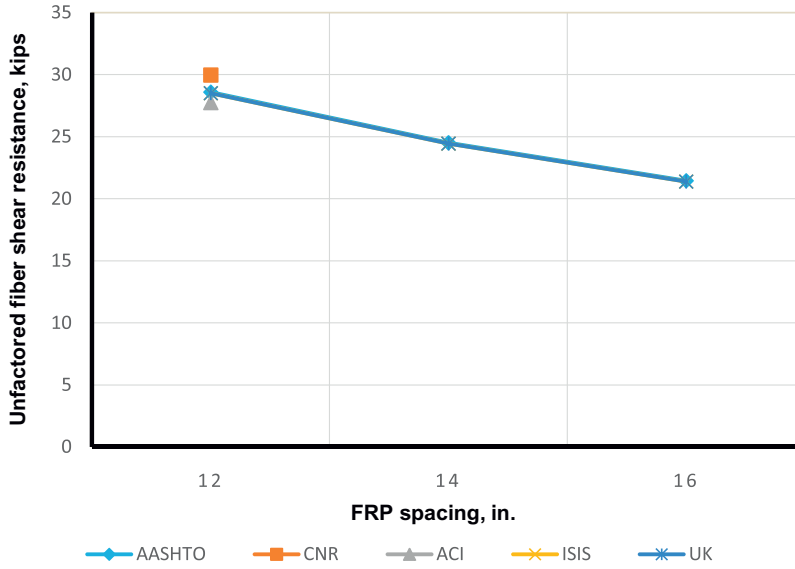

Figure 4.49 Unfactored fiber shear resistance versus FRP spacing, width = 10 in., U-wrap.

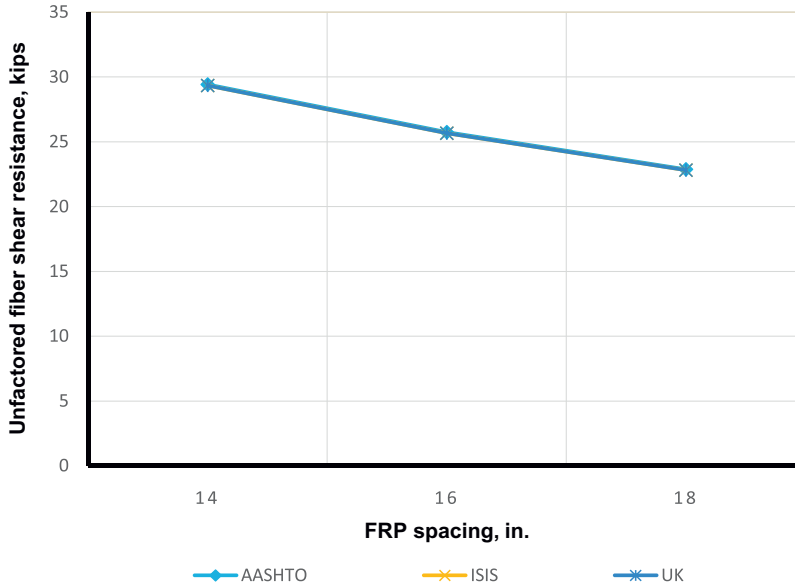

Figure 4.50 Unfactored fiber shear resistance versus FRP spacing, width = 12 in., U-wrap. Note that a 12 in. FRP width exceeds the maximum allowed in CNR (10 in.), and CNR results thus do not appear.

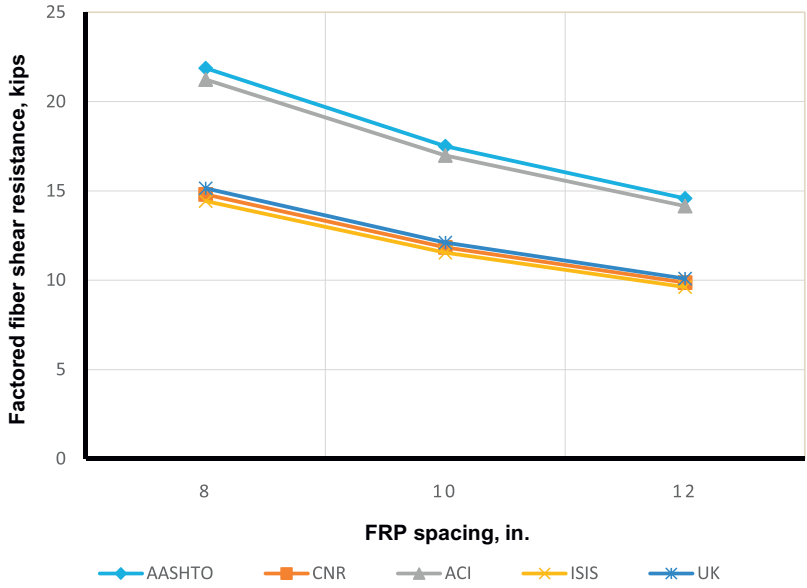

Figure 4.51 Factored fiber shear resistance versus FRP spacing, width = 6 in., U-wrap.

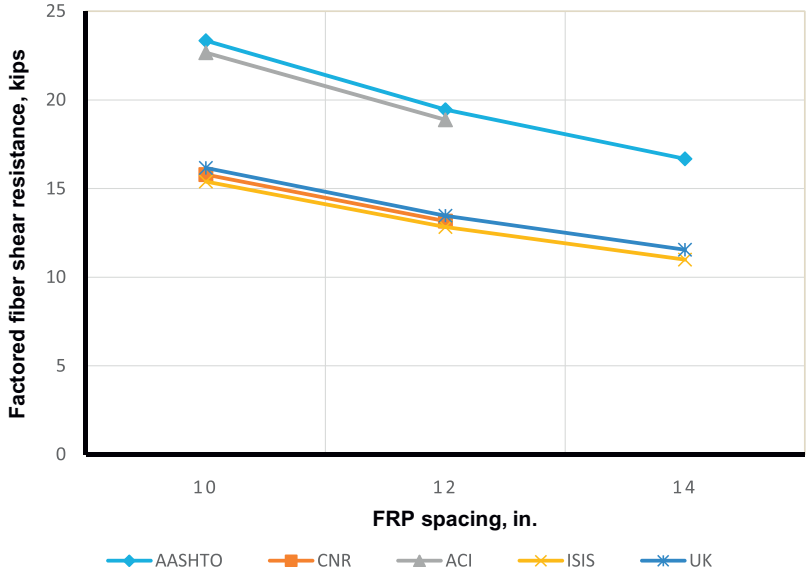

Figure 4.52 Factored fiber shear resistance versus FRP spacing, width = 8 in., U-wrap.

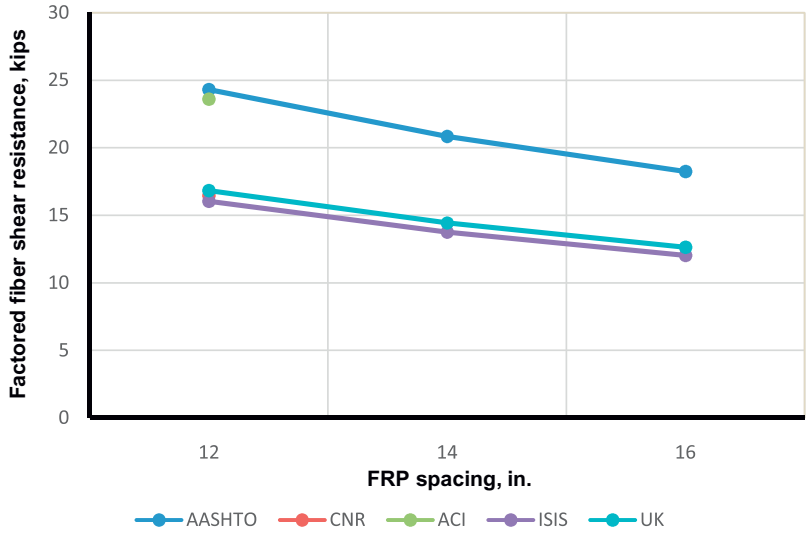

Figure 4.53 Factored fiber shear resistance versus FRP spacing, width = 10 in., U-wrap.

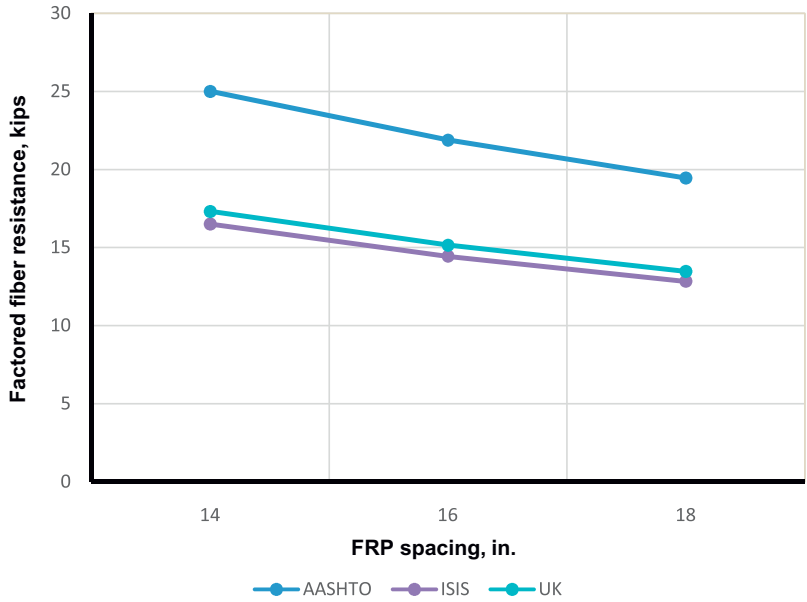

Figure 4.54 Factored fiber shear resistance versus FRP spacing, width = 12 in., U-wrap.

FRP strip case, AASHTO and ACI provide the highest (and similar) design capacities, while the remaining codes provide similar, lower capacities.

Figs. 4.57 and 4.58 compare two-sided to U-wrap results. In all cases, two-sided results consistently provide less capacity than U-wrap, as expected. Note, however, that AASHTO limits the maximum strain of FRP to 0.004 for both U-wrap and two sided schemes, and provides the same formula for shear resistance. Moreover, TR55 does not provide an explicit procedure to calculate two-sided shear capacity.

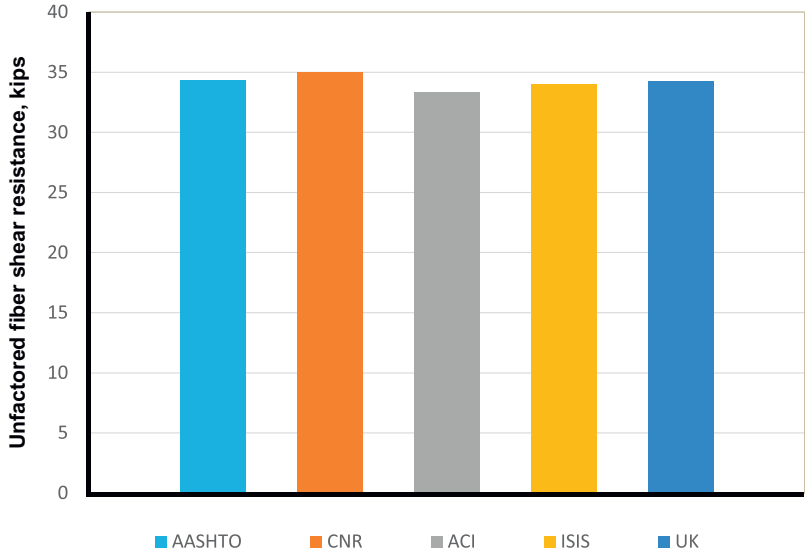

Figure 4.55 Unfactored fiber shear resistance, U-wrap, continuous.

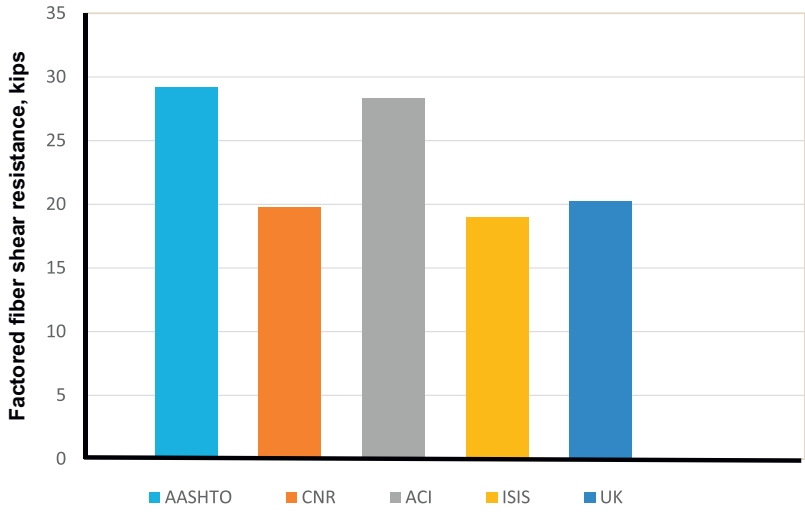

Figure 4.56 Factored fiber shear resistance, U-wrap, continuous.

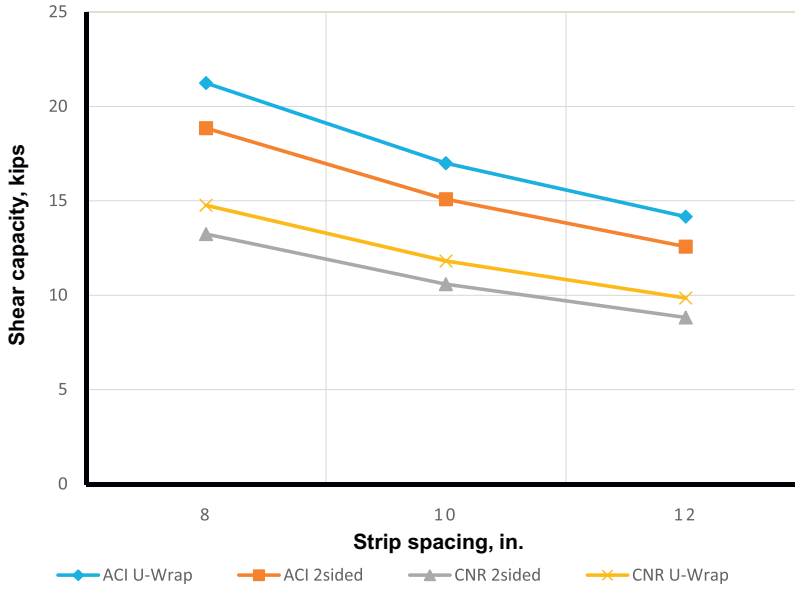

Figure 4.57 Effect of strip spacing on U-wrap and two-sided wraping, $w_f = 6$ in.

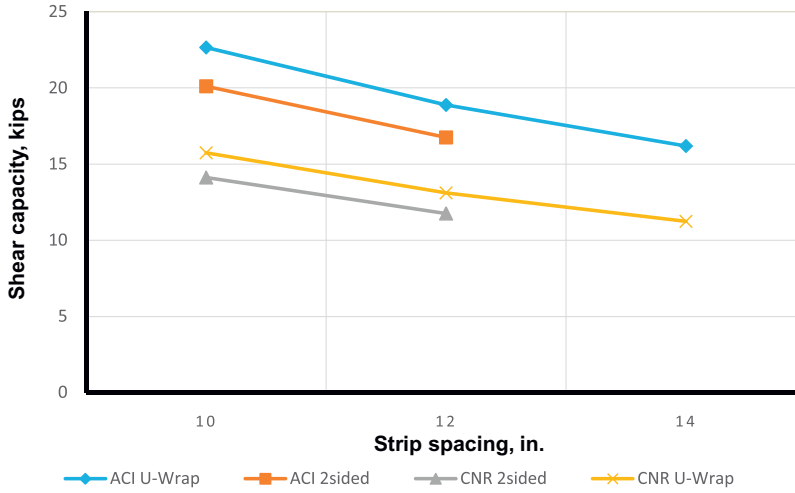

Figure 4.58 Effect of strip spacing on U-wrap and two-sided wraping, $w_f = 8$ in.

JSCE and ISIS do not offer any formula for calculating the shear resistance of two-sided wrap.

In Fig. 4.59 the effect of changing FRP strip width on the components of the total shear resistance (for a constant gap between strips of $d/4$, which is the maximum allowed for ACI code). ACI, AASHTO, and ISIS have somewhat similar

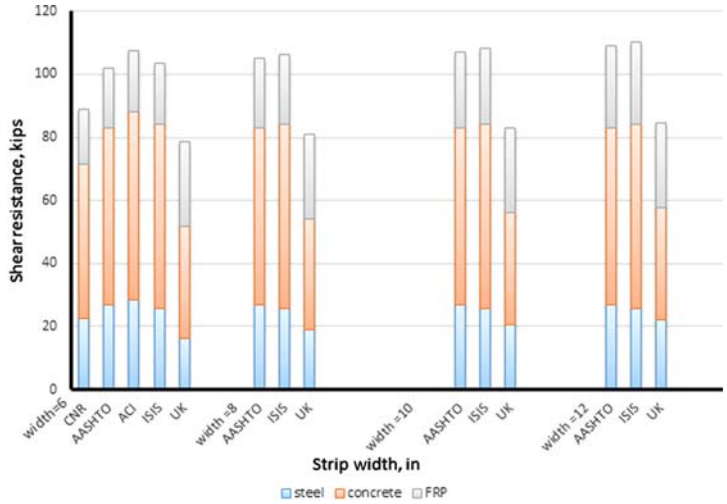

Figure 4.59 Effect of FRP strip width on total shear resistance when gap = *d*/4.

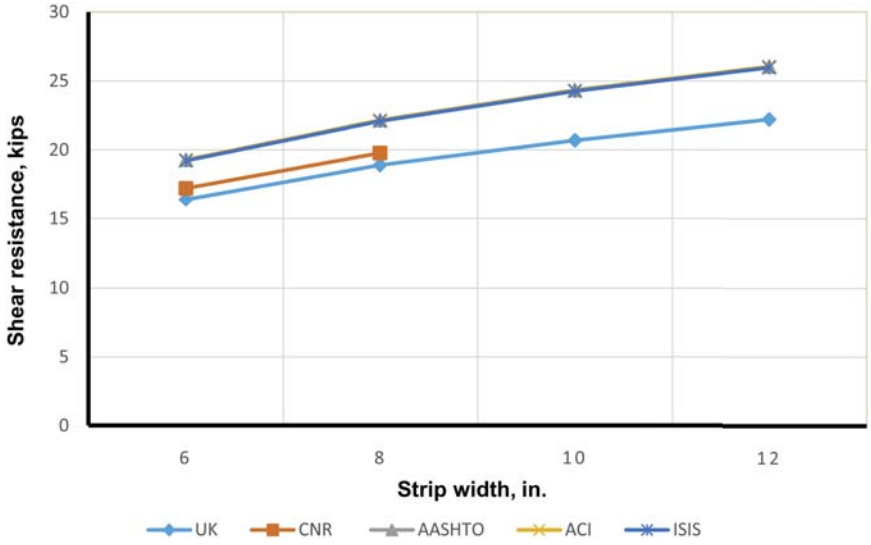

Figure 4.60 Effect of FRP strip width on FRP shear resistance when gap = *d*/4.

results, while TR55 and CNR are most conservative. JSCE does not provide enough information to calculate the shear resistance of steel or concrete. As shown, increasing the FRP strip width does not result in significant changes in shear resistance (note that the maximum spacing allowed in CNR is exceeded in the last two widths shown in the graph, and is therefore not shown). This can be verified with Fig. 4.60, which illustrates the relatively change in FRP capacity with strip width,

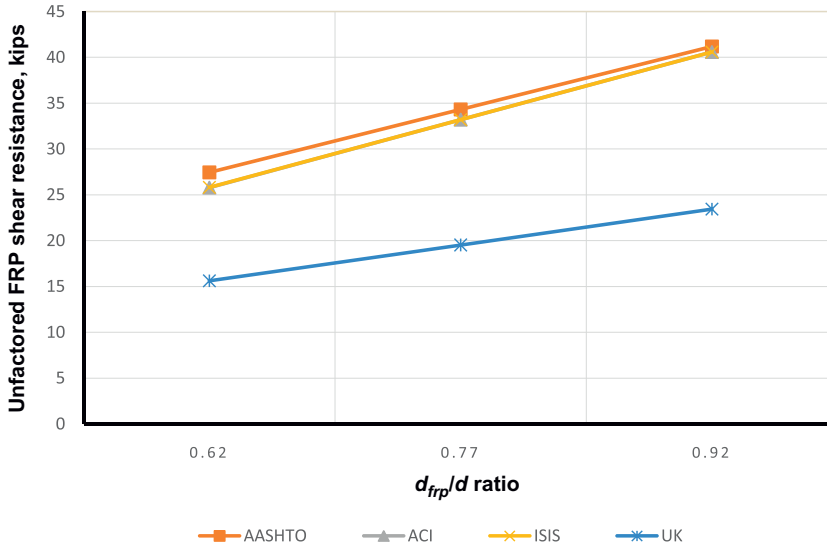

Figure 4.61 Effect of the ratio of d_{frp}/d on unfactored FRP shear resistance.

for a constant gap between strips. Note that a 12 in. strip width exceeds the maximum allowed in CNR. It appears that all codes have similar trends.

Fig. 4.61 presents the effect of the ratio of the effective depth of FRP shear reinforcement to the effective depth of the section on unfactored FRP shear resistance. In the figure the effective depth of the section is taken as 26 in. and the effective depth of FRP is varied from 16 to 24 in. Note that the CNR approach for calculating shear resistance has no relationship to the effective depth of FRP and was thus not included on the graph. As shown, AASHTO and ISIS results are very close, with increasing ratios of (d_{frp}/d) resulting in increased capacities. Although TR55 provides significantly lower capacities, trends are similar.

In Figs. 4.62–4.64 the effect of changing the beam height on the components of total unfactored shear resistance is examined (for the case of continuous U-wrap). In the figures the effective depth of the section is assumed to equal 4 in less than the beam height, while the effective depth of the FRP is assumed to be equal to 0.9 of the effective depth of the section, while the steel stirrups are assumed to be #3 bars. Changing the height of the beam has the most effect on the total shear resistance, which is most sensitive to the concrete component of resistance. ACI provides the highest capacities, although AASHTO and ISIS are similar but slightly lower.

Figs. 4.65–4.67 show the effect of changing beam height on the shear capacity of each of the contributing components (concrete, steel, FRP) individually. In general, AASHTO, ACI, ISIS, and CNR provide similar values for FRP and concrete, while TR55 is significantly more conservative, especially at larger beam depths. Code results are more similar for steel capacity, where ISIS and CNR are most conservative.

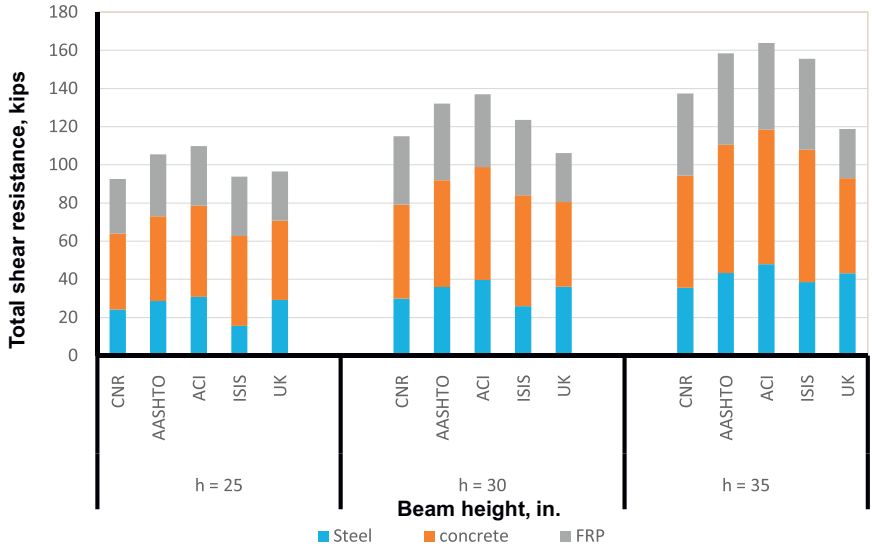

Figure 4.62 Effect of beam height on total shear resistance, steel stirrup spacing = 9 in.

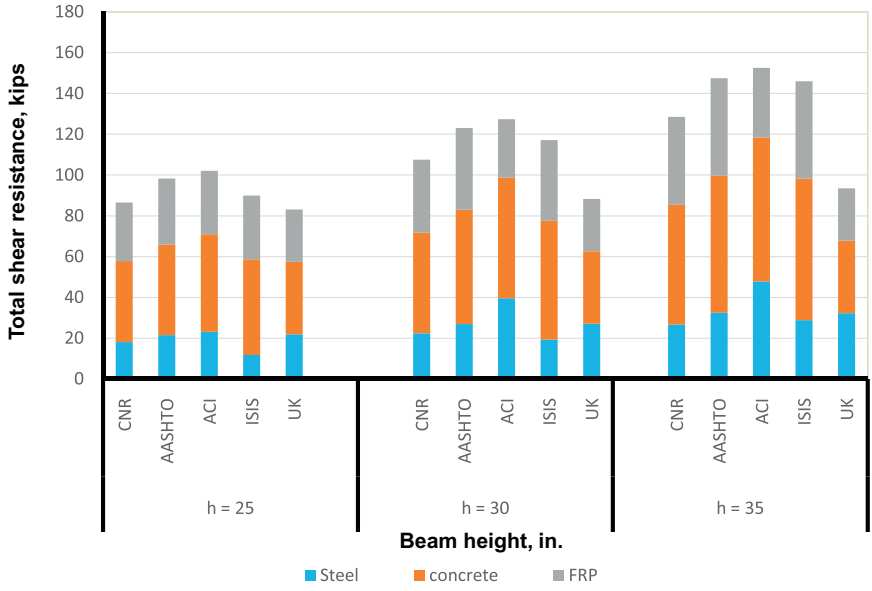

Figure 4.63 Effect of beam height on total shear resistance, steel stirrup spacing = 12 in.

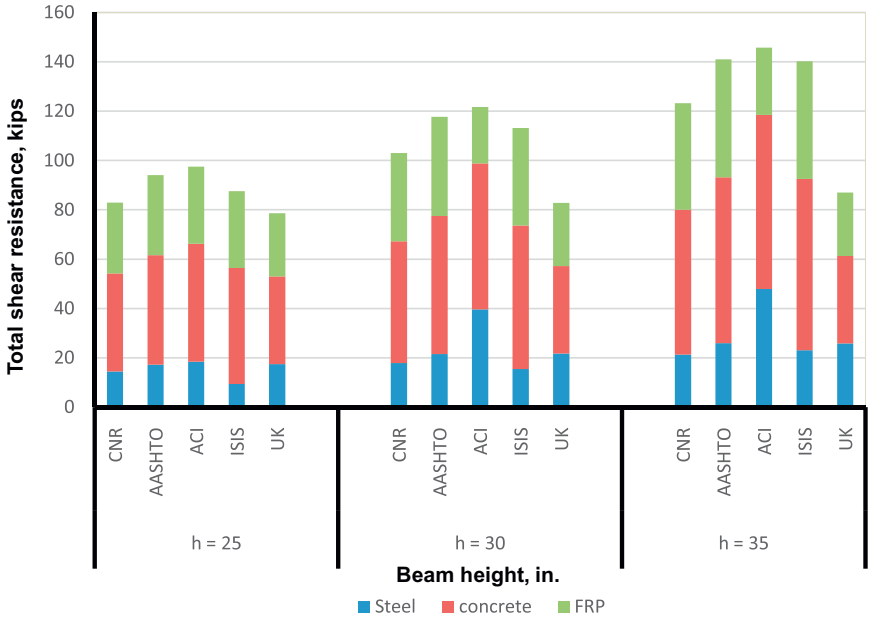

Figure 4.64 Effect of beam height on total shear resistance, steel stirrup spacing = 15 in.

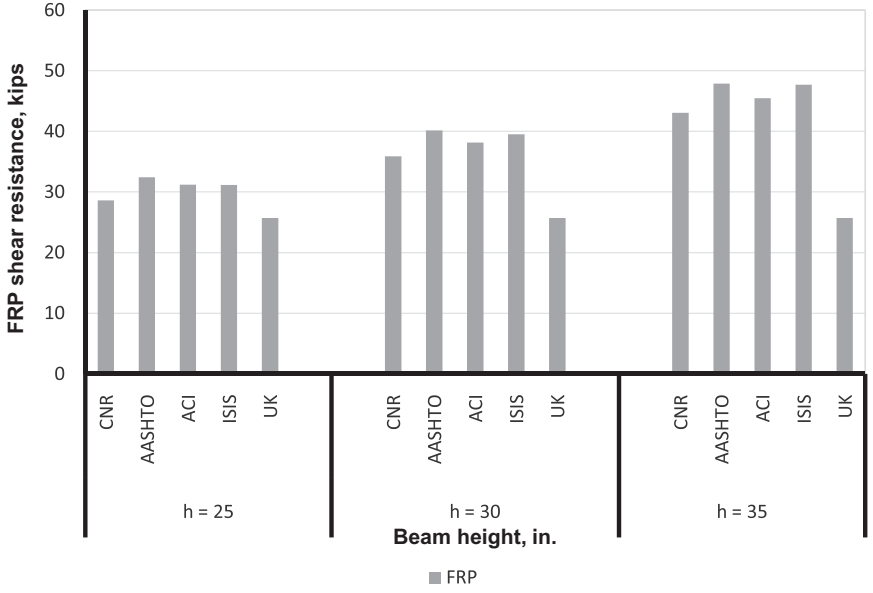

Figure 4.65 Effect of beam height on FRP shear resistance, kips steel stirrup spacing = 9 in.

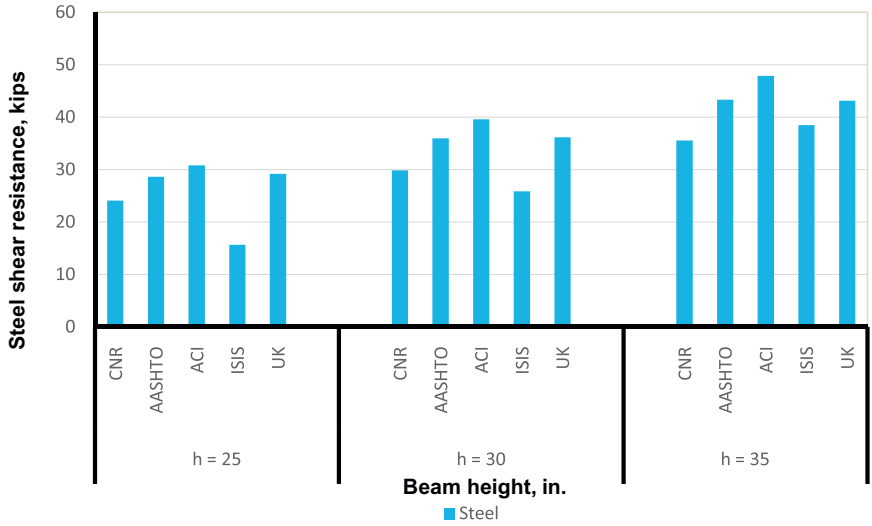

Figure 4.66 Effect of beam height on steel shear resistance, steel stirrup spacing = 9 in.

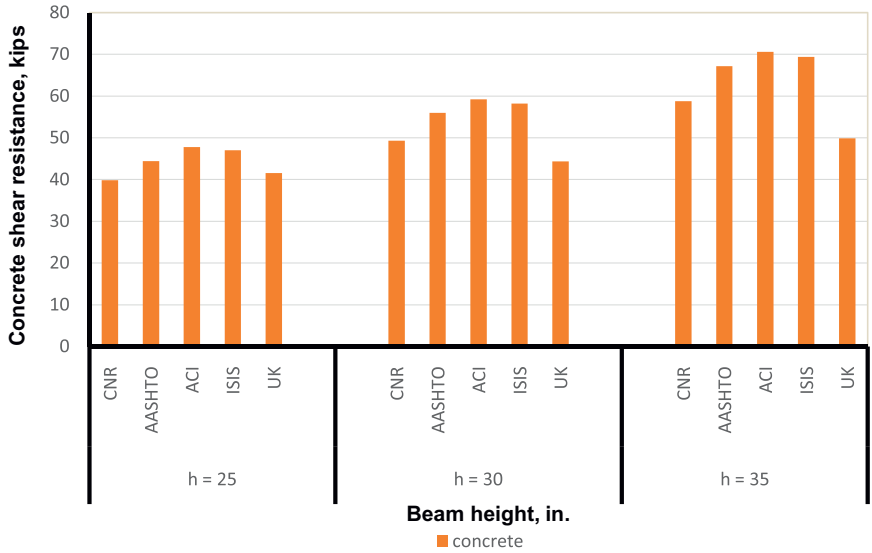

Figure 4.67 Effect of beam height on concrete shear resistance, steel stirrup spacing = 9 in.

4.4 FRP-confinement strengthening of RC/PC bridge members

4.4.1 Introduction

As with previous sections, the items considered for review and comparison in this section are based on the organization of ACI 440.2R-08. These items include

- Design considerations
- Strength reduction factors
- Maximum FRP strain due to confinement
- FRP stress limits
- Design procedures and analysis

4.4.2 Design considerations

4.4.2.1 Strength reduction factors

Table 4.24 presents strength reduction factors recommended for use by different codes. Most range from 0.65 to 0.75, although, as discussed in previous sections, how these factors are applied in design is not consistent among codes.

4.4.2.2 Maximum FRP strain due to confinement

CNR

Failure of an RC confined member may occur by fiber rupture. However, beyond a critical value of hoop strain, the concrete loses effective confinement as it expands laterally and axial strength and stiffness are no longer enhanced with the FRP. As a result, according to CNR, failure of the FRP-confined RC member is also reached when the FRP strain reaches a value of 0.4% or above.

Table 4.24 Strength reduction factor

Code	Reduction factor	
AASHTO	Reduction factor: confinement	0.65
	Resistance factor: Spiral	0.75
	Ties	0.65
CNR	Reduction factor for FRP	0.90
UK	Concrete	0.67
ISIS	Concrete	0.75
	Steel	0.90
	CFRP (embedded in f_l equation)	0.56
ACI	Spiral	0.75
	Ties	0.65

AASHTO

Similar to CNR, AASHTO specifies a FRP strain limit of 0.004 when used for confinement of axial compression members. For comparison, Table 4.25 presents other strain limits depending on the type of stresses applied to the section.

ACI

ACI introduces the following expression to calculate the maximum confinement strain:

$$\varepsilon_{ccu} = \varepsilon_c' \left(1.50 + 12\kappa_b \frac{f_l}{f_c'} \left(\frac{\varepsilon_{fe}}{\varepsilon_c'} \right)^{0.45} \right) \qquad (4.133 - \text{ACI Eq. 12-6})$$

The parameter κ_b accounts for the geometry of the section and can be taken as 1.0 for circular cross-sections. To prevent excessive cracking and potential loss of concrete integrity, the strain calculated in Eq. (4.133) should be limited to the value given in Eq. (4.134) (ACI Eq. 12-7):

$$\varepsilon_{ccu} \leq 0.01 \qquad (4.134 - \text{ACI Eq. 12-7})$$

ISIS

As with CNR and AASHTO, ISIS specifies a maximum confinement strain of 0.004 in the Canadian building code.

$$f_{lFRP} = \frac{2t_{FRP}\phi_{FRP}f_{FRPu}}{D_g} \leq \frac{2t_{FRP}E_{FRP}(0.004)}{D_g} \qquad (4.135 - \text{ISIS Eq. 6-2b})$$

Table 4.25 Maximum FRP strain due to confinement

Code	Maximum strain due to confinement	
AASHTO	Axial compression Axial tension	0.004 0.005
	Max. design (axial tension) completely wrapped $\varepsilon_{fe} = 0.004 \leq 0.75\ \varepsilon_{fu}$	
	Combined axial compression and bending	0.003
ACI	$\varepsilon_{ccu} = \varepsilon_c' \left(1.50 + 12k_b \frac{f_l}{f_c'} \left(\frac{\varepsilon_{fe}}{\varepsilon_c'} \right)^{0.45} \right)$ $\varepsilon_{ccu} \leq 0.01$	
CNR	$\varepsilon_{fd,rid} = \min\left\{ \eta_a . \frac{\varepsilon_{fk}}{\gamma_f}; 0.004 \right\}$	
ISIS	Building code Bridge code	0.004 No limit provided
UK	Confinement Shear	0.010 0.004

The bridge code, however, does not include specific limits on FRP hoop strain, but rather imposes a material reduction factor, ϕ_{FRP}.

$$f_{lFRP} = \frac{2t_{FRP}\phi_{FRP}f_{FRPu}}{D_g} \qquad (4.136 - \text{ISIS Eq. 6-2a})$$

Taking $\phi_{FRP}f_{FRPu} = E_{FRP}(\phi_{FRP}\varepsilon_{FRPu})$, and considering a typical case of MBrace CF130 FRP with $\varepsilon_{FRPu} = 0.0167$ and $\phi_{FRP} = 0.5625$, the resulting factored strain becomes 0.0094, a value which is close to the ACI limit of 0.01.

TR55

Note that although TR55 specifies a maximum strain fixed value of 0.004, which matches the AASHTO and CNR values, this is in fact for the case of shear. When axial confinement is considered, however, the hoop strain limit is specified as 0.01. This value corresponds to an effective enhanced cube strength of $1.5f_{cu}$.

Summary—maximum FRP strain due to confinement

A summary of the FRP strain limits for confined sections is presented in Table 4.25. As shown, most are from 0.003 to 0.005.

4.4.2.3 FRP stress limits

Limits for confinement stress are generally a function of the stress−strain model used by a particular code. AASHTO adopts a bilinear model similar to that of ISIS. AASHTO takes a minimum strain limit of 600 psi to reflect the fact that confinement pressure effectiveness is attained after a certain level of ductility is achieved. Note that AASHTO's maximum confinement stress introduces errors for the case of rectangular columns (D becomes the diagonal length instead of the radius). The errors are tolerated by AASHTO since they are on the conservative side.

ACI and CNR both assume a two-stage stress−strain model; an initial parabolic stage to represent unconfined concrete behavior, followed by a linear stage for confined behavior. The maximum confined stress limits are identical for both codes, while the minimum limits vary slightly.

TR55 discusses several stress−strain behavior models and recommends a model proposed by Lillistone and Jolly (2000). The general expression for FRP-confined concrete stress is presented in Eq. (4.137) (TR55 Eq. 8.3).

$$f_{cc} = \frac{(0.67/\gamma_{mc})(E_i - E_p)\varepsilon_{cc}}{1 + \left\{\dfrac{\varepsilon_{cc}(E_i - E_p)}{f_o}\right\}} + E_p\varepsilon_{cc} \qquad (4.137 - \text{TR55 Eq. 8.3})$$

where E_i = initial tangent modulus of concrete.

$$= 21500\left\{\frac{f_{cu}+8}{10}\right\}^{1/3} \qquad (4.138 - \text{TR55 Eq. 8.4})$$

E_p = postcrushing tangent modulus of concrete.

$$= 1.282\left(\frac{2t_f}{D}\right)E_{fd} \qquad (4.139 - \text{TR55 Eq. 8.5})$$

$$f_o = f_{cu}(E_i - E_p)/(E_i - E_l) \qquad (4.140 - \text{TR55 Eq. 8.6})$$

$$E_l = (f_{cu} + 8)/\varepsilon_{cu} \qquad (4.141 - \text{TR55 Eq. 8.7})$$

To evaluate the maximum confinement pressure, TR55 recommends Eq. (4.142) (TR55 8.16):

$$f_{ccd} = \frac{0.67f_{cu}}{\gamma_{mc}} + 0.05\left(\frac{2t_f}{D}\right)E_{fd} \qquad (4.142 - \text{TR55 Eq. 8.16})$$

Table 4.26 summarizes minimum and maximum confined stress limits.

4.4.3 Analysis and design procedures

4.4.3.1 AASHTO

Axial capacity of confined columns in compression

The design procedure for columns strengthened with FRP is the same as that for reinforced concrete columns without strengthening. However, the concrete compressive strength f'_c is replaced by the increased confined concrete compressive strength f'_{cc}.

The factored axial load resistance, P_r, for a confined column is taken as

For members with spiral reinforcement:

$$P_r = 0.85\phi[0.85f'_{cc}(A_g - A_{st}) + f_yA_{st}] \qquad (4.143 - \text{AASHTO Eq. 5.3.1-1})$$

For members with tie reinforcement:

$$P_r = 0.80\phi[0.85f'_{cc}(A_g - A_{st}) + f_yA_{st}] \qquad (4.144 - \text{AASHTO Eq. 5.3.1-2})$$

where ϕ = resistance factor; A_g = gross area of section (in.^{2}); A_{st} = total area of longitudinal reinforcement (in.^{2}); f_y = yield strength of reinforcement (ksi); f'_{cc} = compressive strength of the confined concrete.

Table 4.26 FRP stress limits

Code	Minimum confined stress	Maximum confined stress
AASHTO	600 psi	$f_l = \phi_{frp}\frac{2N_{frp}}{D} \le \frac{f'_c}{2}\left(\frac{1}{k_e\phi} - 1\right)$
CNR	Confinement is effective if: $f_{l,eff}/f_{cd} > 0.05$	$f_{ccd} = f_{cd} + E_t\varepsilon_{ccu}$
ACI	$f_l/f'_c \ge 0.08$	$f'_{cc,u} = f'_c + E_2\varepsilon_{ccu}$
ISIS	$0.1f'_c$	$0.33f'_c$

The multipliers 0.85 and 0.80 are intended to account for accidental load eccentricity (0.05h and 0.10h for columns with spiral or tied reinforcement, respectively). Columns with larger eccentricities are to be designed using the provisions of AASHTO section 5.5-Axial Tension.

Evaluation of confined compressive strength, f'_{cc}

The compressive strength of the confined concrete, f'_{cc}, is determined from:

$$f'_{cc} = f'_c\left(1 + \frac{2f_l}{f'_c}\right) \qquad \text{(4.145 – AASHTO Eq. 5.3.2.2-1)}$$

where f_l = the confinement pressure due to FRP strengthening for circular columns

$$= \phi_{frp}\frac{2N_{frp}}{D} \le \frac{f'_c}{2}\left(\frac{1}{k_e\phi} - 1\right) \qquad \text{(4.146 – AASHTO Eq. 5.3.2.2-2)}$$

k_e = strength reduction factor applied for unexpected eccentricities,
= 0.80 for tied columns, and
= 0.85 for spiral columns.
N_{frp} = strength per width of FRP reinforcement corresponding to a strain of 0.004;
ϕ_{frp} = 0.65.

For rectangular columns the diameter D is taken as the smaller dimension of the width and depth. When Eq. (4.146) (AASHTO Eq. 5.3.2.2-2) is applied to rectangular columns after replacing D with the smaller dimension of the rectangular section, the factored axial strength estimated from Eq. (4.143) or (4.144) (AASHTO 5.3.1-1 or 5.3.1-2) is conservative. The calculated gain in strength provided by the confinement of a rectangular section is very little compared to that attainable for circular section. As a result, neither minimum nor maximum limits are specified for rectangular sections, since the attainable confinement pressure, which relies on ductility development, is very limited for rectangular columns.

4.4.3.2 ACI

Axial capacity of confined columns in compression

ACI provides an expression similar to AASHTO to evaluate the axial capacity of confined columns. The confined stress−strain behavior model adopted by ACI is based on the stress−strain model developed by Lam and Teng (2003b). The expressions used to evaluate axial design capacity for spiral and tied columns are provided in Eqs. (4.147) and (4.148) (ACI 12-1a and 12-1b). These equations follow ACI 318 column design equations, but concrete compressive strength f'_c is replaced with the confined compressive strength f'_{cc}.

For nonprestressed columns with steel spiral reinforcement:

$$\phi P_n = 0.85\phi[0.85f'_{cc}(A_g - A_{st}) + f_y A_{st}] \qquad \text{(4.147 – ACI Eq. 12-1a)}$$

For nonprestressed with tie reinforcement:

$$\phi P_n = 0.80\phi[0.85f'_{cc}(A_g - A_{st}) + f_y A_{st}] \qquad \text{(4.148 – ACI Eq. 12-1b)}$$

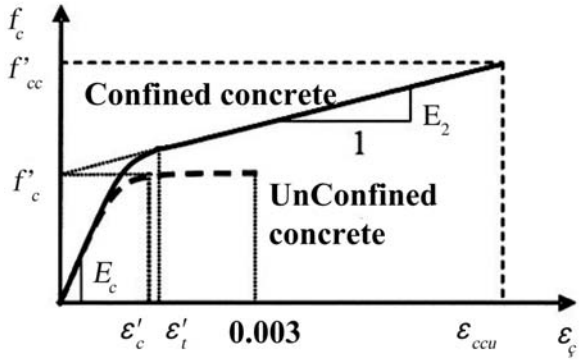

Figure 4.68 ACI stress–strain model for FRP-confined concrete (Lam and Teng, 2003a).

Stress–strain model for confined reinforced concrete columns

The Lam and Teng (2003b) model adopted by ACI is shown in Fig. 4.68. Eq. (4.149) provides the general expression for concrete stress for the nonlinear/unconfined portion as well as the linear/confined portion. Eq. (4.150) evaluates the slope for the linear portion of the stress–strain model, E_2. Eq. (4.151) evaluates the transition strain between the nonlinear and linear portions of the stress–strain curve. Eqs.(4.133) and (4.134) are discussed in Section 4.4.2.2.3.

$$f_c = \begin{cases} E_c\varepsilon_c - \dfrac{(E_c - E_2)^2}{4f'_c}\varepsilon_c^2 & 0 \le \varepsilon_c \le \varepsilon'_t \\ f'_c + E_2\varepsilon_c & \varepsilon'_t \le \varepsilon_c \le \varepsilon_{ccu} \end{cases} \qquad (4.149 - \text{ACI Eq. 12-2a})$$

where E_2 = the slope of the linear portion of the stress–strain model for FRP confined concrete, psi.

$$= \frac{f'_{cc} - f'_c}{\varepsilon_{ccu}} \qquad (4.150 - \text{ACI Eq. 12-2b})$$

$$\varepsilon'_t = \frac{2f'_c}{E_c - E_2} \qquad (4.151 - \text{ACI Eq. 12-2c})$$

$$\varepsilon_{ccu} = \varepsilon'_c\left(1.50 + 12\kappa_b\frac{f_l}{f'_c}\left(\frac{\varepsilon_{fe}}{\varepsilon'_c}\right)^{0.45}\right) \qquad (4.133 - \text{ACI Eq. 12-6})$$

$$\varepsilon_{ccu} \le 0.01 \qquad (4.134 - \text{ACI Eq. 12-7})$$

Evaluation of confined compressive strength f'_{cc}

$$f'_{cc} = f'_c + \psi_f 3.3 \kappa_a f_l \qquad (4.152 - \text{ACI Eq. 12-3})$$

$$f_l = \frac{2E_f n t_f \varepsilon_{fe}}{D} \qquad (4.153 - \text{ACI Eq. 12-4})$$

$$\varepsilon_{fe} = \kappa_\varepsilon \varepsilon_{fu} \qquad (4.154 - \text{ACI Eq. 12-5})$$

κ_ε = strain efficiency factor (accounts for the possibility of premature failure of FRP)
= 0.586 for CFRP

D is the diameter of a circular column. For noncircular cross-sections an equivalent circular cross-section with diameter D equal to the diagonal of the rectangular cross-section is used. The equivalent D value for a rectangular column cross-section is presented in Eq. (4.155) (ACI 12-8):

$$D = \sqrt{b^2 + h^2} \qquad (4.155 - \text{ACI Eq. 12-8})$$

For circular cross-sections the shape factors κ_a and κ_b appearing in Eqs. (4.133) and (4.152) above can be taken as 1.0. For rectangular cross-sections, κ_a and κ_b are expressed in Eqs. (4.156) (ACI Eq. 12-9) and (4.157) (ACI Eq. 12-10), respectively. Their values depend on two parameters: the side-aspect ratio h/b (see Fig. 4.69), and the ratio of the effective area of the confined concrete A_e to the

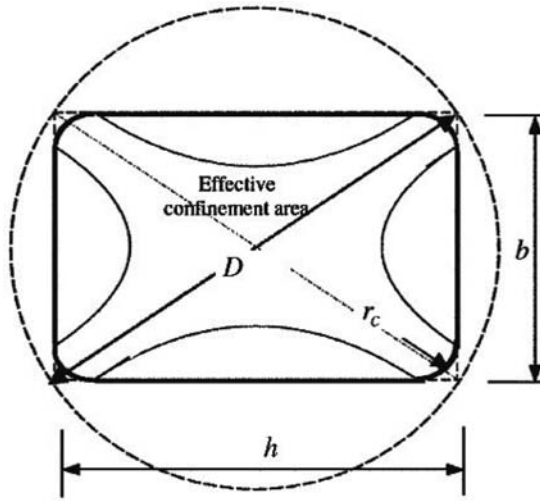

Figure 4.69 Equivalent circular cross-section (Lam and Teng, 2003b).

total area of the concrete section A_c. The ratio A_e/A_c is evaluated in Eq. (4.158) (ACI Eq. 12.11).

$$\kappa_a = \frac{A_e}{A_c}\left(\frac{b}{h}\right)^2 \qquad (4.156 - \text{ACI Eq. 12-9})$$

$$\kappa_b = \frac{A_e}{A_c}\left(\frac{b}{h}\right)^{0.5} \qquad (4.157 - \text{ACI Eq. 12-10})$$

$$\frac{A_e}{A_c} = \frac{1 - \frac{\left[\left(\frac{b}{2}\right)(h-2r_c)^2 + \left(\frac{b}{2}\right)(h-2r_c)^2\right]}{3A_g} - \rho_g}{1-\rho_g} \qquad (4.158 - \text{ACI Eq. 12-11})$$

Serviceability considerations

ACI stipulates that the transverse strain in the concrete should remain below its cracking strain at service load levels, which is to be taken as an equivalent concrete compressive stress limit of $0.65f'_c$. ACI also states that the service stress in the longitudinal steel should remain below $0.60f_y$ to avoid plastic deformation under sustained or cyclic loads.

4.4.3.3 ISIS

Axial capacity of confined columns in compression

The analysis considered in this chapter is based on the S6-06 bridge code equations and procedure. The factored axial resistance of a section in compression, P_r, is given by Eq. (4.159) (ISIS Eq. 6.5a):

$$P_r = 0.80[\alpha_1\phi_c f'_{cc}(A_g - A_s) + \phi_s f_y A_{st}] \qquad (4.159 - \text{ISIS Eq. 6-5a})$$

where

$$\phi_c = 0.75$$

$$\phi_s = 0.9$$

$$\alpha_1 = 0.85 - 0.0015\, f'_c \geq 0.67 \qquad (4.160 - \text{ISIS Eq. 5-1})$$

Evaluation of the confined compressive strength, f'_{cc}

The model used in S6-06 to evaluate the confined compressive strength f'_{cc} is given by Eq. (4.161) (ISIS Eq. 6-3). This equation provides a reasonably conservative estimate of f'_{cc}, based on the research by Thériault and Neale (2000), Teng et al., (2002), and Bisby et al. (2005).

$$f'_{cc} = f'_c + 2f_{l\text{FRP}} \qquad (4.161 - \text{ISIS Eq. 6-3})$$

where

$f'_c \leq 7.25$ ksi (50 MPa)

$f_{l\text{FRP}}$ = confinement pressure due to FRP strengthening at ultimate capacity (MPa)

$$= \frac{2t_{\text{FRP}}\phi_{\text{FRP}}f_{\text{FRP}u}}{D_g} \qquad (4.162 - \text{ISIS Eq. 6-2a})$$

D_g = diameter of a circular column, or diagonal of a rectangular column provided that the section edges are rounded, $h/b \leq 1.5$ (see Fig. 4.69), and $b \leq 31.5$ in. (800 mm).

4.4.3.4 CNR

Axial capacity of FRP-confined members under concentric or slightly eccentric force

Confinement action on reinforced concrete columns becomes significant only after cracking of the concrete and yielding of the steel reinforcement when increased lateral expansion occurs; prior to concrete cracking, the FRP is practically unloaded.

Ultimate strength design requires that both the factored design axial load, N_{Sd}, and the factored axial capacity, $N_{Rcc,d}$, satisfy the following equation:

$$N_{Sd} \leq N_{Rcc,d} \qquad (4.163 - \text{CNR Eq. 4.39})$$

For nonslender FRP confined members the factored axial capacity can be calculated as follows:

$$N_{Rcc,d} = \frac{1}{\gamma_{Rd}} A_c f_{ccd} + A_s f_{yd} \qquad (4.164 - \text{CNR Eq. 4.40})$$

where γ_{Rd} = partial factor taken equal to 1.10; A_c = member cross-sectional area; f_{ccd} = design strength of confined concrete; A_s = area of existing steel reinforcement; f_{yd} = yield strength of existing steel reinforcement.

Evaluation of the confined compressive strength, f_{ccd}

The design strength, f_{ccd}, of the confined concrete is evaluated as follows:

$$\frac{f_{ccd}}{f_{cd}} = 1 + 2.6\left(\frac{f_{1,eff}}{f_{cd}}\right)^{2/3} \qquad (4.165 - \text{CNR Eq. 4.41})$$

where f_{cd} = the design strength of unconfined concrete; $f_{1,eff}$ = the effective confined lateral pressure. For effective confinement, use $(f_{1,eff}/f_{cd}) > 0.05$.

Evaluation of the confined lateral pressure

The effective confined lateral pressure, $f_{1,eff}$, is a function of the member cross-section and FRP configuration, as indicated in the following equation:

$$f_{1,eff} = k_{eff}.f_1 \qquad (4.166 - \text{CNR Eq. } 4.42)$$

where k_{eff} = a coefficient of efficiency (≤ 1), defined as the ratio of the volume, $V_{c,eff}$, of the effectively confined concrete and the volume, V_c, of the concrete member (neglecting the area of existing internal steel reinforcement); f_1 = the confined lateral pressure.

$$= \frac{1}{2}.\rho_f.E_f.\varepsilon_{fd,rid} \qquad (4.167 - \text{CNR Eq. } 4.43)$$

ρ_f = the geometric strengthening ratio as a function of section shape (circular or rectangular) and FRP configuration (continuous or discontinuous wrapping); E_f = Young's modulus of the FRP in the direction of fibers; $\varepsilon_{fd,rid}$ = a reduced FRP design strain.

$$= \min\left\{\eta_a \frac{\varepsilon_{fk}}{\gamma_f}; 0.004\right\} \qquad (4.168 - \text{CNR Eq. } 4.47)$$

η_a = environmental conversion factor (CNR Table 3.4); γ_f = partial factor (CNR Table 3.2)

$$k_{eff} = k_H.k_V.k_a \qquad (4.169 - \text{CNR Eq. } 4.44)$$

Evaluation of k_H, k_V, and k_a

The coefficient of horizontal efficiency, k_H, depends on the cross-section shape. The coefficient of vertical efficiency, k_V, depends on the FRP configuration. Regardless of the section shape the efficiency coefficient, k_a, is used when fibers are spirally installed with an angle α_f with respect to the member cross-section. k_a is evaluated using Eq. (4.170) (CNR Eq. 4.46).

$$k_a = \frac{1}{1 + (\tan \alpha_f)^2} \qquad (4.170 - \text{CNR Eq. } 4.46)$$

For reinforced concrete columns confined using continuous wrapping, $k_V = 1.0$. For the case of discontinuous FRP wrapping, FRP strips are installed with a center-to-center spacing of p_f, and clear spacing of p'_f (see Fig. 4.70). A reduction in

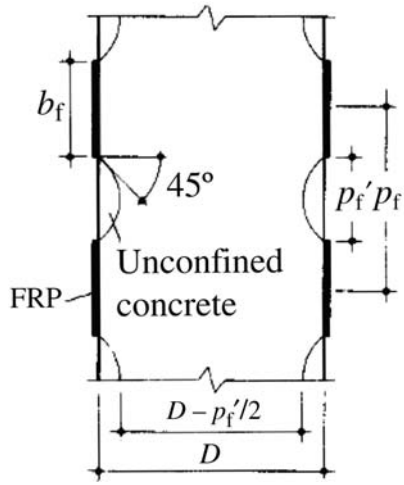

Figure 4.70 Elevation view of circular member confined with FRP strips (CNR).

confinement effectiveness occurs due to the diffusion of stresses (approximately at 45°) between two subsequent wrappings. The reduction is independent of column cross-section shape. The coefficient of vertical efficiency, k_V, can be evaluated using the following expression:

$$k_V = \left(1 - \frac{p_f'}{2d_{\min}}\right)^2 \qquad (4.171 - \text{CNR Eq. } 4.45)$$

where $d_{\min}$ = the minimum cross-sectional dimension of the member; $p_f' \leq (d_{\min}/2)$ for discontinuous wrapping.

For circular cross-sections subjected to either concentric or slightly eccentric axial load, confinement is most effective and $k_H = 1.0$. For members with square or rectangular cross-sections, FRP-confinement produces only marginal increases in the member's compressive strength, and CNR specifies additional special limitations in this case; for example, the strengthening effect of FRP confinement is neglected for rectangular cross-sections having $b/d > 2$, or $\max\{b, d\} > 35.4$ in. (900 mm) unless otherwise demonstrated in experimental tests.

In CNR, similar to other codes, for rectangular cross-sections, the effectively confined concrete area is taken as a fraction of the overall concrete cross-section, due to the "arch effect" as shown in Fig. 4.71. Such an effect depends on the corner radius r_c. CNR recommends the following minimum limit to r_c:

$$r_c \geq 0.79 \text{ in. } (20 \text{ mm}) \qquad (4.172 - \text{CNR Eq. } 4.49)$$

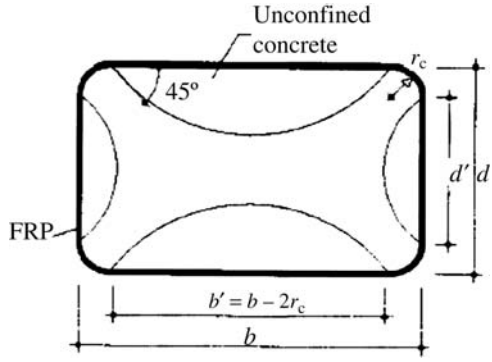

Figure 4.71 Confinement of rectangular sections (CNR).

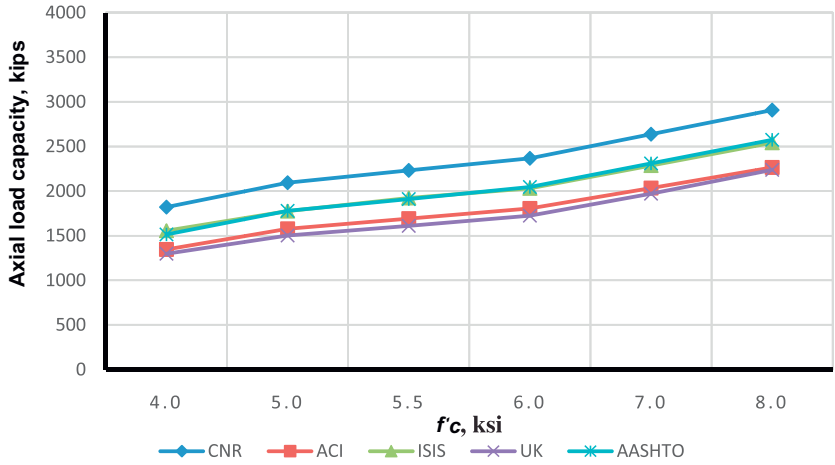

Figure 4.72 Effect of changing f'_c on factored axial load resistance, square column, $\rho = 0.02$.

For rectangular cross-sections the coefficient of horizontal efficiency, k_H, accounts for the arch effect and is evaluated as follows:

$$k_H = 1 - \frac{b'^2 + d'^2}{3A_g} \qquad (4.173 - \text{CNR Eq. } 4.51)$$

4.4.4 Summary

Code results are compared in Figs. 4.72–4.101. Results in the figures are calculated with the following assumptions: a circular cross-section is considered with a

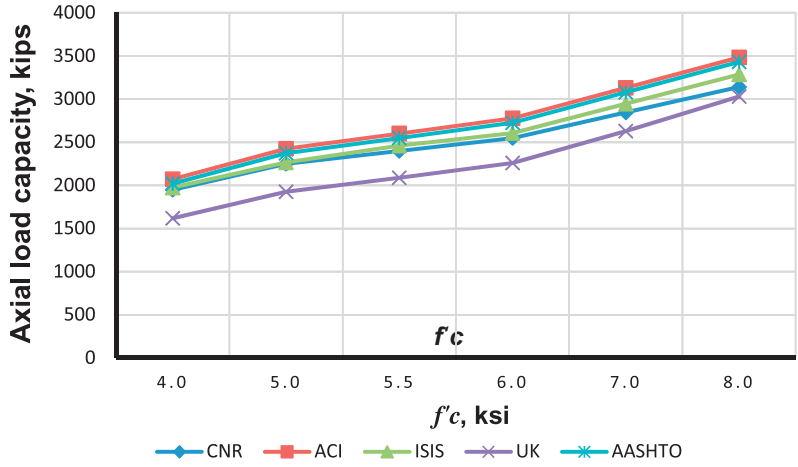

Figure 4.73 Effect of changing f'_c on unfactored axial load resistance, square column, $\rho = 0.02$.

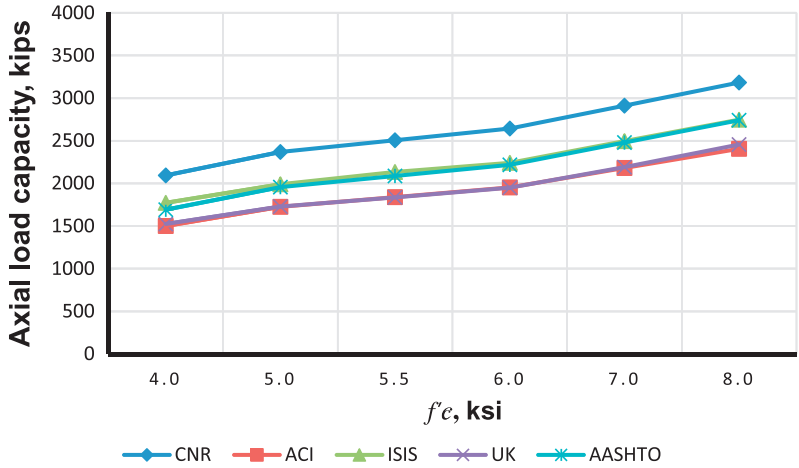

Figure 4.74 Effect of changing f'_c on factored axial load resistance, square column, $\rho = 0.03$.

diameter of 26 in. and a square cross-section with side lengths of 23 in. (both columns have the same area of 530 in.^{2}). When the effects of f'_c are evaluated, FRP wrapping is taken as three plies with a total thickness of 0.02 in. (0.51 mm). Here, BASF MBrace CF130 CFRP is considered. When the amount of CFRP is varied from one, two, three, four, and five plies, f'_c is taken as 4 ksi, and the corresponding CFRP thicknesses are 0.0065, 0.013, 0.0195, 0.026, and 0.033 in., respectively

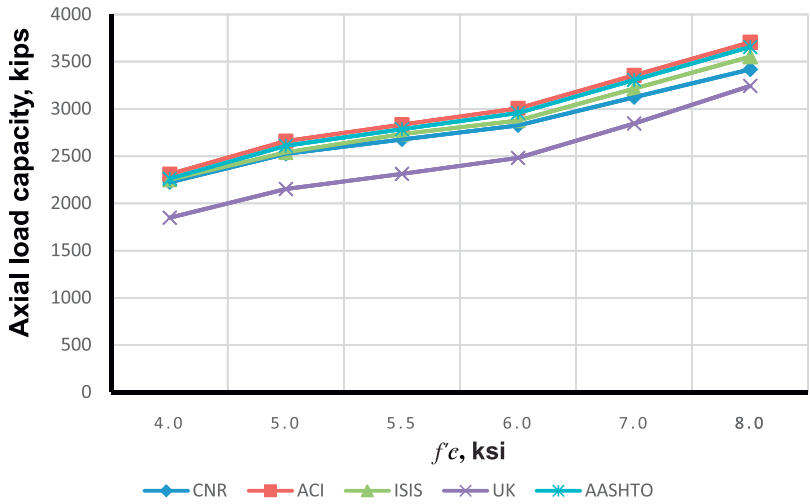

Figure 4.75 Effect of changing f'_c on unfactored axial load resistance, square column, $\rho = 0.03$.

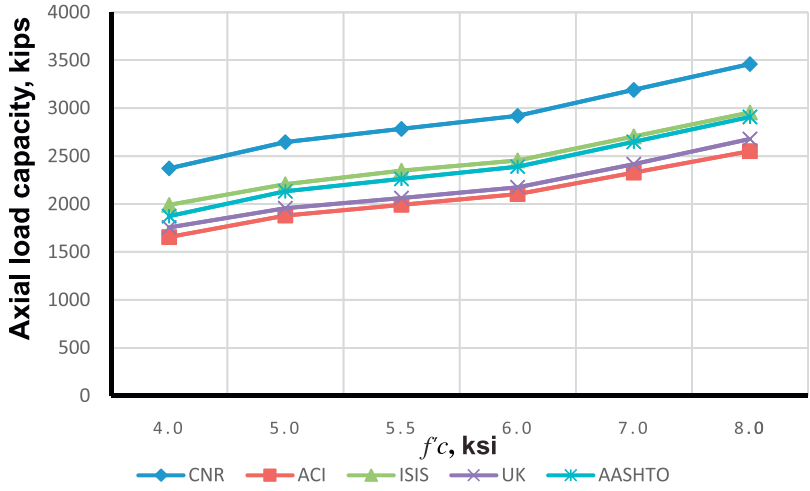

Figure 4.76 Effect of changing f'_c on factored axial load resistance, square column, $\rho = 0.04$.

(0.17, 0.33, 0.50, 0.66, and 0.83 mm). Moreover, for sake of comparison, for AASHTO results, the minimum confinement pressure limit is ignored. Figs. 4.72–4.77 present the effect of changing $f_c^{'}$ on the axial capacity of a square column with different reinforcement ratios (0.02, 0.03, and 0.04). Factored

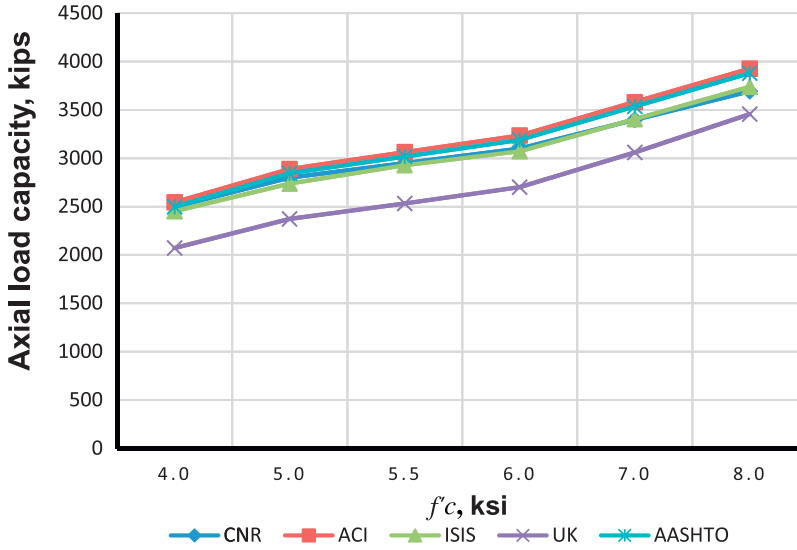

Figure 4.77 Effect of changing f'_c on unfactored axial load resistance, square column, $\rho = 0.04$.

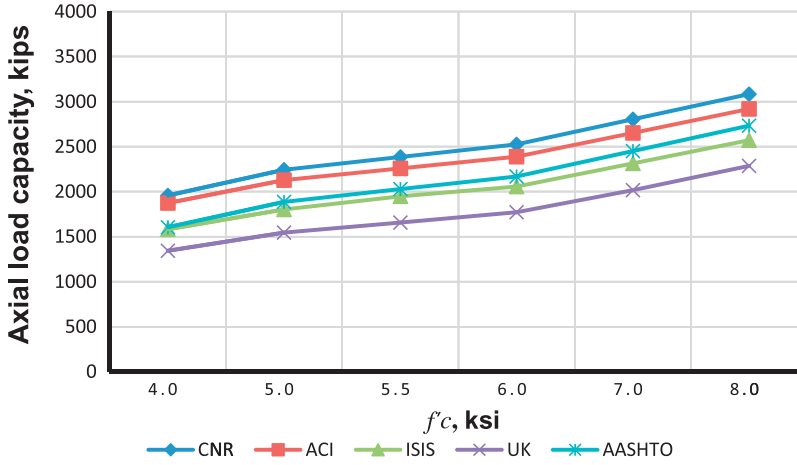

Figure 4.78 Effect of changing f'_c on factored axial load resistance, circular column, $\rho = 0.02$.

(including applicable reduction factors) and unfactored (excluding applicable reduction factors from calculations) axial loads are evaluated. Also note that for TR55, reduction factors are embedded and only the partial safety factor for concrete could be removed for the unfactored cases.

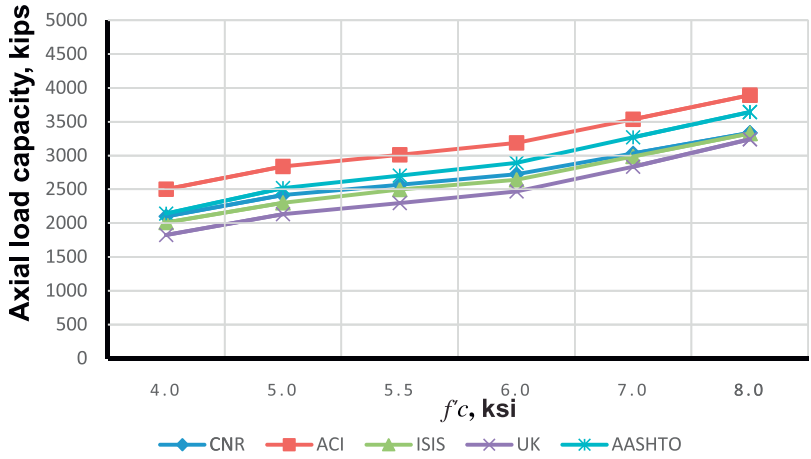

Figure 4.79 Effect of changing f'_c on unfactored axial load resistance, circular column, $\rho = 0.02$.

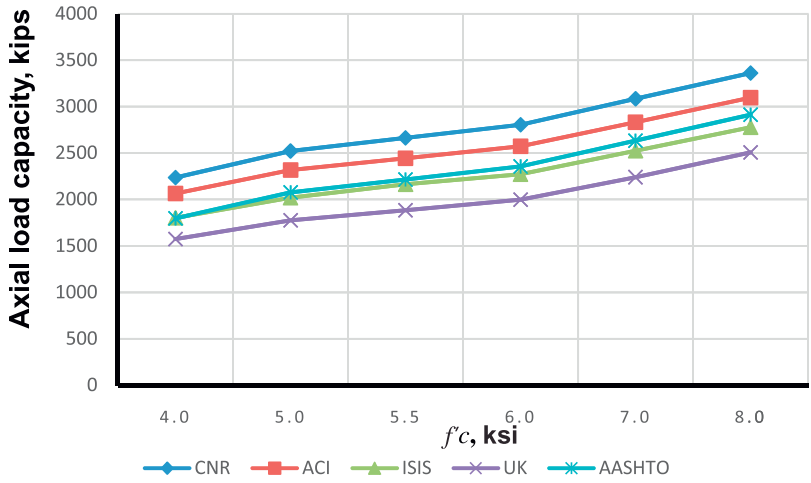

Figure 4.80 Effect of changing f'_c on factored axial load resistance, circular column, $\rho = 0.03$.

It was found that the unfactored results are very similar among codes, and as expected, when the effect of various reduction factors are included, greater differences emerge. Here, CNR is least conservative while the other codes show, in general, closer agreement, with AASHTO and TR55 (as expected, as some implicit reduction factors are present, as noted above) most conservative. It was also found that axial capacity is more sensitive to reinforcement ratio ρ at lower values of $f_c^{'}$ than higher values; at a compressive strength of 8 ksi, no increase in axial load capacity is observed with an increase of ρ from 0.02 to 0.04.

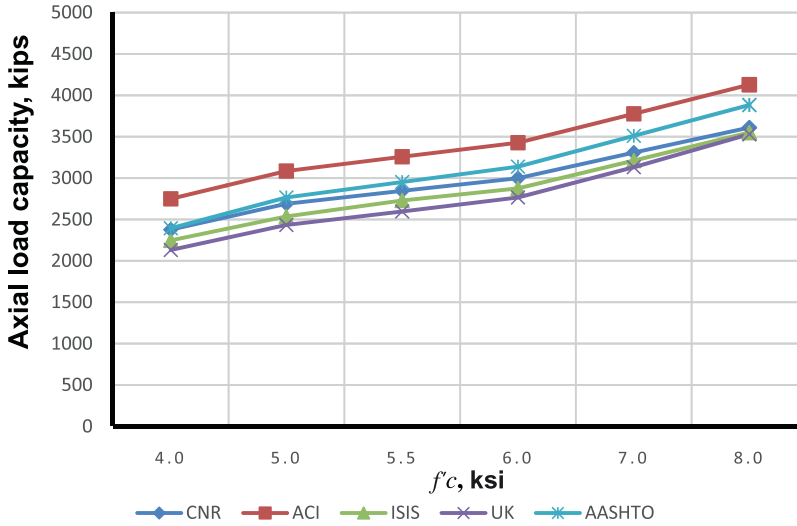

Figure 4.81 Effect of changing f'_c on unfactored axial load resistance, circular column, $\rho = 0.03$.

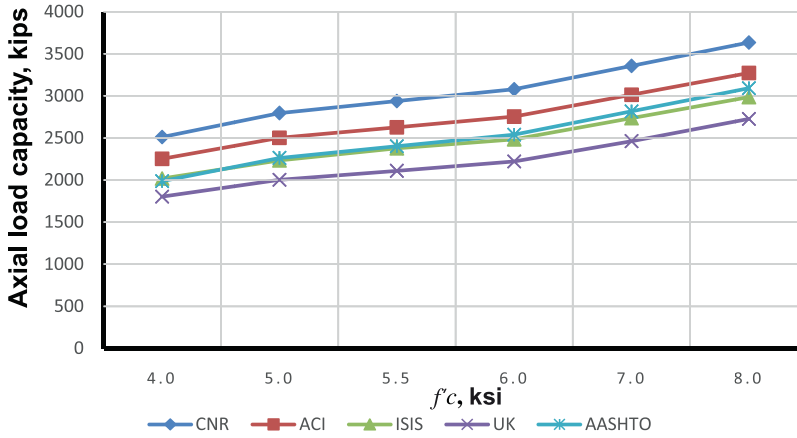

Figure 4.82 Effect of changing f'_c on factored axial load resistance, circular column, $\rho = 0.04$.

In Figs. 4.78–4.83 the effect of changing $f_c^{'}$ on circular column capacity with different reinforcement ratios is examined. As shown, although trends are similar, the circular column generally has greater capacity than the corresponding square column of the same area. Considering the unfactored case, ACI generally has the highest capacity. However, for the factored cases, CNR produces the greatest capacity.

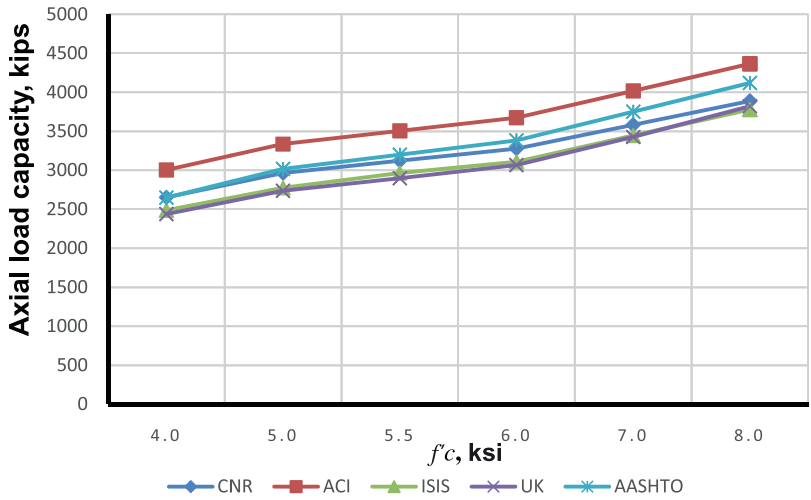

Figure 4.83 Effect of changing f'_c on unfactored axial load resistance, circular column, $\rho = 0.04$.

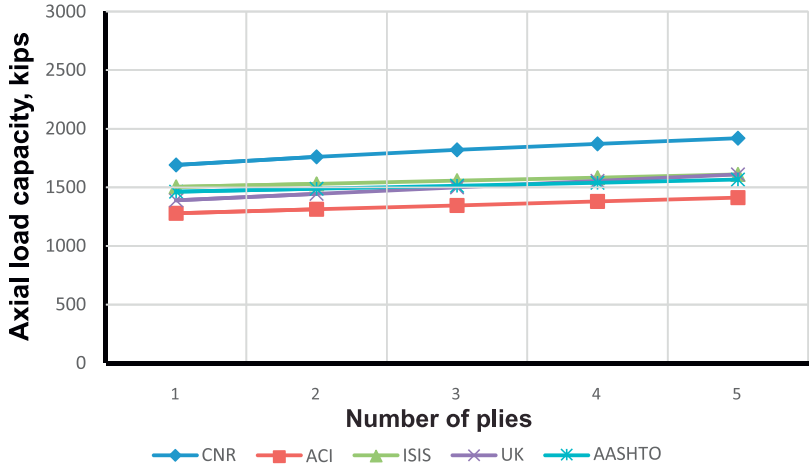

Figure 4.84 Effect of changing number of plies on factored axial load resistance, square column, $\rho = 0.02$.

In Figs. 4.84–4.89 the effect of number of plies on the axial capacity of square columns is shown. In these figures, it can be seen that, for the factored case, CNR has the highest capacity while ACI is most conservative. However, the codes converge to similar values for the unfactored case. Figs. 4.90–4.95 illustrate the effect of changing the number of plies on the axial load capacity of circular columns. For

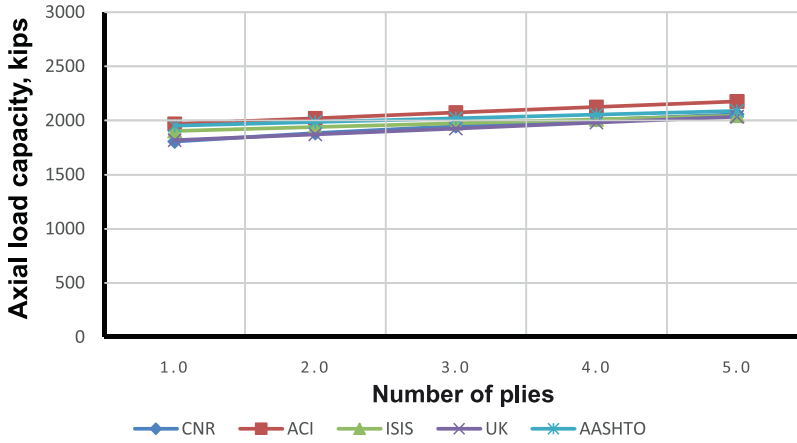

Figure 4.85 Effect of changing number of plies on unfactored axial load resistance, square column, $\rho = 0.02$.

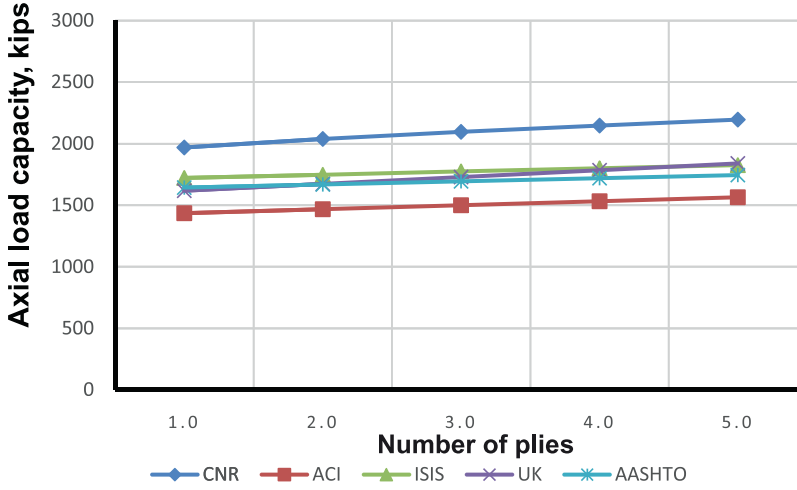

Figure 4.86 Effect of changing number of plies on factored axial load resistance, square column, $\rho = 0.03$.

circular columns, axial capacity was more sensitive to f'_c than the amount of FRP confinement. For the circular column, AASHTO, ISIS, and TR55 are most conservative (as compared to ACI for square columns), while CNR is least conservative in both cases. Figs. 4.96 and 4.97 present the effect of number of plies on axial capacity. It can be seen that increasing the number of layers has little effect on

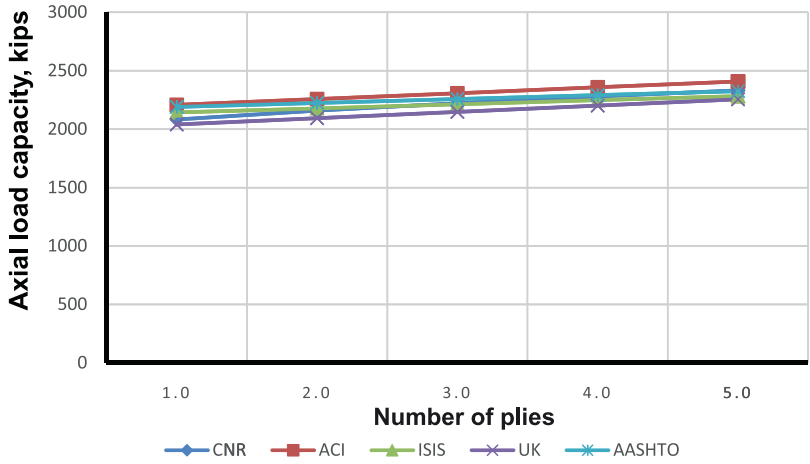

Figure 4.87 Effect of changing number of plies on unfactored axial load resistance, square column, $\rho = 0.03$.

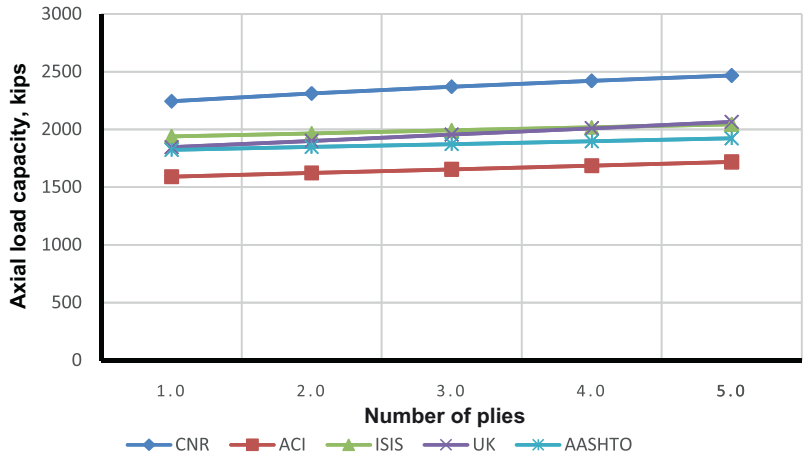

Figure 4.88 Effect of changing number of plies on factored axial load resistance, square column, $\rho = 0.04$.

improving column axial capacity for both circular and square columns, and AASHTO and ISIS (both bridge codes) produce similar results that are slightly more conservative as compared to ACI and CNR.

Figs. 4.98 and 4.99 show the effect of changing f'_c on circular and square column capacity, while Fig. 4.100 compares circular and square column results. As shown earlier, increasing f'_c clearly increases axial capacity, while the bridge codes

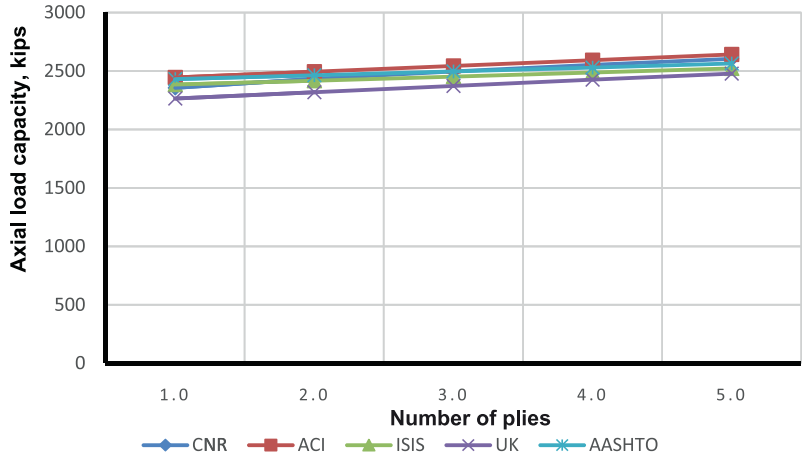

Figure 4.89 Effect of changing number of plies on unfactored axial load resistance, square column, $\rho = 0.04$.

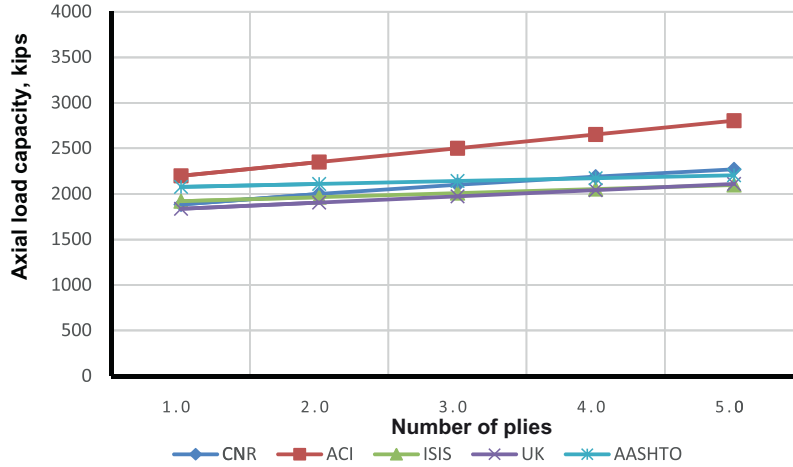

Figure 4.90 Effect of changing number of plies on unfactored axial load resistance, circular column, $\rho = 0.02$.

(AASHTO and ISIS) are slightly conservative in predicting the axial capacity of circular columns, and TR55 is most conservative for square columns. Due to the reduction of effective area of confinement, square columns clearly have lower axial capacity than a corresponding circular column. It is also clear that ACI and CNR produce similar results for circular columns. Fig. 4.101 shows the effect of

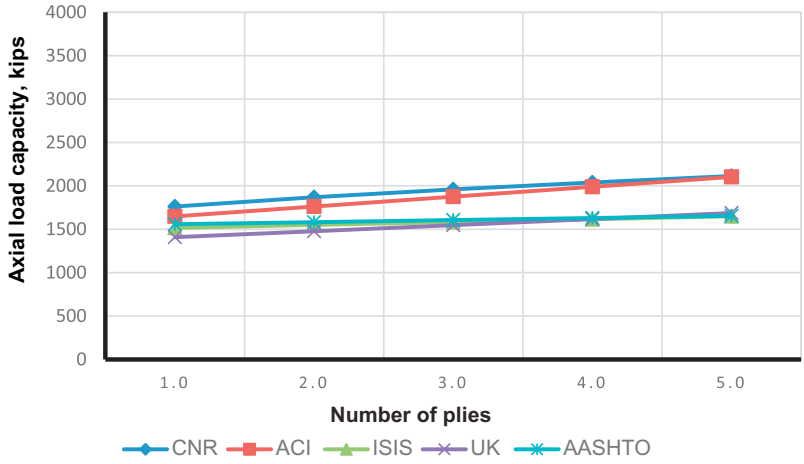

Figure 4.91 Effect of changing number of plies on factored axial load resistance, circular column, $\rho = 0.02$.

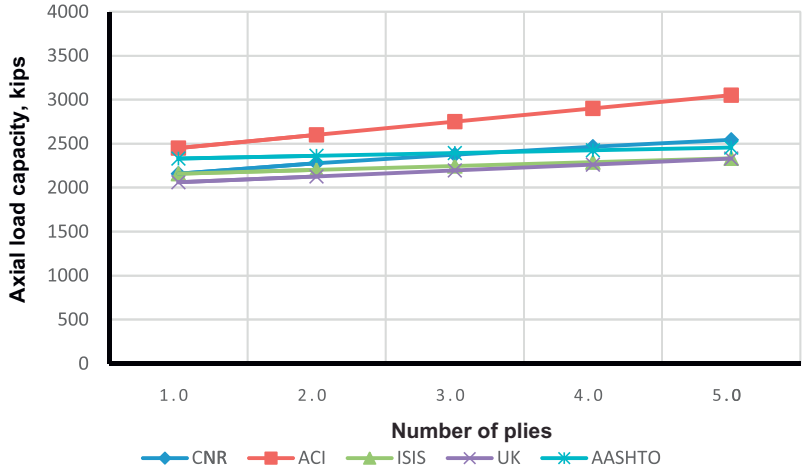

Figure 4.92 Effect of changing number of plies on unfactored axial load resistance, circular column, $\rho = 0.03$.

changing the number of plies on axial load capacity, for both circular and rectangular columns. ACI and CNR provide higher capacities for circular columns while for square columns, ACI is conservative. For both circular and square columns, AASHTO and ISIS produce similar results.

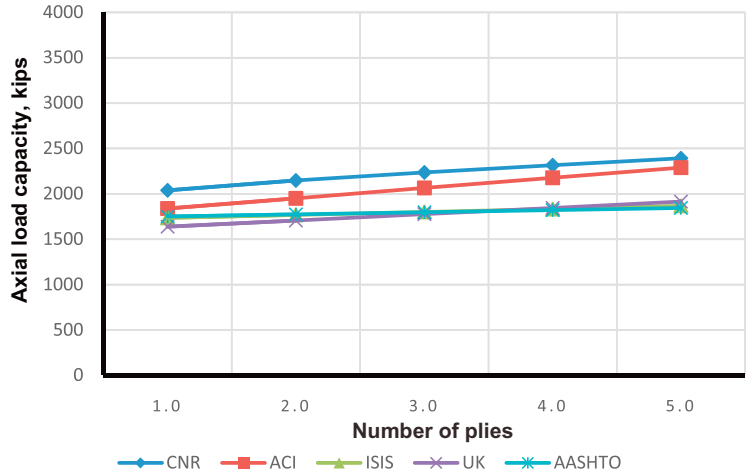

Figure 4.93 Effect of changing number of plies on factored axial load resistance, circular column, $\rho = 0.03$.

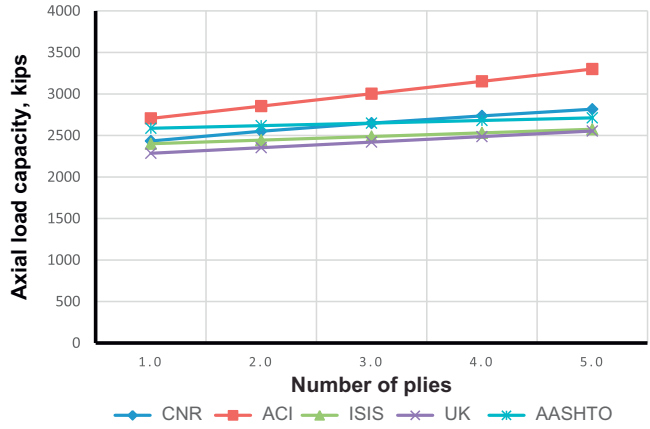

Figure 4.94 Effect of changing number of plies on unfactored axial load resistance, circular column, $\rho = 0.04$.

In summary, the following general observations can be made. The different codes produce more consistent values of capacity when f'_c is varied than when ply number is varied. This is because changing the number of plies results in different FRP stress and strain limits imposed by different codes, which becomes the underlying cause of lack of agreement. Only a small change in axial capacity occurred when ply number changed from 1 to 5, while similarly changing f'_c resulted in large

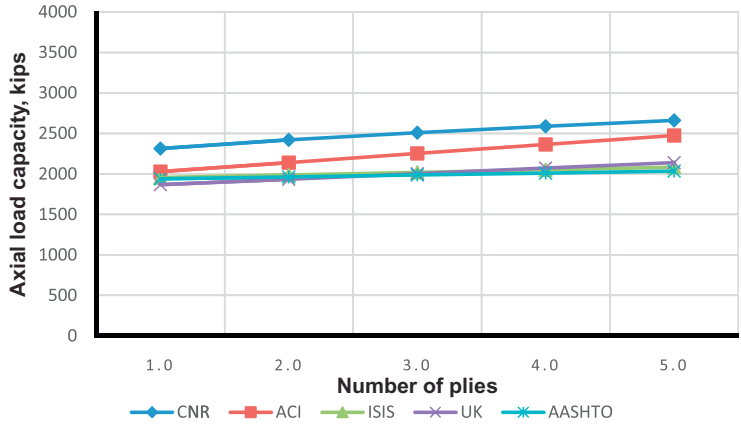

Figure 4.95 Effect of changing number of plies on factored axial load resistance, circular column, $\rho = 0.04$.

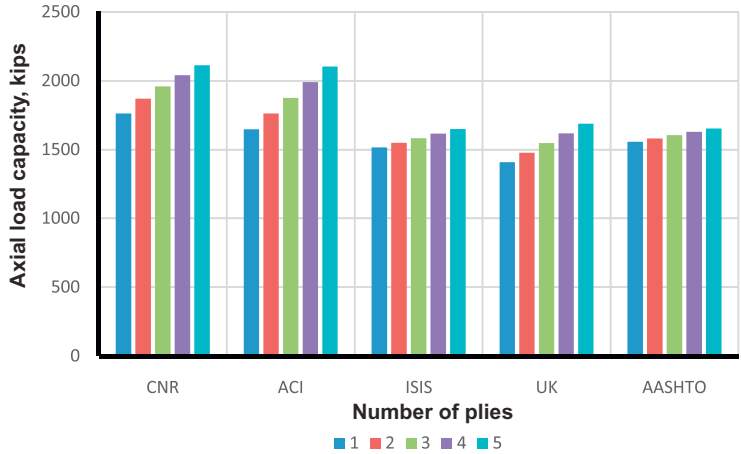

Figure 4.96 Effect of changing number of plies on axial load capacity, circular column, $\rho = 0.02$.

differences in capacity. Overall, CNR is least conservative for most cases, while AASHTO and ISIS produce close results for most cases.

4.5 Witness panels

As further discussed throughout this chapter, witness panels are often part of the FRP system design. The panels are used as test panels to verify the adequacy of the FRP installation. As such, they are to be produced on-site and exposed to the same

Figure 4.97 Effect of changing number of plies on axial load capacity, square column, $\rho = 0.02$.

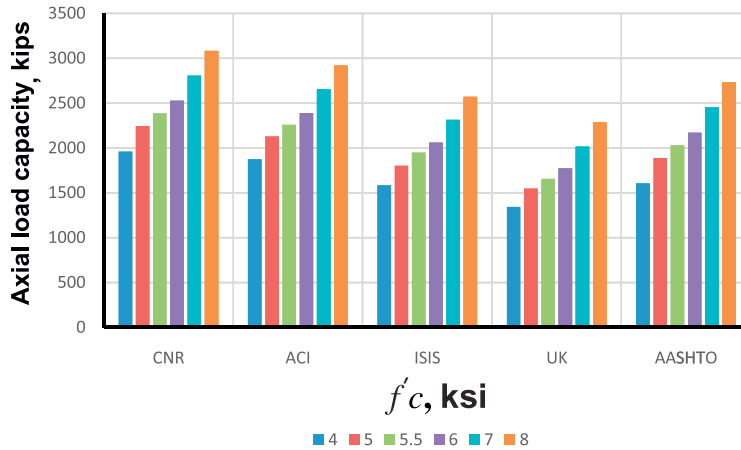

Figure 4.98 Effect of changing f'_c on axial load capacity, circular column, $\rho = 0.02$.

construction and weathering conditions as the strengthening system. Some codes recommend the use of witness panels in general, while others suggest that this decision should be left to the project engineer. Although there are no universal guidelines to their use, in general, as the size, complexity, and importance of the strengthening project increases, the benefits to witness panel fabrication become more compelling. The panels may be actual areas on the structure itself that are similar in character to the strengthened areas. In this case, additional strengthening material is applied on other areas of the structure for later testing. Alternatively the

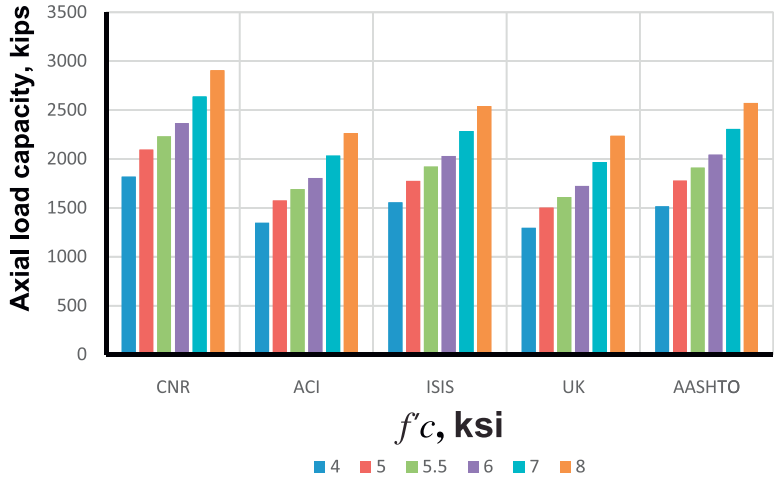

Figure 4.99 Effect of changing f'_c on axial load capacity, square column, $\rho = 0.02$.

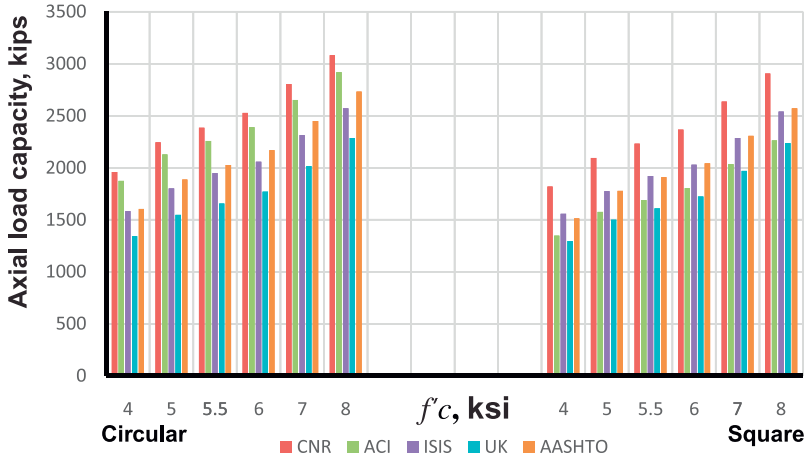

Figure 4.100 Effect of changing f'_c on axial load capacity, both circular and rectangular columns, $\rho = 0.02$.

panels may be smaller, portable specimens apart from the structure. As the panels may remain available for use for long periods of time, they can be used only to verify initial quality of the installation but long-term performance characteristics as well.

Typical witness panel sizes are from 6 to 24 in.^{2} and are best if placed on the structure itself in different locations. In general the number of panels increases with

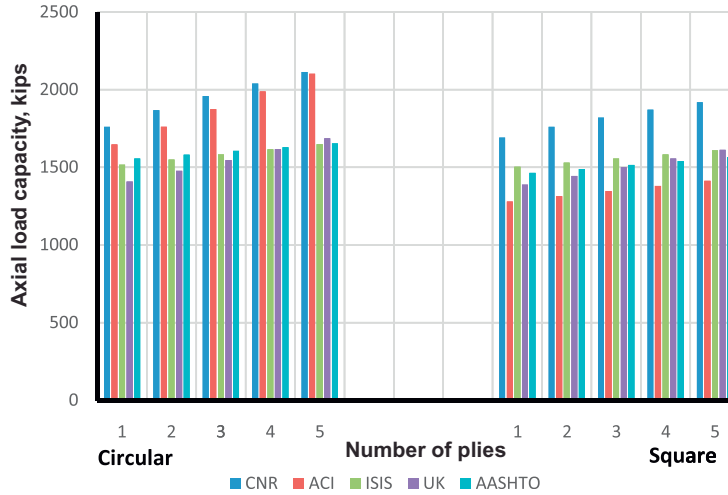

Figure 4.101 Effect of changing number of plies on axial load capacity, both circular and rectangular columns, $\rho = 0.02$.

project complexity as well as the size of the strengthened area. As such, careful planning in the design phase of the project is necessary to decide upon the number and type of panels (i.e., on or off of the structure), and if on the structure, panel placement. Additional details are provided in this chapter and Chapter 8, Recommendations.

This page intentionally left blank

Provisions for installation, quality control, and maintenance

5

5.1 Introduction

This chapter presents an overview of installation provisions of fiber-reinforced polymer (FRP) strengthening systems. Section 5.2 concerns the installation procedures and related matters including shipping, storage, and handling of FRP system components as well as contractor qualifications to perform the work needed. Section 5.3 covers all quality assurance (QA)/quality control (QC) aspects of FRP installation including inspection, evaluation, and acceptance criteria. Section 5.4 covers maintenance and repair including inspection, assessment, and repair techniques.

5.2 Installation of FRP strengthening systems

Installation includes consideration of how materials are stored and transported to the site; the qualification of contractors to conduct the work required; as well as procedures and recommendations used to install the strengthening system.

5.2.1 Shipping, storage, and handling

5.2.1.1 ACI

Shipping

In ACI, packaging, labeling, and shipping for thermosetting-resin materials are to be controlled by the *Code of Federal Regulations 49* (CFR 49). Many materials used in the system may be classified as corrosive, flammable, or poisonous in subchapter C (CFR 49) under "Hazardous Materials Regulations." As such, applicable FRP system materials are to be packaged and shipped in a manner that conforms to appropriate federal and state packaging and shipping codes and regulations.

Storage

To preserve engineering properties and maintain safety while storing FRP materials, ACI suggests that the manufacturers' recommendations are followed. Of particular concern is storage of reactive curing agents, hardeners, initiators, catalysts, and cleaning solvents which have special safety-related requirements. These items should be stored in a manner recommended by the manufacturer as well as the Occupational Safety and Health Administration (OSHA). Catalysts and initiators (usually peroxides) should be stored separately.

Strengthening of Concrete Structures Using Fiber Reinforced Polymers (FRP).
DOI: http://dx.doi.org/10.1016/B978-0-08-100636-8.00005-3

Properties of uncured resin components may change with time, temperature, and humidity. Any component material that has exceeded its shelf life, has deteriorated, or has been contaminated should not be used. FRP materials deemed unusable should be disposed of in a manner specified by the manufacturer and acceptable to state and federal environmental control regulations.

Handling

Thermosetting resins describe a generic family of products that includes unsaturated polyesters, vinyl esters, epoxy, and polyurethane resins. The materials used with them are generally described as hardeners, curing agents, peroxide initiators, isocyanates, fillers, and flexibilizers. ACI notes some general health hazards that may be encountered when handling thermosetting resins, from skin irritation to explosive reactions.

ACI recommends that product hazard labels and associated Material Safety Data Sheets (MSDS), now referred to as Safety Data Sheets (SDS), are to be read and understood by those working with these products. CFR 16, Part 1500 (2009), regulates the labeling of hazardous substances and includes thermosetting-resin materials. ANSI Z-129.1 (2010) provides further guidance regarding classification and precautions. ACI states that disposable suits and gloves are suitable for handling fiber and resin materials. Rubber or plastic gloves resistant to resins and solvents are recommended and should be discarded after each use. Safety glasses or goggles should be used when handling resin components and solvents. Respiratory protection, such as dust masks or respirators, should be used when fiber fly, dust, or organic vapors are present, or during mixing and placing of resins if required by the FRP system manufacturer.

The work place in which composite materials are prepared and installed should be well ventilated, and surfaces should be covered as needed to protect against contamination and resin spills. The manufacturer's literature should be consulted for proper mixing procedures. ACI notes that ambient-cure resin formulations produce heat when curing, which accelerates the reaction. Uncontrolled reactions, including fuming, fire, or violent boiling, may occur in containers holding a mixed mass of resin; therefore such containers should be monitored.

As cleanup can involve flammable solvents, appropriate safety precautions are suggested. However, cleanup solvents are available that do not present flammability concerns. All waste materials are to be disposed of as prescribed by the prevailing environmental authority.

5.2.1.2 ISIS

As with ACI, according to ISIS, the shipping, handling, and storage of all fiber, resin, and FRP materials are to be performed in accordance with the manufacturer's specifications. The shipping, handling, and storage of FRP materials is covered in Clause A16.1.2 of the S6-06 bridge code (CAN/CSA-S6-06, 2006) and Clause 14.3 of the S806-02 building code (CAN/CSA-S806-02, 2002). Governing safety and environmental regulations must be followed, and appropriate documentation is to be provided that specifies composite material properties, installation requirements,

and safety considerations for workers, the environment, and the public. This documentation includes technical data sheets of FRP products, as well as MSDSs.

Shipping

ISIS states that FRP materials are to be packaged and shipped in a manner that conforms to applicable packaging and shipping regulations, with particular concern to thermosetting-resin materials that are classified as corrosive, flammable, or poisonous, that must follow appropriate regulations for hazardous materials. It is the duty of the contractor and supplier to ensure that the packaging and shipping methods used do not negatively impact material properties and performance. All FRP components must be shipped with their respective MSDSs. ISIS recommends that all components of the FRP system are inspected upon delivery to the construction site, and the use of opened or damaged containers should only proceed with written authorization by the project engineer.

Storage

Proper storage of FRP components is in a clean, dry area, sheltered from the sun, which is well ventilated and temperature controlled and in accordance with the manufacturer's recommendations. As with ACI, ISIS notes that special safety requirements are required in the storage and handling of certain components such as reactive curing agents, hardeners, initiators, catalysts, and cleaning solvent. Catalysts and initiators (e.g., peroxides) should be stored separately.

The manufacturer is to provide a recommended shelf life within which the properties of the resin-based materials should continue to meet or exceed the stated performance, and the contractor must follow these time limits. Materials that have exceeded their shelf life or have otherwise exhibited signs of deterioration should be disposed of in a manner specified by the manufacturer.

Handling

ISIS refers to ACI 503R (1998) for detailed handling information and potential hazards of FRP components. However, ISIS recommends that special care should be taken to avoid material contact with water, dust, or other contaminants. Moreover, excessive bending, crushing, and other sources of mechanical damage to the fibers must be avoided. All involved in handling thermosetting resins are to read and understand product labels and MSDSs.

Personal protection precautions include the use of disposable rubber or plastic gloves that are resistant to resins and solvent penetration (which should be discarded after each use), safety glasses or goggles, as well as respiratory protection such as dust masks or respirators when handling resin components and solvents, or for operations where fiber fly, dust, or organic vapors are present. In poorly ventilated areas, the use of respiratory protection is required, preferably with a fresh air supply.

Information regarding proper storage, handling, and mixing resin components and potential hazards should be provided by the manufacturer and made available at the construction site. As with ACI recommendations, ISIS notes that mixed resin containers should be frequently monitored since uncontrolled reactions, including

fuming and fire, may occur. Similarly, ISIS notes that the work place should be adequately ventilated, and surfaces covered as needed to protect against contamination and resin spills.

All waste materials are to disposed of as prescribed by the prevailing environmental authority, and appropriate precautions observed during cleanup, since some cleaning solvents may be flammable.

5.2.1.3 AASHTO

AASHTO does not provide specific recommendations for shipping, storage, and handling. However, NCHRP Report 609 (2008), upon which other AASHTO recommendations are based, offers the following guidelines.

Shipping and storage

All FRP system components must be delivered and stored in the original factory-sealed, unopened packaging with labels identifying the manufacturer, brand name, system identification number and date. Catalysts and initiators are to be stored separately. All components must be protected from dust, moisture, chemicals, direct sunlight, physical damage, fire, and temperatures outside the range specified in system data sheets.

NCHRP 609 notes that typically, temperature in the storage area should be within 50−75°F (10−24°C), unless otherwise noted on the system data sheet, and components should be stored in a dry environment, unless an acceptable moisture level is specified on the system data sheet. It is further stated that any component that has been stored in a condition different from that stated above must be disposed of.

Handling

All FRP components, but especially fiber sheets, must be handled with care according to manufacturer recommendations to protect them from damage and to avoid misalignment or breakage of the fibers. NCHRP 609 notes that higher modulus fibers are more susceptible to misalignment damage, and therefore should be handled with greater care. After cutting, sheets shall be either stacked dry with separators, or rolled gently at a radius no tighter than 12 in (305 mm), or as recommended by the manufacturer.

All components of the FRP system, especially resins and adhesives, must be handled with care to avoid safety hazards, including but not limited to skin irritation and breathing vapors and dusts. Resin mixing is to be monitored to avoid fuming and production of excessive inflammable vapors, fire hazards, or violent boiling. It is the contractor's responsibility to ensure that all components of the FRP system at all stages of work conform to governing environmental and safety regulations.

5.2.1.4 JSCE

Shipping

JSCE recommends that the handling precautions relating to material deterioration and safety during delivery, storage, mixing, processing, and use are to be confirmed

in advance and strictly observed. Materials are to be properly shipped and stored to ensure that no deterioration occurs.

Storage and handling

JSCE notes that continuous fiber sheets and strands are easily damaged before being impregnated with resin, and some types of continuous fibers may deteriorate if exposed to ultraviolet light and moisture. Therefore, in general, the FRP materials should be stored in a cool, dark place without exposure to direct sunlight. As resins are potentially harmful to workers, resin containers must be sealed securely and stored in a cool, dark place. As resins are also flammable, fire precautions should be observed and storage quantities kept within limits prescribed by fire regulations (JSCE references the Japanese Fire Defense Law). JSCE further recommends that consideration is given to the handling manuals prepared by the material manufacturer.

5.2.1.5 TR55

TR55 does not have a specific section discussing shipping, storage, and handling. The code requires, however, that all installation related work abide by governing safety laws (TR55 references The Health and Safety at Work Act and The Control of Substances Hazardous to Health Regulations). The code emphasizes that a certificate of conformity to these laws must be provided with the materials from the supplier.

TR55 provides few additional material storage guidelines, suggesting that all materials should be stored and used strictly in accordance with the manufacturer's instructions, with particular attention to maintaining proper temperature, and for adhesives, a dry storage area. TR55 suggests that adhesive and material delivery dates should be recorded, and these items used in rotation based on the date of arrival. It further states that materials should be stored at the construction site in a way that damage and contamination are avoided.

5.2.1.6 CNR

Shipping and storage

CNR notes that each component of the FRP system is to be suitably packaged and transported according to governing safety regulations. FRP materials are to be stored according to the recommendations provided by the supplier/manufacturer. CNR notes that the properties of nonpolymerized resins may change over time and are affected by moisture and temperature. Temperature may also affect the mixture reactivity and properties of polymerized resin. Suitable environmental conditions for storage are suggested to be from 50 to 75°F (10 to 24°C) and in a dry environment with less than 20% humidity, unless otherwise suggested by the manufacturer.

In storage, care is to be taken to avoid laminate and other preformed material damage due to bending or improper stacking. It is especially important that some potentially hazardous constituents such as reactive reticulating agents, initiators, catalysts, solvents for surface cleaning, etc., are stored according to manufacturer

requirements or official standards. As with other code recommendations, CNR specifies that catalysts and initiators (typically peroxides) are stored separately from other reagents to avoid any accidental contact leading to premature polymerization.

Manufacturers are to indicate the storage time (shelf life) that ensures thermosetting resin properties are maintained. Constituents exceeding their shelf life or suffering degradation or contamination are not to be used, and those deemed unusable are to be disposed of according to manufacturer specifications as well as the governing safety laws.

Handling

CNR states that the manufacturer is to provide the MSDSs for all FRP constituents. It notes that substances used in combination with thermoset resins are typically hardeners, cross linkers, initiators (peroxides), and fillers, and these are associated with potential health hazards. Personnel working with these substances are to read all labels as well as MSDS to minimize risks. When handling fibers and resins, disposable gloves and work-suits, as well as protective glasses are suggested. Rubber or plastic gloves are to be solvent-resistant. In the presence of fiber fragments, dusts or solvent vapors, or when mixing and applying resins, respiratory protection devices are needed, in accordance to the suggestion of the FRP manufacturer. The working site must always be properly ventilated.

5.2.1.7 Summary of shipping, storage, and handling

ACI, ISIS, and CNR stipulate that packaging, labeling, and shipping are to be done in accordance with applicable national and local packaging and shipping codes and regulations. ISIS stresses the need to abide by the manufacturer's guidelines for shipping as well. AASHTO and TR55 have no specific regulations for shipping. JSCE emphasizes the need to properly ship FRP materials to prevent material deterioration during shipping.

AASHTO does not have provisions regarding FRP storage, and storage recommendations are taken from NCHRP 609. ACI, NCHRP 609, ISIS, CNR, and TR55 state that storage of FRP materials should be done in accordance with manufacturer's recommendations to preserve the material properties and maintain worker safety. ACI adds that reactive curing agents and cleaning solvents should also be stored as recommended by OSHA. ACI, NCHRP 609, ISIS, and CNR require that catalysts and initiators (usually peroxides) be stored separately.

Since FRP materials have a prescribed shelf life, there is a chance that stored materials exceed this limit and require disposal. ACI requires that material disposal be conducted in accordance with the manufacturer's guidelines and be acceptable to state and federal environmental control regulations. CNR states that disposal should be done in accordance to the manufacturer as well as the provisions of safety laws and regulations. ISIS relies only on the manufacturer's recommendations for materials disposal. AASHTO has no specific recommendations for materials disposal. However, NCHRP 609, Section 3.4 stipulates that disposal of expired

materials be performed in a manner to protect the environment and follow the manufacturer's recommendations as stated in the MSDS.

Storage temperature, moisture, and other considerations are discussed with varying details among different codes. AASHTO specifies a storage temperature of 50−70°F (10−21°C), a dry enclosure protected from dust, moisture, direct sun, and the risk of fire or damage. CNR recommends the same temperature range as NCHRP 609, but requires a dry environment with a moisture not to exceed 20% or as recommended by the manufacturer. ACI has no specific stated temperature or moisture recommendations but suggests following the recommendations of the manufacturer. TR55 states that storage temperature range is to be in accordance with the manufacturer, while JSCE places emphasis on fire protection of the storage facility based on limits prescribed by the Fire Defense Law. JSCE adds several requirements for storage such as maintaining a cool temperature and a dark environment with no direct exposure to sunlight.

ACI, NCHRP Report 609, ISIS, and CNR require that manufacturer's recommendations are to be used when handling FRP materials to protect against health risks from skin exposure or fume inhalation. ACI refers to CFR 16, Part 1500 for regulations on hazardous substance labeling, and ANSI Z-129.1 for further guidance regarding classifications and precautions. ACI, ISIS, and CNR require individuals handling FRP system components to wear disposable suites, gloves, eye protection, and respirators for safe handling of the materials. The three codes recommend the use of a well-ventilated work place. TR55 and JSCE have no coverage of FRP materials handling. ACI and ISIS state that for cleanup and disposal, the use of cleanup solvents that do not present a high flammability risk is advisable. The codes require that all waste materials be contained and disposed as prescribed be the prevailing environmental authority.

5.2.2 Contractor qualifications

5.2.2.1 ACI

ACI suggests that the FRP system installation contractor should demonstrate competency for surface preparation and application of the FRP system to be installed. This competency can be demonstrated by providing evidence of training and documentation of related work previously completed, or by an actual demonstration of surface preparation and installation. It is recommended that the FRP system manufacturer or its authorized agent should train the contractor's application personnel in the installation procedure for the specific system to be used.

5.2.2.2 ISIS

ISIS stipulates that the contractor is responsible for providing the training of his staff and shall provide proof of the qualification or experience of his staff to the project engineer. The staff, which includes the installation crew, supervisors, and safety officers, must be properly trained on the specific tasks within their responsibility.

For example, a site safety officer must be trained on the course of action in the case of accident in accordance with materials safety regulations provided in the MSDSs.

5.2.2.3 AASHTO

As with ACI, AASHTO recommends that FRP application must be performed by a contractor trained in accordance with the installation procedures specified by the manufacturer. For further information, AASHTO references NCHRP 609 (2008). According to NCHRP 609, the manufacturer/supplier may be prequalified for each FRP system to be installed, after providing the following information:

- System data sheets and MSDS for all components of the FRP system;
- Documentation of a minimum of 5 years' experience with the FRP system, or 25 documented similar field applications with acceptable reference letters from respective owners;
- Documentation of a minimum of 50 test data sets from an independent agency approved by the owner verifying the mechanical properties, aging and environmental durability of the proposed FRP system, and;
- Documentation of the availability of a comprehensive hands-on training program for each FRP system that can be taken by the staff of the contractor/applicator.

The owner may also require the manufacturer/supplier to provide a specified number of samples of the components and the complete FRP system for in-house or independent testing prior to qualification. The training program conducted by the manufacturer/supplier should provide hands-on experience with surface preparation and installation of the same FRP system for which the certificate is issued. The contractor/applicator may be prequalified by the owner for each FRP system, after providing documentation of a minimum of 3 years' experience or 15 similar field applications with acceptable reference letters from respective owners, and a certificate of completed training from the manufacturer/supplier for at least one staff member who will be present on site throughout the project.

5.2.2.4 JSCE

JSCE recommends that work should be performed under the supervision of an engineer who has thorough knowledge of FRP strengthening. However, the code does not specifically discuss criteria for qualifying a contractor.

5.2.2.5 TR55

TR55 recommends that various issues should be taken into account when selecting a contractor. In particular, it suggests that the contractor provides evidence of experience in strengthening work, has QA procedures in place, and is accredited and audited in accordance with ISO 9002. TR55 further suggests that the contractor should be a member of the Concrete Repair Association or has a record of successful projects involving the installation of composites. Moreover, the contractor should provide a detailed statement of the method which will be used to install the composites as well as an assessment of the risks involved. This should include

discussion of the procedure which will be used to minimize the risks to the workforce and to any other persons (especially children) who may be affected by the work. The contractor's personnel should be supplied with the correct protection equipment for use when handling the materials, and trained and qualified in the application technique specified by the manufacturer of the system. Finally, the contractor should provide a safe means of access to the work location and maintain an environment suitable for the successful use of structural adhesives.

5.2.2.6 CNR

CNR does not provide specific recommendations for qualifying a contractor. However, it defines several responsibilities of the contractor as follows. The contractor is to obtain the material indicated by the designer through suppliers/manufacturers who guarantee the quality of their products, and is to ensure that the products are accompanied by technical data sheets, reporting both mechanical and physical characteristics, and possibly laboratory test certificates. Finally, the contractor is to see that these products comply with the provisions indicated by the designer, and if the material with the indicated requirements is not available, the contractor is to work with the designer to find a viable alternative.

5.2.2.7 Summary of contractor qualifications

ACI, ISIS, and TR55 require that the contractor provide evidence of training on the FRP strengthening system to be used, as well as provide evidence of past experience of similar projects. CNR and JSCE do not provide any specific contractor qualifications requirements. AASHTO refers to NCHRP 609 for recommendations with regard to contractor qualifications. This report offers a comprehensive list of qualification requirements for the supplier and the contractor with specifics such as documentation to verify the required years of experience for the supplier (5 years). The report generally requires the submittal of documented evidence for all items needed for qualification (see Section 5.2.2.3).

5.2.3 Installation procedures

5.2.3.1 ACI

ACI notes that procedures for installing FRP systems have been developed by the system manufacturers and often differ between systems. In addition, installation procedures can vary for the same system, depending on the type and condition of the structure. ACI recommends that deviations from the procedures developed by the manufacturer should not be allowed without manufacturer approval.

Temperature, humidity, and moisture considerations

ACI emphasizes that temperature, relative humidity, and surface moisture at the time of installation can affect the performance of the FRP system. It suggests that primers, saturating resins, and adhesives should generally not be applied to cold or

frozen surfaces. When the surface temperature of the concrete surface falls below a minimum level as specified by the FRP system manufacturer, improper saturation of the fibers and improper curing of the resin constituent materials can occur, compromising the integrity of the system. It suggests that a noncontaminating heat source can be used to raise the ambient and surface temperatures during installation.

With regard to moisture, ACI states that resins and adhesives should generally not be applied to damp or wet surfaces unless they have been formulated for such applications. Moreover, FRP systems should not be applied to concrete surfaces that are subject to moisture vapor transmission. ACI warns that the transmission of moisture vapor from a concrete surface through the uncured resin materials typically appears as surface bubbles and can compromise the bond between the FRP system and the substrate.

Equipment

Some installation procedures specify unique equipment designed for the application of that particular system. This equipment can include resin impregnators, sprayers, lifting/positioning devices, and winding machines. ACI suggests that all equipment should be clean and in good operating condition. All supplies and equipment should be available in sufficient quantities to allow continuity in the installation project and QA.

Surface preparation

Successful strengthening with FRP systems is dependent on a sound concrete substrate and proper preparation of the concrete surface, as an improperly prepared surface can result in debonding or delamination. Although ACI presents general guidelines intended to all externally bonded FRP systems, it notes that specific guidelines for a particular FRP system should be obtained from the manufacturer. For general methods of concrete repair and surface preparation, ACI refers to ACI 546R (2004) and ICRI 03730 (2008). ACI suggests that the FRP system manufacturer should be consulted to ensure compatibility of the FRP system with the materials used for repairing the concrete substrate, if necessary. If corrosion-related concrete deterioration is detected, ACI suggests that the cause of the corrosion be addressed, and the associated deterioration repaired before application of the FRP system.

To repair cracks, those wider than 0.010 in. (0.3 mm) can be pressure injected with epoxy before FRP installation, in accordance with ACI 224.1R (2007). Cracks of smaller width may require resin injection or sealing to prevent corrosion of existing reinforcement. ACI refers to ACI 224.1R (2007) for crack-width limitations based on different exposure conditions.

ACI classifies surface preparation into two major categories: bond-critical or contact-critical. Bond-critical applications require an adhesive bond between the FRP and the concrete, and usually involve systems for flexural or shear strengthening. ACI suggests that surface preparation for bond-critical applications

should be in accordance with ACI 546R (2004) and ICRI 03730 (2008). A summary of recommendations is given as follows:

- The surface on which the FRP system is to be applied should be free of loose or unsound materials, and where fibers wrap around the corners of rectangular cross-sections, the corners should be rounded to a minimum 0.5 in. (13 mm) radius to prevent stress concentrations in the FRP as well as voids between the FRP and the concrete. This applies to both vertical and horizontally oriented corners. Note that ACI does not specifically mention allowing an existing or created chamfered edge to substitute for a rounded edge. Roughened corners can be smoothed with putty. Inside corners and concave surfaces may require special detailing to ensure bond between the FRP system and the concrete.
- Consideration should be given to removing obstructions and embedded objects in the concrete before installing the FRP system, and surface preparation can be accomplished with either abrasive or water-blasting techniques. Bug holes and other small surface voids should be completely exposed during surface profiling. After profiling, the surface should be cleaned and protected.
- The concrete surface should be prepared to a minimum concrete surface profile (CSP) 3, as defined by ICRI surface profile chips, and localized out-of-plane variations, including form lines, should not exceed 1/32 in. ($\sim$1 mm) or the tolerances recommended by the FRP system manufacturer.
- Localized variations can be removed by grinding, before abrasive or water blasting, or can be smoothed over using resin-based putty if variations are small. Bug holes and voids should be filled with resin-based putty. All surfaces to be strengthened should be as dry as recommended by the FRP system manufacturer.

Contact-critical applications only require close contact between the FRP and concrete and are generally reserved for confinement strengthening. In applications involving confinement, the surface should be prepared such that continuous contact between the concrete and the FRP system is maintained. Moreover, surfaces to be wrapped should be flat or convex, and large surface voids should be patched. Materials with low compressive strength and elastic modulus, such as plaster, should be removed.

Mixing of resins

According to ACI, the manufacturer should supply recommended batch sizes, mixture ratios, mixing methods, and mixing times, and all mixing should be done according to the manufacturer's recommendations. Resin components should be at the proper temperature and mixed until there is a uniform and complete mixing of components. Resins should be mixed for the prescribed mixing time and visually inspected for uniformity of color. As resin components are often contrasting colors, ACI notes that full mixing is usually achieved when color streaks are eliminated. Resin mixing should be in quantities sufficiently small to ensure that all mixed resin can be used within the resin's pot life.

Application

ACI recommends that FRP systems be selected with consideration for their impact on the environment, including emission of volatile organic compounds and toxicology.

Where required, primer should be applied to all areas on the concrete surface where the FRP system is to be placed. Here, primer should be placed uniformly at the manufacturer's specified rate of coverage. Once applied, the primer should be protected from dust, moisture, and other contaminants before applying the FRP system. Putty should be used in an appropriate thickness and sequence with the primer as recommended by the FRP manufacturer, and only to fill voids and smooth surface discontinuities. Rough edges or trowel lines of cured putty should be ground smooth, and primer and putty should be cured as specified by the FRP system manufacturer before applying the FRP resin or adhesive. Note that after the putty and primer are cured, the FRP system manufacturer may require additional surface preparation before the application of the saturating resin or adhesive.

The use of solvents to clean the FRP surface before applying a coating is not recommended due to the damaging effect that solvents may have on resin, and the FRP system manufacturer should approve the use of any solvent wipe. Coatings should be periodically inspected and maintenance provided as needed to ensure the effectiveness of the coating.

Wet lay-up FRP systems are typically installed by hand using dry-fiber sheets and a saturating resin and should use the manufacturer's installation recommendations. Generally, saturating resin should be applied uniformly to all prepared surfaces where the system is to be placed, then the reinforcing fibers should be gently pressed into the resin. Entrapped air between layers should be released or rolled out before the resin sets. Sufficient resin should be applied to achieve full saturation of the fibers, and successive layers of saturating resin and fibers should be placed before the complete cure of the previous resin layer. If previous layers have cured, interlayer surface preparation, such as light sanding or solvent application as recommended by the system manufacturer, may be required.

Wrapping machines are primarily used for concrete columns. Machine-applied systems can use resin preimpregnated tows or dry-fiber tows; prepreg tows are impregnated with saturating resin off-site and delivered to the work site as spools, while dry fibers are impregnated at the job site during the winding process. ACI emphasizes that the FRP system manufacturer's recommendations should be followed in all application steps. After wrapping, prepreg systems should be cured at an elevated temperature in accordance with the manufacturer's recommendations.

Precured systems include shells, strips, and open grid forms that are typically installed with an adhesive. General recommendations are as follows. Surfaces to be bonded should be clean and prepared in accordance with the manufacturer's recommendations, with a minimum CSP of 3 (ICRI 03732). The adhesive should then be applied uniformly at the rate recommended by the FRP manufacturer. After the precured sheets are placed into the wet adhesive, entrapped air between layers should be released or rolled out before the adhesive sets. Any protective coatings that are used should be compatible with the FRP strengthening system and applied in accordance with the manufacturer's recommendations.

Alignment of FRP materials

Proper FRP alignment is critical, as even small variations in angle (as little as 5 degrees) from that intended can cause a substantial reduction in strength and

stiffness. Therefore materials should be handled such that correct fiber straightness and orientation are preserved, and deviations in ply orientation should be made only if approved by the project engineer. Moreover, kinks, folds, waviness, or other forms of substantial material malformation should be reported for evaluation.

Multiple plies and lap splices

Multiple plies may be used, provided that all plies are fully impregnated with resin the shear strength is sufficient to transfer the shearing load between plies, and the bond strength between the concrete and FRP system is sufficient. Lap splices may be used for long spans as necessary, provided that they are staggered, unless otherwise approved by the project engineer. Lap splice details, including lap length, should be based on testing and installed in accordance with the manufacturer's recommendations. Specific guidelines on lap splices are given in ACI Chapter 13.

Curing

Ambient-cure resins can take several days to reach full cure, and temperature extremes or fluctuations can retard or accelerate curing time. All resins should be cured according to the manufacturer's recommendations, and field modification of resin chemistry should not be permitted. The cure status of installed plies should be verified to be sufficient before placing subsequent plies, and the installation of successive layers should be halted if there is a curing anomaly.

To meet the manufacturer's curing recommendations, FRP systems may require protection such as tents or plastic screens, during installation and curing against adverse temperatures, direct contact by rain, dust, or dirt, excessive sunlight, high humidity, and vandalism. If temporary shoring is required, the FRP system should be fully cured before the shoring is removed. If damage to the FRP system is suspected during installation, the project engineer should be notified and the FRP system manufacturer should consulted for evaluation.

5.2.3.2 ISIS

As with ACI, ISIS stresses the importance of following the specific recommendations of the FRP system manufacturer.

Temperature, humidity, and moisture considerations

ISIS notes that the temperature, humidity, and dew point at the time of installation can affect the performance of the FRP system. It suggests that in general, primers, saturating resins, and adhesives should not be applied to cold or frozen surfaces. Per Clause A16.1.3.5 of the S6-06 bridge code, during the installation of the FRP, ambient air and concrete surface temperature should be 50°F (10°C) or more; the concrete surface temperature should be at least 5°F (3°C) higher than the actual dew point; and atmospheric relative humidity should be less than 85%. To meet these conditions in colder temperatures, it may be necessary to provide a noncontaminating auxiliary heat source to the FRP material during the installation and curing processes.

Moreover, resin and adhesive materials should not be applied to wet surfaces unless they are specifically formulated for this purpose, and FRP materials should not be applied to concrete surfaces that are subject to condensation, vapor transmission, or water ingression unless such issues are clearly addressed by the system design and the resin systems are specifically formulated for use in such conditions.

Equipment

As with ACI, ISIS suggests that all equipment used in the installation process should be clean and in good operating condition and should be accessible for inspection by the project engineer. The contractor should have qualified personnel sufficiently trained to install and operate system-specific equipment such as resin impregnators, sprayers, lifting/positioning devices, and winding machines. All materials, and supplies, and personal protective equipment should be available in sufficient quantities to allow safe construction continuity and QA.

Surface preparation

For concrete surface preparation details, ISIS refers to Clause A16.1.4 of the S6-06 bridge code (2006) and Clause 14.9 of the S806-02 building code (2002). ISIS suggests that the concrete surface preparation should be inspected and approved by the engineer or the supervisor prior to the application of the FRP. Some specific recommendations are as follows. ISIS recommends that the surface preparation should be performed according to the FRP system manufacturer's guidelines. Surfaces in good condition may only require cleaning, but all signs of deterioration, including that caused by steel corrosion, should be repaired prior to the application of the FRP system. Before the repair process, the concrete surface must be free of particles and pieces that no longer adhere to the structure, and cleaned from oil and other contaminants. An inspection and approval of the surfaces is then required before the repair may begin. During the repair, the concrete surfaces must be repaired or reshaped in accordance with the original section, and sections with sharp edges must be rounded to a minimum radius of 1.4 in. (35 mm), in accordance with the S6-06 bridge code (2006), before installing the FRP system.

Cracks wider than 0.01 in. (0.3 mm) should be pressure injected with epoxy in accordance with the guidelines of ACI 224.1R (2007), and smaller cracks in aggressive environments may also require epoxy injection to prevent corrosion of steel reinforcement. All surface repairs should meet the requirements of the FRP system manufacturer.

For bond-critical applications, the method of surface preparation should depend on the existing surface condition. A smooth concrete surface can be sandblasted or otherwise abraded until aggregates become visible according to the relevant preparation recommendations. After blast cleaning, the surface should be protected within an appropriate amount of time prior to the FRP installation. Areas that are very rough can be leveled using a material approved by the manufacturer and/or the engineer, and out-of-plane variations should be within the tolerances recommended

Table 5.1 Maximum depth of depressions on the concrete surface

Type of FRP	Max. depth for length of 12 in. (0.3 m) (in.)	Max. depth for length of 80 in. (2.0 m) (in.)
Plates $\geq$0.04 in. (1.0 mm)	0.16 in. (4.0 mm)	0.39 in. (10.0 mm)
Plates <0.04 in. (1.0 mm)	0.08 in. (2.0 mm)	0.24 in. (6.0 mm)
Sheets	0.08 in. (2.0 mm)	0.16 in. (4.0 mm)

by the FRP system manufacturer, where small holes and voids should be filled with putty or a mortar polymer. The maximum allowed depth of depressions (see Clause A16.1.4 of the S6-06 bridge code) is shown in Table 5.1 (ISIS Table 8.1).

All dirt, oil, existing coatings, or other matter that could interfere with the bond of the FRP should be removed. The concrete surface must have a tensile and shear strength high enough to ensure an efficient bonding; Clause A16.1.4 of the S6-06 bridge code requires a minimum tensile strength of 218 psi (1.5 MPa) as measured by a pull-off tension test in accordance with ASTM D4541 (2002). Rectangular cross-sections should have corners rounded or reshaped to a minimum radius of 1.4 in. (35 mm), and roughened corners should be smoothed with an epoxy gel.

All surfaces to which the strengthening system will be applied should be dry according to the FRP system manufacturer's requirements, and the moisture content should be evaluated according to the requirements of ACI Standard 503.4 (2003).

For contact-critical applications such as confinement, the surface preparation should guarantee a continuous contact between the concrete and the FRP confinement system. Rounding of corners, filling holes, and eliminating depressions are most critical.

For all types of applications, if water seepage through the concrete is found, special resins designed for this bond condition must be used. Both the engineer and the contractor must verify that the pressures will neither cause debonding nor affect the integrity of the reinforced structure. If FRP is to be installed underwater, the method to be used must be prescribed in detail according to the recommendations of the manufacturer and must be approved by the engineer.

Mixing of resins

When mixing resins, all components should be mixed at a proper temperature and in the correct ratio until there is uniform and complete mixing and the product is free from trapped air. The resin mixing should be done in quantities sufficiently small to ensure that all mixed resin will be used within the resin's pot life.

Application

ISIS references Clause A16.1.3 of the S6-06 bridge code for FRP application. ISIS recommends that all materials, including primer, putty, saturating resin and fibers, are part of the same system. ISIS notes that appropriate installation procedures should depend on the specific FRP system and the structure for strengthening.

For hand-applied wet lay-up systems, manufacturer recommendations must be followed in all application steps, and the following additional recommendations are suggested. Putty should be used only to fill voids and smooth surface discontinuities prior to the application of other materials and should be used in an appropriate thickness and in sequence with the primer as recommended by the FRP manufacturer. Primer should be placed uniformly on the prepared surface at the specified rate of coverage and should have sufficiently low viscosity to penetrate the surface of the concrete substrate. Rough putty edges or trowel lines should be smoothed before installation of the fiber sheets.

Hand-applied, wet lay-up materials include dry as well as preimpregnated fiber sheets and fabrics used with a saturating resin applied on site. In the latter case the saturating resin should be applied uniformly to all prepared surfaces where the FRP is to be placed. The resin should have sufficiently low viscosity such that the fiber reinforcement becomes fully impregnated with resin prior to curing. Once the FRP is applied, entrapped air under the sheet or between layers should be released or rolled out before the resin sets. In doing so, it is recommended to work the FRP materials parallel to the fibers, proceeding in one direction from the center or from one extremity and to avoid any backward and forward movements. A protective finish compatible with the proposed system should be applied in accordance with the manufacturer's recommendations.

When using precured systems (i.e., surface bonded plates), the precured laminate surfaces to be bonded should be cleaned and prepared in accordance with the manufacturer's recommendations. Adhesive should be applied uniformly to the prepared surfaces where the laminates are to be placed. Care should be taken to use an application method to avoid entrapping air under the laminate, because such a condition is difficult to detect as well as to rectify. In contrast to hand-applied, wet lay-up materials, stacking multiple layers of FRP plate is usually not permitted, except for the overlapping portion of prefabricated L-shaped stirrups. At intersections of FRP plates, care should be exercised to minimize curvature; grooving the concrete for the layer underneath is sometimes used to allow full contact between the plate and the concrete surface underneath.

For FRP material used to wrap the base of a reinforced concrete column that is in contact with the ground, the wrapping should extend a minimum of 20 in. (500 mm) below the ground surface to prevent water and air infiltration. ISIS also states that FRP stirrup strips for shear reinforcement must be anchored in a satisfactory manner at both extremities; this anchorage is to be specified by the designer.

Alignment of FRP materials

ISIS notes that the alignment of the FRP material is critical, and the ply orientation and stacking sequence must be specified in the design prior to installation. As with ACI, ISIS specifies that sheet and fabric materials should be handled in a manner to maintain the fiber straightness and orientation, as even small variations in the intended orientation angle can cause a reduction in strengthening. Any observed deviation in angle for an installed FRP are to be approved by the project engineer.

Multiple plies and lap splices

ISIS allows the use of multiple layers of FRP materials, provided that all layers are fully impregnated within the resin system, that the resin shear strength is sufficient to transfer the shearing load between layers, and that the FRP-to-concrete adhesive strength is sufficient. However, the project engineer or the manufacturer may limit the maximum number of consecutive layers, and/or define the installation period between successive layers. When several superposed layers of FRP materials are required, care must be taken not to move or otherwise disturb the preceding layers where the resin has not set. In the absence of other prescriptions, a minimum overlap length parallel to the fibers of 6 in. (150 mm) is suggested. If an interruption of the FRP system laying up process occurs, interlayer surface preparation such as cleaning or light sanding may be required.

Curing

FRP materials are to be cured according to the recommendations of the manufacturer. Unless otherwise specified, ISIS recommends the following curing provisions. A minimum curing time of 24 h should be allowed before further work is performed, unless the curing process is accelerated by heating (via a chemical reactant or other external supply). For the entire curing duration, the temperature must be maintained above the minimum required curing temperature; condensation on the surface must be prevented; and chemical contamination from gases, dust, or liquid sprays must be prevented during curing. ISIS notes that although successful rehabilitation of beams under simulated traffic loads have been reported), mechanical stresses should be minimized during curing.

Protective coating

When the surface of the FRP materials is sufficiently dry or hard, a protective coating and/or paint compatible with the installed reinforcement system can be added. A minimum of 24 h should be allowed for the protective coating/paint to dry, or as recommended by the manufacturer. Further, the contractor is required to provide a certificate of compatibility of the protection system prepared by the FRP manufacturer, and the contractor is to provide a guarantee for the performance of the proposed protection system for the expected exposure conditions. The protection system must provide sufficient protection against ultraviolet radiation. It may include a wearing layer if the FRP reinforcement materials are expected to be subjected to abrasive effects. The wearing layer must not be considered to be structural reinforcement, and it must be inspected and maintained regularly. If the FRP reinforcement must be protected against fire, the protection system proposed must be approved by the engineer, and the contractor or manufacturer must guarantee its compliance.

5.2.3.3 AASHTO

AASHTO requirements are written in a similar manner to those given by ACI and ISIS. According to AASHTO, procedures for the installation of FRP systems are developed by the manufacturer and can vary between different systems. Procedures may also vary depending on the type and condition of the structure to be

strengthened. AASHTO notes that the application of FRP systems will not stop the ongoing corrosion of existing steel reinforcement, and the cause of any corrosion should be addressed and corrosion-related deterioration should be repaired prior to application of any FRP system.

Temperature, humidity, and moisture considerations

When temperatures exceed 90°F, the epoxy may be difficult to apply due to an accelerated hardening rate. AASHTO thus recommends that work should be scheduled to avoid high temperatures. If it is necessary to apply epoxy compounds in high temperatures, the work should be supervised by a person experienced in applying epoxy under such conditions. AASHTO also notes that epoxy systems formulated for elevated temperatures are available and should be considered (see ACI 530R-93). At temperatures below 40°F, application difficulties may also occur due to a deceleration of the rate of curing, and the presence of frost or ice crystals may be detrimental to the bond between the FRP and the concrete.

Surface preparation

Prior to FRP application, the concrete surface should be prepared to a minimum CSP 3. Proper preparation and profiling of the concrete surface is necessary to achieve the specified bond strength; improper surface preparation can lead to debonding or delamination. AASHTO recommends that localized out-of-plane variations, including form lines, should not exceed 1/32 in. or the tolerances recommended by the FRP system manufacturer, whichever is smaller. Bug holes and voids are to be filled with epoxy putty. It is recommended that surface preparation be accomplished using abrasive or water-blasting techniques, and all contaminants that could interfere with the bond between the FRP system and concrete substrate should be removed. When fibers are wrapped around corners, corners should be rounded to a minimum radius of 1/2 in. to prevent stress concentrations in the FRP system as well as voids between the FRP and the concrete. Rough edges can be smoothed by grinding or with putty.

5.2.3.4 JSCE

Temperature, humidity, and moisture considerations

When bonding or wrapping with continuous fibers, at each stage of the work it should be verified that environmental conditions are suitable. Suitable conditions for epoxy resin applications are a 41°F (5°C) or higher temperature and humidity no more than 85%. In lower temperatures the construction site should be warmed or a low-temperature primer and resin may be used. If the surface of the concrete is not dry, special primers for wet surfaces should be used. It should also be verified that the concrete surface preparation is suitably performed; that the mixing and coating of primer are appropriately performed; and that the mixing and coating of a smoothing agent are appropriately performed.

To prevent improper hardening of the primer and smoothing agent, the materials should be applied to a dry surface. After application, the primer and smoothing agent should be allowed to harden until firm, and should be checked visually and by touch to make sure there is no dust or moisture on the surface. If there is

condensation or other moisture on the surface before initial hardening, indicated by whitening, the area should be wiped with solvent or the effected portion of primer or smoothing agent removed with sandpaper.

Surface preparation

Prior to application of FRP, JSCE recommends that construction defects, remarkable deterioration, and surface cracking in the concrete should be repaired. These defects include problems such as rock pockets, honeycombs, level differences, or other surface imperfections, which deviate from a smooth surface and can reduce the effectiveness of the FRP strengthening.

When continuous fiber sheets and continuous fiber strands are placed perpendicular to corner angles, the angles should be rounded by chipping, polishing, or the use of a smoothing agent.

To ensure proper bond between the FRP and the concrete surface, deteriorated layers, oils, and other contaminants should be removed from the surface.

Application

When using continuous fiber sheets, JSCE notes that it is critical that the sheets are attached with the specified position, direction, and number of plies. A working diagram matching the actual structure should be prepared based on the design. The diagram should clearly identify the reference point for attachment, the overlap splice positions and the number of plies to enable the sheets to be attached properly. It must also be ensured that the sheet is bonded or sealed securely to the concrete surface, and that the resin is suitably mixed and applied and has thoroughly impregnated the sheet. This is particularly important in the overlap splice sections, where the impregnation resin should thoroughly penetrate between the fibers and sheets. After attaching the continuous fiber sheets, an inspection should be done visually or through sounding to verify the absence of lift, swelling, peeling, slackness, wrinkles, and voids in the epoxy resin impregnation.

When using continuous fiber strands, it must be verified that the strand winding interval is appropriate, the strand winding tension is constant, the strand winding speed is appropriate, the strands are thoroughly impregnated with resin, that the resin has been suitably mixed and applied, and that the impregnation resin is cured thoroughly. JSCE notes that if carbon fiber strands are wound by hand, the tension force applied is not constant, resulting in variations of stress distribution in the strands after completion. Moreover, since the winding speed is not constant, there may also be variations in the degree of permeation of the impregnation resin. These issues may affect the tensile strength of the strands. For these reasons, the use of a machine to wind the strands, to control the winding interval, tension, and speed, is recommended.

JSCE notes that when wrapping FRP around corners, it is important that a sufficient radius of curvature is maintained, as when the radius of curvature is small, as noted by AASHTO, stress concentrations occur, decreasing the effective tensile strength of the FRP. In general the chamfer radius should be between 0.4 in. and

2.00 in. (10−50 mm). However, the type and thickness of FRP used have a large influence on the necessary chamfer radius.

Lap splices

JSCE states that the required lap length is to be determined through testing in accordance with JSCE-E 542 (2000). JSCE note that carbon and aramid fiber sheets have been found to require an overlap splice length of approximately 4 in. (100 mm) at the lower stress level produced in the splice zone and about 8 in. (200 mm) for strengthening for shear capacity and ductility. However, depending on the type of FRP and resin used, the splice strength may be lower than the tensile strength of the FRP and failure may occur in the bonded layers of the splice even if the overlap length is long.

When only one layer of continuous fiber sheet is used for reinforcement, variations in overlap splice strength due to construction errors may significantly influence the splice strength. In such cases, it is recommended to elongate the overlap splice length and to attach one more layer of FRP over the splice section. When more than one layer is used, the overlap splices should not be placed at the same section, since this reduces the overlap splice strength. Overlap splices should not be placed at locations subjected to large bending moments.

Curing

After applied, resin should be cured for a suitable period of time before the next sheet is attached. Before the initial setting of the impregnation resin, JSCE recommends that the surface should be protected with vinyl sheets from rain, dust, and sudden climatic changes. It must also be verified that the impregnation resin is cured thoroughly.

Anchorage length

JSCE notes that an item requiring verification is the end anchorage of FRP, for which it should be confirmed that the strand is wound with the required number of turns at the section to be anchored. The required number of turns for anchorage should be determined through testing. JSCE states that one to two wraps is sufficient anchorage for carbon fiber strands composed of 12,000 filaments.

If mechanical anchorage is to be used, it can be by way of anchor bolts and plates and should be verified by confirming that the anchorage detail has sufficient strength to prevent anchorage failure. JSCE suggests that when reinforcing bridge pier foundations, mechanical anchoring with anchor plates and bolts may be necessary because attaching FRP sheets to the footing surface is generally insufficient anchorage. When FRP is bonded to the sides of beams for shear reinforcement, anchorage should be provided by anchor bolts and plates.

5.2.3.5 TR55

Temperature, humidity, and moisture considerations

Before application of FRP, the concrete surface should be dry for normal applications. If surface dryness is not achievable, a suitable epoxy adhesive for nondry surfaces should be selected.

Suitable environmental conditions including temperature, relative humidity and surface moisture must be maintained during surface preparation, strengthening system application, and the curing period. During surface preparation, environmental control consists of a system to extract dust from the work area and the exclusion of any material that might contaminate the prepared surface. During installation, a clear access path from the adhesive work area to the location of the concrete surface should be maintained in order to minimize contamination risk. During the curing period, the adhesive temperature must be maintained within the specified limits. The work area should be kept dry.

Surface preparation

TR55 suggests that a trial run of the surface preparation process should be conducted to determine the best technique for the FRP system to be used. As with other codes, TR55 notes that the concrete surface must be cleaned to remove contaminants. Even new concrete should be cleaned to remove mold release agents and curing membranes. The preparation process should remove the surface layer to expose small particles of aggregate without causing damage to the substrate. The surface should not be polished or roughened excessively. Sharp edges, shutter marks, or other irregularities should be removed to achieve a flat surface.

Various preparation techniques can be effective, including wet, dry, and vacuum-abrasive blasting; high-pressure washing, with or without emulsifying detergents, and using biocides (where necessary); steam cleaning alone or in conjunction with detergents; and, for smaller areas, mechanical wire brushing or surface grinding. TR55 warns that special care should be taken when using some methods, including mechanical impact methods such as needle gunning and bush hammering, which are often too aggressive and may cause microcracks and/or an irregular concrete texture.

Washing techniques may be ineffective in some cases and can simply spread the contaminants further. The use of solvent-based and sodium hydroxide-based products in the form of a gel or poultice can be effective in drawing out the contaminants, but such products must be then completely removed from the surface. If wet grit-blasting is done, the concrete surface must be allowed to completely dry before proceeding. TR55 further recommends vacuum dry-blasting over "open" blasting, the former of which is safer for workers and the environment.

TR55 states that, prior to FRP installation, defects in the concrete surface should be repaired, and if cementitious repairs are used, they should be allowed 28 days to cure. TR55 notes that it is important that the prepared surface should allow application of the resin in a layer of uniform thickness; the thickness of the adhesive layer is commonly between 0.04 and 0.20 in. (1−5 mm). To facilitate this, the surface should be smoothed by removing any steps and filling hollows with a suitable repair mortar. Minor imperfections in the concrete surface can be treated with epoxy materials which can be applied in thin layers. The flatness of the surface should be such that the gap under a 3.3 ft. (1 m) straight-edge does not exceed 0.20 in. (5 mm). When fabric is to be wrapped around corners, the corners should be rounded to a minimum radius of 0.6 in. (15 mm), or as recommended by the manufacturer. TR55 notes that some bonding systems require the use of a primer to

be applied once the surface preparation is complete if so, primer should be applied in strict accordance with the manufacturer's instructions.

The final assessment of surface quality can be made with pull-off tests. If primer was used, the primed surface should be tested. Here, a minimum of three tests are carried out, as described in BS 1881: Part 207 (1992).

Mixing of resins

All equipment used for the mixing and application of the adhesive and materials should be kept clean and maintained in good operating condition, and all operators should be suitably trained in the use of such equipment. The mixing and application of the adhesive should be in accordance with the manufacturer's instructions. For accurate mix proportioning, prebatched quantities of resins and hardeners should be used. The materials should be mixed thoroughly per the supplier's instructions. The volume of adhesive mixed at one time should be such that it may be applied within the pot life of the adhesive; adhesive remaining at the end of the specified pot life must be discarded.

Application

If the concrete surface is to be strengthened using FRP plates, the mixed adhesive is to be applied to the bonding area by hand, using plastering techniques. The thickness of the adhesive should be maintained from 0.04 to 0.08 in. (1−2 mm). Before applying the adhesive to the FRP plate, the plate surface should be prepared in accordance with the manufacturer's recommendations; in general, this involves application of light abrasion and cleaning with a solvent. No additional treatment is required for materials with an additional peel ply which, upon removal, exposes a clean surface with the appropriate roughness. The adhesive layer should be applied to the plates to form a slightly convex profile across the plate. Extra thickness along the center-line helps to reduce the risk of void formation.

If FRP fabric is to be applied, a handheld foam roller or brush can be used to apply the bonding adhesive to the concrete surface. The adhesive layer should be evenly applied to saturate the concrete surface and adhere to the FRP. Dry fabric can be directly applied to the resin-saturated concrete surface without adhesive being applied to the fabric. For wet fabric, the resin must be applied to the fabric before it is installed. The resin can be applied to the fabric using handheld foam rollers or brushes, or an impregnation machine.

5.2.3.6 CNR

Temperature, humidity, and moisture considerations

CNR recommends that FRP should not be installed in very moist environments, as a high degree of humidity may delay resin curing and affect strengthening effectiveness, especially for wet lay-up applications. Moreover, FRP should not be applied to substrates having a surface humidity greater than 10%, as such conditions could delay the penetration of the primer and generate air bubbles that could compromise bond. Substrate humidity can be evaluated with a hygrometer for mortar or by employing absorbent paper. FRP material should also not be applied if temperatures

are too low, as resin curing and fiber impregnation could be compromised. It is also recommended not to install FRP when the concrete surface is heavily exposed to sunlight. CNR suggests that the range of suitable temperature for FRP application is generally within 50−95°F (10−35°C). In low-temperature environments, artificial heat can be provided. If resin curing takes place under rainy conditions, protective measures should be employed to ensure proper curing.

Surface preparation

Prior to FRP installation, CNR recommends that the soundness of the concrete substrate is checked, and in any case, concrete compressive strength should not be less than 2.18 ksi (15 N/mm^2) below which the FRP strengthening may not be effective. CNR states that deteriorated concrete should be removed, and an assessment of the existing steel reinforcing bars should be made if exposed. Corroded steel bars are to be protected against further deterioration. Once the deteriorated concrete has been removed, suitable measures taken to prevent further corrosion, and additional protective measures, if needed, to prevent other sources of concrete degradation (such as water leakage), concrete restoration using shrinkage-free cement grouts is to be performed. A concrete surface roughness with profile differences greater than 0.4 in. (10 mm) is to be leveled with a compatible epoxy paste, and specific filling materials are to be used for unevenness greater than 0.8 in. (20 mm). Cracks wider than 0.02 in. (0.5 mm) should be stabilized using epoxy injection methods before FRP strengthening can take place. Once the flatness and soundness of the concrete is restored sandblasting should be done to provide a roughness of at least 0.01 in. (0.3 mm); level of roughness can be measured by suitable instruments such as a laser profilometer or an optical profile-measuring device. All inside and outside corners and sharp edges shall be rounded or chamfered to a minimum radius of 0.8 in. (20 mm). Finally, the concrete surface should be cleaned to remove any dust, laitance, or any other bond-inhibiting material.

Application

Proper fibers alignment is to be observed, and waving of FRP reinforcement must be avoided during installation. If carbon fiber is used and there is potential for direct contact between the carbon and existing steel reinforcement, insulating material should be installed to prevent galvanic corrosion. CNR recommends that an anchorage length of at least 8 in. (200 mm) be used for the end portion of FRP systems. Alternatively, mechanical connectors may be used.

Witness areas

If semidestructive tests are planned, it is suggested to provide additional strengthening areas ("witness areas") in properly selected parts of the structure of size of at least 20 in. × 8 in. (500 mm × 200 mm), with a minimum extension of 155 in.^{2} (0.1 m^2), but not less than 0.5% of the overall area to be strengthened. Witness areas are to be strengthened at the same time of the main FRP installation, using the same materials and procedures. In addition, witness areas are to be exposed to the same environmental conditions of the main FRP system and should be uniformly distributed on the strengthened structure.

Protective coating

The FRP system should be protected from direct sunlight, which may produce chemical-physical alterations in the epoxy matrix. This can be achieved with protective acrylic paint, provided that the composite surface is cleaned with soap beforehand. Alternatively, a better protection can be achieved by applying a plaster or mortar layer (preferably concrete based) to the installed system.

For fire protection, two different solutions may be adopted: the use of intumescent panels or the application of protective plasters. In both cases, the manufacturer is to indicate the degree of fire protection provided, as a function of the panel/plaster thickness. The panels, generally based on calcium silicates, are to be applied directly on the FRP system, provided that fibers will not be cut during their installation. Fire-protective coatings that can keep the FRP temperature below 176°F (80°C) for 90 min are also available.

5.2.3.7 Summary of installation procedures

Coverage of installation procedures varies widely among codes. AASHTO and CNR are primarily design codes with little coverage of many aspects of FRP installation. The limited areas that are covered by the two codes include surface preparation of the concrete substrate and site environmental conditions at the time of installation. CNR covers three additional topics; minimum width for crack injection repair; lap splices; and temporary protection of the FRP system during resin curing. AASHTO's lack of coverage is supplemented by NCHRP 609, which provides description of a recommended installation procedure not found in AASHTO. JSCE is similarly brief in coverage and includes site environmental conditions at the time of installation, surface preparation of the concrete substrate, mixing of resin, and lap splicing. TR55 covers the same items as JSCE, with the exception of lap splicing. TR55 also adds detail on FRP application in the form of primer/putty application and wet lay-ups.

The most comprehensive installation procedure detailed in the reviewed codes is provided by ACI and ISIS. The two codes have similar coverage, although ISIS provides more quantitative limits. The topics covered by ACI and ISIS include site environmental conditions at installation, use of equipment, surface preparation, resin mixing, application of the FRP system, protective coatings, alignment of FRP materials, multiple plies and lap splices, resin curing, and temporary protection. Comparative summaries are provided in Tables 5.2–5.4. Table 5.2 compares maximum allowable crack width beyond which concrete injection is required as part of surface repair prior to FRP application. Table 5.3 compares the minimum allowable

Table 5.2 Maximum allowable concrete crack width beyond which injection is required

ACI	ISIS	CNR
0.01 in. (0.3 mm)	0.01 in. (0.3 mm)	0.02 in. (0.5 mm)

Table 5.3 Minimum allowable lap splice length

ISIS	JSCE	CNR
6 in. (150 mm)	4 in. (100 mm) at lower stress levels 8 in. (200 mm) for strengthening of shear capacity and ductility	8 in. (200 mm)

Table 5.4 Minimum radius for roundness of concrete corners

ACI	ISIS	AASHTO	JSCE	CNR	TR55
0.5 in. (13 mm)	1.4 in. (35 mm)	0.5 in. (13 mm)	0.4–2.0 in. (10–50 mm)	0.8 in. (20 mm)	0.6 in. (15 mm)

lap splice length. Table 5.4 compares code recommendations for minimum radius for roundness of concrete corners for FRP application.

5.3 Inspection, evaluation, and acceptance

5.3.1 Introduction

This section reviews inspection procedures, evaluation, and acceptance criteria for the installed FRP strengthening system. An assessment survey inspection, checklist is given in Appendix 2.

Inspection evaluation procedures cover the materials used, conformance to the strengthening design plan, and postinstallation inspection of the finished product to detect any deficiencies such as delamination, air bubbles, fiber waviness or misalignment, and adhesion strength. Evaluation of deficiencies, if any, is conducted based on acceptance criteria that sets limits between acceptable minor deviations and deficiencies that require corrective repairs.

5.3.2 Inspection

5.3.2.1 ACI

ACI states that FRP systems and all associated work should be inspected as required by applicable codes. The inspection should be conducted by or under the supervision of the project engineer or a qualified inspector. The qualified inspector should look for compliance with the design drawings and project specifications. During the installation of the FRP system, daily inspection should be conducted and should note, as applicable:

- Date and time of installation;
- Ambient temperature, relative humidity, and general weather observations;

- Surface temperature of concrete;
- Surface dryness per ACI 503.4 (2003);
- Surface preparation methods and resulting profile using the ICRI-surface-profile-chips;
- Qualitative description of surface cleanliness;
- Type of auxiliary heat source, if applicable;
- Widths of cracks not injected with epoxy;
- Fiber or precured laminate batch number(s) and approximate location in structure;
- Batch numbers, mixture ratios, mixing times, and qualitative descriptions of the appearance of all mixed resins, including primers, putties, saturants, adhesives, and coatings mixed for the day;
- Observations of progress of resin cure;
- Conformance with installation procedures;
- Pull-off test results: bond strength, failure mode, and location;
- FRP properties from tests of field sample panels or witness panels, if required;
- Location and size of any delaminations or air voids; and
- General progress of work.

The inspector should provide the inspection records and witness panels. ACI defines witness panels as structural samples manufactured on site as true representatives of the materials and FRP system used. They are to be kept under the same conditions as the structure for future testing and evaluation. In some cases, FRP system is applied to areas of the structure not in need of strengthening for future testing and assessment. Records and witness panels should be retained for a minimum of 10 years or a period specified by the project engineer. The installation contractor should retain sample cups of mixed resin and maintain a record of the placement of each batch.

5.3.2.2 ISIS

ISIS divides inspection tasks into several phases; inspection of the concrete substrate; materials inspection; and inspections before installation, during installation, and at completion of the project.

Contractor's quality control responsibilities

ISIS requires that the FRP material suppliers, the installation contractors and all others associated with the FRP strengthening project maintain a comprehensive QA and QC program (per Annex A16.2 of S6-06 bridge code). QA is achieved through a set of inspections, measurements, and applicable tests to document the acceptability of the surface preparation and the installation of FRP, and the QC should cover all aspects of the strengthening project and will depend on the size and complexity of the project.

The FRP material suppliers are responsible for training the installation crew and as well as certifying their competency for the surface preparation and installation of the FRP materials. ISIS notes that only qualified inspectors should be used.

FRP materials should be qualified on the basis of the engineer's plans and specifications. ISIS notes that two types of specifications are possible: descriptive or performance. In descriptive specifications, the engineer specifies the length, width, orientation, installation sequence, and other requirements of a particular,

selected FRP material, and perhaps acceptable equivalents. In performance specifications, the engineer specifies requirements in term of strength, stiffness, or other necessary properties and characteristics, and the contractor is responsible for selecting an appropriate FRP system and submitting it for approval.

The FRP manufacturer is to provide documentation demonstrating that the proposed system meets all design requirements such as tensile strength, type of fibers and resin, durability, resistance to creep, bonding to substrate, and glass transition temperature. Independent tests of the FRP constituent materials and laminates fabricated with them are essential and should be mandatory.

Selection of contractors should be based on evidence regarding their qualifications, their demonstrated skills and ability through experience or training for FRP strengthening projects.

Inspection of concrete substrate

The concrete surface should be inspected and tested before application of the FRP material. The inspection should include an examination for surface smoothness, protuberances, holes, cracks, corners, and other imperfections and characteristics. Pull-off tests should be performed to determine the tensile strength of the concrete for bond-critical applications, in accordance with Clause A16.1.4 of the S6-06 bridge code (2006). The degree of surface dryness, including the potential for condensation, should be in accordance with the criteria established by the FRP manufacturer.

Inspection before installation

Inspections of the FRP material is to be conducted before, during and after installation. The inspection program should cover such aspects such as raw materials, the presence and extent of delamination, the cure of the installed system, adhesion, laminate thickness, fiber alignment, and material properties.

Before construction, the FRP material supplier should submit a certification and identification of all FRP materials to be used, and the installation procedure should be submitted with information on shelf life and resin working time related to temperature. Performance tests on the supplied materials should be performed according to the QC test plan and should meet the requirements specified in the engineer's performance specifications. Testing may include parameters such as tensile strength, glass transition temperature, gel time, pot life, as well as the adhesive shear strength.

Inspection during installation and at completion

During construction, special care should be taken to keep all records on the quantity of mixed resin during a 1-day period, the date and time of mixing, the mixture proportions, and identification of all components, ambient temperature, humidity, and other factors that may affect resin properties. These records should also identify the FRP sheets used each day, their location on the structure, the ply count and direction of application, and all other relevant information in accordance with Clause A16.2.3.3 of the S6-06 bridge code.

Sample cups of mixed resin should be prepared according to a predetermined sampling plan and retained for testing to determine the level of cure. Sample FRP plate specimens should be fabricated according to a predetermined sampling plan, under the same ambient conditions and procedures used to apply the FRP material to the concrete surfaces. Performance tests on these FRP specimens may be conducted as needed. Moreover, a visual inspection of fiber orientation, and waviness for specific FRP material systems, should be performed. Fiber misalignment of more than 5 degrees (1/12 slope) from the specified angle should be reported to the engineer.

Inspection at completion

At project completion, the inspector is to check for delamination, the overall quality of cured system, and test for adhesion. Moreover, a record of all final inspection and test results related to the FRP material should be retained. It should include a description of any delamination and repairs, on site bond tests, anomalies and correction reports as well as all test results from designated testing facilities. Samples of the cured FRP materials should be retained by the engineer. The required reports and tests are specified in Clause A16.2.3.4 of the S6-06 bridge code (2006).

5.3.2.3 AASHTO

AASHTO recommends that systems considered for FRP strengthening should be inspected by a licensed engineer or qualified inspector knowledgeable in FRP systems and installation procedures. The following should be recorded at the time of installation:

- Date and time of installation;
- Ambient temperature, relative humidity, and general weather observations and surface temperature of concrete;
- Surface dryness, surface preparation methods, and the resulting surface profile using ICRC surface profile-chips;
- Qualitative description of surface cleanliness;
- Type of auxiliary heat source, if used;
- Widths of cracks not injected with epoxy;
- Fiber or precured laminate batch number(s) and approximate locations in the structure where each was used;
- Batch numbers, mixture ratios, mixing times, and qualitative descriptions of the appearance of all mixed resins, including primers, putties, saturants, adhesives, and coatings mixed for the day;
- Observations of progress of resin curing;
- Conformance with installation procedures;
- Location and size of any delaminations or air voids;
- General progress of work;
- Level of resin curing, in accordance with ASTM D2582 (2009);
- Adhesion strength.

5.3.2.4 JSCE

JSCE recommends that inspections are conducted at each stage of the work, which are: material inspections when first received, inspections of the storage condition of these materials, surface preparation inspections, and, inspections of the bonding or jacketing condition of the FRP after the work is completed. Further description of these inspections is provided below.

Materials and storage inspection

When material is first received, the FRP, primer, smoothing agent, impregnation resin, and other materials should be inspected for quality and damage. Inspection of materials should be done in accordance with the QA sheet, test results, or other relevant documents issued by the manufacturer. If the materials have suffered damage during shipment, long-term storage at the site, or during construction, before use, they should be tested to confirm quality.

The storage condition of the materials is to be inspected as well. In general, materials should be stored indoors in a well-ventilated location away from direct sunlight, flame, and rain, and at appropriate temperature and humidity conditions. Laws relating to storage should be strictly observed.

Inspection of the existing structure

At the site, a detailed inspection of the existing structure to be strengthened should be conducted, with attention to the following:

- Existing structural configuration and site conditions. Due to construction errors or undocumented changes, existing structures may not necessarily have been completed as specified in the available design documents. The dimensions of the existing structure should be verified in advance. Moreover, as climatic conditions affect curing and bond, it is necessary to determine the wind, sunshine, temperature changes, and other conditions expected at the site.
- Necessity for impact protection. If the applied FRP sheets may be damaged by impacts, it is necessary to study whether surface protection should be implemented. Accordingly, the potential for damage to a strengthening system by impacts and the degree of damage to the existing structure from impacts should be estimated.
- Surface quality. Since bond strength is crucial for effectiveness, the degree of surface deterioration and damage of the existing concrete surface should be carefully determined, so necessary repair measures can be implemented.
- Cause and degree of existing deterioration. The deterioration progress of the upgraded concrete structure depends on the type and degree of the causes of deterioration. Accordingly, when damaged concrete structures are upgraded, it is necessary to preexamine the type and degree of external factors causing deterioration. Particularly, when concrete damaged by alkali-aggregate reaction is strengthened, volumetric expansion may occur after construction. Therefore the quantity and area of FRP coverage should be determined by taking account of the amount of residual expansion.

Inspection before, during, and after installation

Before application of FRP, concrete surface preparation is to be inspected with respect to the completeness of sectional restoration work, surface smoothness, processing of corner angles, primer coating, and smoothness.

During and after construction, FRP should be inspected for attachment position, lifting, peeling, slackness, wrinkles, overlap splice length, number of plies, and quantity of the resin coating. Moreover, a bond strength test should be conducted as needed. If the scale of construction is large or construction conditions are severe, it is best to conduct confirmation tests using test specimens fabricated at the site. The same materials as those used on site should be used for tests, and the tests should be performed on the concrete at the site. However, if it is difficult to perform the test on the concrete at the site, the test may be performed on a slab specimen with concrete properties representative of the site concrete. If wound on site, FRP strands are to be inspected for winding position, winding interval, winding tension and winding speed, and that fibers are thoroughly impregnated with resin.

5.3.2.5 TR55

TR55 states that its recommendations for inspection, evaluation, and acceptance are not intended to be a specification, but are meant to suggest what significant points should be included in a specification. TR55 suggests that the manufacturer should supply characteristic values of the mechanical properties to be used for design purposes (e.g., strength, elastic modulus, etc.), which TR55 defines as the mean value minus 2 standard deviations. It further suggests that sufficient tests should be carried out at regular intervals to ensure that the values reported are statistically valid.

Material QC requirements

TR55 suggests that all materials used should have been manufactured under an approved quality scheme, such as ISO 9000, and conform to relevant ISO specifications, Euronorms, or other equivalent international standards. In addition, the traceability of all materials should be ensured and materials should be supplied with a certificate of conformity to the relevant standards. Further, all external or independent testing to determine material properties should be carried out in approved laboratories in accordance with relevant international standards or by the manufacturer under an approved quality scheme. When no international standards exist, an industry or company standard or method with a recognized history should be used.

Inspection before installation

Testing should consist of visual checks on the basic materials and where appropriate, physical tests on the finished elements as detailed below. For fabric materials, the properties of a specified width of finished material should be checked by testing samples. The frequency of testing should be stated in the quality plan. A minimum of one sample should be taken at the start and finish of each production run. Minimum properties to test for should include unit weight, elastic modulus, and tensile strength. Samples of FRP may be made into laminates, using the appropriate specified resin, and the laminate then tested to determine composite properties. Where appropriate, properties should be determined in the transverse direction as well as in the longitudinal direction. All individual rolls of material should be appropriately labeled.

For pultruded plates, the supply of fibers to the pultrusion line should be monitored on a regular basis, with a frequency of at least once per hour. The speed of processing, processing temperature, and other manufacturing parameters should be maintained within agreed limits and checked and recorded regularly. The properties of the plate should be checked by testing samples, and the frequency of testing should be stated in the quality plan. A minimum of one sample should be taken at the start and finish of each production run. The samples should also be checked for dimensional accuracy, and plates should be marked with a unique batch number at regular intervals.

When received from the supplier, all materials should be accompanied by a certificate of conformity to appropriate standards. When received, all materials should be stored and used strictly in accordance with the manufacturer's instructions. Accurate records should be maintained of all materials used (e.g., delivery notes, batch numbers) and, when required, the ambient conditions (e.g., temperature, relative humidity). If plates are used, visual checks should be carried out to ensure that the plate material is as specified and undamaged. When bonded, the plate should be checked by tapping or other means to ensure continuous adhesion.

Inspection during installation

For wet lay-up laminates, visual checks should be carried out on mats, unidirectional tapes/fabrics, woven rovings, and multiaxial fabrics to ensure uniformity and conformity. The completed laminate should be checked visually for defects. When required by the contract, trial pieces to verify properties such as strength and elastic modulus should be made at the same time and by the same process. Care should be taken to ensure that the trial pieces are representative of the material in the finished unit.

5.3.2.6 CNR

CNR contains little information relevant to this topic, and simply indicates that the inspector's responsibilities are to check that the quality of the materials are in compliance with the manufacturer specifications; to verify that all materials have been accepted by the construction manager; and to check the results of any experimental tests required.

5.3.3 Evaluation and acceptance

5.3.3.1 ACI

ACI states that FRP systems should be evaluated and accepted or rejected based on conformance to the design drawings and specifications. FRP system material properties, installation within specified placement tolerances, presence of delaminations, cure of resins, and adhesion to substrate should be included in the evaluation. Placement tolerances including fiber orientation, cured thickness, ply orientation, width and spacing, corner radii, and lap splice lengths should be evaluated. ACI further suggests that witness panels and pull-off tests are to be used to evaluate the

installed FRP system. In-place proof load testing can also be used to confirm the installed behavior of the FRP-strengthened member (Nanni and Gold, 1998).

Evaluation and acceptance before starting the project

Before starting the project, the FRP system manufacturer should submit a certification of specified material properties and identification of all materials to be used. Based on the needs of the project, additional material testing can be conducted if deemed necessary. Evaluation of delivered FRP materials, in accordance with the QC test plan, may include tests for tensile strength, an infrared spectrum analysis, glass transition temperature, gel time, pot life, and adhesive shear strength. Materials that do not meet the minimum requirements as specified by the licensed design professional should be rejected.

For FRP systems such as precured and machine-wound systems, that do not lend themselves to the fabrication of small, flat witness panels, the project engineer can require test panels or samples to be provided by the manufacturer. During installation, sample cups of mixed resin should be prepared according to a predetermined sampling plan and retained for testing to determine the level of cure.

Evaluation and acceptance at project completion

Fiber or precured laminate orientation should be evaluated by visual inspection. Fiber or precured laminate misalignment of more than 5 degrees [approximately 1 in./ft. (80 mm/m)] from that specified should be reported to the engineer for evaluation and acceptance.

The cured FRP system should be evaluated for delaminations or air voids between multiple plies or between the FRP system and the concrete. Inspection methods should be capable of detecting delaminations as small as 2 in.^{2} (1300 mm^2), and may include acoustic sounding (hammer sounding), ultrasonics, and thermography. Delamination size, location, and quantity relative to the overall application area should be considered in the evaluation.

For wet lay-up systems, small delaminations less than 2 in.^{2} (1300 mm^2) are permissible as long as the delaminated area is less than 5% of the total laminate area and there are no more than 10 such delaminations per 10 ft.^{2} (1 m^2). Large delaminations, $>$25 in.^{2} (16,000 mm^2), can significantly affect the performance of the installed FRP and should be repaired by selectively cutting away the affected sheet and applying an overlapping sheet patch of equivalent plies. Delaminations less than 25 in.^{2} (16,000 mm^2) may be repaired by resin injection or ply replacement, depending on the size and number of delaminations and their locations.

For precured FRP systems, ACI states that each delamination should be evaluated and repaired in accordance with the instructions of the project engineer. Upon completion of the repairs, the laminate should be re-inspected to verify that the repair was properly accomplished.

The relative cure of FRP systems can be evaluated by laboratory testing of witness panels or resin-cup samples using ASTM D3418 (2003). The relative cure of the resin can also be evaluated on the project site by physical observation of resin

tackiness and hardness of work surfaces or retained resin samples. The FRP system manufacturer should be consulted to determine the specific resin-cure verification requirements.

Adhesion strength is a critical inspection parameter. For bond-critical applications such as flexural or shear strengthening, tension adhesion testing of cored samples should be conducted using the methods in ACI 503R (1998), ASTM D4541 (2002), or the method described by ACI 440.3R (2004), Test Method L.1. Successful tension adhesion strengths should exceed 200 psi (1.4 MPa) and exhibit failure of the concrete substrate. Lower strengths or failure between the FRP system and concrete or between plies should be reported to the engineer.

Cured thickness also should be verified. Small core samples, typically 0.5 in. (13 mm) in diameter, may be taken to visually ascertain the cured laminate thickness or number of plies; however, taking samples from high stress or splice areas should be avoided. The cored hole can generally be filled and smoothed with a repair mortar or the FRP system putty. However, if required, a 4−8 in. (100−200 mm) overlapping FRP sheet patch of equivalent plies may be applied over the filled and smoothed core hole immediately after taking the core sample.

5.3.3.2 ISIS

The categories covered under evaluation and acceptance by ISIS are similar to those covered in ACI. These include a preinstallation evaluation as well as an evaluation at project completion, which involves checking for items such as fiber orientation, delamination, cure of strengthening system, adhesion, laminate thickness, and material properties.

Evaluation and acceptance before starting the project

For materials qualification, ISIS recommends that FRP systems without fully established properties through appropriate testing should not be considered for use, and all constituent materials should be acceptable by applicable codes and known for their good performance. Mechanical properties of FRP systems should be determined from plate specimens manufactured in a process representative of their field installation, and from tests based on established standards. However, modification of standard procedures may be permitted in order to better represent field assemblies. The specified material qualification programs should include sufficient laboratory testing to measure the repeatability and reliability of critical properties, and testing multiple batches of FRP materials is recommended.

Evaluation and acceptance at project completion

Visual inspection of fiber orientation, and waviness for specific FRP material systems, should be performed; fiber misalignments of more than 5 degrees from the specified angle should be reported to the engineer.

An inspection of the FRP system for delamination should be conducted after the full cure. Delaminations or other anomalies that are detected should be evaluated

considering their size and number relative to the overall application area, as well as their location with respect to structural load transfer. Inspection methods may include acoustic sounding (hammer sounding), ultrasonics, and thermography, and should be capable of detecting delaminations as small as 1 in.^{2} (600 mm^2) as well as any defects with a leading edge greater than 1 in. (25 mm). Repairs are required for delaminations of size greater than 2.3 in.^{2} (1500 mm^2) or 5% of the total laminate area. Cutting away the affected sheet and applying an overlapping sheet patch of equivalent plies may be considered a repair option for delaminated FRP areas. Appropriate bond lengths must be used to ensure the integrity of the repaired area. The repaired area should then be re-inspected, and the resulting delamination map or scan compared with that of the initial inspection to verify that repair soundness.

Evaluation of the relative cure of FRP materials can be performed by laboratory testing of sample plate specimens or resin samples using ASTM Standard D3418 (2003). At the construction site, curing evaluation is achieved by physical observation of resin tackiness and hardness of work surfaces or retained resin samples. For premolded systems, adhesive hardness measurements should be made in accordance with the manufacturer's recommendations.

Tension adhesion testing of cored samples should be conducted using known methods such as those described in ASTM D4541 (2002) or ACI 503R (1998). However, care should be taken to avoid coring in high stress or splice areas. The tested areas must be repaired unless they are located in areas where the FRP is unstressed. Sampling frequency will depend on the size and complexity of the project. Tensile bond strength values less than 220 psi (1.5 MPa) are unacceptable.

The laminate thickness or number of plies used can be inspected with small core samples, typically 0.6 in. (15 mm) in diameter; these cores may be those used for adhesion testing. As with coring for adhesion testing, highly stressed or splice areas should be avoided. After coring, the hole should be filled and smoothed. A 4−8 in. (100−200 mm) overlapping sheet patch of equivalent plies should be applied when required.

Confirmation of the strength and elastic modulus of the FRP materials can be determined using tension tests on panels fabricated from construction site specimens. Tension testing should follow procedures such as those prescribed in Annex F of the S806-02 building code (2002) or ASTM Standard D3039 (2008). The lap strength, tensile strength, and elastic modulus of the FRP materials can also be determined using burst testing of ring specimens. FRP materials can be tested in accordance with existing ASTM test methods, but all exceptions to the method should be listed in the test report. Durability related tests use the same test methods, but require application of specific preconditioning of the specimens.

For verification of the qualification testing results, samples of the FRP system should be prepared at the construction site and tested at an approved laboratory, with the properties to be verified specified. In-place load testing can be used to confirm the behavior of the FRP-strengthened member. Such testing should be performed under the supervision of an experienced engineer and precaution must be exercised to avoid damaging the structure.

5.3.3.3 AASHTO

Contractor submittals

For evaluation and acceptance, AASHTO recommends that the contractor be required to submit evidence of acceptable QC procedures that were followed in the manufacture of the FRP system. The QC procedure should at least include the specifications for raw material procurement, quality standards for the final product, in-process inspection and control procedures, test methods, sampling plans, criteria for acceptance or rejection, and record keeping standards.

The contractor also must provide information describing the fiber, matrix, and adhesive systems to be used that is sufficient to define their engineering properties. Descriptions of the fiber system should include the fiber type, percent of fiber orientation in each direction, and fiber surface treatments. When required by the engineer, the matrix and the adhesive shall be identified by their commercial names and the commercial names of each of their components, along with their weight fractions with respect to the resin system.

Further, AASHTO suggests that the contractor should submit test results that demonstrate that constituent materials and the composite system are in conformance with the physical and mechanical property values stipulated by the engineer. These tests shall be conducted by a testing laboratory approved by the engineer. For each property value, the batches from which test specimens were drawn are to be identified and the number of tested specimens from each batch, and the mean, minimum, and maximum value, as well as the coefficient of variation, must be reported. The minimum number of tested samples is 10.

Moisture content and epoxy requirements

When cured under conditions identical to those of the intended use, the composite material system as well as the adhesive system are to conform to the following requirements. The characteristic value of the glass transition temperature of the composite system, determined in accordance with ASTM D4065 (2012), should be at least 40°F higher than the maximum design temperature, defined in Section 3.12.2.2 of the *AASHTO LRFD Bridge Design Specifications* (2012). The characteristic value of the tensile failure strain in the direction corresponding to the highest percentage of fibers must not be less than 1% if the tension test is conducted according to ASTM D3039 (2008).

When moisture migrates through the matrix and reaches the fiber−matrix interface, adhesion of the matrix to the fibers weakens. AASHTO thus specifies that the moisture content must be limited; the mean and coefficient of variation of the moisture equilibrium content, as determined in accordance with ASTM D5229/D5229M (2010), must not be greater than 2 and 10%, respectively. A minimum sample size of 10 should be used in the calculation of these values.

Environmental conditioning

After conditioning in the various environments listed below, the characteristic value of the glass transition temperature, determined in accordance with ASTM D4065

(2012), and that of tensile strain, determined in accordance with ASTM D3039 (2008), of the composite in the direction of interest shall retain 85% of the required values above. The conditioning environments are as follows:

- Water: Samples shall be immersed in distilled water having a temperature of $100 \pm 3°F$ ($38 \pm 2°C$) and tested after 1000 h of exposure.
- Alternating ultraviolet light and condensation humidity: Samples shall be conditioned in an apparatus under Cycle 1-UV exposure condition according to ASTM G154 (2012) Standard Practice. Samples shall be tested within 2 h after removal from the apparatus.
- Alkali: The sample shall be immersed in a saturated solution of calcium hydroxide (pH ~ 11) at ambient temperature of $73 \pm 3°F$ ($23 \pm 2°C$) for 1000 h prior to testing. The pH level shall be monitored and the solution shall be maintained as needed.
- Freeze−thaw: Composite samples shall be exposed to 100 repeated cycles of freezing and thawing in an apparatus meeting the requirements of ASTM C666 (2008).

Further, if impact tolerance is stipulated by the engineer, impact tolerance should be determined according to ASTM D7136 (2007).

When adhesive material is used to bond the FRP reinforcement to the concrete surface, the following requirements shall be met. After conditioning in the environments noted above, the characteristic value of the glass transition temperature of the adhesive material, determined in accordance with ASTM D4065 (2012), must be at least 40°F higher than the maximum design temperature as defined in Section 3.12.2.2 of AASHTO LRFD Bridge Design Specifications (2012). Moreover, after conditioning in the environments noted above, the bond strength, determined by tests specified by the engineer shall be at least $0.065\sqrt{f'_c}$ (ksi) (Naaman and Lopez, 1999). Also, AASHTO recommends to evaluate whether moisture will collect at the bond lines between the concrete and epoxy adhesive before the epoxy has cured. This may be checked by taping a 4×4 ft. (1.2×1.2 m) polyethylene sheet to the concrete surface. If moisture collects on the underside of the sheet before the time required to cure the epoxy, then the concrete should be allowed to dry sufficiently to prevent the possibility of a moisture barrier forming between the concrete and epoxy per ACI 530R-05 (2005).

Epoxy physical and adhesive properties testing

During installation, sample cups of mixed resin should be prepared according to a predetermined sampling plan and retained for testing to determine the level of curing, in accordance with ASTM D2583 (2007). The relative cure of the resin can also be evaluated on the project site by physical observation of resin tackiness and hardness of the work surfaces and retained resin samples.

For bond-critical (i.e., flexural or shear) applications, tension adhesion testing of cored samples should be conducted using the methods in ACI 530R (2005), ASTM D7234 (2012), or the method described by ISIS (2008). The sampling frequency should be specified. Tension adhesion strengths should exceed 200 psi (1.4 MPa) and exhibit failure of the concrete substrate before failure of the adhesive per ACI 440.2R-08 (2008).

5.3.3.4 JSCE

JSCE recommendations for evaluation and acceptance include criteria for fire safety, collision protection, and finishing work.

Fire safety

In JSCE, the required level of fire safety depends on the structure to be upgraded and the surrounding environment. In general, three levels of safety are available:

- Flame retardant. Here, the combustibility of the FRP is low and it can be confirmed that, even if damaged in a fire, it can be repaired.
- Noncombustible and quasi-noncombustible. In a fire, the FRP sheets are not ignited and no harmful fumes are produced. However, they are not required to maintain their load-carrying capacity during and after the fire.
- Fire-resistant. The structure will not collapse during the fire, and the FRP sheets are required to maintain full strength after the fire and either full or partial strength during the fire, without repair.

For verification of fire safety, a test specimen with the same protective coating as the actual structure should be manufactured and subjected to combustion tests. During the combustion test, ignition, the generation of gases, harmful surface deformation, and changes in the quality of the FRP after the fire are to be studied according to the level of fire safety required.

One simple method of performing the combustion test that can be used to check the flame retardant level of protection is to bring a flame near the FRP and observe whether the sheet is ignited and whether there is any residual flame on the surface of the test specimen when the burner flame is removed.

In a normal fire, the carbon fibers used in FRP do not combust or produce a chemical reaction. Even when ignited with an external flame, the fibers are self-extinguishing once the flame is removed. Therefore they are thought to be flame retardant even without surface covering. In general, when a FRP strengthening system is used, the existing concrete structure supports dead loads and other permanent loads, while the FRP is used to support live loads. Thus even if continuous fiber sheets fail during a fire, there is usually no danger of the structure collapsing immediately. In light of this, JSCE notes that if there is little danger of a fire occurring, no danger of spread if a fire should occur, adequate refugee space is available, and there is little likelihood of danger to human life, then there is no particular need to provide a flame resistant covering on the FRP system.

When preventing combustion during a fire is a design objective and nonflammable or quasi-nonflammable coverings are used with the assumption that the sheets will be repaired after the fire, coverings may generally consist of mortar, a rock wall, or similar materials. One method of checking flame resistance in this design category is to fabricate a test specimen by bonding FRP sheets to the concrete members, then heating the test specimen in a furnace at the prescribed temperature for the prescribed duration, then immediately testing the FRP sheets to determine if the properties of the FRP sheets are altered in undesirable ways.

When the FRP sheets are expected to maintain strength without repair even after the fire, the temperature of the continuous fiber sheets during the fire should be kept below that at which resin decomposes [for epoxy resins, about 500°F (260°C)]. One way to achieve this is to cover with approximately 2 in. (50 mm) of mortar.

Collision resistance

Collision resistance is another area addressed by JSCE. When there is a possibility that the FRP may be subjected to impact, one of several methods may be used to confirm performance requirements. One possibility is that the magnitude of the impact design load is estimated using statistical data, and then performance requirements are to be verified by conducting an impact load test. The normal impact resistance of the structure can be evaluated through drop impact tests and pendulum impact tests. Possible impacts during the service life of the structure can be estimated based on damage surveys of structures thought to have been subjected to the same impacts that the structure being verified is prone to. When it is difficult to make statistical calculations of the impacts applied to the structure during its service life, more simple methods can be used that are based on the results of a survey of existing structures. When the structure is expected to be subjected to impacts only on very rare occasions, verification may be conducted to ensure that, even if the performance drops temporarily after an impact, the structure can be quickly repaired.

Finishing work

Finishing work includes providing coatings for durability, appearance and fire protection. JSCE recommends that upgraded surfaces are finished appropriately to ensure that the performance requirements, including sunlight and weatherproofing, fire resistance, shock resistance, roughness, and appearance, are satisfied. JSCE notes that the excellent durability of FRP has been confirmed through outdoor exposure tests and accelerated exposure tests. However, depending on the type of fiber, durability may be impaired by conditions of use, and hence the finishing should be planned after carefully considering the properties of the FRP. Resin may deteriorate and whiten when exposed to ultraviolet light and ozone, and its appearance is easily marred. Accordingly, when an aesthetic appearance and illumination are required in the environments exposed to direct sunlight, the FRP should be finished with protective paint.

5.3.3.5 TR55

Detailed evaluation and acceptance criteria as presented in ACI and ISIS are missing in TR55. The code, however, introduces test methods for shear and adhesive bond using mechanical and nondestructive test methods. The proposed test method for shear is the double lap shear test. TR55 notes that various nondestructive tests may be used to inspect a completed and cured bond. The most common is acoustic sounding (hammer tapping). Thermography may be used to survey large areas. Pull-off dollies can also be installed at the time of strengthening, and pull-off tests

can be performed at various times to test adhesive strength as a function of time. Similarly, additional double lap shear test specimens can be prepared at the time of strengthening and tested at various times.

TR55 states that delamination risk is dependent on the type of strengthening and the location on the structure. For example, an area of delamination in the wrapping of a column will probably have a limited effect on performance, while delamination of a plate on the soffit of a beam, particularly at points of high shear, will have a significant effect. TR55 references ACI 440 to suggest the extent of delamination that may be acceptable.

For major structures, it may be appropriate to install instrumentation prior to the strengthening to assess the structural response before and after strengthening.

5.3.3.6 CNR

Evaluation and acceptance before starting the project

CNR recommends before starting the project that FRP materials should be subjected to a series of controls to ensure appropriate mechanical and physical characteristics. For construction materials, specific standards are available for the determination of minimum values of physical and mechanical properties, test procedures, as well as acceptance criteria. For further information about mechanical characterization tests for fiber reinforcement materials, CNR refers to the following documents:

- *ACI 440.3R 04 "Guide Test Methods for Fiber-reinforced Polymers for Reinforcing or Strengthening Concrete Structures";*
- *JSCE (1995) "Test methods for continuous fiber reinforcing materials";*
- *JSCE (2000) "Test methods for continuous fiber sheets";*
- *ISO (TC71/SC6N) "Non-conventional strengthening of concrete – Test methods-Part 1: Fiber strengthened polymer (FRP) bars and grids";*
- *ISO (TC71/SC6N) "Non-conventional strengthening of concrete – Test methods-Part 2: Fiber strengthened polymer (FRP) sheets."*

Responsibilities of the construction manager

CNR defines the process of evaluation and acceptance as the responsibility of the construction manager. Additional responsibilities of the construction manager are as follows. The construction manager is to make decisions as to the acceptance of products; check the compliance of the material to the designer's provisions; check the origin of the supplied material (pultruded materials are typically marked by the manufacturer for their identification, while other materials must have labels or tags with the necessary information for traceability); and to check the mechanical and physical characteristics of products using the test certificates provided by the manufacturer. Additional responsibilities are to determine whether experimental tests are to be required to evaluate material quality and compliance with the values provided by the manufacturer. Such tests are to be carried out in laboratories with sufficient experience and equipment to characterize FRP materials. Acceptance criteria may be based on the maximum acceptable deviation of results from the values obtained

during production. In some cases, tests may be required to evaluate both mechanical and physical properties of unconditioned and conditioned specimens to take into account temperature and moisture variation.

CNR defines Type-A and Type-B applications. For Type-A, certification is obtained for each component as well as the final product to be applied. However, it is the decision of the construction manager to require acceptance tests for the installed system. For Type-B applications, each component requires certification but not the FRP system. In this case, the construction manager shall require a number of tests to ensure proper quality of both the FRP system and installation procedures as suggested in CNR sections 4.8.3 and 5.8.3 for reinforced concrete and masonry structures, respectively.

Evaluation and acceptance at project completion

CNR specifies that QC tests are needed during FRP installation. Tests include at least one cycle of semidestructive tests for the mechanical characterization of the installation itself, and at least one nondestructive mapping to ensure uniformity.

For semidestructive tests, both pull-off and shear tearing tests may be conducted. Semidestructive tests shall be carried out on witness panels and, where possible, in noncritical strengthened areas at the rate of one test for every 53.82 ft.^{2} (5 m^2) of application, and in any case, not less than 2 per each type of test. The pull-off test is used to assess properties of the concrete substrate and is carried out by using 0.8 in. (20 mm) thick circular steel plates with a diameter of at least three times the characteristic size of the concrete aggregate, but not less than 1.6 in. (40 mm). These plates are adhered to the surface of the FRP with an epoxy adhesive. After the steel plate is firmly attached to the FRP, it is isolated from the surrounding FRP with a core drill rotating at a speed of at least 2500 rpm. Here, particular care shall be taken to avoid heating of the FRP system while a 0.04−0.08 in. (1−2 mm) incision of the concrete substrate is achieved. FRP application may be considered acceptable if at least 80% of the tests (both tests in case of only two tests) return a pull-off stress not less than 130−174 psi (0.9−1.2 MPa), provided that failure occurs in the concrete substrate.

The shear tearing test is particularly significant to assess the quality of bond between the FRP and concrete. It may be carried out only when it is possible to pull a portion of the FRP system in its plane located close to an edge detached from the concrete substrate. Results may be considered acceptable if at least 80% of the tests (both in the case of two tests) return a peak tearing force not less than 5.4 kips (24 kN).

Nondestructive tests may be used to characterize the uniformity of FRP application, starting from an adequate two-dimensional survey of the strengthened surface with a spatial resolution as a function of the strengthening area (see Table 5.5).

The nondestructive tests described by CNR are:

Stimulated acoustic testing. In a simple version, this test can be conducted by a technician hammering the composite surface and listening to the sound from the impact. However, more objective results may be obtained with automated systems.

Table 5.5 Minimum resolution for defects to be identified with nondestructive tests

Shear stress transfer at interface	Example	Nondestructive test	Surface mapping grid	Minimum resolution for defects thickness
Absent	Wrapping, with the exception of the overlapping area in a single-layer application	Optional	10 in. (250 mm)	0.12 in. (3.0 mm)
Weak	Central area of extensive plane reinforcement	Optional	10 in. (250 mm)	0.12 in. (3.0 mm)
Moderate	Central area of longitudinal flexural strengthening	Suggested	4 in. (100 mm)	0.02 in. (0.5 mm)
Critical	Anchorage area, overlapping areas between layers, stirrups for shear strengthening, interface area with connectors, or an area with large roughness or cracks in the substrate	Required	2 in. (50 mm)	0.004 in. (0.1 mm)

High-frequency ultrasonic testing. This is best conducted with a reflection method using frequencies no less than 1.5 MHz and probes with diameter no greater than 0.98 in. (25 mm), using the technique based on the first peak amplitude variation due to localized defects.

Thermographic test. According to CNR, this is effective only for FRP systems with low thermal conductivity and should not be applied to carbon or metallic FRP strengthening systems unless special precautions are taken, as the heat developed during the test must be smaller than the glass transition temperature of the FRP system.

Acoustic emission test. This test is particularly suited for detecting defects in FRP systems applied on RC structures, as well as delamination of the concrete substrate.

5.3.3.7 Summary of evaluation and acceptance

ACI and ISIS provide similar coverage of evaluation and acceptance criteria including materials evaluation, materials/FRP system qualification tests, and field testing and sample collections. The two codes present criteria for acceptance of fiber alignment, delamination, cure of resin, adhesion strength, and cured thickness.

AASHTO states the contractor's responsibilities for evaluation and acceptance. The contractor is to submit a complete QC plan detailing inspection, sampling, testing, and criteria for acceptance. The contractor is required to also provide detailed information on materials used as part of the FRP system, as well as test results to verify the materials meet required design properties. AASHTO provides a detailed list of acceptance criteria for materials and FRP system including a description of testing required and sample sizing. AASHTO places emphasis on testing materials under various environmental factors.

Table 5.6 Minimum acceptable tension strength of adhesive

ACI	ISIS	CNR
200 psi (1.4 MPa)	220 psi (1.5 MPa)	130−175 psi (0.9−1.2 MPa)

Table 5.7 Maximum allowable area of delamination

ACI	ISIS
2 in.^{2} (1300 mm^2) or 5% of the total laminate area	2.33 in.^{2} (1500 mm^2) or 5% of the total laminate area

JSCE places particular emphasis on three areas; fire resistance, collision safety, and finishing work. The code offers a reasonable coverage of the three areas but lacks coverage in areas of evaluation and acceptance covered by other codes. TR55 does not have clear boundaries separating aspects of QC, inspection, and testing from evaluation and acceptance criteria. So, items discussed in inspection overlaps evaluation and acceptance.

CNR offers a list of reference codes it recommends as basis for its materials/system qualification. The code provides broad guidelines for evaluation and acceptance but lacks detail. The code offers two testing categories: semidestructive and nondestructive. Semidestructive testing includes pull-off and shear tearing tests. Nondestructive testing includes stimulated acoustic testing, acoustic emission testing, and thermographic testing.

A comparison of the minimum acceptable tension strength of adhesive is presented in Table 5.6, and a comparison of the maximum allowable area of delamination is presented in Table 5.7.

5.4 Maintenance and repair

5.4.1 Introduction

This section covers elements of a maintenance program with periodic inspection and testing to identify any damage, degradation, or deficiencies to the FRP strengthening system and to make any necessary repairs. A maintenance assessment is made from test data as well as observations, and may include recommendations to help slow down degradation and propose necessary repairs.

5.4.1.1 ACI

Inspection and assessment

ACI suggests that periodic inspection and assessment are needed to verify the long-term performance of the FRP system. The causes of any damage or deficiencies

detected during routine inspections should be identified and addressed before performing any repairs or maintenance.

A general inspection consists of observation for changes in color, debonding, peeling, blistering, cracking, crazing, deflection, indications of reinforcing-bar corrosion, and other anomalies. Other inspection methods such as ultrasonic, acoustic sounding (hammer tap), or thermographic tests may be used to identify signs of progressive delamination.

Test data and observations are used to assess any damage and the structural integrity of the strengthening system. Testing can include pull-off tension tests or conventional structural load tests. The assessment can include a recommendation for repairing any deficiencies and preventing recurrence of degradation.

Repair techniques

Prior to repair, the causes of the damage must first be identified and addressed. The method of repair should depend on the cause of damage, the type of material, the form of degradation, and the level of damage. Minor damage should be repaired, including localized FRP laminate cracking or abrasions that affect the structural integrity of the laminate. Such damage can be repaired by bonding FRP patches with the same FRP characteristics over the damaged area. The FRP patches should possess the same characteristics, as thickness or ply orientation, as the original laminate. Minor delaminations can be repaired by resin injection.

Major damage, including peeling and debonding of large areas, may require removal of the affected area, reconditioning of the concrete, and replacement of the FRP. ACI does not mention techniques that may be used to remove the damaged FRP. However, some recommendations for removal are provided in Section 8.2.6.2 of this book. FRP patches should be installed in accordance with the material manufacturer's recommendation.

If the surface protective coating is to be replaced, the FRP should be inspected for structural damage or deterioration. The surface coating should be replaced using a process approved by the system manufacturer.

5.4.1.2 ISIS

ISIS does not address long-term maintenance, assessment, and repair.

5.4.1.3 AASHTO

AASHTO recommends that the following documents be considered for evaluation and repair of existing concrete structures and postrepair evaluation criteria:

- *ACI 201.1R: Guide for Making a Condition Survey of Concrete in Service*;
- *ACI 224.1R: Causes, Evaluation, and Repair of Cracks in Concrete*;
- *ACI 364.1R-94: Guide for Evaluation of Concrete Structures Prior to Rehabilitation*;
- *ACI 440.2R-08: Guide for the Design and Construction of Externally Bonded FRP Systems for Strengthening Concrete Structures*;
- *ACI 503R: Use of Epoxy Compounds with Concrete*;
- *ACI 546R: Concrete Repair Guide*;

- *International Concrete Repair Institute (ICRI) ICRI 03730: Guide for Surface Preparation for the Repair of Deteriorated Concrete Resulting from Reinforcing Steel Corrosion*;
- *International Concrete Repair Institute (ICRI) ICRI 03733: Guide for Selecting and Specifying Materials for Repairs of Concrete Surfaces*;
- *NCHRP Report 609: Recommended Construction Specifications Process Control Manual for Repair and Retrofit of Concrete Structures Using Bonded FRP Composites*.

AASHTO states that relevant specifications and guidelines provided by FRP manufacturers should also be carefully reviewed.

5.4.1.4 JSCE

JSCE recommends that concrete structures strengthened with FRP should be maintained with a systematic combination of deterioration prediction, inspection, evaluation and judgment, countermeasures, and records.

Anticipated deterioration should be accounted for in the design and maintenance inspections by upgrading and repairing appropriately. At the time of a maintenance event, more accurate predictions of deterioration should be made.

Inspection and assessment

Inspections consist of initial, daily, periodic, detailed, and extraordinary inspections. These should be based on the performance requirements and the predictions of performance deterioration. Inspections should be conducted visually or using appropriate inspection equipment, with consideration given to both performance requirements and the mechanism of deterioration. Deterioration may affect the FRP material itself or the resin individually, the FRP system as a composite material (interfacial deterioration), and deterioration of bond to the concrete. The visual features of this deterioration may include swelling, peeling, lifting, softening, discoloration, whitening, chalking, cracking, wearing, erosion, pinholes, scratches, deformation, and embrittlement. However, JSCE notes that FRP sheets will block or limit the intrusion of various external substances. As such, improved concrete durability can be anticipated with respect to the salt attack, carbonation, freeze−thaw, alkali-aggregate reaction, chemical attacks, and fatigue. Deterioration may change various properties, including weight, volume, mechanical properties (hardness, bond strength, tensile strength, modulus of elasticity, elongation, etc.), and physical properties (electrical properties, thermal properties, optical properties, etc.). Inspections using a combination of observation as well as suitable inspection equipment should be conducted.

JSCE notes that two stages of evaluations and judgments are used: those based primarily on visual inspections, and those based on detailed inspections. For visual inspections, a judgment is made as to whether a detailed inspection is required. In a detailed inspection, the need for countermeasures is evaluated and judgment is used to select the type of countermeasure.

Repair techniques

Countermeasures are implemented to satisfy performance requirements, based on the results of evaluation and judgment. Countermeasures include stricter inspections, service restrictions, repair of the FRP system, additional upgrading, improvement of appearance, and dismantling and disposal. For minor deterioration, countermeasures should consist primarily of stricter inspections and repair of the FRP system. The method selected should depend on the deterioration mechanism and the extent of changes observed. However, JSCE suggests the following for consideration. For swelling, peeling, and lifting, resin fill can be used, while for cracking, wearing, and erosion, patching can be used. When serious deterioration or deterioration over a wide area is observed, additional FRP upgrading should be performed. In such cases, the existing FRP should be removed and the upgrading plan reexamined.

To implement suitable maintenance, the results of design, construction, inspection, evaluations and judgments, repairs, additional upgrading, and so on, are to be recorded and the records maintained. The ease of maintenance is affected by the upgrading plan and by design and construction. More specifically, the placement of access paths to the structure that allow inspection and monitoring equipment affects ease of maintenance. For this reason, it is recommended to give thorough consideration to maintenance considerations in the upgrading plan, as well as in design and construction.

5.4.1.5 TR55

Inspection and assessment

Similar to ACI, TR55 emphasizes that the FRP strengthening system should be monitored and inspected regularly. A general inspection is recommended once a year, while a detailed inspection is recommended once every 6 years.

A general (visual) inspection primarily consists of a surface inspection. The inspector looks for signs of crazing, cracking, delamination, or evidence of deterioration, in addition to local damage due to impact or surface abrasion. Signs of concrete deterioration in the form of cracking or corrosion should also be reported. Any required identification or warning labels should be checked for, and missing ones should be replaced.

The condition of the FRP protective layer, if any, should also be inspected. Damaged protective coatings should be replaced in accordance with the supplier's recommendations. It is not appropriate to remove the protective layer to facilitate inspection.

A detailed inspection considers various items. Debonding of the FRP from the concrete may be determined by tapping or thermography. However, TR55 reports that no nondestructive tests are available to assess the condition of the adhesive bond. Therefore adhesive bonding is evaluated by pull-off tests on the control specimens at regular intervals. Pull-off tests should be carried out as part of a detailed inspection, although there may be a requirement to test samples more frequently, particularly soon after strengthening.

To facilitate inspection, instrumentation may be installed as part of the assessment process; for example, to measure strains due to live loading on the structure. Such instrumentation can be used to indicate changes in structural response. If significant changes are observed, it is necessary to determine whether they are due to changes in the strengthening system (such as delamination) or due to overall changes in the concrete structure (such as additional cracking or corrosion) so that appropriate action can be taken. The Health and Safety File for the structure should include details of any instrumentation that was installed as part of the strengthening exercise, along with any data obtained before and after strengthening.

Information on the materials used in strengthening should be included in the Health and Safety File for the structure. This File should also include reported minor areas of delamination and any initial faults detected in the strengthening system, identification of critical strengthening regions such as anchorage zones and high-stress regions, and procedures prepared by the engineer on actions to be taken for various forms of damage to the FRP strengthening system, which should be tailored to each particular structure.

In order to facilitate the testing and evaluation of the FRP strengthening system, it is recommended that additional areas of the strengthened structure, away from the regions that were strengthened, are also bonded with the FRP system for future testing that does not impact the system performance. TR55 reports that this approach has been adopted on a number of structures including the Barnes Bridge in Manchester and the John Hart Bridge in British Columbia.

Alternatively, FRP can be bonded to concrete samples which can be stored near the structure. Samples can be inspected and tested as part of the inspection regime. To aid inspection, some or all of the samples should not be covered with any protective layer. They should thus indicate a lower bound of performance of the composites bonded to the structure. Details should be included in the structure's Health and Safety File along with recommendations for the frequency of testing.

Repair techniques

For localized damage to the FRP, repairs can be made with resin injection or plate overlapping. For major damage, such as peeling and debonding of large areas, the defective material should be removed to an extent that material on the periphery of the repair is fully bonded. The concrete surface should then be prepared, and an FRP patch installed that allows adequate overlap between the new and old materials. The compatibility of the proposed repair material with the materials already in place should be checked. The repair material must have similar characteristics to the material in place such as fiber orientation, volume fraction, strength, stiffness, and overall thickness.

5.4.1.6 CNR

CNR recommends that, due to the poor availability of data regarding long-term behavior of FRP systems used for strengthening, appropriate monitoring of the installed FRP system should be performed with periodic semi- and nondestructive

tests. The aim of the monitoring process is to identify potential problems with the temperature of the installed FRP system, environmental humidity, displacements and deformations of the strengthened structure, fiber damage, and defects or delaminations in the installed FRP system.

5.4.1.7 Summary of maintenance and repair

ACI, TR55, and JSCE all present a relatively broad and reasonable coverage of maintenance and repair issues. They each call for development and implementation of a periodic maintenance program including visual inspection, specified testing, an assessment of damage to evaluate the structural integrity of the system, and recommendations for repair. Based on the type and severity of damage, the three codes offer suggestions for appropriate repair methods. CNR's coverage on maintenance and repair is brief, and states the need for periodic monitoring and inspection using semi and nondestructive tests for assessment of the system. No discussion of repair recommendation is presented. ISIS does not cover this topic, while AASHTO does not provide detailed coverage, but refers to a list of specialized documents from ACI, ICRI, and NCHRP for further suggestions.

This page intentionally left blank

Laboratory testing

6

6.1 Durability testing overview

A common concern with fiber-reinforced polymer (FRP) durability is its potential degradation of system engineering properties when exposed to extreme hot or cold temperatures, moisture fluctuation, freeze−thaw cycles, chemical contaminants, such as road salt, and other potential stressors. Unfortunately, such durability data for a specific FRP system within a specific environment are not available. Ideally, a field test could be conducted to assess long-term durability by exposing the system of interest to the climate for which it is intended, and periodically monitoring and assessing its performance over time. This is rarely a viable option, however, due to the expense and time required for such an experimental program, which may take many years or decades of exposure for significant degradation to occur. Alternatively, accelerated laboratory testing can be used to assess durability. Here, FRP specimens are subjected to a surrogate environment that is more severe than the intended environment. But the accelerated environment should not alter the failure modes observed in field. The intent of the severe exposure is to artificially accelerate the degradation rate, such that meaningful deterioration can be observed within a reasonable time and cost. The drawback of such accelerated tests is that the interpretation of the resulting data, and in particular the relationship of the results to expected performance in the intended environment, is not always clear. Another concern is how to quantify degradation. That is, what engineering properties should be tested and what test procedures are to be used. Although many FRP system properties may potentially degrade over time, a primary concern is the strength of the bond between the FRP and concrete. This bond often governs the strength of the system and may degrade more quickly than the FRP material itself. One way to assess this is with a pull-off test, which can be conducted on samples subjected to accelerated weathering.

6.2 Bond durability

In general the test process involves preparing a series of FRP samples suitable for bond testing, then placing the specimens into an environmental chamber and subjecting them to a predetermined environmental acceleration cycle. The samples are periodically removed and subjected to pull-off bond testing. The deterioration rates of different types of samples can be compared for relative durability, or results can be extrapolated to predict long-term performance in the natural environment in some cases, if additional information is available, as discussed below.

Strengthening of Concrete Structures Using Fiber Reinforced Polymers (FRP).
DOI: http://dx.doi.org/10.1016/B978-0-08-100636-8.00006-5

6.2.1 Sample preparation

Numerous sample configurations are viable. However, it is often helpful to work from a known standard and modify if needed. A sample size which is large enough to conduct multiple pull-off tests on but yet compact enough to place in a small environmental chamber and easily handled is given by ASTM C 293, which specifies small beam dimensions of $16 \times 4.3 \times 4.1$ in. or $40.6 \times 10.9 \times 10.4$ cm (length $\times$ height $\times$ width). Because the pull-off tests are concerned with bond strength rather than flexural strength, however, the full depth of the beam (i.e., normal to the surface upon which the FRP will be applied) is not needed. Hence, these test beams might be reduced to approximately half-depth to form dimensions of $16 \times 2.0 \times 4.1$ in. or $40.6 \times 5.1 \times 10.4$ cm.

Simple plywood mold assemblies can be prepared prior to concrete casting (Fig. 6.1). Since multiple specimen pours were to be made, the forms shown in Fig. 6.1 were bolted together to allow disassembly and specimen removal without destroying the formwork. It is recommended that the inner surfaces of such molds are coated with a release agent such as wax or oil to facilitate specimen removal.

It is important that the concrete used reflects the mix design, strength, and other properties representative of the actual structure to which the FRP will ultimately be applied, as the quality of the concrete substrate is particularly important for bond strength. Once poured, fresh concrete properties may be checked with on-site with standard ASTM tests for water/cement ratio (ASTM C 1078 and C 1079), slump (ASTM C 143), air content (ASTM C 231, C 173, or C 138), and any other properties relevant to the project. Recommended procedures to handle sample concrete for

Figure 6.1 Reusable plywood mold for seven specimens.

checking purposes is discussed in ASTM C 172. Moreover, test cylinders should be prepared and later tested to verify anticipated compressive strength (ASTM C 31, C 192, or C 873, and C 39).

As with the concrete used, sample curing should resemble as close as possible the curing conditions of concrete on the structure to which the FRP will be applied. As FRP is usually retrofitted to aged, existing structures, such information is often unavailable. Therefore, unless other conditions are expected, a standard 28-day moist-curing process is recommended. An easy way to achieve this without surface coating or continuously rewetting the specimens is to submerge them in water after removal from the formwork. Of course specimens must be kept continuously moist within the formwork and prior to placement in the water bath, however. At the conclusion of the moist curing process, samples should be allowed to dry for 48 h prior to preparing the surface for FRP application. Surface preparation includes: surface grinding with an angle grinder to remove any weak concrete areas and impurities; grinding to round edges, if U-wrap test configurations will be used; wire brushing the surface to clean depressed areas and surface imperfections; filling large concavities with putty to ensure a level surface, and; cleaning the specimens with compressed air to remove dust prior to FRP application.

Assuming that similar procedures will be used in the field, FRP manufacturer guidelines should be closely followed for installation on the specimens, including the use of appropriate processes, tools, and safety requirements. Here two issues should be noted which require particular attention. First, it is often difficult to fully saturate FRP fabric with high viscosity resin. If this combination of strengthening materials is used, special care is recommended to ensure that the fabric is indeed fully saturated. Higher viscosity resins are generally recommended for FRP sheet (laminates) applications rather than fabrics. Second, strict adherence to the epoxy pot life and its operating temperature range during installation is necessary to avoid an early set of the epoxy and negatively impacting the quality of the final system. Careful adherence to the manufacturer's recommended guidelines and advanced planning of the installation process is crucial. Examples of final specimens with FRP installed are shown in Fig. 6.2.

6.2.2 Test plan and procedures

Accelerated weathering can be conducted in an environmental chamber. Such a chamber is shown in Fig. 6.3, which can be programed to modulate temperature as desired. Although chambers that can also regulate moisture are desirable as they

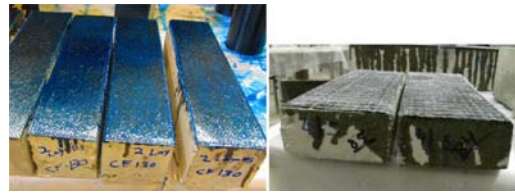

Figure 6.2 Final full- and half-depth samples using FRP wrap (fabric).

Figure 6.3 Tenney environmental chamber.

provide an additional test parameter that can be changed, the moisture extremes, a dry and 100% saturation condition, can be simulated in just about any chamber. For the latter condition, samples can be placed into water baths before insertion into the chamber. The effect of chemical contaminants such as road salt can likewise be simulated, by mixing such additives within the water bath. Here one must take care to avoid containers that may break with water expansion if below-zero temperatures will be utilized.

Various temperature profiles are possible, depending on the anticipated location of the actual structure, the needs of the project, and the desired rate of accelerated degradation. In cold climates, a moist condition freeze−thaw cycle often does most damage, and thus below-zero temperatures should be considered. Although cycling between higher temperature extremes may increase degradation rate and are thus tempting to use to reduce test times, temperatures that greatly exceed those achievable within the anticipated field environment should be avoided; in particular, very high temperatures may artificially soften or even burn some resins. Such elevated temperatures will cause types of damage to the system that would not occur naturally, potentially producing greatly misleading results. An example temperature cycle for a cold climate is shown in Fig. 6.4. Once a temperature test cycle is specified, specimens are subjected to repeated applications of the cycle to induce damage. For example, specimens might be exposed to repetitive application of a 60 cycle sequence, where they are removed and tested after 60, 120, 180, and 240 cycles, and so on. Since there is no clear guidance to determine an optimal cycle length, cycles between 2 and 5 h corresponding to the upper and lower limits suggested in ASTM C666 might be used.

For pull-off testing, the same sample can likely be retested throughout the entire process, as the area of FRP required to conduct a pull-off test is generally quite small, as will be discussed below. However, for other types of specimens, such as those used for flexural or compression tests, the entire specimen is generally greatly

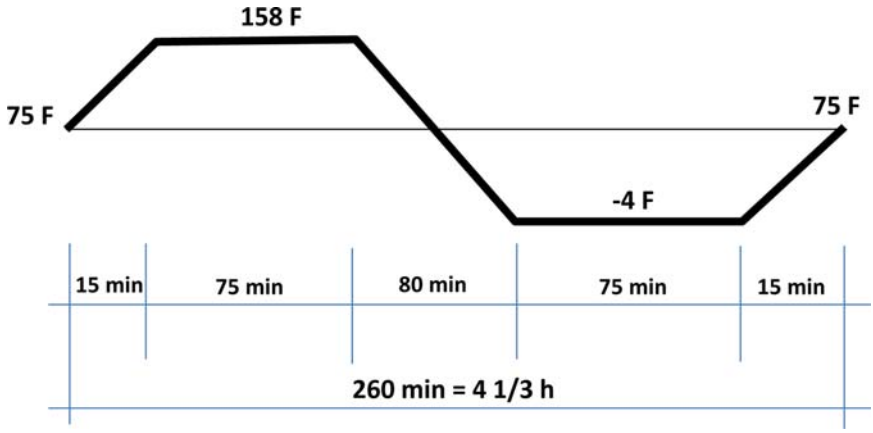

Figure 6.4 Example temperature test cycle.

damaged or destroyed after each test thus cannot be exposed to additional weathering cycles and retested later. In this case, multiple specimens must be used, each subjected to different exposure times. Subjecting each specimen to a different number of exposure cycles introduces additional uncertainty to the test results, however, as of course some natural variation in strength between specimens will occur. This uncertainty can be dealt with by testing multiple specimens at each exposure cycle. Various statistical procedures exist to estimate the number of tests needed to achieve a desired level of confidence in the results, depending on the variability found in the tests.

One such procedure is as follows. Given a group of test results (at a given number of exposure cycles) with standard deviation σ, it is often desired to know how reliable is the mean value calculated from the results. The number of specimen test results needed to determine that the actual mean value of the population falls within $\pm w$ of the calculated mean, at a confidence level C can be estimated from: $n = 1/w^2\left(\sigma k_{\alpha/2}\right)^2$. In this formula, $k_{\alpha/2} = \Phi^{-1}(1-(1-C)/2)$. Common values for C are within the range of 90−99% (i.e., $C = 0.9-0.99$), and Φ^{-1} refers to the inverse standard normal cumulative distribution function. This value can be accessed from tables found in most statistics texts, or in Microsoft Excel with the function NORM.S.INV. This is not an exact process, as the above expression assumes that the standard deviation actually applies to the entire population, which is practically never known, rather than to the small number of test samples taken. However, it can be used as a reasonable starting point in many cases. For example, say four pull-off test results are available after 120 weathering cycles with values of (psi): (453, 620, 536, 482). The resulting mean value is 523, where the standard deviation of this set is 73.4. Say that the actual population mean value is desired to be known within ± 30 psi, at 95% confidence. $k_{\alpha/2}$ is then computed as: $k_{\alpha/2} = \Phi^{-1}(1-(1-0.95)/2) = \Phi^{-1}(0.975) = 1.96$. The number of specimen tests needed for this accuracy is then estimated to be:$n = (1/30^2)(73.4(1.96))^2 = 23$.

6.2.3 Pull-off testing

Pull-off adhesion testing is described by ASTM D4541. However, it requires a pull-off tester to accomplish (for example, the DeFelsko PosiTest AT-A automatic adhesion tester). The test works by adhering a small metal test dolly to the surface of the FRP, cutting through the FRP around the dolly with a hole saw, then using the test machine to pull on the top of the dolly until the bond is broken. The test procedure is as follows:

1. Prepare surfaces. Contaminants are removed from the dolly attachment surface and the sample surface using abrasive pads. Residue left from the abrading process is then removed using a dry cloth or paper towel. The area is then degreased with acetone or alcohol.
2. Apply dolly. Epoxy adhesive (for example, Loctite 907-Hysol) is applied uniformly on the base of the dolly, then the dolly is attached to the sample surface. The dolly is firmly pressed in place and excess adhesive is removed. Fig. 6.5 illustrates dollies that have been adhered to the test surface. In the figure, protective paint was applied to half of the specimen (lower part of figure); the effectiveness of paint to resist weathering was of interest for the specimen shown. Here, 20 mm diameter dollies were used. With the sample size suggested, this allows for the possibility of placing numerous dollies on a single specimen, such that it can be retested in future weathering cycles.

Figure 6.5 Installed dollies.

3. Cut FRP around dolly. It is important to separate the FRP attached to the dolly from the surrounding FRP material to obtain a true measure of adhesion that is not affected by the surrounding fibers. Not doing this may produce significantly higher failure stress values than represented by the actual bond quality. A coring tool that fits over the outside of the dolly, but is as close as possible to the dolly diameter can be used. For the 20 mm dollies shown in Fig. 6.5, a 23 mm outside diameter, diamond-coated hole saw/coring bit was used. For the cutting procedure, the bit should be used with a drill press so the depth around the dolly is evenly and accurately controlled. Extreme care must be taken to ensure that the coring just cuts through the FRP but minimizes scoring the concrete substrate as much as possible, as it was found that the pull-off test results are highly sensitive to the depth of scoring into the concrete.
4. Pull-off test. The test is performed according to the testing machine instructions. The portable test machine shown in Fig. 6.6 uses hydraulic pressure to separate the dolly from the sample surface. The tensile strength value is then displayed on a digital screen and results may be saved to computer through a USB port.

6.2.4 Test results

Once the tests are conducted, results must be analyzed and interpreted. It is usually worthwhile to carefully monitor intermediate test results to ensure that the test plan is progressing as expected. Specimens failing (or not failing) at load levels or

Figure 6.6 Pull-off test underway.

modes that were not anticipated may indicate that the test plan, equipment, or specimens were not prepared or implemented properly. If this occurs, thought should be given to halting the tests before additional specimens and time are expended while the problem is being identified.

6.2.4.1 Pull-off testing

When evaluating pull-off test results, an issue to be aware of is that the failure mode may not be that which was anticipated. That is, depending on various factors, including the strength of the concrete, FRP, and resin; how carefully prepared the surfaces were; how fully saturated with resin is the FRP; as well as the effect of accelerated weathering process, failure might occur in multiple ways, including: true bond failure at the concrete/resin interface; failure of the concrete substrate, where a thin layer of concrete is stripped from the specimen and remains adhered to the FRP and dolly; failure within the FRP material; failure of the bond between the dolly and FRP surface; and a mixed-mode failure, where failure might occur by more than one of these modes.

If bond failure between the dolly and the FRP surface occurs, this test result should of course be disregarded, as it does not represent the strength of the specimen. Better FRP/dolly surface preparation, use of a different adhesive or the process used to handle it, and/or the control of other factors such as temperature, moisture, or contaminants, may be needed in order to prevent future failures of this nature. This type of failure is shown in Fig. 6.7 (looking at the bottom surface of the dolly).

Failure within the FRP is shown in Fig. 6.8. This failure is generally due to the presence of air bubbles within the FRP layers or insufficient resin saturation in general. Such a failure indicates poor system installation practice. If the purpose of the testing is to evaluate an existing structure, the quality of workmanship, or a new preparation technique, then results may be valuable. However, if the tests were to

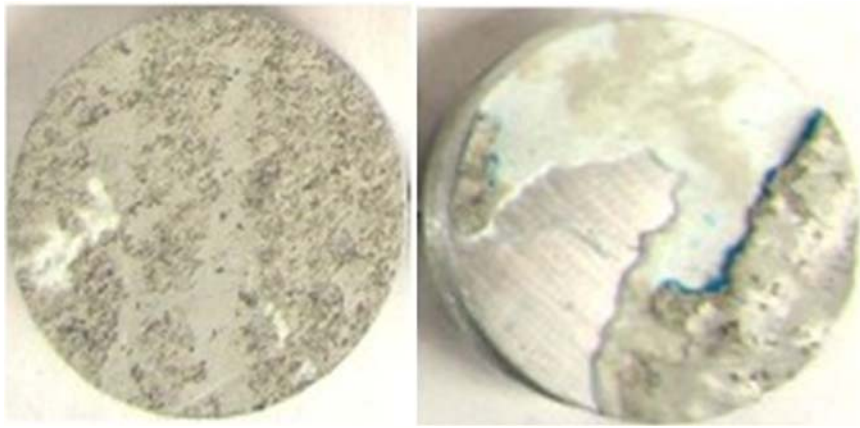

Figure 6.7 Bond failures between dolly and FRP.

be conducted on specimens prepared following manufacturer's requirements and this failure was found in specimens prepared in the laboratory, such results should generally be discarded due to poor specimen preparation.

Unless the strength of the concrete is unusually high, the resin strength unusually low, or the weathering process used greatly damages the resin, most failures on well-prepared specimens will likely be through the concrete substrate, as bond strength of the resin is frequently greater than that of the concrete. This type of failure is shown in Fig. 6.9. A mixed failure of bond/concrete is shown in Fig. 6.10.

Once failure modes have been examined, a decision must be made as to what failure modes to include and which ones to discard. Here, one must determine what are the failure mode(s) of interest that will be used to characterize system performance. A common desire is to consider FRP resin bond failure only. However, as

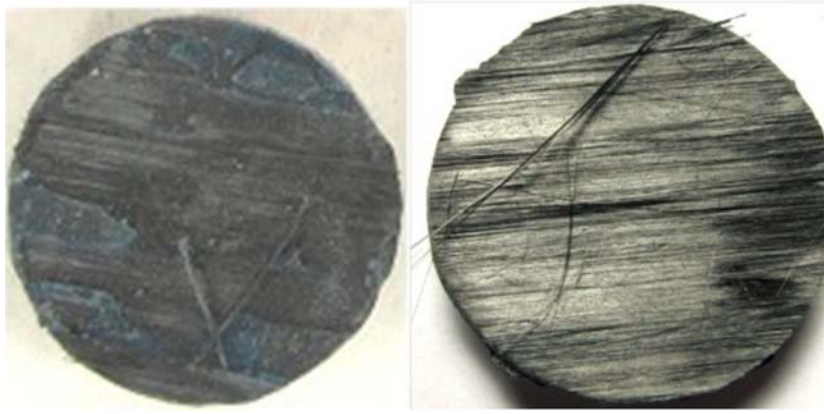

Figure 6.8 Failures within FRP.

Figure 6.9 Failures of concrete substrate.

Figure 6.10 Mixed failures through FRP resin (bond failure) and concrete substrate.

noted previously, this failure may be difficult to capture as the concrete substrate often fails first. In a broader sense, if the concern is debonding of the FRP system, then it is suggested that all failures mentioned above (except dolly bond failure) are included for system evaluation, as any would cause failure of the system, even if a mode such as concrete substrate failure may not directly evaluate the FRP/resin system used.

Note that, as the number of different failure modes that are included in the results increases, the variation in results may increase as well, potentially resulting in large data scatter. This may complicate evaluation of the results.

Another issue that requires resolution is how the results are to be used. In general, as discussed above, if no actual long-term field data are available, then results from accelerated weathering tests can only be used to judge the relative performance of one FRP system over another, but no reliable predictions can be made as to the actual rate of degradation for the same systems placed on a field structure exposed to natural weathering.

If some field data are available for the system, however, even if only for a relatively short period of time such that degradation can be measured (this may require at least a year or more), it may be possible to link the accelerated tests to the field data and make predictions for degradation over much longer periods of time. This can be done by using an acceleration factor, which is discussed below.

6.2.4.2 Evaluation of acceleration factor

An acceleration factor, or parameter, can link the rate of degradation found in accelerated weathering tests conducted in the laboratory to actual rates of degradation measured in the field. This can be very useful, since once the link is established, it can be used to extrapolate to an expected degradation in the field over much longer periods of time.

Although similar FRP systems may be expected to degrade similarly, to best estimate the acceleration factor, it is desirable to use the same FRP system and installation process in the laboratory testing that was used in the field. It is also desirable to gather field data for as long of a time period as possible. There are two ways that the field data can be collected. Ideally, the data are collected from a system directly installed on an existing structure. However, this may not be viable, as some damage will be done to the FRP system during the testing process. Some additional discussion on testing samples on an existing structure is given in Chapter 7, Field testing. Alternatively, test specimens can be constructed and placed outdoors in the same climate for which the system is to installed. In this approach, for each specimen constructed that will be subjected to accelerated testing in the laboratory, an identical specimen should be kept and placed outdoors for natural weathering.

The same pull-off testing technique that is used on the laboratory specimens should be used on the outdoor specimens, although the time interval for testing outdoor specimens should generally be much longer to obtain useful data. For a cold climate, one way to estimate a reasonable starting time interval for outdoor sample testing is to consider the expected number of freeze−thaw cycles. That is, say if indoor specimens are to be tested after each interval of 60 accelerated freeze−thaw cycles in the environmental chamber, one might consider waiting until about 60 natural freeze−thaw cycles have passed in the field to test the natural weathering samples (assuming that 60 cycles of accelerated freeze−thaw tests produced some measurable degradation in the laboratory specimens). The idea here is to avoid testing the natural weathering specimens before any measurable degradation takes place and unnecessarily using up the test specimens. Of course, if measurable degradation is found after 60 cycles of accelerated tests, it does not necessarily mean that degradation will be found after 60 cycles of natural weathering, as the accelerated testing environment is typically much different from the natural environment. Based on the results of the initial testing, some judgment must be used to appropriately schedule future tests.

To evaluate acceleration factor, the time and number of cycles required for the same loss of strength found from the accelerated tests and the natural weathering tests are related. For example, assume a set of outdoor (i.e., natural weathering) specimens were tested, with results shown in Fig. 6.11. In this figure, very long-term data were available (up to 180 months), but such long-term data, although very desirable, are not necessary, as degradation is also apparent only after about 9−12 months of exposure, as shown in the figure. Fig. 6.12 provides similar data that were collected from identical specimens subjected to accelerated weathering tests.

To determine an acceleration factor, the first task is to fit a line through the data in each figure.

Considering the data in Figs. 6.11 and 6.12, notice that the largest losses occur within the first 60 cycles (accelerated) and 9 months (outdoors), then the rate of loss significantly decreases. Although more complex nonlinear fits can be conducted if desired by fitting a curve through the entire time range of data that

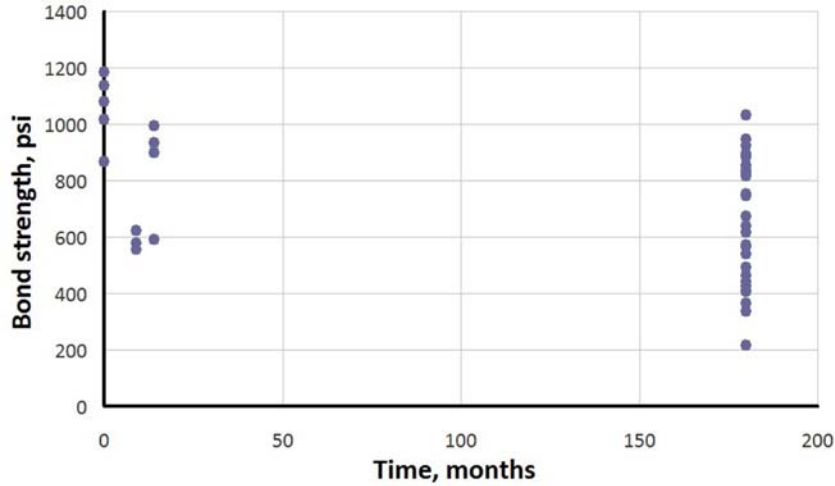

Figure 6.11 Bond strength versus time for outdoor weathering.

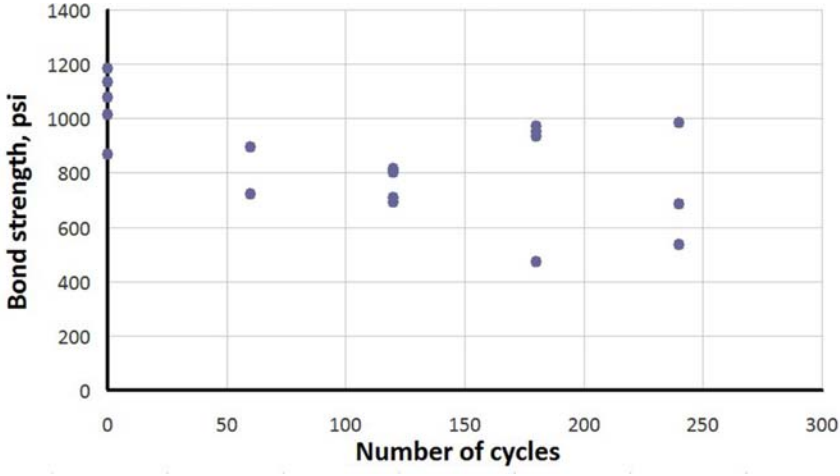

Figure 6.12 Bond strength versus number of cycles for accelerated tests.

were collected if desired, it is assumed that the rate of long-term degradation is of interested rather than prediction of the initial losses that may occur within a few years. In this case, the first data set on the graphs (i.e., time zero) can be eliminated, and a simple linear regression analysis can be conducted to fit lines through the tail of the data for long-term use. These regression fits are given in Figs. 6.13 and 6.14.

As shown in Fig. 6.14, for the accelerated data, the resulting regression line is: $b = 818 - 0.36c$, where b is the bond strength and c is the number of cycles. For

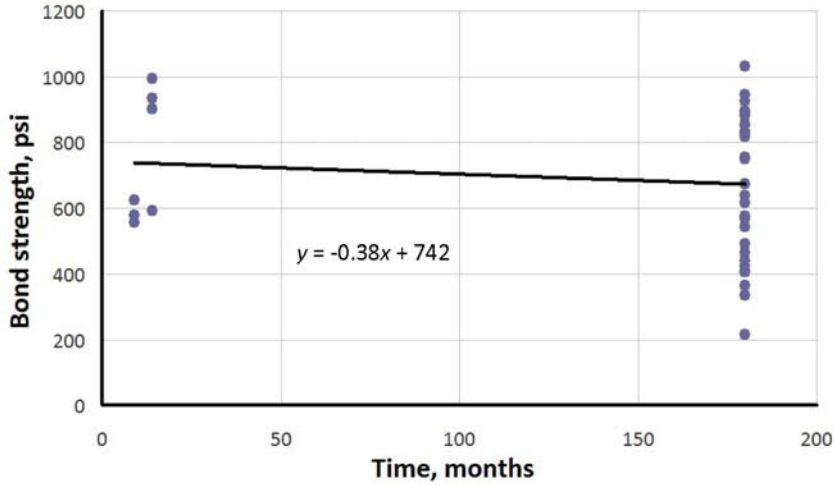

Figure 6.13 Linear regression fit to outdoor weathering data.

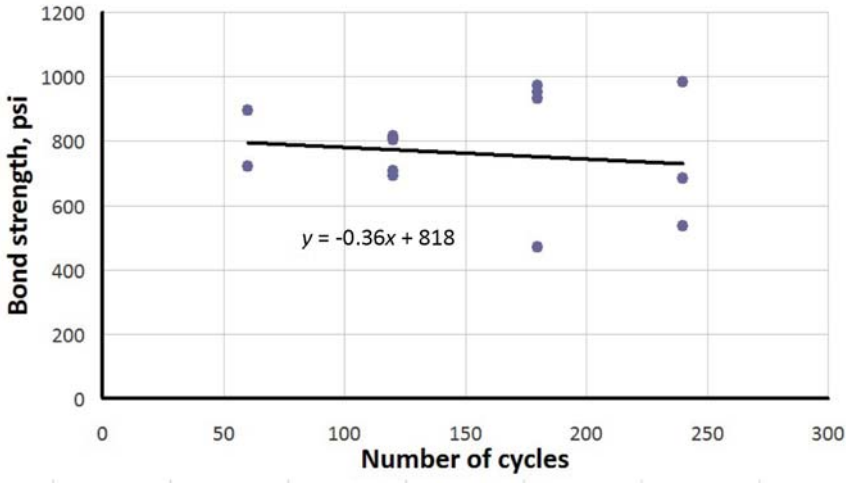

Figure 6.14 Linear regression fit to accelerated weathering data.

the outdoor samples, the line is: $b = 742 - 0.38t$, where t is the time in months. An acceleration factor can now be estimated as follows. Referring to the regression line for the accelerated tests, a loss of say 100 psi of strength (i.e., $b = 718$ psi) is predicted to occur at 278 cycles. Similarly, using the regression line found for the outdoor specimens, it requires 263 months, or 22 years of exposure, for the same loss of strength ($b = 642$). The acceleration factor is therefore estimated to be

278 cycles/22 years = 12.7 cycles per year. That is, about 13 cycles of accelerated testing should produce approximately the same loss of bond strength as 1 year of natural weathering.

Although the short-term data are generally not as useful, a similar short-term acceleration factor can be found by using the same process that was used to develop the long-term factor, but now only the initial loss of strength (i.e., at time zero and at the first 60 cycles) is considered. For example, considering this data shown in Figs. 6.11 and 6.12, for the outdoor specimens, the best-fit regression line between the 0 month and the 9−12 months data was found to be: $b = 1003 - 19t$. For the accelerated specimens, the relationship describing the loss of strength from time 0 to 60 cycles is: $b = 1056 - 4.62c$. This results in an estimated short-term acceleration factor of approximately 207 cycles/48 months = 4.3 cycles/month = 52 cycles/year (valid for about the first year of exposure).

Although they should be used with caution, these relationships can now be used to predict losses of strength of similar FRP systems placed in the same environment by conducting accelerated laboratory testing only, without the need for additional field tests.

Alternatively, if the use of other FRP systems is not a concern, and the single system for which field data are available is the only interest, the regression line or curve fit to the available natural weathering data can be used to directly predict future losses of strength without a need for accelerated laboratory testing. Thus using the acceleration factors or the regression fit to the outdoor weathering data directly, long-term capacity loss can be approximated. In particular, for the outdoor specimens, assuming an initial strength of 1003 psi, bond strength at the end of the first-year loss is expected to be $b = 1003 - 19(12) = 775$ psi, which represents a proportional reduction to 775/1000 = 0.78. In 50 years, for example, the expected bond strength (assuming an initial starting value of 742 psi, per the regression equation) $= 742 - 0.38(49 \times 12) = 519$ psi, or an expected additional proportional reduction to 519/742 = 0.70, which represents a total expected 50-year reduction to $0.775 \times 0.70 = 0.54$ or 54%.

6.3 FRP durability

For some structures, complete FRP components might be added for retrofit. In this case, not only is bond or connection durability of interest, but the durability of the FRP composite material within the component itself. As discussed above, a suitable laboratory accelerated environment should be selected to represent as closely as possible the real climate of interest. Choices for the test environment might involve a wide range from subzero to elevated temperatures. For cold weather environments, ASTM C666 can be modified to condition FRP samples, which is to be further discussed. Unlike externally bonded FRP, for which strength is typically the primary concern, many FRP infrastructural component

designs are stiffness-critical. As such, the environmentally induced failure modes of major interest are those having the greatest effect on the component's stiffness. A common FRP component designed to resist flexure is composed of sandwich construction where the flexural stiffness of the sandwich depends primarily on the stiffness of the composite face skins, the location of the face skins with respect to the neutral axis of the sandwich, and the shear transfer capability of the adhesive bond between the face skins and the core. Failure modes of the composite face skins which are most likely to be affected by environmental conditions are the failure modes associated with the polymer matrix material. The composite face skins typically have a laminated construction with plies at different orientations, but the longitudinal plies (0 degree orientation with respect to longitudinal direction of the composite plate) have the greatest influence on stiffness. The stiffness of longitudinal plies under tension is fiber dominated, and environmentally induced degradation of the polymer matrix would have a small affect on tensile stiffness for reasonable fiber volume fractions. However, the microbuckling failure of longitudinal plies under longitudinal compression is strongly influenced by the stiffness of the polymer matrix, and would therefore be most affected by environmental conditions. Based on these considerations, specimen orientation and test procedures can be designed accordingly.

6.3.1 Test environment

FRP components will usually not only be subjected to variable mechanical loading, but also may have to withstand high and low temperatures, moisture, salt water, etc. In particular, a great concern is the combined effects of low temperature, moisture, and stress on the long-term durability of FRP materials. Therefore it is necessary to perform freeze and thaw tests under loading conditions. To this end, a fixture can be developed that allows application of continuous bending strains to specimens that are simultaneously subjected to freezing and thawing.

ASTM C666 (ASTM 1997) specifies a durability freeze−thaw test for concrete material, alternating the temperature of the specimens from 4.4 to -17.8°C in not less than 2 nor more than 5 h. It is considered to be the most relevant test procedure to characterize the durability of FRP material of interest here, and therefore it is recommended. For a freezing medium, ASTM C666 requires that the specimens are immersed in distilled water. During the winter, especially in the northern states in the United States, de-icing salt is commonly used for roads and bridges. To simulate this condition, a salt solution with 10% sodium chloride by mass can be also used as a medium. Additionally, in-air testing with 0% humidity, representing a completely dry environment, can be conducted. For comparison, a batch of the same specimens may be kept frozen at -17.8°C and tested at the same number of hours of exposure as those subjected to freeze−thaw cycling.

6.3.2 Test methods

The stiffness and strength of the FRP material over the time are important design factors. Thus their potential reductions can be of major concern. The anisotropic nature of the composite dictates that mechanical tests should be carried out in reference to the fiber or off-axis direction. The composite tensile strength and stiffness in the transverse direction and the compressive strength in the longitudinal direction are matrix-dominated, while longitudinal tensile strength and stiffness are fiber-dominated. In addition, the loss factor, a measure of internal damping depending on the degree of microdamage, may also be considered as a performance index for the material. Accordingly, multiple test methods can be used to characterize these performance measures as functions of environmental and stress condition exposure. These methods are discussed next.

6.3.2.1 Destructive flexural strength testing

Flexural testing can be carried out on coupons specimens of the FRP per ASTM D790, Standard Test Methods for Flexural Properties of Unreinforced and Reinforced Plastics and Electrical Insulating Materials. Although various specimen sizes are possible, small specimens require less material, less time to construct, smaller test machine capacity, and are easier to handle. A relatively small span of 63.5 mm (2.5 in.) was used successfully in three-point bending tests of FRP components, 0.14 in. thick (Wu et al., 2006b). This span length provided a span-to-depth ratio of 17.8, larger than the minimum ratio of 16 required by ASTM D790. The resulting flexural strength was taken to be the maximum stress in the outermost fiber location at the moment of specimen fracture.

6.3.2.2 Nondestructive modal testing for storage modulus and loss factor

Modal vibration response measurements using impulsive excitation can be used to determine two additional performance indices of interest, the storage modulus and loss factor. It has been shown that modal vibration testing in either single mode or multimode vibration can be used to determine the storage modulus and damping loss factor of composite materials and their constituents (Gibson, 2000). Modal frequencies and loss factors are sensitive indicators of material integrity. In addition the nondestructive nature of the test is particularly valuable here because the same specimen exposed to possibly deteriorating environments can be consistently and repeatedly tested to monitor possible changes in these performance indices. Modal testing in single mode vibration using the impulse-frequency response method (Suarez et al., 1984; Gibson, 1994, 2000) can be used to measure the flexural modal frequencies and modal loss factors of specimens. In this method, impulsive excitation is applied using an electromagnetic hammer and the transverse displacements of the beam are measured with respect to time by means of a noncontacting eddy current probe positioned near the tip of the beam. Further, a fast Fourier transform is performed to obtain the frequency response function (FRF). The peak locations

in the frequency response spectrum are identified as the natural frequencies of the specimen. The effective storage modulus, representing flexural stiffness, can then be estimated as (Suarez and Gibson, 1987).

$$E = \frac{4\pi^2 f_n^2 \rho A L^4}{\lambda_n^4 I} \tag{6.1}$$

where E = effective storage modulus of beam material; f_n = frequency of nth mode (Hz); I = moment of inertia of beam about its neutral axis; ρ = mass density of the material; A = cross-sectional area of beam; λ_n = eigenvalue for nth mode, which depends on boundary conditions (e.g., $\lambda_1^2 = 22.4$ for first mode of free-free beam); L = free length of the beam.

The loss factor for the nth frequency, which is a measure of internal damping, can be calculated by applying the half-power bandwidth method to the peak located at the nth frequency as (Suarez and Gibson, 1987):

$$\eta_n = \frac{\Delta f}{f_n} \tag{6.2}$$

where η_n = loss factor for the nth frequency; Δf = half-power bandwidth of peak at modal frequency f_n in FRF; f_n = frequency of nth mode (Hz).

6.3.3 Test materials and specimens

Example specimens are described and tested for illustration. The considered specimens are composite plate made of glass fiber and vinyl ester resin, each having dimensions of 38.1 cm (15 in.) by 81.3 cm (32 in.) and a nominal thickness of 3.175 mm (1/8 in.). Each thin plate is made of two layers of glass fiber fabric. Each layer of fabric is made of four plies of unidirectional E-glass fiber bonded and stitched to a randomly oriented E-glass scrim (Table 6.1). The resin used is Derakane 411-PC vinyl-ester (Dow Chemical). The fiber volume fraction for the skin composite is around 50%, so each layer of fabric adds about 1.778 mm (0.07 in.) to the thickness.

Coupon specimens (25.4 mm or 1 in. wide and 254 mm or 10 in. long) can be cut from these plates using a diamond saw blade. The two layer specimens used for testing have an average thickness of 3.556 mm (0.14 in.). All specimens are

Table 6.1 Fabric sublayer properties

Sublayer	Orientation	Fiber-ply weight
1	0°	26.2 oz/yd^2
2	90°	16 oz/yd^2
3	+45°	12 oz/yd^2
4	−45°	12 oz/yd^2
5	Random	6.75 oz/yd^2

subjected to postcuring at 60°C for at least 4 h before either being dried in air at 23°C or soaked in distilled water or salt water to simulate environmental exposure. The cut edges of the specimens are coated with a very thin layer of epoxy to minimize moisture absorption through these edges of the specimens. Soaking time is at least 2 weeks prior to the start of freeze−thaw cycling.

6.3.3.1 Test sequence

As discussed above, the environment factors considered may include the number of thermal cycles, cycle length, exposure time, and media type including distilled water, salt water, and dry air. The combined effect of the environmental factors and specimen prestraining (i.e., to simulate the specimen under service load) should be also investigated. To simulate load imposed on the specimen, a prestraining fixture can be designed as shown in Fig. 6.15 (Wu et al., 2006a). This fixture can bend the specimens about vertical dowels placed in three uniformly offset sets. All dowels are retained at top and bottom so they are in double shear and the displacements of the specimens would be relatively uniform. The middle line of the dowels is set into holes in a channel-guided slide that is displaced by a threaded block and sealed bolt. Prestraining at the level of 25% of the ultimate strain of the specimens might be used, or other degrees of prestraining may be considered as needed. It should be noted that the prestraining is applied in a deflection-controlled manner. The actual level of associated prestress is probably reduced over time due to stress relaxation.

Both destructive flexural and nondestructive vibration modal tests can be used to evaluate possible deterioration of the specimens after subjected to weathering from a predetermined number of freeze/thaw cycles.

6.3.4 Test results

The following results are presented for the purposes of illustration (Wu et al., 2006b).

Fig. 6.16 A shows flexural strength of the specimens after 250 freeze/thaw cycles with and without sustained loads, subjected to 2-h and 5-h cycle tests (designated as 2H and 5H for the specimens without prestraining loads, and 2H-PS and 5H-PS for the specimens with prestraining loads). The storage modulus and loss factor after 250 cycles are shown in Fig. 6.16 B and C, respectively. The storage modulus and loss factor were determined from the nondestructive modal vibration tests using the same specimens throughout each environmental exposure condition. For ease of comparison, relative values are adopted to present the percent changes over the baseline data after 250-cycle exposure to the specified environmental condition. All baseline data are listed in Table 6.2. These data suggest that the 5H-cycle testing with prestraining results in a slightly more severe damage compared to the 2H-testing with prestraining in both distilled water and 10% salt water when judged based on flexural strength and storage modulus, although the differences are not statistically significant. The loss factor does not change noticeably except in salt water. Composite materials would absorb moisture during the thawing regime,

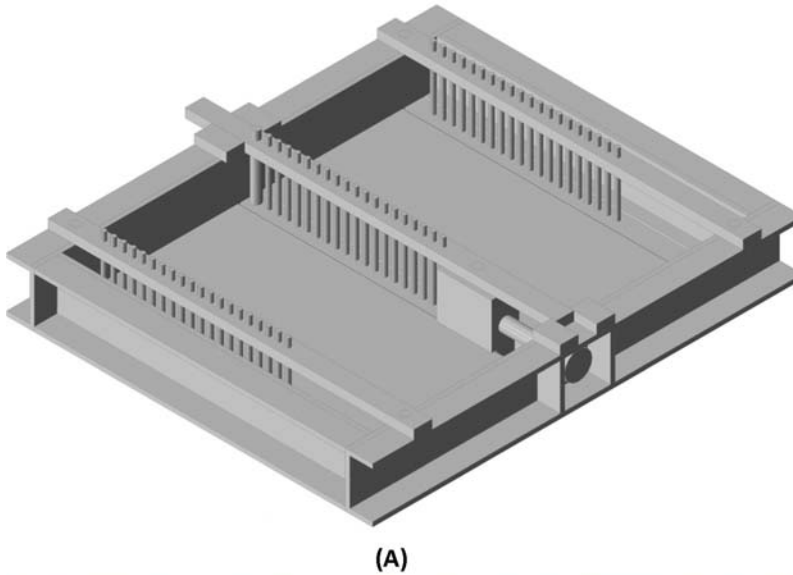

(A)

(B)

Figure 6.15 Prestraining fixture (A) in 3-D drawing, (B) loaded with specimens.

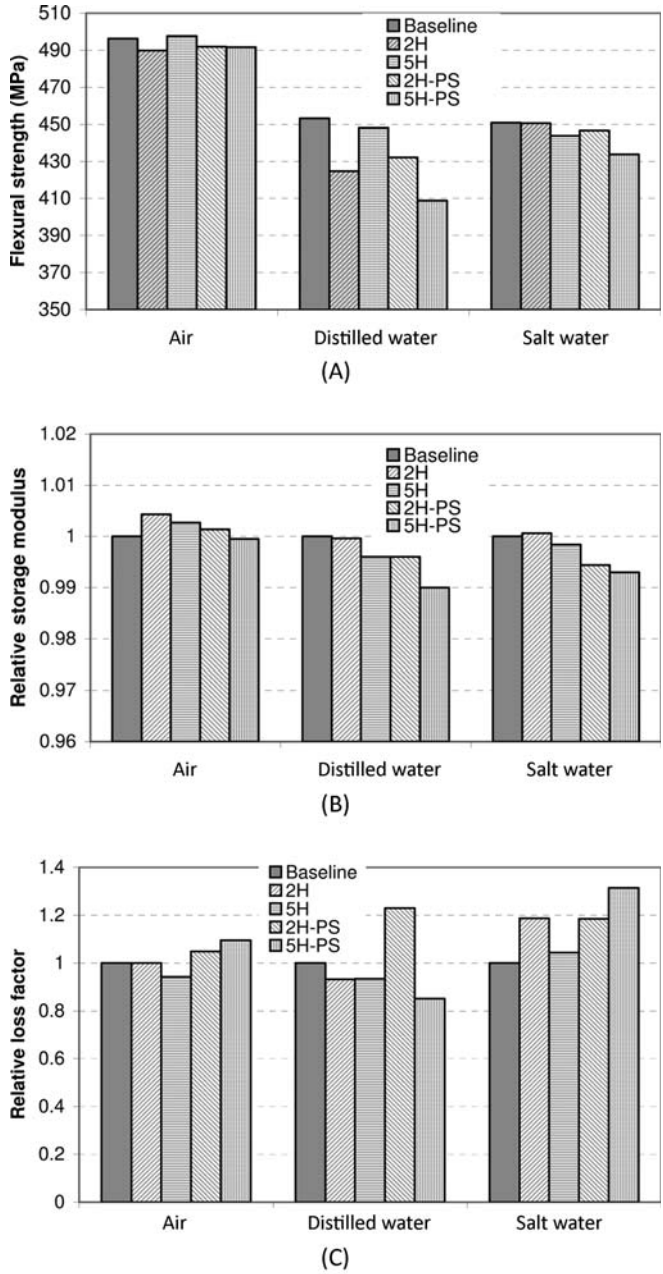

Figure 6.16 Comparison between cycle length of 2 and 5 h after 250 cycles. (A) Flexural strength; (B) Relative storage modulus; (C) Relative loss factor

Table 6.2 Baseline data for storage modulus and loss factor prior to environmental exposure

Specimen ID	Air		Distilled water		Salt water	
	Modulus (GPa)	Loss factor	Modulus (GPa)	Loss factor	Modulus (GPa)	Loss factor
2H	23,358	0.00487	21,394	0.00587	21,963	0.00488
5H	21,892	0.00511	22,746	0.00553	22,460	0.00492
2H-PS	21,631	0.00487	22,838	0.00554	23,170	0.00544
5H-PS	20,909	0.00516	22,174	0.00618	22,549	0.00486

and hence a longer cycle length might permit a higher moisture uptake leading to more deterioration than a shorter cycle length.

A higher loss factor represents a higher level of damping or energy dissipation resulting from more damage or degradation in the test material. It has been previously reported that the loss factor is more sensitive to damage in composites than the storage modulus at elevated temperatures (Gibson, 2000). However, there are no such data available for composite materials at low temperature. In addition, as mentioned above, the coefficient of variation of the loss factor is found to be 12%, which is much higher than that of the flexural strength (7%) and the storage modulus (0.3%). Therefore unless noticeable damage has occurred in the specimens, storage modulus is a better indicator of possible deterioration of the specimens subjected to various exposure conditions. In typical stiffness-critical applications such as a bridge component, it seems reasonable to give more weight to observed changes in modulus than to changes in strength or damping.

Freeze/thaw exposure in dry air resulted in no noticeable changes in flexural strength, storage modulus, and loss factor regardless of cycle length, as shown in Fig. 6.16. This may be attributable to the relatively small temperature difference between 4.4°C and −17.8°C, which might not produce a large enough thermal mismatch between the fibers and the matrix and/or between the plies with different orientations. Thus the thermal cycling in dry air shows no appreciable damage.

Also shown in Fig. 6.16 is that the storage modulus of the prestrained specimens from the 2H cycle testing shows a smaller degree of deterioration compared to that of the 5H-cycle testing after 250 cycles. Note that it takes 5H cycle testing 1250 h to complete 250 cycles, but only 500 h for 2H cycle testing. By the time the 2H specimens undergo 1250-h exposure, they have already accumulated 625 cycles and show a further reduction in storage modulus. These results suggest that the effects of total exposure time and number of thermal cycles on FRP materials are compounded. With these limited data, however, it appears that number of cycles dominates over total exposure time.

This page intentionally left blank

Field testing

7

7.1 Introduction

In Chapter 6, Laboratory testing, it was suggested that, in order to best estimate future levels of fiber-reinforced polymer (FRP) system degradation, some field testing should be done. A drawback with such testing is that the FRP system, if attached to the structure, will experience some damage. In addition to pull-off testing, however, other types of field tests may be useful to assess the bridge performance. Two well-known types of bridge performance testing are strain and/or displacement monitoring under service loads, and proof load testing. These tests can be used to determine strains and/or displacements at critical locations on the structure; to determine load distribution throughout the structure, and in particular, to its girders; and to verify that the structure can indeed carry the loads intended. This information can be used to refine analysis models used to assess the need for FRP installation, to determine with greater accuracy the forces that should be used to design the FRP system, to assess the strains that the system is experiencing, and to validate the load carrying capability of the system. These tests are not meant to be damaging to the structure.

7.2 Field pull-off testing

For the most part, the procedures discussed in Chapter 6, Laboratory testing, can be applied to an as-built structure or witness panel if desired. Here a few additional recommendations are given. First, it may not be reasonable to expect that the quality control used in the field will match that in the laboratory; this is especially true of the installation took place in harsher environmental conditions. Therefore a wider range of test results than found in the laboratory is to be expected. Correspondingly, more tests may be required in the field to establish mean bond failure strength with the level of confidence desired. Second, as FRP systems are usually installed on vertical or upside-down horizontal surfaces, depending on the type of adhesive used, test dollies may not remain firmly adhered to the FRP surface, unlike under the ideal table-top conditions available in the laboratory. One way to ensure that dollies remain in contact with the FRP surface until the adhesive cures is to use a temporary holding mechanism. A cheap and easy solution is to cut pieces from a thin rubber membrane, which can be pulled taught over the in-place dolly and taped to the surrounding surface until the epoxy hardens (Fig. 7.1).

Another issue to consider is that, unless the adhesive used to secure the dollies cures unusually quickly, the pull-off testing must be conducted on a later date than the installation date. For example, the epoxy used to secure the dolly shown in

Strengthening of Concrete Structures Using Fiber Reinforced Polymers (FRP).
DOI: http://dx.doi.org/10.1016/B978-0-08-100636-8.00007-7

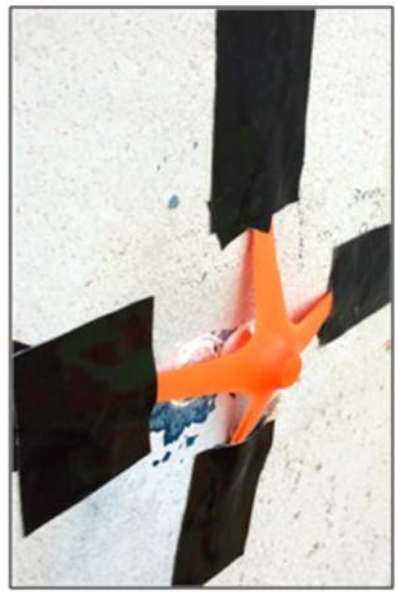

Figure 7.1 Test dolly secured with rubber membrane.

Fig. 7.1 required 3 days to cure and reach full strength, according to the manufacturer. Therefore two different trips to the site were made, with associated concerns for travel, access, and traffic control during installation and testing. During installation, care should be taken to see that, if possible, the environmental conditions (temperature, moisture, contaminants) meet the adhesive manufacturer's recommendations as well, to ensure that the dollies are properly secured and additional trips for reinstallation of failed dolly/FRP system bond are avoided.

The installation process is essentially the same as that for the laboratory specimens: cleaning the surface where test dollies were to be installed; roughening the base surfaces of the dollies to enhance their adhesion; applying epoxy to the base of the dollies; then securing the dollies in place to allow the epoxy to cure. Prior to pull-off testing, after the adhesive is fully cured and the rubber membranes are removed, a portable drill press can be used to cut the FRP around the base of the dollies (Fig. 7.2). As with the laboratory test specimens, care must be taken not to cut into the concrete surface, which can influence test results. A portable adhesion tester can conduct the pull-off test at any surface orientation (Fig. 7.3).

7.3 Load distribution testing

7.3.1 Introduction

It is well known that bridge structures frequently display significantly different behavior than simplified models used for design suggest. One of the most common

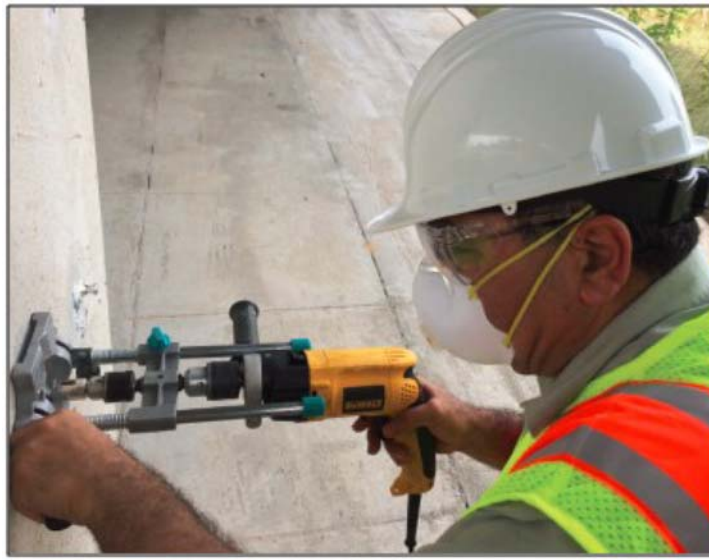

Figure 7.2 Coring FRP material around test dollies with portable drill press.

Figure 7.3 Adhesive bond testing on as-built structure.

analyses of concern for girder bridges is the distribution of vehicular live load to the individual girders. There are various reasons why simplified formula for girder load distribution, such as those found in the AASHTO Bridge Design Specifications, as well as even detailed finite element modeling, may produce results significantly different from those found in actual structures. Some of these reasons include: the presence of elements such as barriers, diaphragms, and sidewalks, which alter the lateral and longitudinal stiffness of the bridge; unintended partial fixity of supports and joints, which are often assumed to be pins or rollers for analysis; differing material properties than assumed; changes in deck thickness, often due to the overlay of a subsequent concrete wearing surface, which may enhance stiffness; and localized damage and deterioration.

Accurate analysis of load distribution becomes important for determining what loads FRP-retrofitted girders must carry. A large body of research, in terms of both field studies and analysis, was generated while studying this issue. Early examples include work based on field tests of bridges conducted by Shepherd and Sidwell (1973), Bakht and Csagoly (1980), Darlow and Bettigole (1989), Bakht and Jaeger (1990), Stallings and Yoo (1993), and among others. Based on this work, it was established that the simple formulas used to distribute load to girders in the AASHTO Standard Specifications (last published as the 17th edition in 2002), as a function of only girder spacing, were inaccurate in many instances. However, even after revised girder distribution factor (DF) expressions were presented, based on finite element studies (Zokaie and Imbsen, 1992) and codified in the first load and resistance factor design version of the AASHTO Bridge Design Specifications in 1994, much additional experimental and computational work on this topic continued. A selection of the many bridge testing and analysis studies to better establish DF include those by Eom and Nowak (2001), who conducted field tests on various steel girder bridges to study DF and dynamic loads, and Eamon and Nowak (2002), who investigated the effects of barriers, sidewalks, and diaphragms. Barr et al. (2001) evaluated DF for skewed prestressed concrete (PC) bridges by field testing and finite element analysis (FEA), while Cai and Shahawy (2004) evaluated the performance of six PC bridges through field testing and FEA, and later (Cai, 2005) proposed adjustments to the AASHTO DF expressions. Similarly, Hughs (2006) evaluated DFs for PC spread box-girder bridges through field testing and FEA, and Cross et al. (2009) who conducted an investigation of 12 bridges to better determine shear DFs. Yousif and Hindi (2007), Dicleli and Erhan (2009), Harris (2010), Fanous et al. (2011), Puckett et al. (2012), and among others, concentrated on computational modeling to improve DF estimation. Other work includes that by Zia et al. (1995), Ebeido and Kennedy (1996), Miller et al. (2004), Oesterle et al. (2004), and Okeil and Elsafty (2005), who studied load distribution on continuous bridges. Although bridge finite element modeling is beyond the scope of this book (successful approaches can be found in many of the references mentioned above), a more reliable method to determine actual load distribution is field testing, the topic of this section.

First, it should be noted that load distribution testing is structure-specific. Due to the various factors discussed in the introductory paragraph to this section, the effect

of which may vary greatly from one bridge to the next, the DFs found on one structure may vary significantly from those associated with another very similar structure. Such testing requires significant advanced planning, and for most bridges, will of course require the permission and cooperation with the bridge owner, generally a local agency or the state Department of Transportation (DOT).

This type of field testing will usually require a minimum of 2 days; 1 day for equipment installation and another day for testing and equipment dismantling. If the installation team has not instrumented a bridge previously, a plan for a minimum of 2 days for installation is recommended. Coordination with the owner is required to develop a traffic control plan for both the test day for on-bridge traffic, as well as for the installation day, if the structure spans a roadway. State and local agencies will have appropriate plans in place for lane closures, as needed. Note that for most types of instrumentation, access to the underside of the bridge girders is necessary for installation. Depending on the accessibility of the structure, some bridges may not be possible to instrument. However, it is reasonable to assume that if the structure is chosen for FRP installation, it should be accessible for instrumentation installation as well.

Several types of instrumentation can be used. Traditional types include the use of reusable strain gauges to measure girder strains and linear variable differential transformers (LVDTs) to measure girder displacements. More modern systems include optical systems to map displacements and strains, and may not require any instrumentation attached to the bridge. The use of this type of system is currently limited, however, and is not discussed further. Although LVDT systems can directly measure girder deflections, in the authors' experience, they are more difficult and time consuming to set up than a strain gauge system, and also require access to a firm surface below the bridge to secure the LVDTs. As such, the use of these gauges usually precludes instrumenting bridges with a waterway or roadway below, limiting their versatility. Thus the following discussion will focus on the use of strain gauges. However, much of the information presented will apply to the use of an LVDT system as well.

7.3.2 Installation plan

After the bridge is selected and verified for accessibility, an instrumentation plan must be developed, where what to be measured and where it will be measured is determined. As noted earlier, actual girder live load distribution is a significant unknown and is a common concern, as this directly affects the magnitude of load to be carried by girders strengthened with FRP systems. Typically, strain gauges are placed at or near midspan of the girders, where strains are greatest under live load. If the structure is continuous, if additional gauges are available, it might also be worthwhile to instrument the negative moment region near interior supports as well. Strain gauges are usually installed on the lower flanges only. Additional strain information on the deck surface would be useful to locate the neutral axis of the girders, but this placement is rarely done as traffic and load vehicles on the bridge may damage such instrumentation. An example of a instrumentation plan for a 2-span

continuous bridge with seven girders is shown in Fig. 7.4, with planned gauge locations given, where 'm' refers to a gauge placed at midspan on the lower girder flange and 's' refers to a gauge placed near the continuous center support on the lower girder flange. In this particular project, there was an insufficient instrumentation available to monitor all girders at both the midspan and support locations, and thus the missing gauges on some girders on the rightmost span.

Depending on the type of sensors available, different attachment methods might be used. If multiple bridges are to be tested, it may be worthwhile to consider purchasing durable, reusable strain gauges meant for field testing, if funds are available. These gauges can be mounted to concrete by epoxying small metal tabs to the surface of the girder flange. Projecting from these tabs is a metal bolt, upon which the gauge can be mounted and secured with a nut, as shown in Fig. 7.5. Such

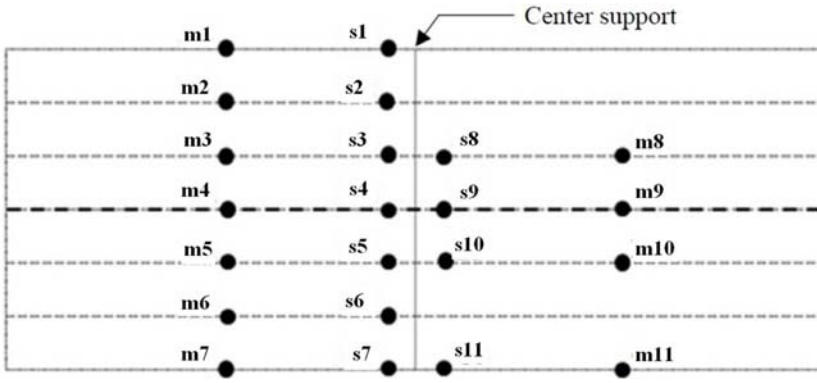

Figure 7.4 Example instrumentation plan.

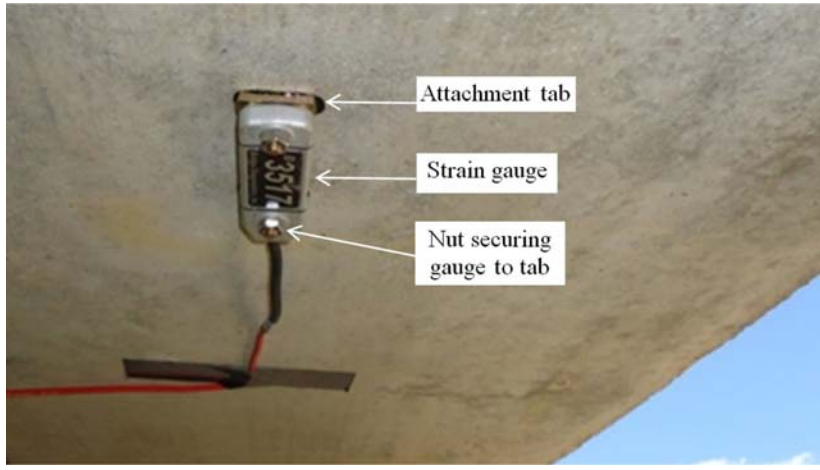

Figure 7.5 Strain gauge mounted to lower flange of PC bridge girder.

gauges are pricy, however. Alternatively, a cheaper but less durable sensor can be fabricated by mounting a small, discardable gauge to a metal coupon, which in turn can be secured to the concrete. Note that the use of very small gauges might capture localized strains not representative of the larger field, particularly if cracks are present in the concrete surface.

Even though reusable gauges are expected to come calibrated from the manufacturer, it is highly recommended to verify gauge accuracy before use. This can be done in the laboratory by mounting each gauge to a steel coupon placed in a tension machine and comparing gauge strains to those found from an alternative source that is known to be accurate.

Before installing instrumentation in the field, it is highly recommended that the sensor and data acquisition system, if new or if not recently used, is given a trial run to verify that it is working properly. This can be done in the laboratory or outdoors, under similar conditions that will be expected in the field. Issues to be especially concerned with are: the adequacy of the gauge mounting procedure; the level of accuracy expected with the system and that needed, considering the inherent noise level present; and the power supply and operation of the system. High quality gauges can be expected to have a practical accuracy within $1-2\%$, and a good data acquisition system a base noise level within $1-2$ microstrain. The level of strain that the girders will experience, as compared to the strain level that they can accurately detect, requires careful thought. In the authors' experience, due to the many factors discussed earlier in this section, bridge girders often experience significantly less strain than simple analyses will indicate. Another consideration is the safety of the system itself; if left overnight, damage due to poor weather or vandalism is possible. Traffic delays and rental of test vehicles are highly undesirable and costly, and thus even small details should not be left to be worked out on test day.

7.3.3 Test plan

A test plan specifies the loads that will be used and where and in what sequence they will be placed on the bridge. For measurement accuracy, it is desirable to produce a high signal/noise ratio. Thus for purposes of monitoring load distribution, it is best to select large loads that will generate strains as high as feasibly possible. The limits to these loads will generally be governed by the state vehicle code where vehicle configurations and maximum allowable legal axle forces are specified. The rental of construction vehicle(s), such as a filled haulers from a gravel yard, for example, may be most cost-efficient. If special circumstances dictate that these loads must be exceeded, the use of a permit load or even the application of very heavy static objects on the bridge might be used, though costs and logistics difficulties increase. The use of static loads on the structure is generally least practical, as the expense and time to conduct such a test may be overwhelming, especially since multiple load positions are highly desirable.

After the load vehicle(s) are determined, the sequence of positioning the vehicles on the bridge must be determined. In general, significant variation in girder strain will occur depending on the longitudinal and lateral position of the vehicles. Thus to

confirm findings as well as to determine the maximum possible proportion of live load that a girder can be expected to take, it is recommended that multiple load cases are investigated. It is also recommended that vehicles are not placed at a particular longitudinal position on the structure, stopped, and then strains are measured. It is very difficult to determine where vehicles should be placed longitudinally on an actual structure to develop the maximum possible girder strains. A much more reliable way is to simply have the vehicles slowly drive (at walking speed) completely across the span. Of course, while trucks are moved across the bridge, it is important that other traffic is stopped such that no other vehicles are present on the span. If data are continuously sampled at a reasonably fast rate (30 Hz is more than sufficient), the maximum load effect possible based on longitudinal position will be achieved. Dynamic tests require additional consideration and are beyond the scope of this chapter. An example test plan is shown in Fig. 7.6. The figure shows diagrams for 15 load runs using two heavy vehicles.

To allow for further analysis, truck axle weights and configuration (axle spacing and transverse axle widths) should be recorded at a weigh station prior to each test. Many gravel yards have weigh stations that can be used if the vehicles are rented there. Moreover, during the tests, the precise longitudinal positions of the vehicles should be recorded. This can be done by video or other reliable means.

7.3.4 Interpreting results

An example of girder strains is shown in Fig. 7.7, which presents a record of midspan strain (from gauges m1 to m7, as shown in Fig. 7.4) as test vehicles move over a two-span continuous structure following run #1, as shown in Fig. 7.6.

As it is unknown what actual loads will travel over the bridge during its lifetime, in the load distribution test, the actual level of strain caused by the test vehicles is not important; rather, it is the maximum proportion of strain that a single girder experiences. This proportional relationship can then be used to better estimate a girder distribution factor (GDF) for design or evaluation for any level of live load that the bridge might experience. GDF can be simply defined as the maximum proportion of total truck live load effect applied on the bridge that is distributed to a single girder. Thus assuming flexural load effects are of interest, GDF, in terms of moment, can be computed as

$$\mathrm{GDF} = \frac{\max(M_i)}{\sum_{i=1}^{n} M_i} \tag{7.1}$$

where M_i is the live load moment carried by girder i and n is the total number of girders. Expressing moment in terms of Young's modulus (E) and bottom section modulus (S) of girder i ($M_i = E_i \varepsilon_i S_i$), assuming E and S are similar for all girders, GDF can be determined in terms of a proportion of measured girder strains at the bottom surface of the girder section (ε):

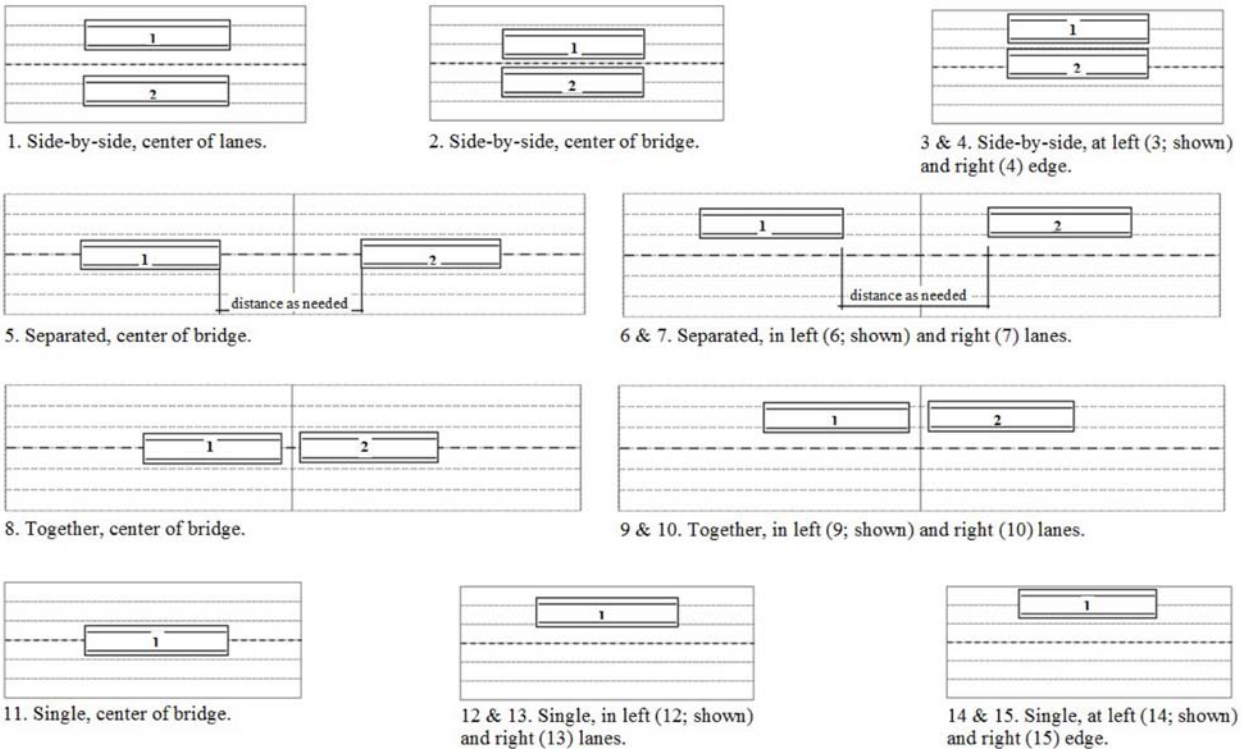

Figure 7.6 Example test plan runs using two vehicles.

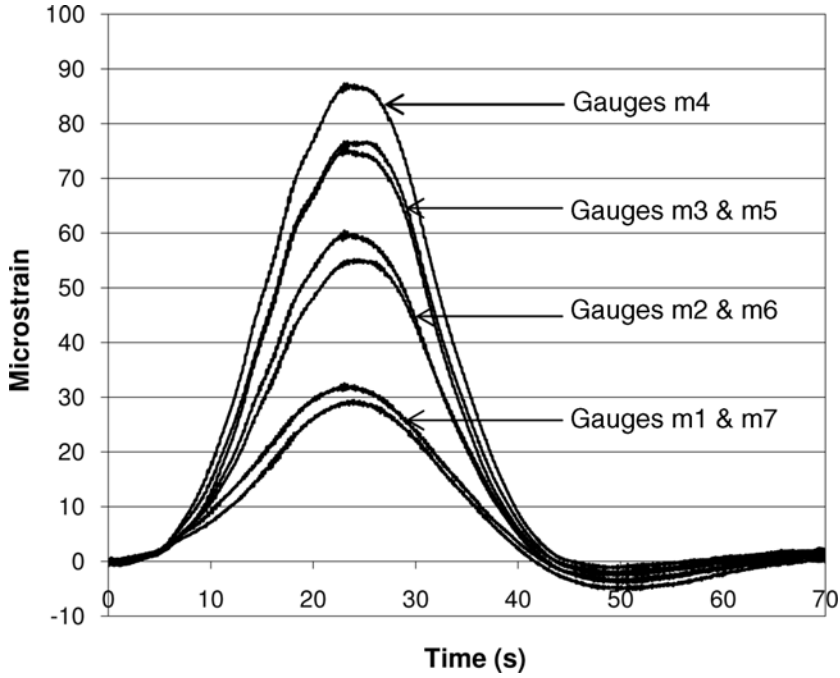

Figure 7.7 Example girder strains as a function of time.

$$\text{GDF} = \frac{\max(\varepsilon_i)}{\sum_{i=1}^{n} \varepsilon_i} \tag{7.2}$$

Thus at any particular point in time in Fig. 7.7, measured girder strains can be inserted into Eq. (7.2) and a GDF determined. Fig. 7.8 shows girder strains that could be used for GDF calculation at time $t = 25$ s, taken from Fig. 7.7. This process can be repeated for the different load cases considered to determine the worst case, as well as for different girders, if more than one girder is under consideration for GDF calculation. Note that in a general design situation, the maximum GDF for any girder is needed. However, for FRP retrofit analysis, the GDF for only the affected girder(s) may be needed.

As discussed above, Eqs. (7.1) and (7.2) assume that that the effective section modulus and Young's modulus of the girders are identical. Of course this is not necessarily true, due to local variations in material properties, cracking, as well as the presence of nonstructural elements on the deck such as barriers, which stiffen exterior girders to a greater extent than those interior to the span. Regardless, the actual variation in the effective girder stiffness is unknown and can only be approximated. These effects were studied previously (Stallings and Yoo, 1993; Nowak and Eom, 2001) and were suggested to have minor differences in GDF. Although one may attempt to adjust GDFs, particularly by including barriers in the estimation

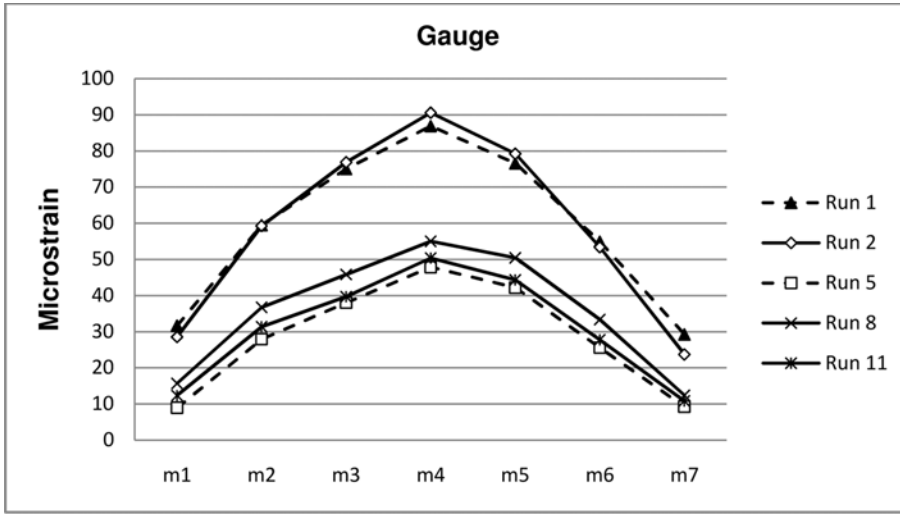

Figure 7.8 Example girder strains at $t = 25$ s.

of exterior girder stiffness, it is common to ignore these unknowns and weigh all girders equally.

7.4 Proof load testing

In some cases, a bridge owner may wish to verify that a particular bridge, after FRP strengthening, can safely carry certain loads that may be imposed on it. Such a verification test is referred to as a proof load test. Assuming that the structure is not to be damaged, it is not possible to determine the ultimate capacity of the bridge. However, a proof load test can be used to confirm that the structure can carry the maximum legal or a given permit load limit, for example.

Although bridge strains or displacements are usually not directly of interest for a proof load test, some type of bridge performance monitoring must be conducted during the test to ensure that the structure is not becoming overloaded and subjected to damage. This can be done by instrumenting the bridge as if it was to be subjected to a load distribution test as discussed in Section 7.3. During the proof load test, girder strains must be monitored to ensure that a precalculated limit strain is not exceeded, as well as to ensure that the structure continues to behave in the linear elastic range. Limit strains of interest might be: allowable strains to prevent FRP debonding; allowable strains to prevent concrete cracking; and reinforcing or prestress steel yielding. For concrete members, steel strains can only be estimated, based on a calculated neutral axis position and the available girder flange strains. This is one instance where instrumenting at the top of the deck as well as the girder lower flange is very useful.

Often, bridges that are chosen for FRP strengthening have a low load rating. For these structures, the desire is typically to repair the structure such that a minimum

operating rating of 1.0 can be achieved so the normal flow of traffic is not restricted. However, determining the appropriate proof load requires careful consideration. Generally, the proof load should be above the maximum legal (or permit) load of interest, to account for uncertainties in the actual traffic loads (i.e., a live load factor should be imposed). Different approaches for calculation of the appropriate proof load level have been proposed and are provided in detail elsewhere (see, for example, Nowak and Saraf, 1996; Lichtenstein, 1998). Some reliability-based guidelines for target proof load calculation have been proposed (Fu and Tang, 1995; Faber et al., 2000).

Factors to consider when selecting an appropriate live load factor include: the traffic level and governing load effect; whether the bridge has fracture-critical details and nonredundant load paths; how often inspections are performed; and the existing condition of the structure. In any case, once the desired proof load level has been calculated, another task which is often troublesome is to determine how the structure will be loaded in order to generate the needed proof load. Due to the imposed live load factor, proof loads often require loads significantly beyond the maximum legal load. As noted in Section 7.3 the use of static loads such as concrete blocks is generally not recommended due to the inconvenience of moving and placing these objects, as well as the relatively long time required for bridge closure. Moving load possibilities include obtaining the use of very heavy special permit vehicles, or the use of heavy construction vehicles which potentially can be brought to the site on legal or routine permit tractor−trailer, then removed and placed on the bridge to generate a concentrated load effect. Although availability may be uncertain, some proof load tests conducted for a state DOT have involved the use of tanks (brought to the site on tractor−trailers) obtained from a nearby national guard station.

Recommendations

8

8.1 Analysis and design recommendations

8.1.1 Criteria for recommendations

In Chapter 4, Design provisions, and Chapter 5, Provisions for installation, quality control, and maintenance, a set of standards for FRP installation were reviewed and most were found to have reasonable coverage of the major design and analysis areas (flexure, shear, confinement). Depending on the policy or legal requirements in-place at a particular location, the choice of provisions to use may not be an option. However, if this decision is yet to be made, or is left to the designer, some of the following criteria might be considered to guide selection of appropriate provisions.

1. Accuracy. It is essential that a recommended provision accounts for the phenomenon that it attempts to address with sufficient accuracy. In general, this can be established with adequate documentation in the code commentary, to demonstrate theoretical soundness and/or convincing experimental evidence for empirically based provisions. Documentation may include references to appropriate technical papers, reports, or other published sources, some of which are included in this book. As shown in earlier chapters, the reviewed codes contain varying levels of documentation for their recommendations.
2. Format compatibility. From a practical point of view, it is important that provisions are compatible with existing bridge design and analysis procedures in place. This is particularly important when considering strength reduction factors that modify expressions for capacity. Such factors may have been developed for building loads, for example, which have different levels of uncertainty than traffic loads. Similarly, manufacturing and environmental factors may reflect conditions that are not representative of those in the climate for which the system will be installed.
3. Clarity and ease of use. Often, provisions produce similar outcomes, but achieve the outcome with different procedures, equations, and processes. Clearly, a balance must be drawn between accuracy and ease of use. A large increase in complexity that provides a minimal gain in accuracy may not be appropriate. Clarity and ease of use can be evaluated in terms of the procedures and models used, and even the symbols and nomenclature used in the relevant expressions. Clarity also concerns similarity to the existing methods that designers are familiar with.

8.1.2 General recommendation and discussion

Based on the criteria considered above, for use in the United States, it is recommended that the AASHTO guidelines (AASHTO *Guide Specification for the Design of Bonded FRP Systems for Repair and Strengthening of Concrete Bridge Elements*)

Strengthening of Concrete Structures Using Fiber Reinforced Polymers (FRP).
DOI: http://dx.doi.org/10.1016/B978-0-08-100636-8.00008-9

are used as the base analysis and design document, with some recommended modifications, as discussed below. The AASHTO Guide covers most areas of concern with good documentation of accuracy, and results calculated from the AASHTO provisions generally fall with the range of outcomes of the other codes considered. Moreover, the document is specifically written for bridge structures and is directly compatible with the AASHTO load and resistance factor design (LRFD) design provisions, which are practically universally used in the United States. The format, notation, and procedures within are also familiar to bridge engineers. A brief summary of the reasoning for recommending the AASHTO provisions is discussed below.

Strengthening limits for fire endurance. ACI 440.2R provides strengthening limitations to allow a structure to maintain a minimum specified strength if the external FRP strengthening system is weakened in a fire. The use of this expression, however, requires evaluation of existing structural capacity at high temperatures, which introduces complexity that may not be desirable. Although AASHTO does not directly address this issue, AASHTO does provide a general strengthening limit expression when FRP is considered. As discussed in Chapter 4, Design provisions, this existing provision provides a strengthening limit outcome similar to that presented by ACI. Therefore the existing AASHTO expression is recommended without modification.

FRP strain limits. To prevent debonding, AASHTO specifies that the FRP strain may not exceed 0.005 less initial strain (for flexure). AASHTO adds a second strain condition to ensure ductile behavior poststeel yielding. AASHTO stipulates that the ultimate FRP strain equals 2.5 times FRP strain at the point of steel yielding. These strain limit requirements are slightly more conservative than some other codes, as discussed in Chapter 4, Design provisions, but are deemed reasonable for reinforced concrete structures. However, as discussed below, these may not be suitable for prestressed concrete girders.

Strength reduction factors for FRP. The majority of codes use a FRP strength reduction factor close to 0.85, as discussed in Chapter 4, Design provisions. Some codes such as TR55 adopt a more detailed procedure to account for different FRP materials, manufacturing processes, and exposure conditions to produce a combined factor for specific cases. This approach offers flexibility, but unfortunately, most of the values recommended are undocumented or rely on manufacturer test data that may not follow common standards or regulations. The common global value adopted by AASHTO of 0.85 is based on the work by Okeil et al. (2007) that is based on reliability analysis and accounting for the brittle nature of carbon FRP (CFRP). Due to the lack of information to justify a more detailed system, and as the AASHTO-specified value is similar to that adopted by other codes, it is recommended for use.

Serviceability, service load limits, creep rupture, and fatigue limits. The AASHTO serviceability limits are $0.80f_y$ for steel, $0.36f'_c$ for concrete, and $0.80f_{fu}$ for CFRP. These values are similar to those adopted by ACI, except for the FRP limit since AASHTO has no considerations for an environmental reduction factor which is built in the ACI factor of $0.55f_{fu}$. Both ACI and AASHTO reference the work of

Yamaguchi et al. (1997) and Malvar (1998) as a basis for fatigue limits. No other codes offer a complete set of serviceability limits. AASHTO fatigue limits are comprehensive as well, with strain limits given for concrete, steel, and FRP, and are recommended.

FRP end peeling. End peeling limits vary from a constant value specified by TR55, an expression by ACI relating the shear force to concrete shear resistance (as a function of section geometry and concrete compressive strength), and expressions by AASHTO that account for FRP thickness, adhesive properties and concrete compressive strength. As shown in Chapter 4, Design provisions, the AASHTO peeling limits compare closely to those of CNR. The work of Naaman and Lopez (1999) is the basis for the limits adopted by AASHTO. Note, however, that this work specifically considered environmental conditions meant for a seasonally cold climate with accompanying freeze−thaw cycles; such conditions may be rather conservative for other climates.

Development length. The expression for development length presented by AASHTO is somewhat different from that of the other codes; it is substantially more sensitive both to f'_c as well as the amount of FRP provided, as shown in Chapter 4, Design provisions. However, the AASHTO expression was developed by Naaman and Lopez (1999) and specifically considered seasonally cold environmental conditions, as discussed above. It is therefore thought to be appropriate or conservative for most North American climates.

Shear and confinement strengthening. Variations in shear and confinement strengthening provisions are minimal among the different codes. Based on this similarity, there is no theoretically compelling reason to deviate from the AASHTO provisions. However, due to the AASHTO requirement that a minimum confinement pressure of 0.6 ksi is met (see Chapter 4: Design provisions), AASHTO may often require a larger amount of FRP than theoretically necessary to increase capacity. Therefore two alternatives are recommended for consideration of confinement strengthening: the AASHTO provisions as well as the ACI provisions. The latter is recommended as it may be more economically feasible than the AASHTO approach for some columns. In particular, as ACI does not specify a minimum required confinement pressure, it may achieve the same strengthening result as AASHTO but with less FRP material.

8.1.3 Recommended modifications to AASHTO provisions

Although the AASHTO provisions are generally recommended, some areas for consideration of modification have been identified. The following are suggested.

8.1.3.1 Environmental reduction factors

AASHTO provides no specific environmental reduction factors. Rather, a minimum assumed interface shear strength is provided ($\tau_{\text{int}} = 0.065\ \sqrt{f'_c}$), which is also used to evaluate peeling (Eq. (4.39)) as well as development length (Eq. (4.52)). Therefore the reduction factor below should be applied to the interface shear strength of the system,

τ_{int}, the value of which is obtained from the manufacturer or from appropriate experimental testing as noted in Section 8.2.4.2.

If bond strength degradation data are available, obtained by a test method such as that suggested in Chapter 6, Laboratory testing, and Chapter 7, Field testing, it is recommended that location-specific reduction factors for CFRP interface bond strength are used. These reduction factors are to be multiplied by the τ_{int} determined for the specific FRP system (not the value of 0.065 $\sqrt{f_c'}$ provided by AASHTO, which is likely much lower than the actual τ_{int}). It should be emphasized that the reduction factor is applied to τ_{int} only and not directly to the section capacity in the form of an overall strength reduction factor. Even if experimentally determined long-term reduction factors are found to be large (for example, close to 0.5 at 75 years), if common epoxy strengths and appropriate surface preparation and installation techniques are used, as in accordance with the recommendations of this chapter, it is likely that no environmental reductions in capacity will occur in most cases. This is because the interface shear strength assumed by AASTHO is very low ($\tau_{int} = 0.065\ \sqrt{f_c'}$), and most FRP installations are expected to have initial τ_{int} values greater than twice this amount. Thus even applying a large, long-term reduction factor for 50−75 years may result in a design shear strength greater than the minimum specified by AASHTO, resulting in a potential increase in peeling strength (Eq. (4.39)) and decrease in allowable development length (Eq. (4.52)).

8.1.3.2 Flexural design when considering compression failures

Although tension failures are clearly desired, in many cases it is not possible to meaningfully strengthen with FRP and maintain a tension-controlled section. This is particularly so for prestressed concrete sections, but this is not directly addressed in AASHTO. In the case of a compression controlled section, it is recommended that in the capacity analysis, the AASHTO-specified FRP strain limit (at ultimate capacity) should correspond to a maximum concrete compressive strain in the girder of 0.003. If the resulting FRP strain is less than 0.005, the FRP reinforcement strength per unit width, N_b, should be calculated based on the FRP strain calculated at concrete compressive failure, not 0.005.

8.1.3.3 Initial strain for prestressed sections

For the strengthening analysis of prestressed concrete sections, the initial strain ε_{bo} at the bottom of the beam (FRP/concrete interface) must be calculated. Although not addressed in AASHTO, this expression can be theoretically derived and is given in ACI, which is recommended for use (ACI Eq. 10-18):

$$\varepsilon_{boi} = \frac{-p_e}{E_c A_{cg}}\left(1 + \frac{e y_b}{r^2}\right) + \frac{M_{DL} y_b}{E_c I_g} \tag{8.1}$$

where ε_{pi} = initial strain level in prestressed steel reinforcement, in./in. (mm/mm); p_e = effective force in prestressing reinforcement (after allowance for all prestress losses), lb (N); A_{cg} = cross-sectional area of beam, in.^{2} (mm^2); E_c = modulus of elasticity of concrete, psi (MPa); e = eccentricity of prestressing steel with respect to centroidal axis of member in. (mm); r = radius of gyration of section, in. (mm). y_b = distance from extreme bottom fiber to section centroid, in. (mm); M_{DL} = dead load moment, lb-in (N-mm); I_g = moment of inertia, in.^{4} (mm^4).

8.1.3.4 Strength reduction factors and ductility provisions considering prestressed sections

To ensure ductility, AASHTO limits specify that the strain developed in the FRP reinforcement at section ultimate capacity must be equal to or greater than 2.5 times the strain in the FRP reinforcement at the point where the centroid of steel tension reinforcement yields. With a maximum useable strain of 0.005 at the FRP reinforcement/concrete interface, the maximum effective strain developed in the FRP reinforcement is $\varepsilon = 0.005 - \varepsilon_{bo}$, where ε_{bo} is the initial tensile strain at the bottom concrete surface as a result of the moment due to dead load (the existing tensile strain prior to FRP installation). When the FRP is applied, the steel will have some initial strain due to dead load moment (ε_d). Since the FRP is bonded to the outside of the beam, it is placed further away from the neutral axis in the section than the steel. Therefore the FRP will have a minimum strain value of $\varepsilon_y - \varepsilon_d$ when the steel yields, where ε_y is steel yield strain. Following the AASHTO provisions, at ultimate flexural capacity, strain in the FRP must be greater than the minimum possible value of 2.5 ($\varepsilon_y - \varepsilon_d$). For prestressed beams, the steel effective prestrain (ε_p) must also be considered, such that the strain in the FRP at ultimate flexural capacity must be greater than $2.5(\varepsilon_y - \varepsilon_d - \varepsilon_p)$. However, for the high-grade steel used for prestressing, ε_y is large, and the value of $2.5(\varepsilon_y - \varepsilon_d - \varepsilon_p)$ may exceed the allowable FRP strain limit of $0.005 - \varepsilon_{bo}$. This limitation will not allow any flexural FRP strengthening to be applied to prestressed beams in many cases. Reasonable changes in the concrete constitutive model does not alter this result. ACI provisions solve this problem by allowing such sections to be strengthened, but to account for the possible loss in ductility, the section strength is penalized with a lower resistance factor. However, for the practical cases of prestressed concrete girders investigated, it was found that the ACI approach often leads to high requirements of FRP reinforcement as well as a resistance factor of 0.65. The former occurs because the ACI debonding limit, which limits the usable strain in the FRP (Eq. (4.8)), is a function of the amount of FRP applied; as the amount of FRP is increased to meet flexural demand, this strain limit decreases. It was found that the resulting value is often lower than the value of 0.005 specified with the AASHTO provisions. Moreover, as FRP area is increased, strain in the prestressing steel at failure generally decreases, thus lowering resistance factor, often to 0.65. Therefore direct use of the ACI strengthening provisions with prestressed griders was also found to be impractical in many cases. Therefore an alternative approach is recommended for consideration, based on a modification of the existing AASHTO procedure.

This approach utilizes the AASHTO FRP strain limit addressed in Section 8.1.2. For consistency, the same methodology is recommended for both nonprestressed as well as prestressed sections, with appropriate adjustments in strain limits. This approach combines AASHTO and ACI limits and reduction factor concepts to produce a more practical strengthening procedure for some cases. For nonprestressed sections the resistance factor for flexural capacity for concrete beams with FRP strengthening is recommended to be taken as

$$\begin{cases} \phi = 0.90 \quad \text{for} \quad (\varepsilon_{\text{FRP}u} \geq 2.5\varepsilon_{\text{FRP}y} \text{ and } \varepsilon_t \geq 0.005) \\ \phi = \min \begin{cases} 0.65 + \left(\dfrac{0.25}{1.5}\right)(\varepsilon_{\text{FRP}u} - 1) \text{ for } \varepsilon_{\text{FRP}y} < \varepsilon_{\text{FRP}u} < 2.5\varepsilon_{\text{FRP}y} \\ 0.65 + \dfrac{0.25(\varepsilon_t - \varepsilon_{sy})}{0.005 - \varepsilon_{sy}} \text{for } \varepsilon_{sy} < \varepsilon_t < 0.005 \end{cases} \\ \phi = 0.65 \text{ for } \varepsilon_{\text{FRP}u} \leq \varepsilon_{\text{FRP}y} \text{ OR } \varepsilon_t \leq \varepsilon_{sy} \end{cases} \tag{8.2}$$

where ε_t = strain in the lowest layer (i.e., furthest away from the compression side of the beam) of steel at ultimate capacity, where ultimate capacity is limited by either (whichever occurs first) concrete crushing, FRP rupture, or FRP debonding (at an assumed maximum interface strain of 0.005 given by AASHTO); $\varepsilon_{\text{FRP}u}$ = strain in the FRP at ultimate capacity; $\varepsilon_{\text{FRP}y}$ = strain in the FRP when steel yields.

The above factor is to be applied to the entire flexural capacity expression, including steel and FRP-based capacity components. In addition the FRP portion of capacity is further reduced by the additional resistance factor given as

$$\begin{cases} \phi_{\text{FRP}} = 0.85/0.90 = 0.94 \quad \text{when } \phi = 0.9 \\ \phi_{\text{FRP}} = 0.38\,\phi + 0.6 \quad \text{when } 0.65 < \phi < 0.9 \\ \phi_{\text{FRP}} = 0.85 \quad \text{when } \phi = 0.65 \end{cases} \tag{8.3}$$

Note that practically, due to the usable FRP strain limit specified by AASHTO of 0.005, $\phi = 0.90$ cannot be achieved due to the requirement of $\varepsilon_t \geq 0.005$. However, in most cases, if maximum FRP strain is set to 0.005, ε_t will only be slightly less than this value, resulting in ϕ between 0.85 and 0.90.

For prestressed concrete members (using 250−270 ksi prestress steel), the following is recommended:

$$\begin{cases} \phi = 0.90 \text{ for } (\varepsilon_{\text{FRP}u} \geq 2.5\varepsilon_{\text{FRP}y} \text{ and } \varepsilon_{ps} \geq 0.013) \\ \phi = \min \begin{cases} 0.65 + \left(\dfrac{0.25}{1.5}\right)(\varepsilon_{\text{FRP}u} - 1) \quad \text{for } \varepsilon_{\text{FRP}y} < \varepsilon_{\text{FRP}u} < 2.5\varepsilon_{\text{FRP}y} \\ 0.65 + \dfrac{0.25(\varepsilon_{ps} - 0.010)}{0.013 - 0.010} \quad \text{for } 0.010 < \varepsilon_{ps} < 0.013 \end{cases} \\ \phi = 0.65 \quad \text{for } \varepsilon_{\text{FRP}u} \leq \varepsilon_{\text{FRP}y} \text{ or } \varepsilon_{ps} \leq 0.010 \end{cases} \tag{8.4}$$

where ε_{ps} = the prestressing steel strain (at steel centroid) at ultimate capacity. The same FRP reduction factor as above is applied to the FRP portion of resistance.

$$\varepsilon_{ps} = \varepsilon_{pe} + \frac{pe}{A_C E_C}\left(1 + \frac{e^2}{r^2}\right) + \varepsilon_{p\text{net}} \leq 0.035 \tag{8.5}$$

$$\varepsilon_{pe} = \frac{f_{pe}}{E_p} \tag{8.6}$$

$$\varepsilon_{p\text{net}} = \frac{d_p - c}{h - c}\varepsilon_{frp}^{u} \tag{8.7}$$

Note that practically, due to the usable FRP strain limit specified by AASHTO of 0.005, $\varepsilon_{ps} \leq 0.010$ and thus $\phi = 0.65$. However, the above equations retain validity if the AASHTO FRP strain limit of 0.005 is adjusted to a new value. Increasing this value will allow an increase in the strength reduction factor for prestressed members beyond 0.65.

In most cases, this approach will provide a resistance factor that is very close (slightly conservative) to that specified by AASHTO if AASHTO ductility criteria are met. If AASHTO criteria are not met, beam strengthening is allowed but with a reduced resistance factor similar to the ACI approach as a function of beam ductility.

Here the reader is strongly cautioned. Note that, to determine the most appropriate resistance factors and associated strain limits, a structural reliability analysis of FRP-strengthened prestressed concrete girders is needed. However, this analysis is beyond the scope of this book. Therefore with the recognition that the existing AASHTO provisions were not specifically developed for strengthening prestressed concrete bridge girders, the procedure presented above may be a reasonable alternative to consider until desired reliability or revised guidelines results become available. Some design examples using the recommendations are given in Chapter 9, Design examples.

8.2 Installation, quality control, and maintenance recommendations

For all sources examined, there is a nearly universal suggestion or requirement to follow the FRP system manufacturer's recommendations. Therefore it is recommended that:

1. The installer obtains documentation of manufacturer recommendations for installation, quality control (QC), and maintenance, as available, and that these recommendations are followed. Deviation from these recommendations are to be made only for compelling reasons and should have approval of the design engineer only after careful review.

The proposed deviation should be accompanied with sufficient documentation and/or justification, preferably with quantitative analysis and/or experimental test data.

2. If the manufacturer does not provide recommendations in a particular instance, the guidelines presented below are recommended. In all cases, it is suggested the manufacturer is consulted for comment on the provisions before use.

A checklist of inspection items following the recommendations below is given in Appendix 2.

8.2.1 Shipping, storage, and handling

8.2.1.1 Shipping

As AASHTO has no specific shipping recommendations, in general, the ACI shipping guidelines are recommended. In particular, packaging, labeling, and shipping for thermosetting-resin materials are to be controlled by the *Code of Federal Regulations 49* (CFR 49), in which some FRP system materials may be classified as corrosive, flammable, or poisonous in subchapter C (CFR 49). As such, FRP system constituent materials are to be packaged and shipped in a manner that conforms to all applicable federal and state packaging and shipping codes and regulations. The following additional provisions are suggested:

It is the duty of the contractor and supplier to ensure that the packaging and shipping methods used do not negatively impact material properties and performance.

All FRP components must be shipped with their respective safety data sheets (SDSs).

All components of the FRP system are to be inspected upon delivery to the construction site, and the use of opened or damaged containers should only proceed with written authorization by the project engineer.

8.2.1.2 Storage

Although AASHTO provides no storage guidelines, ACI Article 5.2 offers the most complete coverage of storage and disposal of expired materials, and these provisions are recommended in general, with the following additional comments.

All FRP system components must be stored in the original factory-sealed, unopened packaging with labels identifying the manufacturer, brand name, system identification number, and date.

Proper storage of FRP components is in a clean, dry area, sheltered from direct sunlight, which is well ventilated and temperature controlled within 50−75°F (10−24°C). Catalysts and initiators (e.g., peroxides) should be stored separately.

As possible, components stored on the jobsite should be periodically inspected in accordance with the inspection checklist presented in Appendix C; components that have been stored in a condition different from that stated above are to be rejected.

Of particular concern are reactive curing agents, hardeners, initiators, catalysts, and cleaning solvents which have special safety-related requirements and are to be stored in securely sealed containers in a manner recommended by OSHA. As resins are also flammable, fire precautions should be observed and storage quantities kept within limits prescribed by fire regulations.

The manufacturer is to provide a recommended shelf life within which the properties of the resin-based materials should continue to meet or exceed the stated performance, and the contractor must follow these time limits.

Any component material that has exceeded its shelf life has deteriorated or has been damaged or otherwise contaminated should not be used. Care must be taken to avoid laminate and other preformed material damage due to bending or improper stacking. FRP materials deemed unusable should be disposed of in a manner acceptable to state and federal environmental control regulations.

8.2.1.3 Handling

ACI Article 5.3 provides the most complete coverage of safe handling of FRP materials as compared to other codes. ACI is therefore generally recommended for use, with the following additional comments.

Information regarding proper storage, handling, and mixing resin components and potential hazards should be made available at the construction site.

Product hazard labels and associated SDSs are to be read and understood by those working with these products. CFR 16, Part 1500 (2009), regulates the labeling of hazardous substances and includes thermosetting-resin materials. Such labeling guidelines should be followed.

Disposable suits and gloves resistant to resins and solvents should be used for handling fiber and resin materials, where gloves should be discarded after each use. Safety glasses or goggles should be used when handling resin components and solvents, and surfaces should be covered as needed to protect against contamination and resin spills.

Respiratory protection, such as dust masks or respirators, should be used when fiber fly, dust, or organic vapors are present, or during mixing and placing of resins. The workplace in which composite materials are prepared and installed should be well ventilated; in poorly ventilated areas, the use of respiratory protection with a fresh air supply is recommended.

Uncontrolled reactions, including fuming, fire, or violent boiling, may occur in containers holding a mixed mass of resin; therefore such containers should be monitored.

As cleanup can involve flammable solvents, appropriate safety precautions are suggested. All waste materials are to be disposed of as prescribed by the prevailing environmental authority.

It is the contractor's responsibility to ensure that all components of the FRP system at all stages of work conform to governing environmental and safety regulations.

All FRP components, but especially fiber sheets, must be handled with care to protect them from damage and to avoid misalignment or breakage of the fibers;

excessive bending, crushing and other sources of mechanical damage to the fibers must be avoided. Higher modulus fibers are particularly susceptible to such damage. After cutting, sheets should be either stacked dry with separators, or rolled gently at a radius no tighter than 12 in. (305 mm). Special care should be taken to avoid material contact with water, dust, or other contaminants.

8.2.2 Manufacturer and contractor qualification

For manufacturer and contractor qualification, AASHTO refers to NCHRP 609, which gives relatively comprehensive qualification requirements as compared to other sources. NCHRP 609 is thus recommended as a qualification guide, with the following summary of these recommendations, as well as additional comments.

FRP application must be performed by a contractor specifically trained in accordance with the installation procedures specified by the manufacturer. These procedures may differ from one system to another, and thus general knowledge of FRP installation is of itself not sufficient.

The proposed manufacturer may be prequalified for each FRP system to be installed, after providing the following information to a qualified engineer for review and consideration:

- System data sheets and SDS for all components of the FRP system;
- Documentation of a minimum of 5 years experience with the FRP system, or 25 documented similar field applications with acceptable reference letters from respective owners;
- Documentation of test data sets from an independent agency verifying the mechanical properties, aging, and environmental durability of the proposed FRP system, and;
- Documentation of the availability of a comprehensive hands-on training program for each FRP system that can be taken by the staff of the contractor/applicator.

The design engineer may further opt to require the manufacturer to provide samples of the components, as well as of the complete FRP system for in-house or independent testing prior to qualification.

The training program conducted by the manufacturer should provide hands-on experience with surface preparation and installation of the specific FRP system which is to be installed.

Additionally, it is recommended that:

The engineer may further opt to require that the contractor demonstrate competency by an actual demonstration of surface preparation and installation.

The contractor must provide a detailed statement of the method which will be used to install the composites as well as an assessment of the risks (failing to meet system performance requirements as well as health and construction hazards) involved. This should include discussion of the procedure which will be used to minimize these risks. The contractor should further provide description of a plan that will be used to maintain an environment on-site that is suitable for the successful use of structural adhesives. Note that many of these items are typical requirements for the contractor-submitted QC plan.

8.2.3 Installation

Most codes reviewed provided similar recommendations. Provisions provided by ACI are generally most complete and are recommended, with some additional provisions from AASHTO and other codes, as detailed below.

8.2.3.1 Temperature, humidity, and moisture considerations

Primers, saturating resins, and adhesives should generally not be applied to cold or frozen surfaces, which can affect bond as well as rate of curing, and the presence of frost or ice crystals may be detrimental to the bond between the FRP and the concrete. In particular, ambient air and concrete surface temperature should be 50°F (10°C) or more; the concrete surface temperature should be at least 5°F (3°C) higher than the actual dew point; and atmospheric relative humidity should be less than 85%. A noncontaminating heat source can be used to raise the ambient and surface temperatures during installation if needed.

During application of epoxy, work should be scheduled to avoid air and surface temperatures exceeding 90°F (32°C). If necessary, then the work should be supervised by a person experienced in applying epoxy under such conditions. Epoxy systems formulated for elevated temperatures are available and should be considered as well (see ACI 530R-93). It is also recommended not to install FRP when the concrete surface is heavily exposed to sunlight.

Adhesives should not be applied to damp or wet surfaces with surface humidity greater than 10%, unless they have been formulated for such applications. Substrate humidity can be evaluated with a mortar hygrometer or other quantitative means. Moreover, FRP systems should not be applied to concrete surfaces that are subject to condensation, moisture vapor transmission, or water ingression, unless such issues are clearly addressed by the system design and the resin systems are specifically formulated for use in such conditions. ACI Standard 503.4 (2003) provides additional moisture content requirements. Note that the transmission of moisture vapor from a concrete surface through the uncured resin materials typically appears as surface bubbles and can compromise the bond between the FRP system and the substrate. Condensation or other moisture on the resin surface before initial hardening, indicated by whitening, the area should be wiped with solvent or the effected portion of primer or smoothing agent removed with sandpaper.

8.2.3.2 Equipment

All equipment should be clean, in good operating condition, and accessible for inspection by the project engineer. Note that some FRP systems recommend or require specific equipment for application, such as resin impregnators, sprayers, lifting/positioning devices, and winding machines. The contractor is to have qualified personnel sufficiently trained to install and operate such system-specific equipment, such as by training and/or certification from the FRP system manufacturer, if available. All materials, and supplies, and personal protective equipment

should be available in sufficient quantities to allow safe construction continuity and quality assurance (QA).

8.2.3.3 Substrate repair

The surface on which the FRP system is to be applied should be free of loose and unsound materials; unfit existing conditions may require repair. The quality of the substrate can be checked with testing. Compressive strength should not be less than 2.2 ksi (15 N/mm^2), and the concrete surface must have a minimum tensile strength of 220 psi (1.5 MPa), as measured by a pull-off tension test in accordance with ASTM D4541 (2002). For concrete surfaces that require repair, general methods are provided in ACI 546R (2004) and ICRI 03730 (2008). However, the concrete surfaces must be repaired or reshaped in accordance with the original section.

Before any epoxy or putty-based products are applied for repair, and all contaminants that could interfere with the bond should be removed. The concrete surface preparation should be inspected and approved by the project engineer before such repairs. If cementitious materials are used for repair, they should be allowed to sufficiently cure (i.e., when it is expected to have reached its minimum specified compressive strength) before further surface preparation. If corrosion-related concrete deterioration is detected, the cause of the corrosion should be addressed, and the associated deterioration repaired before application of the FRP system.

To repair cracks, those wider than 0.010 in. (0.3 mm) should be pressure injected with epoxy before FRP installation, in accordance with ACI 224.1R (2007). Cracks of smaller width may require resin injection or sealing to prevent corrosion of existing reinforcement. ACI 224.1R (2007) provides additional crack-width limitations based on different exposure conditions.

If there is uncertainty in the best approach, a trial run of the surface preparation process should be conducted to determine an effective technique for the FRP system to be used, and approved by the project engineer.

8.2.3.4 Surface smoothness

For contact-critical applications such as confinement (i.e., those in which loss of bond between the concrete and FRP is not critical, but contact between the surfaces must be maintained), the surface preparation should guarantee a continuous contact between the concrete and the FRP confinement system. After repair (if needed) the concrete surface should be prepared to a minimum concrete surface profile (CSP) 3, as defined by ICRI surface profile chips, and localized out-of-plane variations, including form lines, should not exceed 1/32 in. (1 mm). Localized variations can be removed by grinding or can be smoothed over using resin-based epoxy if variations are small. It is best that epoxy materials are applied in thin layers to build up to the desired flatness. Bug holes and voids should be filled with resin-based putty.

Table 8.1 Maximum depth of depressions on the concrete surface

Type of FRP	Max. depth for length of 12 in. (0.3 m) (in.)	Max. depth for length of 80 in. (2.0 m) (in.)
Plates ≥ 0.04 in. (1.0 mm)	0.16 in. (4.0 mm)	0.40 in. (10.0 mm)
Plates < 0.04 in. (1.0 mm)	0.08 in. (2.0 mm)	0.24 in. (6.0 mm)
Sheets	0.08 in. (2.0 mm)	0.16 in. (4.0 mm)

However, before application of any fillers, the surface must be appropriately cleaned to ensure bond of the repair materials. The maximum size allowed for small depressions is shown in Table 8.1.

Rectangular cross-sections should have corners rounded to a minimum radius of at least 0.5−1.4 in. (13−35 mm). This applies for corners both horizontally and vertically oriented. Chamfered corners are not recommended as a substitute for rounded corners. Larger radii should be used if forming and bonding the FRP to the member corner becomes difficult, which may occur as the thickness and stiffness of the FRP material used increases. Rough corners should be smoothed with epoxy or putty. Inside corners and concave surfaces may be difficult for FRP application, may require special attention to ensure that bond is achieved between the FRP and the concrete.

8.2.3.5 Surface cleanliness

Before application of the FRP the concrete surface should be cleaned to remove any dust, laitance, oils, dirt, or any other bond-inhibiting material. Even new concrete should be cleaned to remove mold release agents and curing membranes.

Various cleaning techniques can be effective, including wet, dry, and vacuum-abrasive blasting; high-pressure washing, with or without emulsifying detergents, and using biocides (where necessary); steam cleaning alone or in conjunction with detergents; and, for smaller areas, mechanical wire brushing or surface grinding. However, the use of some impact methods such as needle gunning and bush hammering may be too aggressive and are to be carefully monitored, as they may cause microcracks and/or an irregular concrete texture.

Washing techniques may be ineffective in some cases and can simply spread contaminants further; surface cleanliness should be carefully checked. If solvent-based and sodium hydroxide-based products are used, they must be completely removed from the surface. Vacuum dry-blasting is recommended over “open” blasting, the former of which is safer for workers and the environment. After cleaning the surface should be protected from contamination prior to FRP installation if necessary. The concrete surface preparation should be inspected and approved by the project engineer before application of the FRP.

8.2.3.6 Resin mixing

Resin components should be mixed at the proper temperature, proportions and the appropriate time until there is a uniform and complete mixing of components that is free from trapped air. For accurate mix proportioning, prebatched quantities of resins and hardeners are recommended. As resin components are often contrasting colors, full mixing is usually achieved when color is uniform and streaks are eliminated; the mixed result should be visually inspected for this condition. Resin mixing should be in quantities sufficiently small to ensure that all mixed resin can be used within its pot life; adhesive remaining at the end of the specified pot life must be discarded. Strict adherence to the epoxy pot life and operating temperature range during installation is necessary to avoid negatively impacting the quality of installation. Correspondingly, advanced planning is crucial.

8.2.3.7 Application of FRP systems

All materials, including primer, putty, saturating resin, and fibers, should be part of the same system. If the use of primer is required of the FRP system, it should be uniformly applied to all surfaces of the concrete where the FRP system is to be placed. Primer should have sufficiently low viscosity to penetrate the surface of the concrete substrate. In particular, it is recommended that higher viscosity resins are limited to plates, and special care is taken to ensure full saturation of FRP fabrics. Once applied, the primer should be protected from dust, moisture, and other contaminants, and allowed to cure before applying the FRP. It should be checked visually and by touch to make sure it is cured and that there is no dust or moisture on the surface.

For FRP installation, a working diagram matching the actual structure should be prepared based on the design. The diagram should clearly identify the reference point for attachment, the overlap splice positions, and the number of plies to be attached.

For wet layup systems, which are typically installed by hand using dry fiber sheets and a saturating resin, the resin should be applied uniformly to all prepared concrete surfaces where the system is to be placed, then the reinforcing fibers gently pressed into the resin. Note that dry fabrics can be directly applied to the resin-saturated concrete surface without adhesive being applied to the fabric, but for wet fabric systems, the resin must be applied to the fabric before it is installed. Resin with sufficient quantity and sufficiently low viscosity should be applied to achieve full saturation of the fibers. A handheld foam roller or brush can be used to apply the bonding adhesive to the concrete surface or resin, as required; an impregnation machine can also be used to apply resin to the fabric for wet fabric systems. Entrapped air between layers should then be released or rolled out before the resin sets. In doing so, it is recommended to work the FRP materials parallel to the fibers, proceeding in one direction from the center or from one extremity and to avoid any backward and forward movements. After attaching the continuous

fiber sheets, an inspection should be done visually or through sounding to verify the absence of lift, swelling, peeling, slackness, wrinkles, and voids in the epoxy resin impregnation.

When using precured systems such as surface bonded plates, the precured-laminate surfaces to be bonded should be properly prepared. This may involve application of light abrasion and cleaning. No additional treatment is required for materials with an additional peel ply which, upon removal, exposes a clean surface with the appropriate roughness. The mixed adhesive is then to be applied to the concrete bonding area by hand, using plastering techniques. The thickness of the adhesive should be maintained from 0.04 to 0.08 in. (1−2 mm). The adhesive layer should be applied to the plates to form a slightly convex profile across the plate. Extra thickness along the center-line helps to reduce the risk of void formation. Stacking multiple layers of FRP plate is usually not permitted, except for the overlapping portion of prefabricated L-shaped stirrups. At intersections of FRP plates, care should be exercised to minimize curvature; grooving the concrete for the layer underneath is sometimes used to allow full contact between the plate and the concrete surface.

A protective finish compatible with the proposed system that provides ultraviolet light protection should be applied when the surface of the FRP material has sufficiently cured and has been cleaned. Alternatively, protection can be achieved by applying a plaster or mortar layer (preferably concrete based) to the installed system. The protective coating may include a wearing layer for protection against abrasive conditions as well, but such a layer is not to be considered as structural reinforcement.

If required for fire protection, intumescent panels or the application of protective plasters may be used. In both cases, the degree of fire protection provided is to be specified, as a function of the panel/plaster thickness. The panels, generally based on calcium silicates, are to be applied directly on the FRP system, provided that fibers will not be cut during their installation. The protection system proposed must be approved by the engineer.

The contractor is to provide a certificate of compatibility of the protective system and the FRP system, prepared by the manufacturer, and the contractor is to provide a guarantee for the performance of the proposed protection system for the expected exposure conditions. Once applied, a minimum of 24 h should be allowed for the protective coating to dry.

When FRP material is used to wrap the base of a reinforced concrete column that is in contact with the ground, the wrapping should extend a minimum of 20 in. (500 mm) below the ground surface to prevent water and air infiltration.

When using continuous fiber strands, the use of a machine to wind the strands, to control the winding interval, tension, and speed, is recommended. In this case, it must be verified that the strand winding interval is appropriate, the strand winding tension is constant, the strand winding speed is appropriate, the strands are thoroughly impregnated with resin, the resin has been suitably mixed and applied, and that the impregnation resin is cured thoroughly.

If the carbon fiber is used and there is a potential for direct contact between the carbon and existing steel reinforcement, insulating material should be installed to prevent galvanic corrosion.

8.2.3.8 Alignment

The ply orientation and stacking sequence must be specified in the design prior to installation. Materials should be handled such that correct fiber straightness and orientation are preserved. Moreover, kinks, folds, waviness, or other forms of substantial material malformation must be reported for evaluation, as well as angle deviations greater than 5 degrees.

8.2.3.9 Multiple plies and lap splices

When multiple plies are used, it must be verified the resin shear strength is sufficient to transfer the shearing load between plies, and the bond strength between the concrete and FRP system is sufficient. The former can be verified with representative specimen test results (i.e., shear or flexure) provided by the manufacturer/installer. However, the project engineer may limit the maximum number of consecutive layers allowed, and/or restrict the installation period between successive layers. When several superposed layers are used, care must be taken not to move or otherwise disturb the preceding layers where the resin has not set. If an interruption of the FRP system layup process occurs, interlayer surface preparation such as cleaning or light sanding may be required. All plies must be fully impregnated with resin.

Lap splices may be used, provided that they are staggered, unless otherwise approved by the project engineer. Lap splice details, including required lap length, should be based on testing. Specific guidelines on lap splices are given in ACI Chapter 13. In the absence of manufacturer requirements, a minimum lap splice length of 8 in. (200 mm) is recommended. If only one layer of FRP sheet is used within a lap or splice, it is recommended to elongate the overlap splice length and to attach one more layer of FRP over the splice section. When more than one layer is used, the overlap splices should not be placed at the same section, since this reduces the overlap splice strength. Overlap splices should not be placed at locations subjected to large bending moments.

8.2.3.10 Curing

Ambient-cure resins may take several days to reach full cure, and temperature fluctuations can retard or accelerate curing time. The cure status of installed plies should be verified to be sufficient before placing subsequent plies, and the installation of successive layers should be halted if there is a curing anomaly. Successive layers of saturating resin and fibers should be placed before the complete cure of the previous layer; if previous layers have cured to an advanced degree, interlayer surface preparation, such as light sanding or solvent application, may be required.

A minimum curing time of 24 h should be allowed before further work is performed, unless the curing process is accelerated by heating. For the entire curing duration the temperature must be maintained above the minimum required curing temperature; condensation on the surface must be prevented; and chemical contamination from gases, dust or liquid sprays must be prevented. Mechanical stresses on the FRP should be minimized during curing. Before the initial setting of the impregnation resin the surface should be protected with vinyl sheets from rain, dust, excessive sunlight, high humidity, and sudden climatic changes, as necessary. If temporary shoring is used, the FRP system should be fully cured before the shoring is removed.

8.2.4 Inspection

The completeness and quality of inspection procedures for different stages of work vary among the standards reviewed. ISIS inspection procedures are in general recommended to help assess the exiting concrete surface condition and determine the repair method needed, if any. The ISIS inspection procedure to verify the quality of the concrete surface repair prior to FRP application is also recommended. AASHTO and ACI have similar inspection procedures to monitor the quality of the FRP installation. These procedures are reasonably detailed and discuss documentation, sample collection, the use of witness panels, and applicable testing. The AASHTO procedures are ultimately recommended for this purpose. Finally the inspection procedure to be used at the completion of the installation as presented by ISIS is recommended, due to its comparative completeness. A summary of these recommended provisions, with additional suggestions, is provided below.

Inspection should be conducted by or under the supervision of the project engineer or a qualified inspector knowledgeable of FRP systems and installation procedures. In general the inspector should look for compliance with the design drawings and project specifications, with details discussed below.

Note that two types of specifications are feasible: descriptive or performance. In a descriptive-focused specification, the engineer specifies the length, width, orientation, installation sequence, and other requirements of a particular, selected FRP material, and perhaps acceptable equivalents. In a performance-focused specification the engineer specifies requirements in terms of strength, stiffness, or other necessary properties and characteristics, and the contractor is responsible for selecting an appropriate FRP system and submitting it for approval. Either type of specification is acceptable, provided that sufficient quantitative analysis and/or test data is provided to demonstrate that the required performance requirements will be met with the proposed strengthening plan.

The time and effort spent on the inspection is expected to reasonably correlate with the importance level of the structure, as well as the size and complexity of the strengthening scheme. Also of consideration is how critical is the consequence of nonsatisfactory system performance. Moreover, the extent of the inspection may be influenced in part by what is initially uncovered. For example, the identification

of one or several flaws in the beginning of the inspection phase, or of a systematic error in application, should lead to a more detailed and extensive scrutiny of the system.

However, this is not to suggest that some structures are to be inspected more casually than others. Rather, some strengthening schemes, by nature of their construction, will inherently require more inspection effort. For example, Section 8.2.4.4 (see below) recommends that the number of witness panels constructed varies with the size of the strengthened area. In any case the extent of the planned inspection effort should be influenced by the factors noted in the paragraphs above.

8.2.4.1 Quality assurance and control program

FRP material suppliers, installation contractors, and other relevant parties associated with the FRP strengthening project are to maintain and submit for review a comprehensive quality assurance (QA) and QC program. QA is achieved through a set of inspections, measurements, and applicable tests to document the acceptability of the surface preparation and the installation of FRP, and the QC should cover all aspects of the strengthening project and will depend on the size and complexity of the project.

All materials used should be manufactured under an approved quality scheme (for example, such as ISO 9000), and conform to a relevant specification or international standard. In addition, the traceability of all materials should be ensured. All external or independent testing to determine material properties should be carried out in approved laboratories in accordance with relevant standards or by the manufacturer under an approved quality scheme. The types and frequency of testing should be stated in the quality plan. A minimum of one sample should be taken at the start and finish of each production run.

8.2.4.2 Material inspection

The FRP manufacturer is to provide documentation demonstrating that the proposed system meets all design requirements such as (but not limited to) tensile strength, type of fibers and resin, durability, resistance to creep, bonding to substrate, and glass transition temperature. Independent test results, performed according to the QC test plan for the FRP constituent materials and laminates, are required. Test results may include parameters such as tensile strength, glass transition temperature, gel time, pot life, as well as the adhesive shear strength. Note this last value is needed to apply the environmental reduction factors recommended in Section 8.1.3.1.

When material is first received, the FRP, primer, smoothing agent, impregnation resin, and other materials should be inspected for quality and damage. Inspection of materials should be done in accordance with the quality assurance sheet, test results, or other relevant documents issued by the manufacturer. If the materials have suffered damage during shipment, storage at the site, or during construction, they should be rejected or tested to confirm quality.

When received from the supplier, all materials should be accompanied by a certificate of identification and conformity to appropriate standards. Accurate records should be maintained of all materials used (e.g., delivery notes, batch numbers) and, when required, the ambient conditions (e.g., temperature, relative humidity). Visual checks should be carried out to ensure that the material is as specified.

The storage condition of the materials is to be inspected as well, as discussed earlier in these recommendations.

8.2.4.3 Inspection of concrete substrate

The concrete surface should be inspected and tested before application of the FRP material. The inspection should include an examination for completeness of restoration work, processing of corner angles, primer coating, surface smoothness, protuberances, holes, cracks, corners, and other imperfections and characteristics. Pull-off tests should be performed to determine the tensile strength of the concrete for bond-critical applications, as discussed earlier in these recommendations. The degree of surface dryness, including the potential for condensation, should be verified in accordance with the criteria established by the FRP manufacturer.

8.2.4.4 Inspections during installation

During construction, special care should be taken to keep all records on the quantity of mixed resin during a 1-day period, the date and time of mixing, the mixture proportions, and identification of all components, ambient temperature, humidity, and other factors that may affect resin properties. These records should also identify the FRP sheets used each day, their location on the structure, the ply count and direction of application, and all other relevant information. This information is useful even if witness panels are tested for acceptance. This is because it is possible that witness panel tests may be found satisfactory even though the manufacturer's requirements for installation are not met. Such a finding may suggest the possibility of long-term durability problems with the installation, even though the initial quality appears satisfactory.

As specified by the project engineer, witness panels are to be manufactured on-site and applied on equivalent concrete surfaces using the same preparation and installation procedures as used on the structure. Ideally the witness areas are in the form of additional strengthening areas applied on the actual structure of size of at least 2−5 ft.^{2}, but not less than 0.5% of the overall area to be strengthened. Witness areas are to be strengthened at the same time of the main FRP installation and are as uniformly distributed on the structure as possible. The panels are to be kept under the same conditions as the strengthened structure for future testing and evaluation, and fabricated and tested according to a predetermined sampling plan. It is generally recommended that at least some witness panels are constructed for all strengthening installations.

During the installation of the FRP system, daily inspection should be conducted and should note, as applicable:

- Date and time of installation;
- Ambient temperature, relative humidity, and general weather observations;
- Surface temperature of concrete;
- Surface dryness per ACI 503.4 (2003);
- Surface preparation methods and resulting profile using the ICRI-surface-profile-chips;
- Qualitative description of surface cleanliness;
- Type of auxiliary heat source, if applicable;
- Widths of cracks not injected with epoxy;
- Fiber or precured laminate batch number(s) and approximate location in structure;
- Batch numbers, mixture ratios, mixing times, and qualitative descriptions of the appearance of all mixed resins, including primers, putties, saturants, adhesives, and coatings mixed for the day;
- Observations of progress of resin cure;
- Conformance with installation procedures;
- Pull-off test results: bond strength, failure mode, and location;
- FRP properties from tests of field sample panels or witness panels, if required;
- Location and size of any delaminations or air voids;
- General progress of work;
- Level of resin curing, in accordance with ASTM D2582 (2009); and
- Adhesion strength.

The FRP system should be further inspected with particular attention to attachment position, orientation and alignment, laminate thickness, waviness, lifting, peeling, slackness, wrinkles, overlap splice length, number of plies, and quantity of the resin coating. If wound on site, FRP strands are to be inspected for winding position, winding interval, winding tension and winding speed, and that fibers are thoroughly impregnated with resin.

8.2.4.5 Project completion

At project completion, a record of all inspections and test results related to the project should be retained. It should include a summary assessment of any problems identified and repairs, on-site bond tests, anomalies, as well as all test results from designated testing facilities.

8.2.5 Evaluation and acceptance

Evaluation is covered thoroughly in ACI Article 7.2 (see Chapter 4 of this book), while Chapter 14 of ACI discusses specification requirements and submittals required by the contractor. FRP sample specification requirements are also provided in NCHRP 609, which expand on the requirements stated in Chapter 14 of ACI. AASHTO covers acceptance criteria scope and detail well. Thus the evaluation procedures presented by ACI and acceptance criteria presented by AASHTO, supplemented with NCHRP 609, together offer a thorough, compatible, and complementary

treatments of this topic and are recommended. These procedures, together with additional suggestions from other standards, are summarized below.

FRP systems should be evaluated and accepted or rejected based on conformance to the design drawings and specifications. In general, items that were inspected require evaluation. A summary of most critical issues is given below.

8.2.5.1 Materials

As noted earlier in the recommendations, for evaluation and acceptance, the contractor is required to submit evidence of acceptable QC FRP system manufacturing procedures. This should at least include the specifications for raw material procurement, quality standards for the final product, in-process inspection and control procedures, test methods, sampling plans, criteria for acceptance or rejection, and record keeping standards. Some acceptable test results are given later in this section. For those not specified, including material and bond properties, unless the project engineer has reason to specify otherwise, no additional specific limitations are recommended, provided that the required design values are met.

The contractor also must provide information describing the fiber, matrix, and adhesive systems to be used that is sufficient to define their engineering properties. Descriptions of the fiber system should include the fiber type, percent of fiber orientation in each direction, and fiber surface treatments. The matrix and the adhesive should be identified by their commercial names and the commercial names of each of their components, along with their weight fractions with respect to the resin system.

Further, the contractor is to submit test results that demonstrate that constituent materials and the composite system are in conformance with the physical and mechanical property values stipulated by the engineer. These tests are to be conducted by a testing laboratory approved by the engineer. For each property value, the batches from which test specimens were drawn are to be identified and the number of tested specimens from each batch, and the mean, minimum, and maximum value, as well as the coefficient of variation, must be reported. The minimum number of tested samples is 10. In accordance with the QC test plan, test results may include tensile strength, elastic modulus, an infrared spectrum analysis, glass transition temperature, gel time, pot life, and adhesive shear strength, among other parameters relevant to the project. Tensile testing should follow a standard procedure, such as that described by ASTM D3039 (2008).

For FRP systems such as precured and machine-wound systems, that do not lend themselves to the fabrication of small, flat witness panels, the engineer can require test panels or samples provided by the manufacturer.

For bond-critical applications, tension adhesion testing of cored samples (on the structure, after installation) should be conducted using a standard method such as that described in ACI 530R (2005), ASTM D4541 (2002), ASTM D7234 (2012), or the method described by ACI 440.3R (2004), Test Method L.1. Successful tension adhesion strengths should exceed 200 psi (1.4 MPa) and exhibit failure of the concrete substrate. Lower strengths or failure between the FRP system and concrete

or between plies should be reported to the engineer. Care should be taken to avoid coring in high stress or splice areas. The tested areas must be repaired unless they are located in areas where the FRP is unstressed. As noted above, sampling frequency may be influenced by the size, complexity, and importance of the project, among other factors.

In-place load testing can also be used to confirm the installed behavior of the FRP-strengthened member. For major structures, it may be appropriate to install instrumentation prior to the strengthening to assess the structural response before and after strengthening.

Once the above information is gathered, the composite material system as well as the adhesive system are to be evaluated for conformance to the requirements that follow. It is assumed that the test specimens were cured under conditions equivalent to those during installation. Ideally, these tests are performed on witness panel samples created for all strengthening projects. However, if the project engineer approves, previous test results of an identical FRP system may be considered for evaluation.

1. The characteristic value of the glass transition temperature of the composite system, determined in accordance with ASTM D4065 (2012), should be at least 40°F higher than the maximum design temperature, defined in Section 3.12.2.2 of the *AASHTO LRFD Bridge Design Specifications* (2012). The characteristic value of the tensile failure strain in the direction corresponding to the highest percentage of fibers must not be less than 1% if the tension test is conducted according to ASTM 3039 (2008).
2. The mean and coefficient of variation of the moisture equilibrium content, as determined in accordance with ASTM D 5229/D 5229M (2010), must not be greater than 2 and 10%, respectively. A minimum sample size of 10 should be used to calculate these values.
3. After conditioning in the various environments listed below, the characteristic value of the glass transition temperature, determined in accordance with ASTM D4065 (2012), and that of tensile strain, determined in accordance with ASTM D3039 (2008), of the composite in the direction of interest, is to retain 85% of the required values given in item (1), above. The conditioning environments are as follows:
   a. Water: Samples shall be immersed in distilled water having a temperature of 100 ± 3°F (38 ± 2°C) and tested after 1000 h of exposure.
   b. Alternating ultraviolet light and condensation humidity: Samples shall be conditioned in an apparatus under Cycle 1-UV exposure condition according to ASTM G154 (2012) Standard Practice. Samples shall be tested within 2 h after removal from the apparatus.
   c. Alkali: The sample shall be immersed in a saturated solution of calcium hydroxide (pH $\sim$11) at ambient temperature of 73 ± 3°F (23 ± 2°C) for 1000 h prior to testing. The pH level shall be monitored and the solution shall be maintained as needed.
   d. Freeze–thaw: Composite samples shall be exposed to 100 repeated cycles of freezing and thawing in an apparatus meeting the requirements of ASTM C666 (2008).
4. If impact tolerance is stipulated by the engineer, impact tolerance should be determined according to ASTM D7136 (2007).
5. When adhesive material is used to bond the FRP reinforcement to the concrete surface, the following requirements are to be met:
   a. After conditioning in the environments noted in item (3), the characteristic value of the glass transition temperature of the adhesive material, determined in accordance with ASTM D 4065 (2012), must be at least 40°F higher than the maximum

design temperature as defined in Section 3.12.2.2 of AASHTO LRFD Bridge Design Specifications (2012).

b. Before conditioning, the concrete−FRP interface (resin) shear strength is to be at least $(0.065\sqrt{f'_c})/RF$, where RF is the reduction factor given in Section 8.1.3.1 of this chapter, for the anticipated number of design years (f'_c in ksi). After conditioning, the bond strength as well as the concrete−FRP interface (resin) shear strength are to be at least $0.065\sqrt{f'_c}$ (ksi).

If specified in the project, for verification of fire safety, a test specimen with the same protective coating as the actual structure should be manufactured and subjected to combustion tests. During the combustion test, ignition, the generation of gases, harmful surface deformation, and changes in the quality and strength of the FRP and laminates after the fire are to be studied according to the level of fire safety required.

8.2.5.2 Cure

The relative cure of FRP systems can be evaluated by laboratory testing of witness panels or resin-cup samples using ASTM D3418 (2003) and ASTM D2583 (2007). The relative cure of the resin can also be evaluated on the project site by physical observation of resin tackiness and hardness of work surfaces or retained resin samples. The FRP system manufacturer should be consulted to determine the specific resin-cure verification requirements.

It should be evaluated whether moisture will collect at the bond lines between the concrete and epoxy adhesive before the epoxy has time to cure. This may be checked by taping a 4×4 ft. (1×1 m) polyethylene sheet to the concrete surface. If moisture collects on the underside of the sheet before the time required to cure the epoxy, then before application of the adhesive, the concrete should be allowed to dry sufficiently to prevent the possibility of a moisture barrier forming between the concrete and epoxy per ACI 530R-05 (2005).

8.2.5.3 Orientation, placement, and thickness

Installation within specified placement tolerances including width and spacing, corner radii, and lap splice lengths should be evaluated, as well as fiber and precured-laminate orientation and waviness. Misalignment of more than 5 degrees (approximately 1 in/ft. [80 mm/m]) from that specified is generally not acceptable without further evaluation, and should be reported to the project engineer.

Cured thickness and/or number of plies used should be verified. Small core samples, typically 0.5 in. (13 mm) in diameter, may be taken to visually ascertain the cured laminate thickness or number of plies; however, taking samples from high stress or splice areas should be avoided. These cores may be those used for adhesion testing. The cored hole can generally be filled and smoothed with a repair mortar or the FRP system putty. However, if required, a 4−8 in. (100−200 mm) overlapping FRP sheet patch of equivalent plies may be applied over the filled and smoothed core hole immediately after taking the core sample.

8.2.5.4 Delamination

The cured FRP system should be evaluated for delaminations or air voids between multiple plies or between the FRP system and the concrete. Inspection methods should be capable of detecting delaminations as small as 2 in.^{2} (1300 mm^2) and may include acoustic sounding (hammer sounding), ultrasonics, and thermography. Delamination size, location, and quantity relative to the overall application area should be considered in the evaluation. For wet layup systems, the need for delamination repair depends on the size and number of delaminations. Small delaminations less than 2 in.^{2} (1300 mm^2) are permissible as long as the delaminated area is less than 5% of the total laminate area and there are no more than 10 such delaminations per 10 ft.^{2} (1 m^2). Delaminations exceeding these limits are to be repaired by either resin injection or ply replacement, depending on delamination size. Large delaminations, greater than 25 in.^{2} (16,000 mm^2), should be repaired by selectively cutting away the affected sheet and applying an overlapping sheet patch of equivalent plies with appropriate overlap length. Delaminations less than 25 in.^{2} (16,000 mm^2) may be repaired by either resin injection or ply replacement. For precured FRP systems, each delamination should be evaluated and repaired in accordance with the instructions of the engineer. Upon completion of repairs, the laminate should be reinspected to verify that the repair was properly accomplished.

8.2.6 Maintenance and repair

A maintenance program involves periodic inspection and testing to identify any damage, degradation, or deficiencies to the FRP strengthening system and to make any necessary repairs. A maintenance assessment is made from test data as well as observations and may include recommendations to help slow down degradation and propose repairs.

AASHTO provides a comprehensive reference list of ACI, NCHRP, and International Concrete Repair Institute (ICRI) documents dealing with the necessary evaluation criteria for repair as well as postrepair evaluation. ACI is one of the listed references which offers a brief, but concise account of inspection and assessment, repair of the strengthening system, and repair of surface coatings (ACI Chapter 8). JSCE Article 9.3 offers some coverage of repair techniques as well (see Chapter 5.2.3). As ACI Chapter 8 is also implicitly included in AASHTO, this, in addition to some of the provisions given by JSCE Article 9.3 for repair techniques (Chapter 5.2.3 of this book) are generally recommended, with a summary of these provisions and additional suggestions given below.

8.2.6.1 Maintenance inspections

To verify the long-term performance of the FRP system, a general inspection is recommended at least once a year, while a detailed inspection is recommended at least once every 6 years.

A general (visual) inspection primarily consists of a surface inspection. The inspector looks for changes in color, signs of crazing, cracking, delamination/debonding, peeling, blistering, deflection, or evidence of other deterioration, in addition to local damage due to impact or surface abrasion and other damage and anomalies. Signs of concrete deterioration in the form of cracking or steel reinforcement corrosion should also be reported. The condition of the FRP protective layer, if any, should also be inspected.

Other inspection methods such as ultrasonic, acoustic sounding (hammer tap), or thermographic tests should be used to identify signs of progressive delamination. Although acoustic sounding is recommended for a general inspection, more accurate, and time-consuming techniques may be reserved for a detailed inspection.

A detailed inspection should attempt to more accurately quantify the performance and condition of the FRP system. Most signs of FRP degradation, including debonding, can be determined with the test methods noted above. However, adhesive bond strength must be evaluated by puIl-off tests on the control specimens and should be carried out as part of a detailed inspection. As noted earlier in these recommendations, to quantify the performance of the FRP strengthening system during inspection, and in particular, bond strength, it is recommended that additional areas of the strengthened structure, away from the regions that were strengthened, are also bonded with the FRP system for future testing at the time of installation. Alternatively, FRP can be bonded to long-term witness panels that are stored near the structure, to be inspected and tested as part of the inspection regime.

8.2.6.2 Repair

The causes of any damage or deficiencies detected during inspections should be identified and addressed before performing any repairs or maintenance.

The method of repair should depend on the cause of damage, the type of material, the form of degradation, and the level of damage. Even minor damage should be repaired, including localized FRP laminate cracking or abrasions that may affect the structural integrity of the laminate.

For cracking, wearing, and abrasion, patching should be used. Here, FRP patches are bonded over the damaged area. The FRP patches should possess the same characteristics as the material in place, such as fiber orientation, volume fraction, strength, stiffness, and overall thickness. Minor delaminations over small areas that include swelling, peeling, and lifting can be repaired by resin injection.

For major damage, such as peeling and debonding of large areas, the defective material should be removed to an extent that material on the periphery of the repair is fully bonded. There is little information available about effective methods of FRP removal. However, a technique that has been successfully used involves first cutting the FRP fabric into pieces of manageable size with an appropriate tool such as an angle grinder, then peeling the sheets from the concrete surface with a crowbar or similar prying tools. Since the adhesion strength of the resin is often greater than that of the concrete surface itself, the concrete surface may peel off

with the FRP sheet. This will then require repair of the substrate and resmoothing the surface, as described in Sections 8.2.3.3 and 8.2.3.4. An FRP patch can then be installed that allows for adequate overlap between the new and old materials. The use of chemicals to facilitate FRP sheet removal which may penetrate and damage the concrete surface is not recommended, as the extent of such damage may be difficult to detect and this may cause future bond problems. Due to the lack of standard procedures guiding FRP removal, it is recommended that the contractor submit his plan for FRP removal to the project engineer for approval.

When serious deterioration or deterioration over a wide area is observed, additional FRP upgrading should be performed. In such cases the existing FRP should be removed and the upgrading plan reexamined.

If the surface protective coating is to be replaced, the FRP should be further inspected for structural damage or deterioration once the coating is removed.

Specific repair techniques for concrete are well-documented. The following additional guides are recommended for identifying and repairing such damage:

- *NCHRP Report 609: Recommended Construction Specifications Process Control Manual for Repair and Retrofit of Concrete Structures Using Bonded FRP Composites*;
- *ACI 201.1R: Guide for Making a Condition Survey of Concrete in Service*;
- *ACI 224.1R: Causes, Evaluation, and Repair of Cracks in Concrete*;
- *ACI 364.1R-94: Guide for Evaluation of Concrete Structures Prior to Rehabilitation*;
- *ACI 503R: Use of Epoxy Compounds with Concrete*;
- *ACI 546R: Concrete Repair Guide*;
- *International Concrete Repair Institute (ICRI) ICRI 03730: Guide for Surface Preparation for the Repair of Deteriorated Concrete Resulting from Reinforcing Steel Corrosion*;
- *International Concrete Repair Institute (ICRI) ICRI 03733: Guide for Selecting and Specifying Materials for Repairs of Concrete Surfaces.*

Design examples

9

9.1 Introduction

In this chapter, six examples are provided to illustrate the design procedures recommended in Chapter 8, Recommendations (see Section 8.1.3): four consider beams and two consider columns. Two additional examples of the American Concrete Institute (ACI) procedure for strengthening columns are provided for comparison. The examples below assume that the strengthened structure is within the State of Michigan. This becomes important only because the maximum design temperature (based on the location of the structure) must be known in order to determine the adequacy of the glass transition temperature of the epoxy used in the fiber-reinforced polymer (FRP) system. Within the examples, reference is made to various documents using the following abbreviations:

AASHTO: *AASHTO Guide Specifications for Design of Bonded FRP Systems for Repair and Strengthening of Concrete Bridge Elements, 1st Ed.* (2014).
LRFD: AASHTO LRFD Bridge Design Specifications (2012).
NCHRP: *NCHRP Report No. 655 (2010).*
ACI: *440.2R, Guide for the Design and Construction of Externally Bonded FRP Systems (2008).*

List of examples

Example 1: Flexural strengthening of a reinforced concrete girder (modified AASHTO).
Example 2: Flexural strengthening of prestressed concrete girder (modified AASHTO).
Example 3: Shear strengthening with two-sided wrap (AASHTO).
Example 4: Shear strengthening with U-wrap (AASHTO).
Example 5: Axial strengthening of a confined circular column (AASHTO).
Example 6: Axial strengthening of a confined square column (AASHTO).
Example 7: Axial strengthening of a confined circular column (ACI).
Example 8: Axial strengthening of a confined square column (ACI).

9.1.1 Flexural strengthening of a simply supported cast in-place reinforced concrete girder

This example illustrates the flexural strengthening of a reinforced concrete T-beam with an externally bonded carbon FRP (CFRP) system to accommodate higher loading.

Strengthening of Concrete Structures Using Fiber Reinforced Polymers (FRP).
DOI: http://dx.doi.org/10.1016/B978-0-08-100636-8.00009-0

Structure information:
Bridge span = 55 ft.
Concrete compression strength, $f'_c = 4$ ksi
Reinforcing steel yield strength, $f_y = 60$ ksi
Steel reinforcement = 10 #10 ($A_s = 12.70$ in.^{2})
Effective flange width, $b_{\text{eff}} = 72$ in. (Fig. 9.1)
Ultimate tensile strain in the FRP reinforcement, $\varepsilon_{frp}^{tu} = 0.0167$
Strength in the FRP reinforcement at 1.67% strain, $P_{frp} = 3.57$ kips/in.
Shear modulus of the adhesive, $G_a = 160$ ksi
Glass transition temperature = 165°F
New nominal loads for strength I limit state: $M_{DC} = 540$ kip-ft, $M_{DW} = 50$ kip-ft, $M_{L+\text{I}} = 1075$ kip-ft
New nominal loads for fatigue limit state: $M_{L+\text{I}} = 550$ kip-ft
Factored shear force at the reinforcement end-termination, $V_u = 150$ kips.
Step 1:
Determine if the FRP reinforcement material is in compliance with AASHTO Section 2.2.4.1, which specifies that the glass transition temperature must be higher than the maximum design temperature by 40°F. The maximum design temperature, $T_{\text{Max Design}}$, is determined from Article 3.12.2.2 of load and resistance factor design (LRFD) for the location of the bridge (Michigan):

$$T_{\text{Max Design}} = 105^\circ\text{F}$$
$$T_{\text{Max Design}} + 40^\circ\text{F} = 105^\circ\text{F} + 40^\circ\text{F} = 145^\circ\text{F} < T_g = 165^\circ F$$

Step 2:
Establish the linear stress−strain relationship of the FRP reinforcement based on the design assumptions specified in Article 3.2 of AASHTO and compute the tensile strength according to a strain value of 0.005.

$$N_b = \frac{0.005}{0.0167}(3.57) = 1.07 \text{ kip/in.}$$

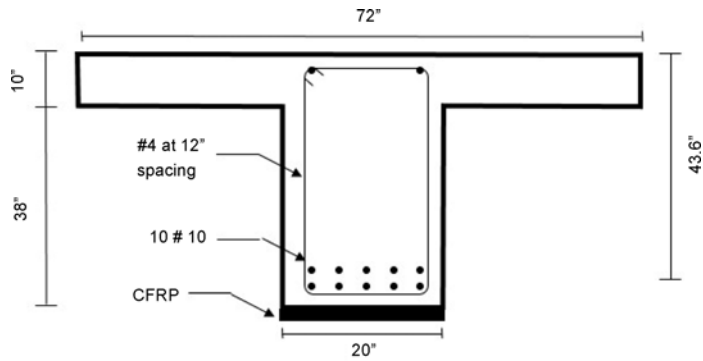

Figure 9.1 RC beam section.

Step 3:

Neglecting the possible contribution of steel in the compression zone to flexure strength, the depth of the concrete compressive stress block is

$$a = \frac{A_s f_y}{0.85 f'_c\, be} = \frac{12.7 \times 60}{0.85 \times 4 \times 72} = 3.11 \text{ in.}$$

Since $a < h_f = 10$ in., the stress block is within the flange and calculation is correct.

The depth of neutral axis $c = (a/\beta 1) = (3.11/0.85) = 3.66$ in.

Strain in the tension steel is

$$\frac{\varepsilon_s}{0.003} = \frac{d - c}{c}$$

$$\varepsilon_s = \frac{43.6 - 3.66}{3.66} \times 0.003 = 0.033$$

Since $\varepsilon_s = 0.033 > (f_y/E_s) = \dfrac{60}{29,000} = 0.0021$, the assumption that the tension steel yielded is correct.

$$M_n = A_s f_y \left(d - \frac{a}{2}\right)$$

$$M_n = 12.70 \times 60 \left(43.6 - \frac{3.11}{2}\right) = 32,038 \text{ kip-in.}$$

Since $\varepsilon_t \geq 0.005$, $\phi = 0.9$.

$$\phi M_n = 0.9 \times 32,038 \text{ kips-in.} = 28,834 \text{ kip-in.} = 2403 \text{ kip-ft.}$$

Step 4:

Determine if the existing beam requires strengthening.

The factored moment for the Strength I limit state is

$$M_u = 1.25\, M_{DC} + 1.5\, M_{DW} + 1.75\, M_{L+I} = 1.25 \times 540 + 1.5 \times 50 + 1.75 \times 1075 = 2631 \text{ kip-ft.}$$

Since $\phi M_n < M_u$, the beam requires strengthening.

Step 5:

For a preliminary estimate of the amount of FRP reinforcement necessary, the following approximation is used:

$$\text{Tension force required of FRP, } T_{frp} \approx \frac{M_u - \phi M_n}{h} = \frac{(2631 - 2403) \times 12}{48} = 57 \text{ kips}$$

$$\text{Number of layers of FRP required, } n = \frac{T_{frp}}{N_b b_{frp}} = \frac{57}{1.07 \times 18} = 2.96$$

Try three layers, for which $T_{frp} = n \times N_b \times b_{frp} = 3 \times 1.07 \times 18 = 57.7$ kips

Step 6:

Compute the factored flexural resistance of the strengthened T-beam.

By trial and error, the depth of the neutral axis can be determined from strain compatibility and force equilibrium.

Guess $c = 7.36$ in.

Strain in concrete

$$\varepsilon_c = \frac{c}{h-c}\varepsilon_{frp}^{u} = \frac{7.36}{48-7.36} \times 0.005 = 9 \times 10^{-4}$$

where 0.005 is the assumed FRP limiting strain.

Modulus of concrete

$$E_c = 57\sqrt{f'_c} = 57\sqrt{4000} = 3605 \text{ ksi}$$

Since $\varepsilon_c < 0.003$, use the parabolic concrete stress block model:

$$\varepsilon_0 = \frac{1.71 \times f'_c}{E_c} = \frac{1.71 \times 4}{3605} = 0.0019 \qquad \text{(NCHRP 3.2)}$$

$$\frac{\varepsilon_c}{\varepsilon_0} = \frac{9 \times 10^{-4}}{0.0019} = 0.48$$

$$\beta_2 = \frac{\text{Ln}\left[1 + (\varepsilon_c/\varepsilon_0)^2\right]}{(\varepsilon_c/\varepsilon_0)} = \frac{\text{Ln}\left[1 + (0.48)^2\right]}{0.48} = 0.43 \qquad \text{(NCHRP 3.3)}$$

In general, when $\varepsilon_c < 0.003$, the force in the concrete compression block is most accurately determined by integrating the nonlinear concrete stress curve as given by AASHTO 3.2-1 over the compressive area of the section (see example 2). However, a simpler approximation might be used for rectangular stress blocks as suggested in Chapter 3, Composite mechanics, of NCHRP 655 (Zureick et al., 2010) as $C = 0.9 f'_c \beta_2 \, c \, b_e$. The latter is shown here for brevity.

Compression force in the concrete:

$$C = 0.9 f'_c \, \beta_2 \, c \, b_e = 0.9 \times 4 \times 0.43 \times 7.36 \times 72 = 820 \text{ kips}$$

Strain in the steel:

$$\varepsilon_s = \frac{d-c}{c}\varepsilon_c = \frac{43.6-7.36}{7.36}\times 9\times 10^{-4} = 4.92\times 10^{-3} > \varepsilon_y = \frac{f_y}{E_s} = \frac{60}{29{,}000} = 0.00207$$

Tension force in steel:

$$T_s = A_s f_y = 12.7 \times 60 = 762 \text{ kips}$$

Tension force in the FRP reinforcement:

$$T_{frp} = n \times N_b \times b_{frp} = 3 \times 1.07 \times 18 = 57.7 \text{ kips}$$

Total tension force:

$$T = T_{frp} + T_s = 57.72 + 762 = 820 \text{ kips}$$

Since equilibrium is satisfied ($T = 819 \approx C = 820$), the neutral axis position is correct.

If $T \neq C$, a new guess for the neutral axis is required.

Step 7:

Determine the initial strain resulting from the service dead load

$$\text{Modular ratio } n = \frac{E_s}{E_c} = \frac{29{,}000}{3605} = 8.04$$

Assuming that the neutral axis lies within the flange of the T-section, the depth of the neutral axis can be computed from:

$$y_n = \frac{nAs}{be}\left(-1+\sqrt{1+\frac{2dbe}{nAs}}\right) = \frac{8.04\times 12.70}{72}\left(-1+\sqrt{1+\frac{2\times 43.6\times 72}{8.04\times 12.70}}\right) = 9.79 \text{ in.}$$

Since $y_n < t_f$, the assumption is correct.

Cracked moment of inertia

$$Icr = \frac{bh^3}{3} + n\,As(d-y_n)^2 = \frac{72\times 9.79^3}{3} + 8.04\times 12.70\times(43.6-9.79)^2$$
$$= 139{,}241 \text{ in.}^4$$

Initial tensile stress at the bottom concrete surface

$$\sigma_{bo} = \frac{Md(h-y_n)}{Icr} = \frac{590\times 12(48-9.79)}{139{,}241} = 1.94 \text{ ksi}$$

At the time of installation of the externally bonded FRP, the dead load initial strain at the bottom surface of the beam is

$$\varepsilon_{bo} = \frac{\sigma_{bo}}{E_c} = \frac{1.94}{3605} = 5.39 \times 10^{-4}$$

Step 8:
Calculate resistance factor and the design moment capacity:

$$M_r = \phi([A_s f_s(ds - k_2 c)] + \phi_{frp}(h - k_2 c))$$

$$\text{With } k_2 = 1 - \frac{2\left[\left(\frac{\varepsilon_c}{\varepsilon_0}\right) - \arctan\left(\frac{\varepsilon_c}{\varepsilon_0}\right)\right]}{\beta_2\left(\frac{\varepsilon_c}{\varepsilon_0}\right)^2} = 1 - \frac{2[(0.48) - \arctan(0.48)]}{0.431 \times (0.48)^2} = 0.35$$

(NCHRP 3.5)

Per recommendations in Section 8.1.3.4:

$$\begin{bmatrix} \phi = 0.9 & \text{for} & (\varepsilon^u_{frp} \geq 2.5\ \varepsilon^y_{frp} \text{ and } E_t \geq 0.005) \\ \phi = \min \begin{bmatrix} 0.65 + \left(\frac{0.25}{1.5}\right)\left(\varepsilon^u_{frp} - 1\right) & \text{for} & \varepsilon^y_{frp} < \varepsilon^u_{frp} < 2.5\ \varepsilon^y_{frp} \\ 0.65 + \left(\frac{0.25\ (E_t - \varepsilon^y_s)}{0.005 - \varepsilon^y_s}\right) & \text{for} & \varepsilon^y_s < \varepsilon_t < 0.005 \end{bmatrix} \\ \phi = 0.65 & \text{for} & (\varepsilon^u_{frp} \leq \varepsilon^y_{frp} \text{ or } \varepsilon_t \leq \varepsilon^y_s) \end{bmatrix}$$

Where strain in the FRP at steel yield is

$$\varepsilon^y_{frp} = \frac{h - c}{d - c}(\varepsilon^y_s) - \varepsilon_{bo} = \frac{48 - 7.36}{43.6 - 7.36}(0.0021) - 5.39 \times 10^{-4} = 0.0018$$

The ratio of FRP ultimate strain to strain at steel yield is

$$\frac{\varepsilon^u_{frp}}{\varepsilon^y_{frp}} = \frac{0.005}{0.0018} = 2.81$$

This exceeds the minimum required value of 2.5 as specified by AASHTO. If this ratio <2.5, the design is not valid.

Strain in the bottom layer of steel at ultimate capacity is

$$\varepsilon_t = \frac{d_t - c}{h - c}(\varepsilon^u_{frp}) = \frac{45.5 - 7.36}{48 - 7.36}0.005 = 0.0047$$

$$\phi = 0.65 + \left(\frac{0.25(\varepsilon_t - \varepsilon_s^y)}{0.005 - \varepsilon_s^y}\right) = 0.65 + \left(\frac{0.25\,(0.0047 - 0.0021)}{0.005 - 0.0021}\right) = 0.87$$

Per recommendations in Section 8.1.3.4 the additional reduction factor to the FRP contribution to moment capacity is

$$\begin{bmatrix} \phi_{frp} = 0.94 & \text{when } \phi = 0.9 \\ \phi_{frp} = 0.38\phi + 0.6 & \text{when } 0.65 < \phi < 0.9 \\ \phi_{frp} = 0.85 & \text{when } \phi = 0.65 \end{bmatrix}$$

$$\phi_{frp} = 0.38\ \phi + 0.6 = 0.38 \times 0.87 + 0.6 = 0.932$$

The final moment capacity of the strengthened section is

$$M_r = 0.87[12.7 \times 60(43.6 - 0.35 \times 7.36) + 0.932 \times 57.72 \times (48 - 0.35 \times 7.36)]$$
$$= 29463 \text{ kip-in.} = 2445 \text{ kip-ft.}$$
$$M_r = 2455 \text{ kip-ft.} < M_u = 2631 \text{ kip-ft.}$$

Since $M_r < M_u$, the strength is insufficient. Solutions are to increase the strength of FRP, the number of layers, or width of FRP (as feasible).

Increasing the number of layers to $n = 7$, following the above procedure, the location of neutral axis and M_r can be found as

$c = 7.71$ in. and $M_r = 2683$ kip-ft. $> M_u = 2631$ kip-ft., which is sufficient capacity.

Step 9:

Compute required development length.

Development length required:

$$L_d = \frac{T_{frp}}{\tau_{int}\, b_{frp}} = \frac{134.68}{0.065 \times \sqrt{4} \times 18} = 57.56 \text{ in.} = 4.8 \text{ ft.}$$

Step 10:

Check fatigue limit state.

For the fatigue load combination: $0.75M_{L+I} = 0.75 \times 550 = 412.5$ kip-ft. $= 4950$ kip-in.

Cracking moment

$$M_{cr} = f_r \frac{I_g}{y_t}$$

where

$$f_r = 0.24\sqrt{f'_c} = 0.24\sqrt{4} = 0.48 \text{ ksi}$$

$I_g = 310,417 \text{ in.}^4$

$y_t = 30.68 \text{ in.}$

$$M_{cr} = 0.48\frac{310,417}{30.68} = 4857 \text{ kip-in.}$$

$M_{cr} = 4857 \text{ kip-in.} \leq 4950 \text{ kip-in.}$ O.K.

Strain in the concrete, steel reinforcement, and FRP reinforcement, respectively, due to the fatigue load combination:

$$\varepsilon_c = \frac{M_f z}{I_T E_{frp}} = \frac{(550)(12)(10.14)}{16,616 \times 33,000} = 1.22 \times 10^{-4} < 0.36\frac{f'_c}{E_c} = 0.36\frac{4}{3605} = 4 \times 10^{-4}$$

$$\varepsilon_s = \frac{M_f(d-z)}{I_T E_{frp}} = \frac{(550)(12)(43.6-10.14)}{16,616 \times 33,000} = 4 \times 10^{-4} < 0.8\,\varepsilon_y$$
$$= 0.8 \times 0.0021 = 1.66 \times 10^{-3}$$

$$\varepsilon_{frp} = \frac{M_f(h + n\,t_{frp} - z)}{I_T E_{frp}} = \frac{(550)(12)\,(48 + 7 \times 0.0065 - 10.14)}{16,616 \times 33,000}$$
$$= 4.56 \times 10^{-4} < \eta\,\varepsilon^u_{frp} = 0.8(0.0167) = 0.013$$

Step 11:
Check reinforcement end-termination peeling

$M_u = 810 \text{ kip-ft.}$

$V_u = 150 \text{ kips}$

Shear modulus of FRP

$$G_a = \frac{E_a}{2(1+\upsilon)} = \frac{440}{2(1+0.35)} = 163 \text{ ksi}$$

Moment of inertia of beam section including FRP (use transformed section), $I_T = 16,616 \text{ in.}^4$

Peeling stress, $f_{\text{peel}} = \tau_{av}\left[\left(\frac{3E_a}{E_{frp}}\right)\frac{t_{frp}}{t_a}\right]^{1/4}$

where

Average shear stress at FRP/concrete interface

$$\tau_{av} = \left[V_u + \left(\frac{G_a}{E_{frp}\, t_{frp}\, t_a} \right)^{\frac{1}{2}} M_u \right] \frac{t_{frp}(h - z)}{I_T}$$

$$\tau_{av} = \left[150 + \left(\frac{163}{33,000 \times 7 \times 0.0065 \times 0.020} \right)^{\frac{1}{2}} \times 810 \times 12 \right]$$

$$\frac{7 \times 0.0065 \times (48 - 10.14)}{16,616} = 2.36 \text{ ksi}$$

$$f_{\text{peel}} = 1.83 \left[\left(\frac{3 \times 440}{33,000} \right) \frac{7 \times 0.0065}{0.02} \right]^{1/4} = 1.29 \text{ ksi} > 0.065\sqrt{4} = 0.13$$

Since $f_{\text{peel}} >$ limit, mechanical anchors at the FRP reinforcement are required.

9.1.2 Flexural strengthening of a simply supported prestressed concrete girder

This example illustrates the flexural strengthening of a PC I-beam with an externally bonded CFRP system to accommodate higher loading.

Structure information:

Concrete compressive strength of the deck, $f'_{cd} = 4$ ksi

$\beta_1 = 0.85$ (for $f'_c \leq 4.0$ ksi)

Modulus of elasticity, $E_c = 57\sqrt{f'_c} = 57\sqrt{4000} = 3605$ ksi

New nominal loads for Strength I Limit State: $M_{DC} = 1700$ kip-ft., $M_{DW} = 200$ kip-ft. and $M_{L+I} = 1525$ kip-ft.

Precast beam: AASHTO-Type IV, with concrete compressive strength $f'_c = 5$ ksi

Total height including deck slab, $h_T = 64$ in.

Flange thickness, $h_f = 9$ in.

Effective width of the Flange, $b_{eff} = 96.38$ in.

Internal shear reinforcement = #3 at 12 in. spacing.

The distance from the extreme compression fiber to the center of gravity of the strands at the midspan, $d_p = 57.62$ in.

Beam pretensioning strands:

Area of one tendon, $A_{ps} = 0.153$ in.^{2}

Diameter = 0.5 in.

Total area of the 26 strands, $A_{ps} = 3.98$ in.^{2}

Ultimate stress, $f_{pu} = 270$ ksi

Yield strength, $f_{py} = 0.9\, f_{pu} = 243$ ksi

Modulus of elasticity, $E_p = 28,500$ ksi

Initial pretensioning at service limit state, $f_{pe} = 0.8\ f_{py} = 194$ ksi

Factor related to the type of strands,

$$k = 2\left(1.04 - \frac{f_{py}}{f_{pu}}\right) = 0.28 \text{ for low relaxation strands} \qquad \text{(LRFD 5.7.3.1.1-2)}$$

FRP reinforcement:

Shop-fabricated carbon fiber/epoxy composite plates
Plate thickness, $t_f = 0.039$ in.
Tensile strain in the FRP reinforcement at failure, $\varepsilon_{frp}^{tu} = 0.013$
Tensile strength in the FRP reinforcement at 1% strain, $P_{frp} = 9.3$ kips/in.
Glass transition temperature, $T_g = 165°\text{F}$ (Fig. 9.2).

Step 1:

Determine if the FRP reinforcement material is in compliance with AASHTO Section 2.2.4.1, which specifies that the glass transition temperature must be higher than the maximum design temperature by 40°F. The maximum design temperature, $T_{\text{Max Design}}$, is determined from Article 3.12.2.2 of the AASHTO LRFD Bridge Design Specifications for the location of the bridge (Michigan):

$$T_{\text{Max Design}} = 105°\text{F}$$
$$T_{\text{Max Design}} + 40°\text{F} = 105°\text{F} + 40°\text{F} = 145°\text{F} < T_g = 165°F$$

Step 2:

For simplicity, neglecting the possible contribution of steel in the compression zone to flexural strength, the depth of the neutral axis is

$$c = \frac{A_{ps}f_{pu} + A_s f_y}{0.85f'_c\beta_1 b + kA_{ps}\left(\frac{f_{pu}}{d_p}\right)} \qquad \text{(LRFD 5.7.3.1.1-4)}$$

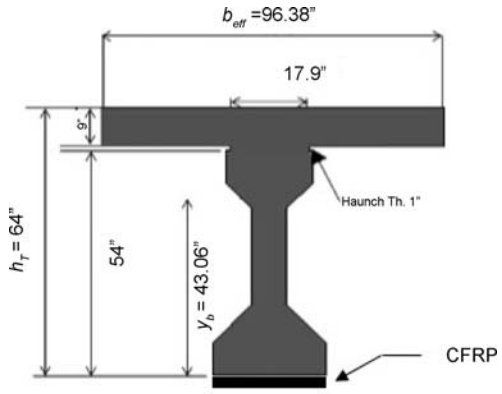

Figure 9.2 PC beam section.

$$c = \frac{(3.98)(270) + 0}{(0.85)(4)(0.85)(96.38) + (0.28)(3.98)\left(\frac{270}{57.62}\right)} = 3.79 \text{ in.}$$

The depth of concrete compressive block: $a = \beta_1 c = (0.85)(3.79) = 3.22$ in.

Since $a < h_f$, the stress block is within the flange and the calculation of a is correct.

$$M_n = A_{ps} f_{ps}\left(d_p - \frac{a}{2}\right) \qquad \text{(LRFD 5.7.3.2.2-1)}$$

The above equation is simplified from LRFD 5.7.3.2.2-1 because no compression reinforcement or mild tension reinforcement is considered and the section behaves as a rectangular section.

$$f_{ps} = f_{pu}\left(1 - k\frac{c}{d_p}\right) \qquad \text{(LRFD 5.7.3.1.1-1)}$$

$$f_{ps} = 270\left(1 - 0.28\frac{3.79}{57.62}\right) = 265 \text{ ksi}$$

$$M_n = 3.98 \times 265 \times \left(57.62 - \frac{3.22}{2}\right) = 59074 \text{ kip-in.} = 4923 \text{ kip-ft.}$$

$$\phi M_n = 1 \times 59,074 \text{ kip-in.} = 59,074 \text{ kip-in.} = 4923 \text{ kip-ft.}$$

Step 3:

Determine if the beam requires strengthening.

The factored moment for the Strength I limit state is

$$\begin{aligned} M_u &= 1.25\,M_{DC} + 1.5\,M_{DW} + 1.75\,M_{L+I} = 1.25 \times 1700 + 1.5 \times 200 + 1.75 \times 1525 \\ &= 5094 \text{ kip-ft.} \\ &= 61,128 \text{ kip-in.} \end{aligned}$$

Since $\phi M_n < M_u$, the beam requires strengthening.

Step 4:

Determine the initial strain resulting from the service dead load per recommendations in Section 5.2.2.3:

$$\varepsilon_{bo} = \frac{-p_e}{E_c A_{cg}}\left(1 + \frac{e\,y_b}{r^2}\right) + \frac{M_{DL}\,y_b}{E_c I_g}$$

where radius of gyration, $r = 22.04$ in.; effective prestressing strain, $p_e = A_{ps}f_{pe} = 3.98 \times 194 = 773$ ksi; eccentricity of prestressing force, $e = 36.68$ in.; gross moment of inertia, $I_g = 768{,}283$ in.^{4}; cross-sectional area, $A_{cg} = 1674$ in.^{2}; distance from extreme bottom fiber to the section centroid, $y_b = 43.06$ in.

$$\varepsilon_{bo} = \frac{-773}{3605 \times 1674.28}\left(1 + \frac{36.68 \times 43.06}{22.04^2}\right) + \frac{1700 \times 12 \times 43.06}{3605 \times 768{,}283} = -2.3 \times 10^{-4}$$

Step 5:

Establish the linear stress−strain relationship of the FRP reinforcement based on the design assumptions specified in Article 3.2 of AASHTO and compute the tensile strength according to a strain value of 0.005.

$$N_b = \frac{0.005}{0.01}(9.3) = 4.65 \text{ kip/in.}$$

Step 6:

Compute the factored flexural resistance of the strengthened I-beam. By trial and error, the depth of the neutral axis can be determined from strain compatibility and force equilibrium.

Guess $c = 11.3$ in.

Maximum strain in concrete

$$\varepsilon_c = \frac{c}{h-c}\varepsilon_{frp}^{u} = \frac{11.3}{64 - 11.3} \times 0.005 = 0.00107$$

where 0.005 is the assumed FRP limiting strain.

Since the neutral axis is below the deck, the stress block contains concrete areas of two different strengths. This may preclude the use of a simple expression such as $C = 0.9f'_c\beta 2\ cb_e + kA_{ps}(f_{pu}/d_p)$ to calculate the compressive force in the concrete accurately. Here the parabolic concrete stress block model will integrated over the separate areas to better approximate forces.

For the deck:

$$\varepsilon_0 = \frac{(1.71 \times f'_c)}{E_c} = \frac{1.71 \times 4}{3605} = 0.0019 \qquad \text{(NCHRP 3.2)}$$

The stress−strain relationship is

$$f_c = \frac{2(0.9f'_c)\left(\frac{\varepsilon_c}{\varepsilon_o}\right)}{1 + \left(\frac{\varepsilon_c}{\varepsilon_o}\right)^2} \qquad \text{(NCHRP 9.8 AASHTO 3.2-1)}$$

Relating concrete strain ε to distance y from the neutral axis:

$$\varepsilon = y\left(\frac{\varepsilon_{\max}}{c}\right) = y\left(\frac{0.00107}{11.3}\right) = 0.000095y$$

Inserting this relationship into the stress−strain curve above (and using $f'_c = 4$ ksi for the deck):

$$f_c = \frac{2(0.9(4))\left(\frac{0.000095y}{0.0019}\right)}{1 + \left(\frac{0.000095y}{0.0019}\right)^2} = \frac{0.359y}{1 + (0.0498y)^2}$$

Integrating (numerically) through the depth of the 9 in deck:

$$\int_{2.3}^{11.3} \frac{0.359y}{1 + (0.0498y)^2} dy = 19.0$$

Multiplying by the deck width to obtain total force: $C_{\text{deck}} = 19.0 \times 96.38 = 1831$ kips.

Repeating this process for the beam:

$$\varepsilon_0 = \frac{(1.71 \times f'_c)}{E_c} = \frac{1.71 \times 5}{3605} = 0.0024$$

Note that this peak stress will not be experienced, as this would correspond to a location in the deck if the deck were made of 5 ksi concrete; however, this will establish the shape of the lower portion of the stress curve found in the beam.

$$f_c = \frac{2(0.9(5))\left(\frac{0.000095y}{0.0024}\right)}{1 + \left(\frac{0.000095y}{0.0024}\right)^2} = \frac{0.356y}{1 + (0.040y)^2}$$

Integrating (numerically) through the depth of compression zone in the beam:

$$\int_{0}^{2.3} \frac{0.356y}{1 + (0.040y)^2} dy = 0.94$$

Multiplying by the beam width to obtain total force: $C_{\text{beam}} = 0.94 \times 17.9 = 17$ kips.

Total compressive force in the concrete = 1831 + 17 = 1848 kips.

Tension force in the FRP reinforcement.

Guided by step 5 in Example 1 and through trial and error, it is found that seven plies are required to accommodate the ultimate moment.

$$T_{frp} = n \times N_b \times b_{frp} = 7 \times 4.65 \times 24 = 781 \text{ kips}$$

Tension force in the prestressed steel:

$$T_{ps} = A_{ps} f_{pu} = 3.98 \times 270 = 1074 \text{ kips}$$

Total tension force:

$$T = T_{frp} + T_{ps} = 781 + 1074 = 1855 \text{ kips}$$

Since equilibrium is satisfied ($T = 1855 \approx C = 1848$), the neutral axis position is correct. If $T \neq C$, a new guess for the neutral axis is required.

Step 7:

Calculate resistance factor and the design moment capacity per recommendations in Section 8.1.3.4:

$$\left[\begin{array}{ll} \phi = 0.9 & \text{for} \quad (\varepsilon_{frp}^{u} \geq 2.5\, \varepsilon_{frp}^{y} \text{ and } E_{ps} \geq 0.013) \\ \phi = \min \left[\begin{array}{ll} 0.65 + \left(\dfrac{0.25}{1.5}\right)(\varepsilon_{frp}^{u} - 1) & \text{for} \quad \varepsilon_{frp}^{y} < \varepsilon_{frp}^{u} < 2.5\, \varepsilon_{frp}^{y} \\ 0.65 + \left(\dfrac{0.25\,(E_{ps} - 0.010}{0.013 - 0.010}\right) & \text{for} \quad 0.010 < \varepsilon_{ps} < 0.013 \end{array}\right] & \\ \phi = 0.65 & \text{for} \quad (\varepsilon_{frp}^{u} \leq \varepsilon_{frp}^{y} \text{ or } \varepsilon_{ps} \leq 0.010) \end{array}\right]$$

where

$$\varepsilon_{ps} = \varepsilon_{pe} + \frac{p_e}{A_c E_c}\left(1 + \frac{e^2}{r^2}\right) + \varepsilon_{\text{pnet}} \leq 0.035$$

$$\varepsilon_{pe} = \frac{f_{pe}}{E_p} = \frac{194}{28,500} = 0.0068$$

$$\varepsilon_{pe} = \frac{d_p - c}{h - c}\varepsilon_{frp}^{u} = \frac{57.62 - 11.3}{64 - 11.3} \times 0.005 = 0.0044$$

$$\varepsilon_{ps} = 0.0068 + \frac{773}{1674 \times 3605}\left(1 + \frac{36.68^2}{22.04^2}\right) + 0.0044 = 0.0117$$

The strain in the FRP at the point where the prestressing steel yields is

$$\varepsilon_{frp}^{y} = \frac{h - c}{d_p - c}\varepsilon_{ps}^{y} - \varepsilon_{bo}$$

$$\varepsilon_{ps}^{y} = \frac{f_{ps}}{E_{ps}} = \frac{243}{28,500} = 0.0085$$

$$\varepsilon_{frp}^{y} = \frac{64 - 11.3}{57.62 - 11.3} \times 0.0085 - (-2.3 \times 10^{-4}) = 0.0099$$

$\varepsilon_{frp}^{u} = 0.005 \leq \varepsilon_{frp}^{y} = 0.0099$. Thus $\phi = 0.65$ and $\phi_{frp} = 0.85$.
The final moment capacity is generally given as

$$M_r = \phi([A_{ps} f_{ps}(dp - k_2 c)] + \phi_{frp} T_{frp}(h - k_2 c)) \qquad \text{(AASHTO 3.4.1.1-1)}$$

However, since the neutral axis crossed into the beam, the stress block is no longer rectangular; also, two different concrete strengths are present. Therefore the simple expression used to calculate the stress block centroid position ($k_2 = 1 - (2[(\varepsilon_c/\varepsilon_0) - \arctan(\varepsilon_c/\varepsilon_0)]/\beta_2(\varepsilon_c/\varepsilon_0)^2)$) cannot be used. Rather, the centroid of the T-shaped stress block must be calculated.

The centroid can be calculated in general by

$$\overline{y} = \frac{\int_{y1}^{y2} y f(y) dy}{\int_{y1}^{y2} f(y) dy}$$

The flange stress block centroid is then:

$$\overline{y} = \frac{\int_{2.3}^{11.3} \frac{0.359y^2}{1 + (0.0498y)^2} dy}{\int_{2.3}^{11.3} \frac{0.359y}{1 + (0.0498y)^2} dy} = 7.58 \text{ in. (from bottom of flange)}$$

The beam stress block centroid is

$$\overline{y} = \frac{\int_{0}^{2.3} \frac{0.356y^2}{1 + (0.040y)^2} dy}{\int_{0}^{2.3} \frac{0.356y}{1 + (0.040y)^2} dy} = 1.44 \text{ in (from neutral axis)}$$

The centroid of the combined T-shaped block is (from neutral axis): $((7.58 + 2.3) \times 1831 + (1.44) \times 17)/(1831 + 17) = 9.80$ in. Measured from the top of the section, $11.3 - 9.80 = 1.5$ in. $= k_2 c$.

$$f_{ps} = f_{pu}\left(1 - k\frac{c}{f_{pu}}\right) = 270\left(1 - 0.28\frac{11.3}{270}\right) = 266 \text{ ksi}$$

$$M_r = \phi([A_{ps} f_{ps}(dp - k_2 c)] + \phi_{frp}\, T_{frp}(h - k_2 c))$$

$$M_r = 0.65([3.98 \times 266 \times (57.62 - 1.5)] + 0.85 \times 781 \times (64 - 1.5)) = 65587 \text{ kip-in.} = 5465 \text{ kip-ft.}$$

$M_r = 5465$ kip-ft. $> M_u = 5094$ kip-ft. O.K.

9.1.3 Shear strengthening of a prestressed concrete beam using two-sided wrap

This example illustrates the shear strengthening of a PC I-beam with a two-sided CFRP system. Note that the process and results are identical if a three-sided (U-wrap) system that otherwise has the same configuration is applied.

Structure information:

Bridge span = 42 ft.

Concrete compressive strength of the deck, $f'_{cd} = 4$ ksi

Modulus of elasticity, $E_c = 57\sqrt{f'_c} = 57\sqrt{4000} = 3605$ ksi

$\beta_1 = 0.85$ (for $f'_c \leq 4.0$ ksi)

Factored shear force, $V_u = 150$ kips

Precast beam: AASHTO-Type IV, with concrete compressive strength $f'_c = 5$ ksi.

Total height including deck slab, $h_T = 64$ in.

Flange thickness, $h_f = 9$ in.

Width of the web, $b_v = 8$ in.

Effective width of the flange, $b_{\text{eff}} = 96.38$ in.

Distance from the center of gravity of strands to the bottom fiber of the beam, $Y_{bs} = 6.38$ in.

The distance from the extreme compression fiber to the center of gravity of the strands at midspan, $d_p = 57.62$ in.

Beam pretensioning strands:

Area of one tendon, $A_{ps} = 0.153$ in.^{2}

Diameter = 0.5 in.

Total area of the 26 strands, $A_{ps} = 3.98$ in.^{2}

Ultimate stress, $f_{pu} = 270$ ksi

Modulus of elasticity, $E_p = 28{,}500$ ksi

Factor related to the type of strands

$$k = 2\left(1.04 - \frac{f_{py}}{f_{pu}}\right) = 0.28 \text{ for low relaxation strands} \qquad \text{(LRFD 5.7.3.1.1-2)}$$

Internal steel shear reinforcement:

#3 stirrups at 12 in. spacing

$A_v = 0.22$ in.^{2}

$s_v = 12$ in.

$\alpha = 90$ degree

Yield strength, $f_y = 60$ ksi

Modulus of elasticity, $E_s = 29{,}000$ ksi

FRP reinforcement:

Thickness, $t_f = 0.0065$ in.

Failure strength, $f_{fu} = 550$ ksi.

Modulus of elasticity, $E_f = 33{,}000$ ksi.

Failure strain, $\varepsilon_{fu} = 0.0167$ in./in. (Fig. 9.3).

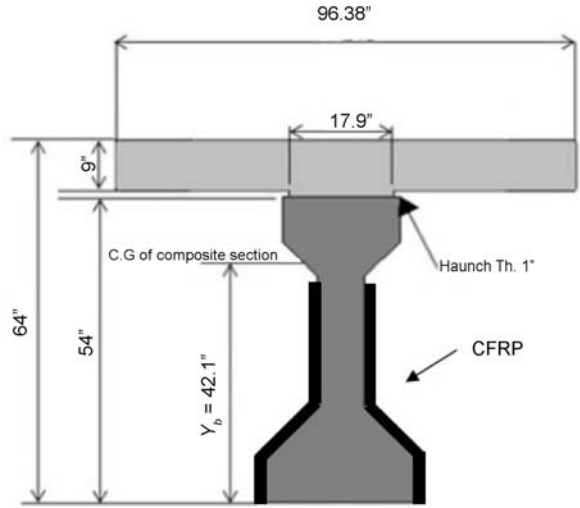

Figure 9.3 PC beam section.

Step 1:

Determine the nominal shear resistance. The effective shear depth, d_v, is taken as the distance measured perpendicular to the neutral axis between the resultants of the tensile and compressive forces due to flexure; it need not be taken to be less than the greater of $0.9d_e$ or 0.72 h (LRFD Article 5.8.2.9).

For simplicity, neglecting the possible contribution of steel in the compression zone to flexural strength, the depth of the neutral axis is

$$c = \frac{A_{ps}f_{pu} + A_s f_y}{0.85f'_c\beta_1 b + kA_{ps}\left(\frac{f_{pu}}{d_p}\right)}$$

$$c = \frac{(3.98)(270) + 0}{(0.85)(4)(0.85)(96.38) + (0.28)(3.98)\left(\frac{270}{57.62}\right)} = 3.79 \text{ in.}$$

The depth of concrete compressive block: $a = \beta_1 c = (0.85)(3.79) = 3.22$ in.

Since $a < h_f$, the stress block is within the flange and the calculation is correct.

d_e = effective depth from the extreme compression fiber to the centroid of the tensile force in the tension reinforcement = $h_c - Y_{bs} = 64 - 6.38 = 57.62$ in.

Check governing case of d_v:

$$d_{v1} = d_e - \frac{a}{2} = 57.62 - \left(\frac{3.22}{2}\right) = 56.01 \text{ in.}$$

$$d_{v2} = 0.9d_e = (0.9)(57.62) = 51.85 \text{ in.}$$

$$d_{v3} = 0.72\ \text{h} = (0.72)(64) = 46.08\ \text{in.}$$

$$d_v = \max\ (56.01,\ \ 51.85,\ \ 46.08) = 56.01\ \text{in.}$$

The nominal shear resistance provided by the concrete, V_c, is calculated in accordance with LRFD Eq. (5.8.3.3-3) as

$$V_c = 0.0316\ \beta \sqrt{f'_c}\ b_v\ d_v$$

For this example, the simplified method is followed ($\theta = 45$ degrees and $\beta = 2$). However, the iterative AASHTO LRFD Sectional Method could also be used if desired.

$$V_c = 0.0316\ (2)\left(\sqrt{5}\right)(8)(56.01) = 63\ \text{kips}$$

The nominal shear resistance provided by the internal steel reinforcement is

$$V_s = \frac{A_v f_y d_v (\cot\theta + \cot\alpha)\sin\alpha}{S} = \frac{(0.22)(60)(56.01)(1)(1)}{12} = 62\ \text{kips} \qquad \text{(LRFD 5.8.3.3-4)}$$

The nominal shear resistance provided by the vertical component of prestressing strands is $V_p = 0$ (this example assumes straight strands; harped or draped strands will have a V_p component).

The nominal shear resistance of the member is

$$V_n = V_c + V_s + V_p = 63 + 62 + 0 = 125\ \text{kips}$$

Step 2:

Check whether strengthening is required.

Strength reduction factor for shear: $\phi = 0.9$

$$\phi\ V_n = 0.9(125) = 112.5\ \text{kips}$$

$\phi V_n = 112.5\ \text{kips} < V_{u\text{-crit}} = 150\ \text{kips}$. Therefore the beam requires strengthening.

Step 3:

Selection of FRP strengthening scheme (Fig. 9.4).

A two-sided (noncontinuous) configuration is used without an anchorage system. The FRP sheets will be applied at 90 degrees with respect to the longitudinal axis of the girder. Note that the following calculation to determine FRP shear resistance for the two-sided scheme is identical for a U-wrap scheme.

Assume one layer of FRP is sufficient, $n_f = 1$

Width of FRP sheets, $W_f = 8$ in.

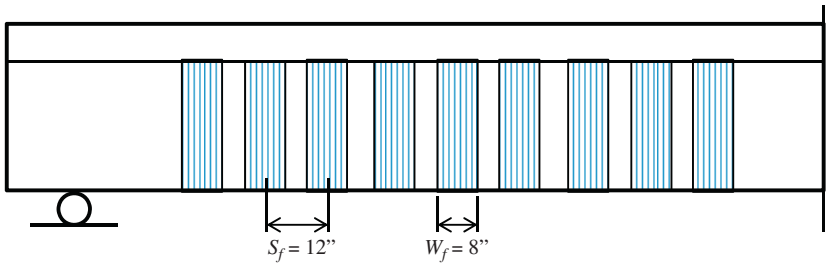

Figure 9.4 FRP reinforcement scheme.

Center-to-center spacing of FRP sheets, $S_f = 12$ in.
Orientation of FRP sheets, $\alpha_f = 90$ degrees
Effective depth of FRP sheets, $d_f = d_p - h_f$: $d_f = 57.62 - 9 = 48.62$ in.
Check if the selected spacing (12 in.) is acceptable. Shear stress in concrete is

$$V_u = \frac{V_{u\text{-crit}} - \phi\, Vp}{\phi b v d v} = \frac{150}{0.9 \times 8 \times 56.01} = 0.38 \text{ ksi} \qquad \text{(LRFD 9.11)}$$

Maximum spacing of FRP strips:

$$S_{\max} = \begin{bmatrix} \min(0.8\, d_v,\ 24) & \text{if } V_u < 0.125\, f'_c & \text{(LRFD 5.8.2.7 - 1)} \\ \min(0.4\, d_v, 12) & \text{if } V_u \geq 0.125\, f'_c & \text{(LRFD 5.8.2.7 - 2)} \end{bmatrix}$$

$0.125\, f'_c = 0.125 \times 5 = 0.63$ ksi
Since $V_u = 0.38$ ksi < 0.63 ksi, $S_{\max} = \min\ (0.8 d_v,\ 24) = \min\ (0.8 \times 56.01,\ 24) =$ 24 in. Since 12 in. < 24 in., the selected spacing is acceptable.
Step 4:
Determine FRP shear resistance, V_{frp}
The FRP reinforcement ratio is

$$\rho_f = \frac{2\, n_f t_f w_f}{b_v\, s_f} = \frac{2 \times 1 \times 0.0065 \times 8}{8 \times 12} = 1.083 \times 10^{-3} \qquad \text{(AASHTO 4.3.2-2)}$$

The FRP strain reduction factor for side bonding or U-wrap without anchorage is

$$0.066 \leq R_f = 3\, (\rho_f \times E_f)^{-0.67} \leq 1.0 = 3 \times (1.083 \times 10^{-3} \times 33,000)^{-0.67} = 0.27 \qquad \text{(AASHTO 4.3.2-5)}$$

The effective strain $\varepsilon_{fe} = R_f\, \varepsilon_{fu} \leq 0.004$

$$\varepsilon_{fe} = 0.27 \times 0.0167 = 0.0046$$

The effective strain is thus taken as 0.004.

$$V_{frp} = \rho_f E_f \varepsilon_{fe} b_v d_f (\sin(\alpha_f) + \cos(\alpha_f))$$
$$V_{frp} = 1.083 \times 10^{-3} \times 33{,}000 \times 0.004 \times 8 \times 48.62 (\sin(90) + \cos(90)) = 56 \text{ kips}$$
(AASHTO 4.3.2-1)

Step 5:
Determine the design shear resistance of the member.

$$\phi_{V_n\text{-total}} = \phi(V_c + V_p + V_s) + \phi_{frp} V_{frp}$$
$$= 0.9(63 + 0 + 62) + (0.85 \times 56) = 160 \text{ kips}$$
$$\phi_{V_n\text{-total}} = 160 \text{ kips} > V_{u\text{-crit}} = 150 \text{ kips. Thus one layer of FRP is sufficient.}$$
(AASHTO 4.3.1-1)

Step 6:
Check maximum FRP shear reinforcement limitations.

$$V_n \leq 0.25 f'_c b_v d_v + V_p$$
$$V_n = V_c + V_s + V_{frp} = 63 + 62 + 56 = 181 \text{ kips} \leq 0.25 \times 5 \times 8 \times 56.01 + 0 = 560 \text{ kips}$$
(AASHTO 5.8.3.3-2)

Thus the web crushing failure limit is O.K.

9.1.4 Shear strengthening of a T-beam using U-wrap

This example illustrates the shear strengthening of a T-beam with a U-wrap system.
Structure information:
Concrete compressive strength, $f'_c = 3$ ksi
Modulus of elasticity $E_c = 57\sqrt{f'_c} = 57\sqrt{3000} = 3122$ ksi
$\beta_1 = 0.85$ (for $f'_c \leq 4.0$ ksi)
Factored shear force, $V_u = 200$ kips
Beam height, $h_T = 48$ in.
Width of the web, $b_v = 18$ in.
Effective flange width, $b_{\text{eff}} = 54$ in.
Tensile reinforcement = 10#11, $A_s = 15.60$ in.^{2}
Internal steel shear reinforcement:

#4 stirrups at 12 in. spacing
$A_v = 0.40$ in.^{2}
$s_v = 12$ in.
$\alpha = 90$ degree
Yield strength, $f_y = 60$ ksi
Modulus of elasticity, $E_s = 29{,}000$ ksi

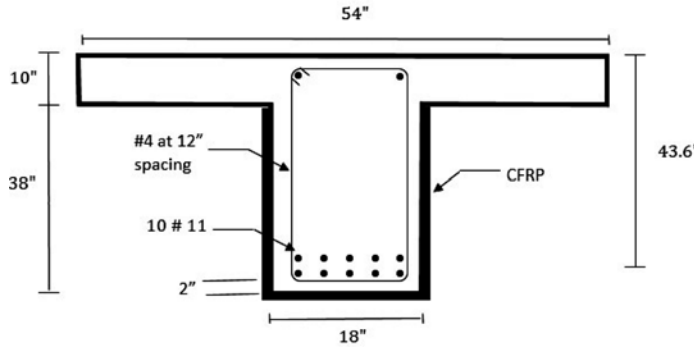

Figure 9.5 RC beam section.

FRP reinforcement:

Thickness, $t_f = 0.0065$ in.
Failure strength, $f_{fu} = 550$ ksi
Modulus of elasticity, $E_f = 33{,}000$ ksi
Failure strain, $\varepsilon_{fu} = 0.0167$ in./in. (Fig. 9.5).

Step 1:
Determine the nominal shear resistance.

The effective shear depth, d_v, is taken as the distance, measured perpendicular to the neutral axis, between the resultants of the tensile and compressive forces due to flexure; it need not be taken to be less than the greater of $0.9d_e$ or 0.72 h (LRFD Article 5.8.2.9).

For simplicity, neglecting the possible contribution of steel in the compression zone to flexural strength, the depth of the neutral axis is

$$c = \frac{(A_s f_y)}{(0.85\,\beta f'_{cb}} = \frac{(15.60 \times 60)}{(0.85 \times 0.85 \times 3 \times 54)} = 8.00 \text{ in.}$$

$$a = \beta_1\, c$$

$$a = 0.85 \times 8.00 = 6.80 \text{ in.}$$

Check governing case of d_v:

$$d_{v1} = d - \frac{a}{2} = 43.60 - \frac{6.80}{2} = 40.20 \text{ in.}$$

$$d_{v2} = 0.9d = 0.9 \times 43.60 = 39.24 \text{ in.}$$

$$d_{v3} = 0.72\, h_T = 0.72 \times 48 = 34.56 \text{ in.}$$

$$d_v = \max(d_{v1},\ d_{v2},\ d_{v3}) = \max(40.20,\ 39.24,\ 34.56) = 40.20 \text{ in.}$$

The nominal shear resistance provided by the concrete, V_c, is calculated in accordance with LRFD Eq. (5.8.3.3-3) as

$$V_c = 0.0316\,\beta\sqrt{f'_c}\,b_v\,d_v \qquad \text{(LRFD 5.8.3.3-3)}$$

For this example, the simplified method is followed: ($\theta = 45$ degrees and $\beta = 2$). However, the iterative AASHTO LRFD Sectional Method could also be used if desired.

$$V_c = 0.0316(2)\left(\sqrt{3}\right)(18)(40.20) = 79 \text{ kips}$$

The nominal shear resistance provided by the internal steel reinforcement is

$$V_s = \frac{A_v f_y\, d_v\, (\cot\theta + \cot\alpha)\sin\alpha}{S} = \frac{(0.40)(60)(40.20)(1)(1)}{12} = 80 \text{ kips} \qquad \text{(LRFD 5.8.3.3-4)}$$

The nominal shear resistance provided by the vertical component of prestressing strands is $V_p = 0$ (this example assumes straight strands; harped or draped strands will have a V_p component).

The nominal shear resistance of the member is

$$V_n = V_c + V_s + V_p = 79 + 80 + 0 = 159 \text{ kips}$$

Step 2:

Check whether strengthening is required.

Strength reduction factor for shear $\phi = 0.9$

$$\phi\, V_n = 0.9(159) = 143 \text{ kips}$$

$\phi V_n = 143$ kips $< V_{\text{u-crit}} = 200$ kips. Therefore the beam requires strengthening.

Step 3:

Selection of FRP strengthening scheme.

A U-wrap (continuous) configuration is used without an anchorage system at the ends of the sheets. The FRP sheets will be applied at 90 degrees with respect to the longitudinal axis of the girder. Note that the following calculation to determine the FRP shear resistance for the U-wrap without anchorage is identical for a side bonding scheme without anchorage.

Assume one layer of FRP is sufficient, $n_f = 1$

Orientation of FRP sheets, $\alpha_f = 90$ degrees

Effective depth of FRP sheets, $d_f = d - h_f = 33.60$ in.

Step 4:

Determine FRP shear resistance, V_{frp}

The FRP reinforcement ratio is

$$\rho_f = \frac{2\, n_f t_f}{b_v} \qquad \text{(AASHTO 4.3.2-2)}$$

$$= \frac{2 \times 1 \times 0.0065}{18} = 7.22 \times 10^{-4}$$

FRP strain reduction factor for U-wrap without anchorage or side bonding is

$$0.088 \le R_f = 3(\rho_f \times E_f)^{-0.67} \le 1.0 \qquad \text{(AASHTO 4.3.2-5)}$$

$$3 \times (7.22 \times 10^{-4} \times 33,000) - 0.67 = 0.36$$

The effective strain $\varepsilon_{fe} = R_f \varepsilon_{fu}$

$$\varepsilon_{fe} = 0.36 \times 0.0167 = 0.006$$

$$V_{frp} = \rho_f E_f \varepsilon_{fe} b_v d_f (\sin(\alpha_f) + \cos(\alpha_f))$$
$$V_{frp} = 7.22 \times 10^{-4} \times 33,000 \times 0.006 \times 18 \times 33.60 (\sin(90) + \cos(90)) = 86 \text{ kips}$$
(AASHTO 4.3.2-1)

Step 5:
Determine the design shear resistance of the member:

$$\phi_{V_{n\text{-total}}} = \phi(V_c + V_p + V_s) + \phi_{frp} V_{frp}$$
$$= 0.9(79 + 0 + 80) + (0.85 \times 86) = 216 \text{ kips} \qquad \text{(AASHTO 4.3.1-1)}$$

$\phi_{V_{n\text{-total}}} = 216$ kips $> V_{\text{u-crit}} = 200$ kips. Thus one layer of FRP is sufficient.
Step 6:
Check maximum FRP shear reinforcement limitations.

$$V_n \le 0.25 f'_c b_v d_v + V_p$$
$$V_n = V_c + V_s + V_{frp} = 79 + 80 + 86 = 245 \text{ kips} \le 0.25 \times 3 \times 18 \times 40.20 + 0 = 542 \text{ kips}$$
(AASHTO 5.8.3.3-2)

Thus the web crushing failure limit is O.K.

9.1.5 Axial strengthening of a confined circular column

This example illustrates the confinement strengthening of a circular column.
Structure information:
Column height = 24 ft.
Column diameter = 28 in.
Compressive strength of concrete, $f'_c = 4$ ksi
Spiral spacing = 12 in.
Vertical reinforcement, A_{st} = 12#8 bars

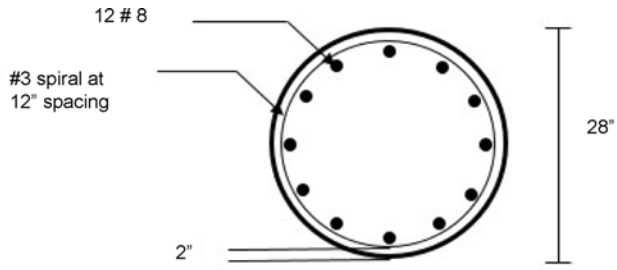

Figure 9.6 Circular column section.

$P_u = 1800$ kips
FRP reinforcement:

Thickness, $t_f = 0.013$ in.
Failure strength, $f_{fu} = 550$ ksi
Modulus of elasticity, $E_f = 33{,}000$ ksi
Failure strain, $\varepsilon_{fu} = 0.0167$ in./in.
Tensile strength of a single layer FRP reinforcement at 1.67% strain, $P_{frp} = 7.14$ kips/in./ply (Fig. 9.6).

Step 1:
Determine the axial strength of the column and check if it requires strengthening.

$$A_g = \frac{\pi D^2}{4} = \frac{\pi \times 28^2}{4} = 615 \text{ in.}^2$$

$$P_n = 0.85[0.85 f'_c (A_g - A_{st} - A_{ps}) + f_y A_{st} - A_{ps}(f_{pe} - E_p \varepsilon_{cu})]$$
$$P_n = 0.85[0.85 \times 4(615 - 9.48 - 0) + 60 \times 9.48 - 0] = 2233 \text{ kips}$$
(LRFD 5.7.4.4-2)

$$P_r = \phi P_n = 0.75 \times 2233 = 1675 \text{ kips} \quad \text{(LRFD 5.7.4.4-1)}$$

$P_r = 1675$ kips $< P_u = 1800$ kips. Therefore the column requires strengthening.
Step 2:
Compute the FRP reinforcement strength at a strain of 0.004. Note that the limit for confinement in AASHTO is different from that for flexure.

$$N_{frp} = \frac{0.004 \times 7.14}{0.0167} = 1.71 \text{ kip/in.}$$

Step 3:
Determine the required confined concrete strength.

$$P_r = 0.85 \phi [0.85 f'_{cc} (A_g - A_{st}) + f_y A_{st}] \geq P_u \quad \text{(AASHTO 5.3.1-1)}$$

From which:

$$f'_{cc} \geq \frac{\left[\left(\frac{p_u}{0.85\ \phi}\right) - \text{fyAst}\right]}{[0.85\ (\text{Ag} - \text{Ast})]} = \frac{\left[\left(\frac{1800}{0.85 \times 0.75} - 60 \times 9.48\right)\right]}{[0.85\ (615 - 9.48)]} = 4.38 \text{ ksi}$$

$$f'_{cc} = f'_c\left(1 + 2\frac{f_l}{f'_c}\right) \geq 4.38 \text{ ksi}$$
$$= 4\left(1 + 2\frac{f_l}{4}\right) \geq 4.38, \text{ therefore } f_l \geq 0.19 \text{ ksi} \qquad \text{(AASHTO 5.3.2.2-1)}$$

As per Article 5.3.2.2 of AASHTO, the confinement pressure shall be greater or equal to 600 psi but less than that specified in equation 5.3.3.3-2 as follows:

$$f_l = 0.6 \text{ ksi} \leq \left(\frac{f'_c}{2}\right)\left(\frac{1}{k_e\ \phi} - 1\right) = \left(\frac{4}{2}\right)\left(\frac{1}{0.85 \times 0.75} - 1\right) = 1.14 \text{ ksi} \quad \text{O.K.}$$

$$N_{frp} = \frac{f_l D}{2\ \phi_{frp}} = \frac{0.6 \times 28}{2 \times 0.65} = 12.92 \text{ ksi/in.} \qquad \text{(AASHTO 5.3.2.2-2)}$$

Required number of plies:

$$n = \frac{N_{frp}}{N_{frpo}} = \frac{12.92}{1.71} = 7.56$$

Try eight layers. The column axial strength is computed as follows:

$$f_l = \phi_{frp}\frac{2N_{frp}}{D} = 0.65\frac{2(8)(1.71)}{28} = 0.64 \text{ ksi}$$

$$f_l = 0.64 \leq \left(\frac{f'_c}{2}\right)\left(\frac{1}{k_e\phi} - 1\right) = 1.137 \text{ ksi} \quad \text{O.K.}$$

$$f'_{cc} = f'_c\left(1 + 2\frac{f_l}{f'_c}\right) = 4\left(1 + 2\frac{0.64}{4}\right) = 5.28 \text{ ksi}$$

$$P_r = 0.85[0.85f'_{cc}(A_g - A_{st}) + f_y A_{st}] \geq P_u$$
$$= 0.85[0.85 \times 5.28(615 - 9.48) + 60 \times 9.48] = 2793 \text{ ksi}$$

$$P_r = \phi P_n = 0.75 \times 2793 = 2095 \text{ kips} > P_u = 1800 \text{ kips.}$$

Thus the selected number of layers are sufficient.

9.1.6 Axial strengthening of a square column

Structure information:

Column height = 24 ft.
Section dimensions = 28 in.^{2}
Compressive strength of concrete, $f'_c = 4$ ksi
Transverse reinforcement = #3 bars at 12 in.
Vertical reinforcement = 12#8 bars
$P_u = 2100$ kips
FRP reinforcement:

Thickness, $t_f = 0.013$ in.
Failure strength, $f_{fu} = 550$ ksi
Modulus of elasticity, $E_f = 33{,}000$ ksi
Failure strain, $\varepsilon_{fu} = 0.0167$ in./in. Tensile strength of a single layer FRP reinforcement at 1.67% strain, $Pfrp = 7.14$ kips/in./ply (Fig. 9.7).

Step 1:

Determine the axial strength of the column.

$$P_n = 0.80[0.85f'_c(A_g - A_{st} - A_{ps}) + f_y A_{st} - A_{ps}(f_{pe} - E_p\varepsilon_{cu})] \quad \text{(LRFD 5.7.4.4-3)}$$

$$P_n = 0.80[0.85 \times 4 \times (784 - 9.48 - 0) + 60 \times 9.48 - 0] = 2562 \text{ kips}$$

$$P_r = \phi P_n = 0.75 \times 2562 = 1922 \text{ kips} \quad \text{(LRFD 5.7.4.4-1)}$$

$P_r = 1922$ kips $< P_u = 2100$ kips. Therefore the column requires strengthening.

Step 2:

Compute the FRP reinforcement strength at a strain of 0.004. Note that the limit for confinement in AASHTO is different from that for flexure.

$$N_{frp} = \frac{0.004 \times 7.14}{0.0167} = 1.71 \text{ kip/in.}$$

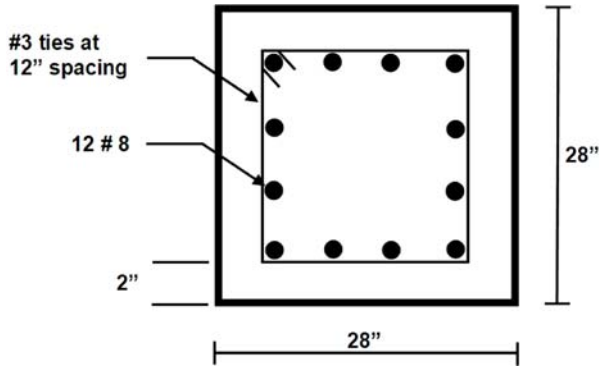

Figure 9.7 Square column section.

Step 3:
Determine the required confined concrete strength.

$$P_r = 0.80\,\phi[0.85f'_{cc}(A_g - A_{st}) + f_y A_{st}] \geq P_u \qquad \text{(AASHTO 5.3.1-2)}$$

From which:

$$f'_{cc} \geq \frac{\left[\left(\frac{p_u}{0.80\,\phi}\right) - f_y A_{st}\right]}{[0.85\,(A_g - A_{st})]} = \frac{\left[\left(\frac{2100}{0.8 \times 0.75}\right) - 60 \times 9.48\right]}{[0.85\,(784 - 9.48)]} = 4.45 \text{ ksi}$$

$$f'_{cc} = f'_c\left(1 + 2\frac{f_l}{f'_c}\right) \geq 4.45 \text{ ksi}$$
$$= 4\left(1 + 2\frac{f_l}{4}\right) \geq 4.45, \text{ therefore } f_1 \geq 0.23 \text{ ksi} \qquad \text{(AASHTO 5.3.2.2-1)}$$

As per Article 5.3.2.2 of AASHTO, the confinement pressure shall be greater or equal to 600 psi but less than that specified in equation 5.3.3.3-2 as follows:

$$f' = 0.60 \text{ ksi} \leq \left(\frac{f'_c}{2}\right)\left(\frac{1}{k_e \cdot \phi} - 1\right) = \left(\frac{4}{2}\right)\left(\frac{1}{0.8 \times 0.75} - 1\right) = 1.33 \text{ ksi} \quad \text{O.K.}$$

$$N_{frp} = \frac{f_1 D}{2\,\phi_{frp}} = \frac{0.6 \times 28}{2 \times 0.65} = 12.92 \text{ kip/in.}$$

Required number of plies

$$n = \frac{N_{frp}}{N_{frpo}} = \frac{12.92}{1.71} = 7.56$$

Try eight layers. The column axial strength is computed as follows:

$$f_1 = \phi_{frp}\frac{2N_{frp}}{\mathrm{D}} = 0.65\frac{2(8)(1.71)}{28} = 0.64 \text{ ksi}$$

$$f'_{cc} = f'_c\left(1 + 2\frac{fl}{f'_c}\right) = 4\left(1 + 2\frac{0.64}{4}\right) = 5.27 \text{ ksi}$$

$$P_n = 0.8[0.85f'_{cc}(A_g - A_{st}) + f_y A_{st}] \geq P_u$$
$$= 0.8[0.85 \times 5.27(784 - 9.48) + 60 \times 9.48] = 3231 \text{ ksi}$$

$$P_r = \phi P_n = 0.75 \times 3231 = 2423 \text{ kips} > P_u = 2100 \text{ kips}$$

Thus the selected number of layers are sufficient.

9.1.7 Axial strengthening of a confined circular column (ACI procedure)

This example considers the same column as in Section 9.1.5.

Structure information:
Column height = 24 ft.
Column diameter = 28 in.
Compressive strength of concrete, $f'_c = 4$ ksi
Spiral spacing = 12 in.
Vertical reinforcement, $A_{st} = 12\#8$ bars
$P_u = 1800$ kips
FRP reinforcement:

Thickness, $t_f = 0.013$ in.
Failure strength, $f_{fu} = 550$ ksi
Modulus of elasticity, $E_f = 33{,}000$ ksi
Failure strain, $\varepsilon_{fu} = 0.0167$ in./in.
Tensile strength of a single layer FRP reinforcement at 1.67% strain, $P_{frp} = 7.14$ kips/in./ply (Fig. 9.8).

Step 1:
Determine the axial strength of the column.

$$P_n = 0.85[0.85 f'_c(A_g - A_{st}) + f_y A_{st}]$$

$$P_n = 0.85[0.85 \times 4(615 - 9.48) + 60 \times 9.48] = 2233 \text{ kips}$$

$$P_r = \phi P_n = 0.75 \times 2562 = 1675 \text{ kips}$$

$P_r = 1675$ kips $< P_u = 1800$ kips. Therefore the column requires strengthening.
Step 2:
Compute the design FRP material properties.

$$f_{fu} = C_E f^*_{fu}$$

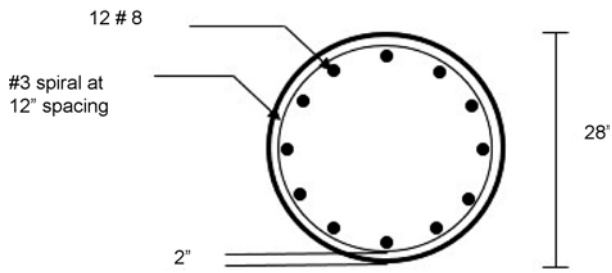

Figure 9.8 Circular column section.

C_E for CFRP equals 0.85 for exterior exposure (bridges and piers).

$$f_{fu} = 0.85 \times 550 = 468 \text{ ksi}$$

$$\varepsilon_{fu} = C_E \varepsilon_{fu}^* = 0.85 \times 0.0167 = 0.0142$$

Step 3:
Determine the required maximum compressive strength of confined concrete, f'_{cc}.

$$f'_{cc} = \frac{1}{0.85(A_g - A_{st})}\left(\frac{\phi P_{n,\text{req}}}{0.85\phi} - f_y A_{st}\right)$$

$$f'_{cc} = \frac{1}{0.85(615 - 9.48)}\left(\frac{1800}{0.85 \times 0.75} - 60 \times 9.48\right) = 4.38 \text{ ksi}$$

Step 4:
Determine the maximum confining pressure due to FRP jacket, f_l.

$$f_l = \frac{f'_{cc} - f'_c}{0.95 \times 3.3 \times k_a}$$

κ_a and κ_b for circular cross section can be taken as 1.0.

$$f_l = \frac{4.38 - 4}{0.95 \times 3.3 \times 1} = 0.12 \text{ ksi}$$

Step 5:
Determine the required number of plies.

$$n = \frac{f_l D}{2E_f t_f \varepsilon_{fe}}$$

$$\varepsilon_{fe} = \kappa_\varepsilon \varepsilon_{fu} = 0.55 \times 0.0142 = 0.0078$$

$$n = \frac{0.12 \times 28}{2 \times 33,000 \times 0.013 \times 0.0078} = 0.50$$

Try one layer.

$$f_l = \frac{2\, nE_f t_f \varepsilon_{fe}}{D} = \frac{2 \times 1 \times 33,000 \times 0.013 \times 0.0078}{28} = 0.24 \text{ ksi}$$

Checking the minimum confinement ratio:

$$\frac{f_l}{f'_c} = \frac{0.24}{4} = 0.06$$

which is not equals or greater than 0.08.

Thus try two layers:

$$f_l = \frac{2\, nE_f t_f \varepsilon_{fe}}{D} = \frac{2 \times 2 \times 33,000 \times 0.013 \times 0.0078}{28} = 0.48$$

$$\frac{f_l}{f'_c} = \frac{0.48}{4} = 0.12 \geq 0.08 \quad \text{O.K.}$$

Step 6:

Verify that the ultimate axial strain of the confined concrete, $\varepsilon_{ccu} \leq 0.01$.

$$\varepsilon_{ccu} = \varepsilon'_c \left(1.5 + 12\kappa_b \frac{f_l}{f'_c} \left(\frac{\varepsilon_{fe}}{\varepsilon'_c} \right)^{0.45} \right)$$

where

$$\varepsilon'_c = \frac{1.71 f'_c}{E_c} = \frac{1.71 \times 4}{3605} = 0.0019$$

$$\varepsilon_{ccu} = 0.0019 \left(1.5 + 12 \times 1 \times 0.12 \left(\frac{0.0078}{0.0019} \right)^{0.45} \right) = 0.008 < 0.01 \quad \text{O.K.}$$

Step 7:

Determine the column axial strength.

$$f'_{cc} = f'_c + (0.95 \times 3.3 \times \kappa_a \times f_l) = 4 + (0.95 \times 3.3 \times 1 \times 0.48) = 5.50 \text{ ksi}$$

$$P_n = 0.8[0.85 f'_{cc}(A_g - A_{st}) + f_y A_{st}]$$

$$= 0.85[0.85 \times 5.50(615 - 9.48) + 60 \times 9.48] = 2890 \text{ kips}$$

$$P_r = \phi\, P_n = 0.75 \times 3289 = 2167 \text{ kips} \geq 1800 \text{ kips}$$

Thus the selected number of layers are sufficient.

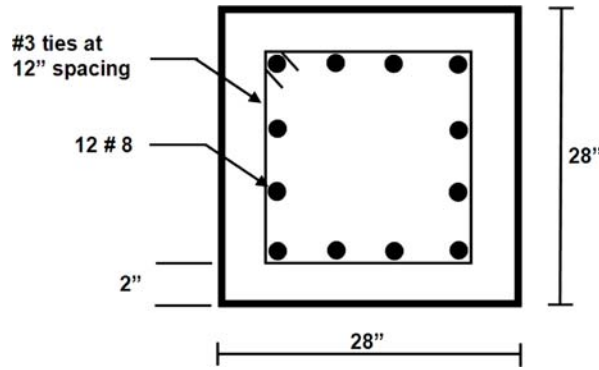

Figure 9.9 Square column section.

9.1.8 Axial strengthening of a confined square column (ACI procedure)

This example considers the same column as in Section 9.1.6.

Structure information:
Column height = 24 ft.
Column dimension = 28 in.^{2}
Compressive strength of concrete, $f'_c = 4$ ksi
Transverse reinforcement = #3 bars at 12 in.
Vertical reinforcement = 12#8 bars
$P_u = 2100$ kips
FRP reinforcement:

Thickness, $t_f = 0.013$ in
Failure strength, $f_{fu} = 550$ ksi
Modulus of elasticity, $E_f = 33{,}000$ ksi
Failure strain, $\varepsilon_{fu} = 0.0167$ in./in.
Tensile strength of a single layer FRP reinforcement at 1.67% strain, $P_{frp} = 7.14$ kips/in./ply (Fig. 9.9).

Step 1:
Determine the axial strength of the column.

$$P_n = 0.80[0.85 f'_c(A_g - A_{st}) + f_y A_{st}]$$

$$P_n = 0.80[0.85 \times 4(784 - 9.48) + 60 \times 9.48] = 2562 \text{ kips}$$

$$P_r = \phi P_n = 0.65 \times 2562 = 1665 \text{ kips}$$

$P_r = 1665$ kips $< P_u = 2100$ kips. Therefore the column requires strengthening.
Step 2:
Compute the design FRP material properties.

$$f_{fu} = C_E f^*_{fu}$$

$C_E = 0.85$ for exterior exposure (bridges and piers).

$$f_{fu} = 0.85 \times 550 = 468 \text{ ksi}$$

$$\varepsilon_{fu} = C_E \varepsilon_{fu}^* = 0.85 \times 0.0167 = 0.0142$$

Step 3:
Determine the required maximum compressive strength of confined concrete, f'_{cc}.

$$f'_{cc} = \frac{1}{0.85(A_g - A_{st})}\left(\frac{\phi P_{n,\text{req}}}{0.80\phi} - f_y A_{st}\right)$$

$$f'_{cc} = \frac{1}{0.85(784 - 9.48)}\left(\frac{2100}{0.80 \times 0.65} - 60 \times 9.48\right) = 5.27 \text{ ksi}$$

Step 4:
Determine the maximum confining pressure due to FRP jacket, f_l.

$$f_l = \frac{f'_{cc} - f'_c}{0.95 \times 3.3 \times k_a}$$

$$\kappa_a = \frac{A_e}{A_c}\left(\frac{b}{h}\right)^2$$

$$\frac{A_e}{A_c} = \frac{1 - \dfrac{\left[\left(\dfrac{b}{h}\right)(h-2r_c)^2 + \left(\dfrac{h}{b}\right)(b-2r_c)^2\right]}{3A_g} - \rho_g}{1 - \rho_g}$$

$$= \frac{1 - \dfrac{\left[\left(\dfrac{28}{28}\right)(28-2\times0.5)^2 + \left(\dfrac{28}{28}\right)(28-2\times0.5)^2\right]}{3\times784} - 0.012}{1 - 0.012} = 0.373$$

$$\kappa_a = \frac{A_e}{A_c}\left(\frac{b}{h}\right)^2 = 0.373\left(\frac{28}{28}\right)^2 = 0.373$$

$$f_l = \frac{5.27 - 4}{0.95 \times 3.3 \times 0.373} = 1.09$$

Step 5:
Determine the required number of plies.

$$n = \frac{f_l \sqrt{b^2 + h^2}}{2E_f t_f \varepsilon_{fe}}$$

$$\varepsilon_{fe} = \kappa_\varepsilon \varepsilon_{fu} = 0.55 \times 0.0142 = 0.0078$$

$$n = \frac{1.09 \times \sqrt{28^2 + 28^2}}{2 \times 33,000 \times 0.013 \times 0.0078} = 6.45$$

Try seven layers.

$$f_l = \frac{2\, nE_f t_f \varepsilon_{fe}}{\sqrt{b^2 + h^2}} = \frac{2 \times 7 \times 33,000 \times 0.013 \times 0.0078}{\sqrt{28^2 + 28^2}} = 1.18 \text{ ksi}$$

Checking the minimum confinement ratio:

$$\frac{f_l}{f'_c} = \frac{1.18}{4} = 0.295 \geq 0.08 \quad \text{O.K.}$$

Step 6:
Verify that the ultimate axial strain of the confined concrete, $\varepsilon_{ccu} \leq 0.01$.

$$\varepsilon_{ccu} = \varepsilon'_c \left(1.5 + 12\kappa_b \frac{f_l}{f'_c} \left(\frac{\varepsilon_{fe}}{\varepsilon'_c} \right) \right)^{0.45}$$

where

$$\varepsilon'_c = \frac{1.71\, f'_c}{E_c} = \frac{1.71 \times 4}{3605} = 0.0019$$

$$\kappa_b = \frac{A_e}{A_c} \left(\frac{h}{b} \right)^{0.5} = 0.373 \left(\frac{28}{28} \right)^{0.5} = 0.373$$

$$\varepsilon_{ccu} = 0.0019 \left(1.5 + 12 \times 0.373 \times 0.295 \left(\frac{0.0078}{0.0019} \right)^{0.45} \right) = 0.0076 < 0.01 \quad \text{O.K.}$$

Step 7:
Determine the column axial strength.

$$f'_{cc} = f'_c + (0.95 \times 3.3 \times \kappa_a \times f_l) = 4 + (0.95 \times 3.3 \times 0.373 \times 1.18) = 5.38 \text{ ksi}$$

$$P_n = 0.8[0.85f'_{cc}(A_g - A_{st}) + f_y A_{st}]$$
$$= 0.8[0.85 \times 5.38(784 - 9.48) + 60 \times 9.48] = 3289 \text{ kips}$$

$$P_r = \phi P_n = 0.65 \times 3289 = 2137 \text{ kips} \geq 2100 \text{ kips}$$

Thus the selected number of layers are sufficient.

Appendix A: Nomenclature

A.1 AASHTO

A_f, A_{frp}	effective area of FRP reinforcement for shear-friction (in.^{2})
A_g	gross area of column section (in.^{2})
A_h	area of one leg of the horizontal reinforcement (in.^{2})
A_s	area of nonprestressed tension reinforcement (in.^{2})
A'_s	area of compression reinforcement (in.^{2})
A_{st}	total area of longitudinal steel reinforcement (in.^{2})
A_{vf}	area of steel reinforcement required to develop strength in shear-friction (in.^{2})
b	width of rectangular section (in.)
b_{frp}	width of the FRP reinforcement (in.)
b_v	effective shear web width (in.)
b_w	girder width (in.)
$\boldsymbol{c}$	depth of the concrete compression zone (in.)
C	clamping force across the crack face (kips)
d_f, d_{frp}	effective FRP shear reinforcement depth (in.)
d_s	distance from extreme compression surface to the centroid of nonprestressed tension reinforcement (in.)
d_v	effective shear depth (in.)
D_g	external diameter of circular column (in.)
E_a	modulus of elasticity of adhesive (ksi)
E_c	modulus of elasticity of the concrete (ksi)
E_f, E_{frp}	modulus of the FRP reinforcement in the direction of structural action
f_c	stress in concrete at strain, ε_c (ksi)
f'_c	28 day compressive strength of the concrete (ksi)
f'_{cc}	compressive strength of confined concrete (ksi)
f_{frpu}	characteristic value of the tensile strength of FRP reinforcement (ksi)
f_{lfrp}	ultimate confinement pressure due to FRP strengthening (ksi)
f_{peel}	peel stress at the FRP reinforcement concrete interface (ksi)
f_s	stress in the steel tension reinforcement at development of nominal flexural resistance (ksi)
f'_s	stress in the steel compression reinforcement at development of nominal flexural resistance (ksi)
f_y	specified yield stress of steel reinforcement (ksi)
f_{yf}	yield strength of steel reinforcement for shear-friction (ksi)
G_a	characteristic value of the shear modulus of adhesive (ksi)
h	depth of section (in.); overall thickness or depth of a member (in.)
I_T	moment of inertia of an equivalent FRP transformed section, neglecting any contribution of concrete in tension (in.^{4})
k_a	coefficient that defines the effectiveness of the specific anchorage system

k_e	strength reduction factor applied for unexpected eccentricities
k_2	multiplier for locating resultant of the compression force in the concrete
l_u	unsupported length of compression member (in.)
L_d	development length (in.)
M_r	factored resistance of a steel-reinforced concrete rectangular section strengthened with FRP reinforcement externally bonded to the beam tension surface (kip-in.)
M_u	factored moment at the reinforcement end-termination (kip-in.)
N_b	FRP reinforcement strength per unit width at a tensile strain of 0.005 (kips/in.)
N_{frp}^{e}	effective strength per unit width of the FRP reinforcement (kips/in.)
$N_{frp,w}(r)$	tensile strength of a closed (wrapped) jacket (kips/in.)
N_s	FRP reinforcement strength per unit width at a tensile strain of 0.004 (kips/in.)
N_{ut}	characteristic value of the tension strength per unit width of the FRP reinforcement (kips/in.)
P_r	factored axial load resistance (kips)
r	girder corner radius (in.)
s_v	spacing of FRP reinforcement (in.)
T_{frp}	tension force in the FRP reinforcement (kips)
$\boldsymbol{T_r}$	factored torsion strength of a concrete member strengthened with an externally bonded FRP system (kip-in.)
t_a	thickness of the adhesive layer (in.)
t_{frp}	thickness of the FRP reinforcement (in.)
V_c	nominal shear strength provided by the concrete (kips)
V_{frp}	nominal shear strength provided by the externally bonded FRP reinforcement (kips)
V_{ni}	nominal shear-friction strength (kips)
V_p	component of the effective prestressing force in the direction of applied shear (kips)
V_r	factored shear strength of a concrete member strengthened with an externally bonded FRP system (kips)
V_s	nominal shear strength provided by the transverse steel reinforcement (kips)
V_u	factored shear force at the reinforcement end-termination (kips)
v_u	effective shear stress (ksi); see AASHTO LRFD 5.8.2.9
w_{frp}	total width of FRP reinforcement (in.)
y	distance from the extreme compression surface to the neutral axis of a transformed section, neglecting any contribution of concrete in tension (in.)
α	angle between FRP reinforcement principal direction and the longitudinal axis of the member; angle between the shear-friction reinforcement and the shear plane (degree)
α_1	ratio of average stress in rectangular compression block to the specified concrete compressive strength
ε_c	strain in concrete
ε_{frp}	strain in FRP reinforcement
ε_{frp}^{ut}	characteristic value of the tensile failure strain of the FRP reinforcement
ε_o	the concrete strain corresponding to the maximum stress of the concrete stress–strain curve
μ	coefficient of friction
η	strain limitation coefficient that is less than unity
ν_a	Poisson's ratio of adhesive
τ_a	characteristic value of the limiting shear stress in the adhesive (ksi)

τ_{int} interface shear transfer strength (ksi)
ϕ_{frp} resistance factor for FRP component of resistance

A.2 ACI 440.2R 08

a_b smaller cross-sectional dimension for rectangular FRP bars, in. (mm)
A_c cross-sectional area of concrete in compression member, in.^{2} (mm^2)
A_e cross-sectional area of effectively confined concrete section, in.^{2} (mm^2)
A_f area of FRP external reinforcement, in.^{2} (mm^2)
$A_{f\text{anchor}}$ area of transverse FRP U-wrap for anchorage of flexural FRP reinforcement
A_{fv} area of FRP shear reinforcement with spacing s, in.^{2} (mm^2)
A_g gross area of concrete section, in.^{2} (mm^2)
A_p area of prestressed reinforcement in tension zone, in.^{2} (mm^2)
A_s area of nonprestressed steel reinforcement, in.^{2} (mm^2)
A_{si} area of i-th layer of longitudinal steel reinforcement, in.^{2} (mm^2)
A_{st} total area of longitudinal reinforcement, in.^{2} (mm^2)
$\boldsymbol{b}$ width of compression face of member, in. (mm)
short side dimension of compression member of prismatic cross section, in. (mm)
b_b larger cross-sectional dimension for rectangular FRP bars, in. (mm)
b_w web width or diameter of circular section, in. (mm)
$\boldsymbol{c}$ distance from extreme compression fiber to the neutral axis, in. (mm)
C_E environmental reduction factor
$\boldsymbol{d}$ distance from extreme compression fiber to centroid of tension reinforcement, in. (mm)
d_f effective depth of FRP flexural reinforcement, in. (mm)
d_{fv} effective depth of FRP shear reinforcement, in. (mm)
d_i distance from centroid of i-th layer of longitudinal steel reinforcement to geometric centroid of cross section, in. (mm)
d_p distance from extreme compression fiber to centroid of prestressed reinforcement, in. (mm)
$\boldsymbol{D}$ diameter of compression member of circular cross section, in. (mm)
$\boldsymbol{D}$ diagonal distance of prismatic cross-section (diameter of equivalent circular column), in. (mm) $= \sqrt{b^2 + h^2}$
e_s eccentricity of prestressing steel with respect to centroidal axis of member at support, in. (mm)
e_m eccentricity of prestressing steel with respect to centroidal axis of member at midspan, in. (mm)
E_2 slope of linear portion of stress−strain model for FRP-confined concrete, psi (MPa)
E_c modulus of elasticity of concrete, psi (MPa)
E_f tensile modulus of elasticity of FRP, psi (MPa)
E_{ps} modulus of elasticity of prestressing steel, psi (MPa)
E_s modulus of elasticity of steel, psi (MPa)
f_c compressive stress in concrete, psi (MPa)
f'_c specified compressive strength of concrete, psi (MPa)
$\overline{f'_c}$ mean ultimate tensile strength of FRP based on a population of 20 or more tensile tests per ASTM D3039, psi (MPa)
$\sqrt{f'_c}$ square root of specified compressive strength of concrete
f'_{cc} compressive strength of confined concrete, psi (MPa)

f'_{co} compressive strength of unconfined concrete; also equal to $0.85 f'_c$, psi (MPa)
$f_{c,s}$ compressive stress in concrete at service condition, psi (MPa)
f_f stress level in FRP reinforcement, psi (MPa)
f_{fd} design stress of externally bonded FRP reinforcement, psi (MPa)
f_{fe} effective stress in the FRP; stress level attained at section failure, psi (MPa)
$f_{f,s}$ stress level in FRP caused by a moment within elastic range of member, psi (MPa)
f_{fu} design ultimate tensile strength of FRP, psi (MPa)
f^*_{fu} ultimate tensile strength of the FRP material as reported by the manufacturer, psi (MPa)
f_l maximum confining pressure due to FRP jacket, psi (MPa)
f_{ps} stress in prestressed reinforcement at nominal strength, psi (MPa)
f_{pu} specified tensile strength of prestressing tendons, psi (MPa)
f_s stress in nonprestressed steel reinforcement, psi (MPa)
f_{si} stress in the i-th layer of longitudinal steel reinforcement, psi (MPa)
$f_{s,s}$ stress level in nonprestressed steel reinforcement at service loads, psi (MPa)
f_y specified yield strength of nonprestressed steel reinforcement, psi (MPa)
$\boldsymbol{h}$ overall thickness or height of a member, in. (mm)
long side cross-sectional dimension of rectangular compression member, in. (mm)
h_f member flange thickness, in. (mm)
I_{cr} moment of inertia of cracked section transformed to concrete, in.^{4} (mm^4)
I_{tr} moment of inertia of uncracked section transformed to concrete, in.^{4} (mm^4)
k ratio of depth of neutral axis to reinforcement depth measured from extreme compression fiber
k_1 modification factor applied to k_v to account for concrete strength
k_2 modification factor applied to k_v to account for wrapping scheme
k_f stiffness per unit width per ply of the FRP reinforcement, lb/in. (N/mm); $k_f = E_f t_f$
l_{db} development length of near-surface-mounted (NSM) FRP bar, in. (mm)
l_{df} development length of FRP system, in. (mm)
L_e active bond length of FRP laminate, in. (mm)
M_{cr} cracking moment, in.-lb (N-mm)
M_n nominal flexural strength, in.-lb (N-mm)
M_{nf} contribution of FRP reinforcement to nominal flexural strength, lb-in. (N-mm)
M_{np} contribution of prestressing reinforcement to nominal flexural strength, lb-in. (N-mm)
M_{ns} contribution of steel reinforcement to nominal flexural strength, lb-in. (N-mm)
M_s service moment at section, in.-lb (N-mm)
M_{snet} service moment at section beyond decompression, in.-lb (N-mm)
M_u factored moment at a section, in.-lb (N-mm)
$\boldsymbol{n}$ number of plies of FRP reinforcement
n_f modular ratio of elasticity between FRP and concrete = E_f / E_c
n_s modular ratio of elasticity between steel and concrete = E_S / E_C
p_e effective force in prestressing reinforcement (after allowance for all prestress losses), lb (N)
p_n nominal axial compressive strength of a concrete section, lb (N)
P_{fu} mean tensile strength per unit width per ply of FRP reinforcement, lb/in. (N/mm)
P^*_{fu} ultimate tensile strength per unit width per ply of FRP reinforcement, lb/in. (N/mm); $P^*_{fu} = f^*_{fu}\, t_f$

$\boldsymbol{r}$	radius of gyration of a section, in. (mm)
r_c	radius of edges of a prismatic cross-section confined with FRP, in. (mm)
R_n	nominal strength of a member
$R_{n\phi}$	nominal strength of a member subjected to elevated temperatures associated with a fire
S_{DL}	dead load effects
S_{LL}	live load effects
t_f	nominal thickness of one ply of FRP reinforcement, in. (mm)
T_g	glass-transition temperature, °F(°C)
T_{gw}	wet glass-transition temperature, °F(°C)
T_{ps}	tensile force in prestressing steel, lb (N)
V_c	nominal shear strength provided by concrete with steel flexural reinforcement, lb (N)
V_f	nominal shear strength provided by FRP stirrups, lb (N)
V_n	nominal shear strength, lb (N)
V_s	nominal shear strength provided by steel stirrups, lb (N)
w_f	width of FRP reinforcing plies, in. (mm)
y_b	distance from centroidal axis of gross section, neglecting reinforcement, to extreme bottom fiber, in./in. (mm/mm)
y_t	vertical coordinate within compression region measured from neutral axis position. It corresponds to transition strain ε_t', in. (mm)
α_1	multiplier on fc' to determine intensity of an equivalent rectangular stress distribution for concrete
α_L	longitudinal coefficient of thermal expansion, in./in./°F (mm/mm/°C)
α_T	transverse coefficient of thermal expansion, in./in./°F (mm/mm/°C)
β_1	ratio of depth of equivalent rectangular stress block to depth of the neutral axis
ε_b	strain level in concrete substrate developed by a given bending moment (tension is positive), in./in. (mm/mm)
ε_{bi}	strain level in concrete substrate at time of FRP installation (tension is positive), in./in. (mm/mm)
ε_b	strain level in concrete, in./in. (mm/mm)
ε_c'	maximum strain of unconfined concrete corresponding to f_c', in./in. (mm/mm); may be taken as 0.002.
ε_{ccu}	ultimate axial compressive strain of confined concrete corresponding to $0.85fcc'$ in a lightly confined member (member confined to restore its concrete design compressive strength), or ultimate axial compressive strain of confined concrete corresponding to failure in a heavily confined member.
$\varepsilon_{c,s}$	strain level in concrete at service, in./in. (mm/mm)
ε_{ct}	concrete tensile strain at level of tensile force resultant in posttensioned flexural members, in./in. (mm/mm)
ε_{cu}	ultimate axial strain of unconfined concrete corresponding to $0.85fco'$ or maximum usable strain of unconfined concrete, in./in. (mm/mm), which can occur at $0.85fc'$ or 0.003, depending on the obtained stress−strain curve
ε_f	strain level in the FRP reinforcement, in./in. (mm/mm)
ε_{fd}	debonding strain of externally bonded FRP reinforcement, in./in. (mm/mm)
ε_{fe}	effective strain level in FRP reinforcement attained at failure, in./in. (mm/mm)
$\overline{\varepsilon_{fu}}$	mean rupture strain of FRP reinforcement based on a population of 20 or more tensile tests per ASTM D3039, in./in. (mm/mm)
ϵ_{fu}^*	ultimate rupture strain of FRP reinforcement, in./in. (mm/mm)

ε_{pe} effective strain in prestressing steel after losses, in./in. (mm/mm)
ε_{pi} initial strain level in prestressed steel reinforcement, in./in. (mm/mm)
$\varepsilon_{p\text{net}}$ net strain in flexural prestressing steel at limit state after prestress force is discounted (excluding strains due to effective prestress force after losses), in./in. (mm/mm)
ε_{ps} strain in prestressed reinforcement at nominal strength, in./in. (mm/mm)
ε_s strain level in nonprestessed steel reinforcement, in./in. (mm/mm)
ε_{sy} strain corresponding to yield strength of nonprestressed steel reinforcement, in./in. (mm/mm)
ε_t net tensile strain in extreme tension steel at nominal strength, in./in. (mm/mm)
ε_t' transition strain in stress−strain curve of FRP-confined concrete, in./in. (mm/mm)
κ_a efficiency factor for FRP reinforcement in determination of $f_{cc}^{'}$ (based on geometry of cross-section)
κ_b efficiency factor for FRP reinforcement in determination of ε_{ccu} (based on geometry of cross-section)
κ_v bond-dependent coefficient for shear
κ_ε efficiency factor equal to 0.55 for FRP strain to account for the difference between observed rupture strain in confinement and rupture strain determined from tensile tests
ρ_f FRP reinforcement ratio
ρ_g ratio of area of longitudinal steel reinforcement to cross-sectional area of a compression member (As/bh)
ρ_s ratio of nonprestressed reinforcement
σ standard deviation
τ_b average bond strength for NSM FRP bars, psi (MPa)
ϕ strength reduction factor
ψ_f FRP strength reduction factor
0.85 for flexure (calibrated based on design material properties)
0.85 for shear (based on reliability analysis) for three-sided FRP U-wrap or two-sided strengthening schemes
0.95 for shear fully wrapped sections

A.3 ISIS

Note: In some instances, documents S6-06 and S806-02 may use different symbols for the same parameter, hence the occasional dual symbols.

a depth of an equivalent rectangular stress block (mm)
A_F, A_{FRP} area of cross-section of an FRP bar, plate, sheet, or tendon (mm^2)
A_g gross area of section (mm^2)
A_{ps}, A_p area of prestressing tendons in tension zone (mm^2)
A_{ps} total area of steel tendons (mm^2)
A_s area of steel tension reinforcement (mm^2)
A'_s area of compression steel reinforcement (mm)
A_{sf} area of tension steel reinforcement which equilibrates the compression force in the slab portion of a T-section (mm)
A_{sj} area of intermediate longitudinal steel reinforcement placed on the sides of the element (mm)
A_{sw} remaining area of tension steel reinforcement in a T-section (mm)

A_v	area of shear steel reinforcement perpendicular to the axis of a member within a distance, s (mm^2)
$\boldsymbol{b}$	width of a rectangular section (mm)
b_e	effective width of compression face of member (mm)
b_{FRP}	width of FRP shear reinforcement measured perpendicular to the longitudinal axis of the element (mm)
b_v	effective web width within depth, d_v (mm)
b_w	width of web of a T-section (mm)
$\boldsymbol{c}$	distance from extreme compression face to neutral axis (mm)
$\boldsymbol{c'}$	distance from the neutral axis to the position where the compression strain is ε_c' in the concrete (mm)
C_b	distance from extreme compression face to neutral axis for balanced conditions (mm)
C_c	compressive resultant force from the concrete stressed lower than f_c' (N)
C_{cc}	compressive resultant force from the confined concrete (N)
C_f	compressive resultant force from the concrete in the slab portion of a T-section (N)
C_s	compressive resultant force from the compression steel (N)
C_w	compressive resultant force from the concrete in the web portion of a T-section (N)
$\boldsymbol{d}$	effective depth of a reinforced concrete component, being the distance from the extreme compression face to the centroid of the tension steel reinforcement (mm)
$\boldsymbol{d'}$	distance from extreme compression face to the centroid of compression steel reinforcement (mm)
$\boldsymbol{d_{sj}}$	distance from extreme compression face to the position of intermediate steel reinforcement (mm)
$\boldsymbol{d_v}$	S6-06: the effective shear depth for internal steel, as defined in Clause 8.9.1.5 of CSA S6-06 (mm)
$\boldsymbol{D}$	dead load (N)
$\boldsymbol{D_f}$, d_{FRP}	effective shear depth for FRP, calculated similar to d_v for steel reinforcement in accordance with Clause 8.9.1.5 of CSA S6-06, or the distance from extreme compression fiber to centroid of tension FRP reinforcement (mm)
D, D_g	diameter of a circular column or equivalent diameter of a rectangular column (mm)
$\boldsymbol{E_c}$	modulus of elasticity of concrete (MPa)
$\boldsymbol{E_f}$	modulus of elasticity of the fibers (MPa)
$\boldsymbol{E_F}$, E_{FRP}	modulus of elasticity of FRP (MPa)
$\boldsymbol{EI}$	flexural stiffness of the element (N-mm^2)
E_m	modulus of elasticity of the resin matrix (MPa)
E_p	modulus of elasticity of steel tendons (MPa)
E_s	modulus of elasticity of steel (MPa)
f_c	compression stress in concrete (MPa)
f_c'	specified compressive strength of concrete (MPa)
f_{cc}'	compressive strength of confined concrete (MPa)
f_{cr}	cracking strength of the concrete (MPa)
f_f	tensile strength of the fibers (MPa)
$\boldsymbol{f_F}$, f_{FRP}	tensile stress in a given direction, generally the fiber direction, of a FRP (MPa)
$\boldsymbol{f_{Fu}}$, f_{FRPu}	specified tensile strength of an FRP bars, plates, sheets, or tendons (MPa)
f_l,f_{lFRP}	confinement pressure due to FRP strengthening at the ULS (MPa)

f_m tensile strength of the resin matrix (MPa)
f_{po} stress in prestressed steel reinforcement when stress in the surrounding concrete is zero (MPa)
f_{pu} specified tensile strength of prestressing steel (MPa)
f_s tensile stress in steel reinforcement (MPa)
f'_s compressive stress in steel reinforcement (MPa)
f_{se} effective stress in the prestressing steel after losses (MPa)
f_Y specified yield strength of steel reinforcement (MPa)
$\boldsymbol{F}$ live load capacity factor
F_{sj} resultant force from the intermediate steel (N)
$\boldsymbol{h}$ overall thickness of a component (mm)
lateral dimension of the cross-section in the direction considered (mm)
longer dimension of a column (mm)
h_f slab thickness (mm)
h_{FRP} height of FRP bonded on the lateral side of the member (mm)
$\boldsymbol{k}$ effective length factor for compression elements
k_1 concrete strength factor as defined in Clause 16.11.3.2 of CSA S6-06
k_2 a nondimensional factor as defined in Clause 16.11.3.2 of CSA S6-06
k_c confinement coefficient
k_e strength reduction factor applied for unexpected eccentricities
k_l confinement parameter
K_ν bond reduction coefficient for externally bonded FRP stirrups
l_a minimum required anchorage length for externally bonded FRP beyond the point where no strengthening is required (mm)
l_n clear span of flexural member (mm)
l_u unsupported length of a compression member (mm)
$\boldsymbol{L}$ width of shear wall (mm)
unsupported length of a flexural member measured from center to center of supports (m)
live load (N)
L_e effective anchorage length of external FRP shear reinforcement (mm)
M_1 value of the smaller end moment at the ULS due to factored loads acting on a compression member, to be taken as positive if the member is bent in single curvature and negative if it is bent in double curvature (N-mm)
M_2 value of the larger end moment at the ULS due to factored loads acting on a compression member, always taken as positive (N-mm)
M_f factored moment at a section (N-mm)
M_r factored flexural resistance of a section in bending (N-mm)
M_{rf} resisting moment corresponding to slab portion of a T-section (N-mm)
M_{rw} resisting moment corresponding to web portion of a T-section (N-mm)
N_f factored axial load normal to the cross-section occurring simultaneously with, V_f (N)
P_D axial dead load (N)
P_E axial earthquake load (N)
P_f factored axial load at a section at the ULS (N)
P_L axial live load (N)
P_r factored axial load resistance (N)
factored axial resistance of a section in compression with minimum eccentricity (N)

P_{ro}	factored axial load resistance at zero eccentricity of the unconfined section (N)
r	radius of gyration of gross cross-section (mm)
s	spacing of steel shear reinforcement measured parallel to the longitudinal axis of the member (mm)
S_F, S_{FRP}	spacing of externally bonded FRP bands on concrete for shear strengthening measured along the axis of the member or unit width (i.e., 1.0) of a continuous FRP shear reinforcement (mm)
S_{ze}	equivalent crack spacing parameter (mm)
t_i, t_{FRP}	total thickness of externally bonded FRP plates or sheets (mm)
T_{FRP}	tensile resultant force from the longitudinal FRP (N)
$T_{FRP,force}$	tensile resultant force from the longitudinal FRP bonded on the tension face (N)
$T_{FRP,side}$	resultant force from the longitudinal FRP subjected to tension and bonded on the sides of the section (N)
T_g	glass-transition temperature (°C)
T_{gw}	wet glass-transition temperature (°C)
T_s	tensile resultant force from the tension steel (N)
V_c	factored shear resistance attributed to the concrete (N)
ν_f	volumetric ratio of fibers within the FRP
V_f	factored shear force at the section (N)
V_F, V_{FRP}	factored shear resistance provided by FRP shear reinforcement (N)
ν_m	volumetric ratio of resin matrix within the FRP
V_P	factored shear resistance provided by the component in the direction of the applied shear of all the effective prestressing forces; positive if resisting the applied shear (N)
V_r	factored shear resistance (N)
V_s	factored shear resistance provided by steel shear reinforcement (N)
w_{FRP}	width of FRP sheet measured perpendicular to the direction of main fibers (mm)
α	depth of an equivalent rectangular stress block (mm)
α_1	ratio of average stress in rectangular compression block to the specified concrete compressive strength
α_D	load factor for dead load
α_L	load factor for live load
α, α_P	angle of inclination of steel tendon force to the longitudinal axis of the member
β, θ	angle of inclination of the transverse reinforcement to the longitudinal axis of the member
β_1	ratio of the depth of rectangular compression block to the depth of the neutral axis
β_v, β	factor to account for the shear resistance of cracked concrete
γ_c	mass density of concrete (kg/m)
δ	design lateral drift ratio
Δf_c	additional concrete stress due to confinement (MPa)
ε_c	strain in concrete
ε_{ci}	initial strain in concrete
ε'_c	strain in concrete at f'_c
ε'_{cc}	strain in concrete at f'_{cc}
ε_{cu}	ultimate compressive strain of concrete
$\varepsilon_{Fi}, \varepsilon_{ft}$	initial tensile strain at the location of FRP before applying FRP
$\varepsilon_F, \varepsilon_{FRP}$	strain in FRP reinforcement
ε_{FRPe}	effective strain in FRP

ε_{FRPt}	maximum permitted tensile strain in FRP flexural strengthening system
$\varepsilon_{Fu}, \varepsilon_{FRPu}$	ultimate strain of FRP
ε_s	tensile strain in tension steel reinforcement
ε'_s	compressive strain in compression steel reinforcement
ε_{si}	initial tensile strain in tension steel reinforcement
ε'_{si}	initial compressive strain in compression steel reinforcement
ε_{sj}	tensile strain in intermediate steel reinforcement
ε_x	longitudinal strain
ε_y	yield strain of steel
$\boldsymbol{\theta}$	angle of inclination of the principal diagonal compressive stress to the longitudinal axis of the member
$\boldsymbol{\lambda}$	parameter depending on the density of concrete
ϕ_c	resistance factor for concrete
ϕ_F, ϕ_{FRP}	resistance factor for FRP
ω_D	linear dead load (kN/m)
ω_L	linear live load (kN/m)

A.4 CNR-DT 200/2004

$(.)_c$	value of quantity (.) for concrete
$(.)_{cc}$	value of quantity (.) for confined concrete
$(.)_d$	design value of quantity (.)
$(.)_f$	value of quantity (.) for the fiber-reinforced composite
$(.)_k$	characteristic value of quantity (.)
$(.)_{mc}$	value of quantity (.) for confined masonry
$(.)_R$	value of quantity (.) as resistance
$(.)_s$	value of quantity (.) for steel
$(.)_S$	value of quantity (.) as demand
A_c	area of concrete cross-section, net of steel reinforcement
A_f	area of FRP reinforcement
A_{fw}	area of FRP shear reinforcement
A_l	overall area of longitudinal steel reinforcement
A_{sw}	area of one stirrup leg
As_1	area of steel reinforcement subjected to tension
A_{s2}	area of steel reinforcement subjected to compression
b_f	width of FRP reinforcement
d	distance from extreme compression fiber to centroid of tension reinforcement
E_c	Young's modulus of elasticity of concrete
E_f	Young's modulus of elasticity of FRP reinforcement
E_{fib}	Young's modulus of elasticity of fiber itself
E_m	Young's modulus of elasticity of matrix
E_s	Young's modulus of elasticity of steel reinforcement
f_{bd}	design bond strength between FRP reinforcement and concrete (or masonry)
f_{bk}	characteristic bond strength between FRP reinforcement and concrete (or masonry)
f_c	concrete compressive strength (cylindrical)
f_{ccd}	design strength of confined concrete
f_{cd}	design concrete compressive strength
f_{ck}	characteristic concrete compressive strength

f_{ctm}	mean value of concrete tensile strength
f_{fd}	design strength of FRP reinforcement
f_{fdd}	design debonding strength of FRP reinforcement (mode 1)
$f_{fdd,2}$	design debonding strength of FRP reinforcement (mode 2)
f_{fed}	effective design strength of FRP shear reinforcement
f_{fk}	characteristic strength of FRP reinforcement
f_{fpd}	design debonding strength of FRP reinforcement
f_l	confining lateral pressure
$f_{l,\mathrm{eff}}$	effective confining pressure
f_{mk}	characteristic compressive strength of masonry
f_{mk}^{h}	characteristic compressive strength of masonry in the horizontal direction
f_{mcd}	characteristic compressive strength of FRP-confined masonry
f_{md}	design compressive strength of masonry
f_{md}^{h}	design compressive strength of masonry in the horizontal direction
f_{mtd}	design tensile strength of masonry
f_{mtk}	characteristic tensile strength of masonry
f_{mtm}	mean value of the tensile strength of masonry
f_{vd}	design shear strength of masonry
f_{vk}	characteristic shear strength of masonry
f_y	yield strength of longitudinal steel reinforcement
f_{yd}	design yield strength of longitudinal steel reinforcement
f_{ywd}	design yield strength of transverse steel reinforcement
$F_{\mathrm{max},d}$	design value of the maximum tensile force transferred by FRP reinforcement to the concrete support
F_{pd}	design value of the maximum anchorage force transferred by FRP reinforcement bonded on a masonry structure in the presence of a force perpendicular to the bonded surface area
G_a	shear modulus of adhesive
G_c	shear modulus of concrete
h	section depth
I_o	moment of inertia of cracked and un-strengthened reinforced concrete section
I_1	moment of inertia of cracked and FRP-strengthened reinforced concrete section
I_c	moment of inertia of transformed section
I_f	moment of inertia of FRP reinforcement about its centroidal axis, parallel to the beam neutral axis
k_{eff}	coefficient of efficiency for confinement
k_H	coefficient of efficiency in the horizontal direction
k_V	coefficient of efficiency in the vertical direction
k_α	Coefficient of efficiency related to the angle of fibers respect to the longitudinal axis
l_b	bond length
l_e	optimal bond length
M_{Rd}	flexural capacity of FRP-strengthened member
M_{Sd}	factored moment
M_o	bending moment acting before FRP strengthening
M_1	bending moment applied to the RC section due to loads applied after FRP strengthening
$N_{Rcc,d}$	axial capacity of FRP-confined concrete member
$N_{Rmc,d}$	axial capacity of FRP-confined masonry

N_{Sd}	factored axial force
p_b	distance between layers of bars in the confinement of masonry columns
p_f	spacing of FRP strips or discontinuous FRP U-wraps
P_{fib}	weight fraction of fibers
P_m	weight fraction of the matrix
s	interface slip
s_f	interface slip at full debonding
t_f	thickness of FRP laminate
T_g	glass-transition temperature of the resin
T_m	melting temperature of the resin
T_{Rd}	torsional capacity of FRP-confined concrete member
$T_{Rd,f}$	FRP contribution to the torsional capacity
$T_{Rd,\max}$	torsional capacity of the compressed concrete strut
$T_{Rd,s}$	steel contribution to the torsional capacity
T_{Sd}	factored torsion
T_x	Yarn count in x direction
V_{fib}	volumetric fraction of fibers
V_{Rd}	shear capacity of FRP-strengthened member
$V_{\mathrm{Rd,ct}}$	concrete contribution to the shear capacity
$V_{\mathrm{Rd,max}}$	maximum concrete contribution to the shear capacity
$V_{\mathrm{Rd,s}}$	steel contribution to the shear capacity
$V_{\mathrm{Rd,f}}$	FRP contribution to the shear capacity
$V_{\mathrm{Rd,m}}$	masonry contribution to the shear capacity
V_{Sd}	factored shear force
w_f	width of FRP laminate
x	distance from extreme compression fiber to neutral axis
α_{fE}	safety coefficient for fabric stiffness
α_{ff}	safety coefficient for fabric strength
γ_m	partial factor for materials
γ_{Rd}	partial factor for resistance models
Γ_{Fk}	characteristic value of specific fracture energy
Γ_{Fd}	design value of specific fracture energy
ε_{o}	concrete strain on the tension fiber prior to FRP strengthening
ε_c	concrete strain on the compression fiber
ε_{ccu}	design ultimate strain of confined concrete
ε_{co}	concrete strain on the compression fiber prior to FRP strengthening
ε_{cu}	ultimate strain of concrete in compression
ε_f	strain of FRP reinforcement
ε_{fd}	design strain of FRP reinforcement
$\varepsilon_{fd,rid}$	reduced design strain of FRP reinforcement for confined members
ε_{fk}	characteristic rupture strain of FRP reinforcement
ε_{fdd}	maximum strain of FRP reinforcement before debonding
ε_{mcu}	ultimate compressive strain of confined masonry
ε_{mu}	ultimate compressive strain of masonry
ε_{s1}	strain of tension steel reinforcement
ε_{s2}	strain of compression steel reinforcement
ε_{yd}	design yield strain of steel reinforcement
η	conversion factor
ν_{fib}	Poisson's ratio of fibers

ν_m Poisson's ratio of matrix
ρ_{fib} fiber density
ρ_m matrix density
σ_c stress in the concrete
σ_f stress in FRP reinforcement
σ_s stress in tensile steel reinforcement
σ_{Sd} stress normal to masonry face acting on the bonded surface area between FRP reinforcement and masonry
$\tau_{b,e}$ equivalent shear stress at the adhesive-concrete interface
ϕ_u curvature at ultimate
ϕ_y curvature at yielding

A.5 TR-55

$\boldsymbol{A_f}$ area of FRP
$\boldsymbol{A_{fa}}$ area of effectively anchored additional FRP tensile reinforcement
$\boldsymbol{A_{fa}}$ area of FRP shear reinforcement
A_s area of tensile steel reinforcement
A_s' area of compression steel reinforcement
$\boldsymbol{b}$ width of section
b_a width of adhesive layer
b_f width of plate
b_w beam width or plate spacing for solid slab
$\boldsymbol{d}$ effective depth of section
$\boldsymbol{d'}$ effective depth of compression steel
d_f effective depth of FRP shear reinforcement
$\boldsymbol{D}$ diameter of column
E_c modulus of elasticity of concrete
E_f modulus of elasticity of FRP
E_{fd} design elastic modulus of FRP
E_{fk} characteristic elastic modulus of FRP
E_i initial tangent modulus of concrete
E_o, E_1 secant modulus of concrete
E_p postcrushing tangent modulus
E_s modulus of elasticity of steel
$E_{\theta\theta}$ hop modulus of FRP
f_{cc} confined concrete compressive strength
f_{ccd} design confined concrete compressive strength
f_{cck} characteristic confined concrete compressive strength $= f_{co} + 4.1 \times 0.85\, f_{fu}\, t_f/R$
f_{ck} characteristic compressive cylinder strength of concrete$\approx 0.85 f_{cu}$
f_{co} unconfined concrete compressive strength
f_{ctm} tensile strength of concrete $= 0.18\ (f_{cu})^{2/3}$
f_{cu} characteristic compressive cube strength of concrete
f_f design tensile strength of FRP
f_{fd} ultimate design tensile strength of FRP
f_{fk} characteristic tensile strength of FRP
f_{fm} mean tensile strength of FRP
f_0 intercept of postcrushing tangent modulus with the stress axis $= f_{cu}(E_i - E_p)/(E_i - E_l)$

f_r	confinement pressure
f_y	characteristic tensile strength of steel reinforcement
$f_y^{'}$	compressive strength of steel reinforcement
F_f	tensile force in FRP
F_s	tensile force in steel reinforcement
$F_s^{'}$	compressive force in steel reinforcement
$\boldsymbol{G}$	dead load
$\boldsymbol{h}$	overall depth of member
I_{ce}	second moment of area of existing concrete equivalent transformed cracked section
I_{cs}	second moment of area of strengthened concrete transformed cracked section
l_t	anchorage length
$l_{t,\max}$	maximum anchorage length
L_e	effective bond length
$\boldsymbol{M}$	design ultimate moment
M_{add}	additional required moment capacity
M_0	moment capacity of existing beam
M_r	design resistance moment of strengthened section
$M_{r,b}$	balanced moment of resistance
M_s	service moment based on unfactored permanent loads
M_u	ultimate moment
$\boldsymbol{Q}$	live load
$\boldsymbol{R}$	radius of column
s_f	spacing of FRP strips
T_k	characteristic bond failure force
$T_{k,\max}$	ultimate bond failure force
t_f	thickness of FRP
V	ultimate shear force at the plate end
V_{Rc}	shear resistance of concrete
V_{Re}	shear resistance of existing member
V_{Rf}	shear resistance of FRP
V_{Rl}	shear resistance of links
$V_{R,\max}$	maximum shear resistance of member
V_{Rs}	shear resistance of strengthened member
V_s	shear force due to ultimate loads
V_{sd}	design shear force
$V_{\max}$	maximum permissible shear stress
w_f	width of FRP shear reinforcement strips
w_{fe}	effective width of FRP
x	depth of neutral axis of existing member
$\boldsymbol{z}$	lever arm
α_c	modular ratio of steel to concrete
α_f	modular ratio of FRP to concrete
$\boldsymbol{\beta}$	angle between FRP and the longitudinal axis of the member = 45° or 90°
γ_{mA}	partial safety factor for adhesive
γ_{mc}	partial safety factor for concrete
γ_{mE}	partial safety factor for modulus of elasticity of FRP
γ_{mF}	partial safety factor for FRP
γ_{mf}	partial safety factor for strength of FRP
γ_{mm}	partial safety factor for manufacture of FRP

γ_{ms} partial safety factor for steel
ϵ_{cc} axially confined concrete strain
ϵ_{ccu} ultimate axial confined concrete strain = $\epsilon_{fu}/\nu_c \left(1 + \sqrt{\frac{f_{c0}R}{f_{fu}t_f}}\right)$
ϵ_{cft} final tensile strain of concrete
ϵ_{cic} initial compressive strain of concrete due to M_s
ϵ_{cit} initial tensile strain of concrete due to M_s
ϵ_{cu} ultimate compressive strain of (unconfined) concrete = 0.0035
ϵ_{fe} effective FRP strain
ϵ_{fk} characteristic failure strain of FRP
ϵ_{fu} design ultimate strain of FRP
ϵ_y yield strain of steel = 0.002
υ_c poisson's ratio for concrete = 0.2
ρ_f FRP shear reinforcement ratio
$\boldsymbol{\tau}$ longitudinal shear stress

This page intentionally left blank

Appendix B: Inspection checklist

The following checklist summarizes the primary items recommended in earlier chapters to verify successful fiber-reinforced polymer (FRP) system installation.

General

- "As-built" plans are being updated to reflect field revisions.

Contractor submittal and training

- Contractor has submitted a quality control plan and safety data sheets (SDSs).
- Contractor has submitted qualifications of the installation crew.
- Contractor has submitted calibration documentation of measuring and testing equipment.
- Site staff members properly trained and informed regarding technical inspection and testing requirements.
- Site staff members are properly trained on emergency and accident procedures.

Materials

- Material property test results are based on a minimum of 10 samples per test.
- Fiber properties including tensile strength, modulus, and ultimate strain are provided.
- The mean and coefficient of variation of the moisture equilibrium content are determined per ASTM D 5229 and are not greater than 2% and 10%, respectively.
- Epoxy property information includes epoxy tensile strength, modulus, infrared spectrum analysis, glass transition temperature, gel time, pot life, and adhesive shear strength.
- The glass transition temperature is determined per ASTM D4065 and is at least 40°F higher than the maximum design temperature (see Section 3.12.2.2 of the *AASHTO LRFD Bridge Design Specifications*).
- After conditioning as specified below the glass transition temperature and tensile strain is to retain 85% of the required values. The conditioning environments are:
  - Water: Samples are immersed in distilled water having a temperature of 100 ± 3°F and tested after 1000 h of exposure.
  - Alternating UV and humidity: Samples are conditioned under Cycle 1-UV exposure per ASTM G154, and tested within 2 h after removal.
  - Alkali: Samples are immersed in calcium hydroxide (pH $\sim$11) at ambient temperature for 1000 h prior to testing.
  - Freeze–thaw: Samples are exposed to 100 repeated cycles of freezing and thawing per ASTM C666.
- If impact tolerance is stipulated by the engineer, it is determined per ASTM D7136.
- Daily inspection during installation should include the following test measurements:
  - Ambient temperature, relative humidity, and general weather observations.
  - Surface temperature of concrete.
  - Surface dryness per ACI 503.4.
  - Level of resin curing in accordance with ASTM D2582.
  - Adhesion strength, to exceed 200 psi.

- The submitted sample results have been from certified mill analyses and third-party laboratories.
- All materials meet acceptance requirements.
- All materials not meeting acceptance requirements have been properly disposed.
- The following design parameters are clearly listed on the structural engineering submittals for a nonprestressed beam flexural strengthening project. Note: Depending on the specific design application, not all of the following parameters may be needed:
  - Concrete compressive strength of precast beam,
  - Modulus of elasticity of concrete,
  - Reinforcing steel yield strength,
  - Steel reinforcement area,
  - Modulus of elasticity of steel,
  - Internal shear reinforcement and its spacing,
  - FRP plate/sheet thickness,
  - Ultimate tensile strain in the FRP at failure,
  - Tensile strength in the FRP at ultimate strain,
  - Glass transition temperature,
  - Shear modulus of the adhesive,
  - Modulus of elasticity of fiber,
  - Total height of beam including deck slab,
  - Flange thickness,
  - Effective width of the flange,
  - Bridge span length,
  - Distance from extreme compression fiber to steel centroid,
  - New nominal loads for fatigue limit state,
  - Shear force at reinforcement end-termination,
  - New load capacity needed.
- In the case of a prestressed concrete beam designed for flexural strengthening, the following parameters may be added to the above list:
  - Concrete compressive strength of the deck,
  - Area of prestress tendons,
  - Diameter of tendons,
  - Initial pretensioning at service limit state,
  - Yield strength,
  - Ultimate stress,
  - Type of strands,
  - Distance from extreme compression fiber to strand centroid.
- When designing for shear strengthening of a nonprestressed member, the following parameters may be needed:
  - Concrete compressive strength of precast beam,
  - Modulus of elasticity of concrete,
  - Reinforcing steel yield strength,
  - Steel reinforcement area,
  - Modulus of elasticity of steel,
  - Internal shear reinforcement and its spacing,
  - FRP plate/sheet thickness,
  - Ultimate tensile strain in the FRP at failure,
  - Tensile strength in the FRP at ultimate strain,
  - Modulus of elasticity of FRP,
  - Tensile strength of FRP at ultimate strain,

Orientation of FRP sheets,
Width of FRP sheets,
Center-to-center spacing of FRP sheets,
Total height of beam including deck slab,
Flange thickness,
Effective width of the flange,
Bridge span length,
Distance from extreme compression fiber to steel centroid,
Effective depth of FRP sheets,
Width of the web,
New shear capacity needed.

- When designing for shear strengthening of a prestressed member, the following parameters may be added to the above list:
  Concrete compressive strength of the deck,
  Area of prestress tendons,
  Diameter of tendons,
  Initial pretensioning at service limit state,
  Yield strength of tendons,
  Ultimate stress of tendons,
  Type of strands,
  Effective depth from extreme compression fiber to centroid of reinforcement.
- Design parameters required for column wrapping (confinement) include:
  Concrete compressive strength,
  Reinforcing steel yield strength,
  Steel reinforcement area,
  Tie or spiral spacing,
  Area of strands,
  Initial pretensioning at service limit state,
  Modulus of elasticity of strands,
  FRP sheet thickness,
  Ultimate tensile strain of the FRP
  Modulus of elasticity of FRP
  Tensile strength of FRP at ultimate strain,
  Column geometry,
  Column height,
  Ultimate axial load to resist.

FRP shipping, storage, and handling

- All packages received include SDSs.
- Packages are inspected upon delivery for damage.
- FRP systems are stored in accordance with the manufacturer's guidelines.
- Catalysts and initiators are stored separately.
- Chemical components are securely sealed per OSHA standards.
- Flammable resins are stored in accordance with fire regulations.
- Expired materials are disposed of in accordance with environmental control regulations.
- Hazardous materials such as thermosetting resins are properly labeled.
- SDSs are accessible to all at the project site and are read and understood by personnel handling hazardous materials.
- Proper gear (suits, gloves, dust masks, respirators, etc.) is available for handling resins, solvents, and fiber materials.

- The resin mixing area is well ventilated.
- Waste materials are disposed in accordance with environmental regulations.

Removal and restoration of defective surfaces prior to concrete placement

- The perimeters of existing spalls have been identified and saw cut to a minimum depth of 0.75 in. to prevent feathered edges.
- Cracks in the concrete wider than 0.01 in. spaced closer than 1.5 in. and cracks wider than 1/32 in. have been filled using pressure injected epoxy.
- After removal of all defective areas, contractor inspected and cleaned the substrate from any dust, laitance, grease, oil, curing compounds, wax, impregnations, foreign particles, and other bond-inhibiting materials.
- All exposed steel has been sandblasted clean prior to concrete placement.
- The contractor applied bonding and reinforcement protection to all exposed reinforcement and concrete surfaces prior to concrete placement.

Inspection of surface preparation prior to FRP application

- All inside and outside corners and sharp edges were rounded or chamfered to a minimum radius of 1/2 in.
- The restored concrete surface is smooth and uniform with a maximum out of plane deviation of 1/32 in.
- All voids with diameters larger than 1/2 in. and depressions greater than 1/16 in. were filled cured.
- Cracks in the concrete wider than 0.01 in. spaced closer than 1.5 in. and cracks wider than 1/32 in. have been filled using pressure injected epoxy.
- The surface was checked and cleaned of any dust, laitance, grease, oil, curing compounds, wax, impregnations, surface lubricants, paint coatings, stains, foreign particles, weathered layers, and any other bond-inhibiting materials.
- The substrate concrete compressive strength was checked to be 2.2 ksi or greater, and tensile strength to be 220 psi or greater.

Application conditions

- The ambient temperature and temperature of concrete surface were within the range of 50−90°F.
- Contact surfaces were completely dry at the time of installation of the FRP system.
- The weather forecast predicts dry conditions. If rain began, the application was stopped untill dry conditions returned.

Installation of wet lay-up systems

- Field data including temperature, surface condition, and relevant field observations were documented.
- Witness panels were prepared with a size of at least 300−775 $in.^2$, but not less than 0.5% of the overall area to be strengthened.
- Resin was mixed in quantities sufficiently small to ensure its use within manufacturer recommended pot life.
- Excess resin was disposed of when it exceeded its pot life, or when it began to generate heat or showed signs of increased viscosity.
- The ambient and concrete surface temperatures were present as specified in the contract drawings and recommended by the manufacturer.

- Excess primer was disposed of when it exceeded its pot life.
- The putty, if necessary, was applied as soon as the primer became tack-free or until non-sticky to the fingers.
- The surfaces of primer and putty were protected from dust, moisture and other contaminants before the FRP system was applied.
- The fiber sheet was placed properly and pressed gently onto the wet saturant.
- Any entrapped air between the fiber sheet and concrete was released.
- Rolling was conducted in the fiber direction for unidirectional fiber sheets.
- Sufficient saturant was applied on top of the fiber sheet as an overcoat to fully saturate the fibers.
- Lap splice lengths were as specified in the contract drawings, and at least 8 in.
- There was no deviation in fiber alignment by more than 5 degree.
- The FRP system was protected as necessary until it was fully cured.

Identification of defective work

- No voids or air encapsulation (pockets) were found between the concrete and the layers of primer, resin and/or adhesive, or within the composite itself.
- Delaminations larger than 2 in.^{2} (1300 mm^2) were scanned for (using acoustic sounding, ultrasonic, or thermography). If more than 10 such delaminations were detected in 10 ft.^{2}, they were repaired.
- There is no wrinkling or buckling of fiber, fiber tows, or discontinuities due to fracture of the fibers.
- There are no resin-starved areas or areas with nonuniform impregnation/wet-out.
- There are no cracks, blisters, or peeling of the surface coating.
- There is no under-cured or incompletely cured polymer.
- There are no incorrectly placed reinforcement configurations.

Postinstallation quality control tests

- A surface inspection was performed for any swelling, bubbles, voids, or delaminations after at least 24 h of initial resin cure. If advanced equipment is unavailable, an acoustic tap test was performed with a hard object to identify delaminated areas by sound. All voids were marked and assessed for size to determine if repair is needed.
- Direct pull-off testing according to ASTM D4541, ASTM D7234, or the method described by ACI 440.3R (2004), Test Method L.1, was conducted. Successful tension adhesion strengths should exceed the greatest of 200 psi or 0.065 $\sqrt{f_c'}$ ksi, and exhibit failure of the concrete substrate.
- Areas after unsuccessful bonding tests were repaired according to the procedures established in the contract drawings and specifications.

Long-term maintenance inspections

- An annual general inspection is conducted, primarily visual in nature. In the annual inspection, the inspector looks for changes in color, signs of crazing, cracking, delamination/debonding, peeling, blistering, deflection, or evidence of other deterioration, in addition to local damage due to impact or surface abrasion.
- A detailed inspection is conducted at least once every 6 years, where the inspection attempts to more accurately quantify the performance and condition of the FRP system. Pull-off testing and test evaluation for debonding and FRP degradation are performed as part of detailed testing.

This page intentionally left blank

References

AASHTO, 2002. Standard Specifications for Highway Bridges. seventeenth ed. American Association of State Highway and Transportation Officials, Washington, DC.

AASHTO, 2012. Guide Specifications for Design of Bonded FRP Systems for Repair and Strengthening of Concrete Bridge Elements. first ed. American Association of State Highway and Transportation Officials, Washington, DC.

AASHTO LRFD, 1994. Bridge Design Specifications. first ed. American Association of State Highway and Transportation Officials, Washington, DC.

AASHTO LRFD, 2010. Bridge Design Specifications. fifth ed. American Association of State Highway and Transportation Officials, Washington, DC.

AC 125, 2010. Acceptance Criteria for Concrete and Reinforced and Unreinforced Masonry Strengthening Using Externally Bonded Fiber-Reinforced Polymer (FRP) Composite Systems, International Code Council.

ACI 201.1R-08, 2008. Guide for Conducting a Visual Inspection of Concrete in Service. American Concrete Institute, Farmington Hills, MI.

ACI 201.2R-08, 2008. Guide to Durable Concrete. American Concrete Institute, Farmington Hills, MI.

ACI 224.1R, 2007. Causes, Evaluation, and Repair of Cracks in Concrete Structures. American Concrete Institute, Farmington Hills, MI.

ACI 318-11, 2011. Building Code Requirements for Structural Concrete and Commentary. American Concrete Institute, Farmington Hills, MI.

ACI 364.1R-94, 1994. Guide for Evaluation of Concrete Structures Prior to Rehabilitation. American Concrete Institute, Farmington Hills, MI.

ACI 440.2R-08, 2008. Guide for the Design and Construction of Externally Bonded FRP Systems for Strengthening Concrete Structures. American Concrete Institute, Farmington Hills, MI.

ACI 440.3R-04, 2004. Guide Test Methods for Fiber-Reinforced Polymers (FRPs) for Reinforcing or Strengthening Concrete Structures. American Concrete Institute, Farmington Hills, MI.

ACI 440R-07, 2007. Report on Fiber-Reinforced Polymer (FRP) Reinforcement for Concrete Structures. American Concrete Institute, Farmington Hills, MI.

ACI 503.4, 2003. Standard Specification for Repairing Concrete with Epoxy Mortars. American Concrete Institute, Farmington Hills, MI.

ACI 503R, 1998. Use of Epoxy Compounds with Concrete. American Concrete Institute, Farmington Hills, MI.

ACI 530-05, 2005. Building Code Requirements for Masonry Structures. American Concrete Institute, Farmington Hills, MI.

ACI 546R, 2004. Concrete Repair Guide. American Concrete Institute, Farmington Hills, MI.

ACI SP-215, 2003. Field Applications of FRP Reinforcement: Case Studies. American Concrete Institute, Farmington Hills, MI.

Aiello, M.A., Galati, N., Tegola, L.A., 2001. Bond analysis of curved structural concrete elements strengthened using FRP materials. In: Fifth International Symposium on Non-Metallic (FRP) Reinforcement for Concrete Structures (FRPRCS-5), Cambridge-Thomas Telford, London, pp. 680–688.

Akers, S.A.S., Studinka, J.B., 1989. Ageing behaviour of cellulose fibre cement composites in natural weathering and accelerated tests. Int. J. Cem. Comp. Ltwt. Concr. 11 (2), 93–97.

American National Standards Institute (ANSI), 2010. Z-129.1, Hazardous Industrial Chemicals Precautionary Labeling.

Ang, H.-S., Tang, W.H., 2007. Probability Concepts in Engineering. John Wiley & Sons, NJ.

Ansley, M., et al., 2009. Thermo-Mechanical Durability of Carbon Fiber Reinforced Polymer Strengthened Reinforced Concrete Beams. Final Report, Florida DOT, Project No. BD550-06.

Araki, N., Matsuzaki, Y., Nakano, K., Kataoka, T., Fukuyama, H., 1997. Shear capacity of retrofitted RC members with continuous fiber sheets, Non-Metallic (FRP) Reinforcement for Concrete Structures, 1. Japan Concrete Institute, Tokyo, Japan, pp. 515–522.

Arduini, M., et al., 1999. II confinamento passivoo di elementi compressi in calcestruzzo con fogli di material composito. Industria Italiana Del Cementa.

Arduini, M., Nanni, A., 1997. Behavior of pre-cracked rc beams strengthened with carbon FRP sheets. J. Compos. Constr. 1 (2), 63–70.

ASTM C666/C666M, 2008. Standard Test Method for Resistance of Concrete to Rapid Freezing and Thawing.

ASTM D2582, 2009. Standard Test Method for Puncture-Propagation Tear Resistance of Plastic Film and Thin Sheeting.

ASTM D2583-07, 2007. Standard Test Method for Indentation Hardness of Rigid Plastics by Means of a Barcol Impressor.

ASTM D3039/D3039M-08, 2008. Standard Test Method for Tensile Properties of Polymer Matrix Composite Materials.

ASTM D3418, 2003. Standard Test Method for Transition Temperatures and Enthalpies of Fusion and Crystallization of Polymers by Differential Scanning Calorimetry.

ASTM D4065-12, 2012. Standard Practice for Plastics: Dynamic Mechanical Properties: Determination and Report of Procedures.

ASTM D4541, 2002. Standard Test Method for Pull-Off Strength of Coatings Using Portable Adhesion Testers.

ASTM D5229/D5229M, 2010. Standard Test Method for Moisture Absorption Properties and Equilibrium Conditioning of Polymer Matrix Composite Materials.

ASTM D7136/D7136M, 2007. Standard Test Method for Measuring the Damage Resistance of a Fiber-Reinforced Polymer Matrix Composite to a Drop-Weight Impact Event.

ASTM D7234-12, 2012. Standard Test Method for Pull-Off Adhesion Strength of Coatings on Concrete Using Portable Pull-Off Adhesion Testers.

ASTM E632-82, 1996. Standard Practice for Developing Accelerated Tests to Aid Prediction of the Service Life of Building Components and Materials. ASTM, West Conshohocken, PA.

ASTM G154, 2012. Standard Practice for Operating Fluorescent Ultraviolet (UV) Lamp Apparatus for Exposure of Nonmetallic Materials.

Bakht, B., Csagoly, P.F., 1980. Diagnostic testing of a bridge. J. Struct. Div. 106 (7), 1515–1529.

Bakht, B., Jaeger, L.G., 1990. Bridge testing. A surprise every time. J. Struct. Eng. N. Y. 116 (5), 1370–1383.

Bank, L.C., Puterman, M., Katz, A., 1998. The effect of material degradation on bond properties of FRP reinforcing bars in concrete. ACI Mater. J. 95 (3), 132–143.

Bank, L.C., Gentry, T.R., Thompson, B.P., Russell, J.R., 2002. Model Specification for Composites for Civil Engineering Structures. Transportation Research Record 1814, Transportation Research Board of the National Academies, Washington, DC.

Barnes, R.A., Mayes, G.C., 1999. "Fatigue performance of concrete beams strengthened with CFRP plates". J. Compos. Constr. 3 (2), 63–72.

Barr, P.J., Eberhard, M.O., Stanton, J.F., 2001. Live-load distribution factors in prestressed concrete girder bridges. J. Bridge Eng. 6 (5), 298–306.

Belarbi, A., Bae, S.-W., Ayoub, A., Kuchma, D., Mirmiran, A., Okeil, A., 2011. Design of FRP Systems for Strengthening Concrete Girders in Shear, NCHRP Report 678. Transportation Research Board, Washington, DC.

Bisby, L.A., Green, M.F., Kodur, V.K.R., 2005. Fire endurance of fiber-reinforced polymer-confined concrete columns. ACI Struct. J. 102 (6), 883–891.

Bizindavyi, L., Neale, K.W., 1999. Transfer length and bond strengths for composite bonded to concrete. ASCE J. Compos. Const. 3 (4), 153–160.

Blaschko, M., Niedremeier, R., Zilch, K., 1998. Bond failure modes of flexural members strengthened with FRP, Proceedings of the Second International Conference on Composites in Infrastructure, ICCI'98, vol. 1. Department of Civil Engineering and Engineering Mechanics, University of Arizona, Tucson, AR, pp. 315–327.

Bousias, S., Triantafillou, T., Fardis, M., Spathis, L., O'Regan, B., 2004. Fiber-reinforced polymer retrofitting of rectangular reinforced concrete columns with or without corrosion. ACI Struct. J. 101 (4), 512–520.

Bousselham, A., Chaallal, O., 2006. Behavior of reinforced concrete T-beams strengthened in shear with carbon fiber-reinforced polymer—an experimental study. ACI Struct. J. 103 (3).

Brewer, J.C., Lagace, P.A., 1988. Quadratic stress criterion for initiation of delamination. J. Compos. Mater. 22, 1141–1155.

Brosens, K., Van Gemert, D., 1999. Anchorage design for externally bonded carbon fiber reinforced polymer laminates. In: Proceedings of Fourth International Symposium on FRP Reinforcement for Concrete Structures, Baltimore, USA, pp. 635–645.

BS 1881-207, 1992. Testing Concrete. Recommendations for the Assessment of Concrete Strength by Near-to-Surface Tests.

Buyukozturk, O., Hearing, B., 1998. Failure behaviour of precracked concrete beams retrofitted with FRP. J. Compos. Construct. 2 (3), 138–144.

Cai, C.S., 2005. Discussion on AASHTO LRFD load distribution factors for slab-on-girder bridges. Practice Periodical on Structural Design and Construction. 10 (3), 171–176.

Cai, C.S., Shahawy, M., 2004. Predicted and measured performance of prestressed concrete bridges. J. Bridge Eng. 9 (1), 4–13.

CAN/CSA S806-02, 2002. Design and Construction of Building Structures with Fibre-Reinforced Polymers.

Canadian Standards Association, 2006. CAN/CSA-S6-06, Canadian Highway Bridge Design Code. Mississauga, Canada.

Carey, S.A., Harries, K.A., 2005. Axial behavior and modeling of small-, medium-, and large-scale circular sections confined with CFRP jackets. ACI Struct. J. 102 (4), 596–604.

Carolin, A., Taljsten, B., 2005. Experimental study of strengthening for increased shear bearing capacity. ASCE J. Comp. Constr. 9 (6), 488–496.

CEB-FIP, 2001. Externally Bonded FRP Reinforcement for RC Structures. Technical Report Bulletin 14. International Federation for Structural Concrete, Geneva, Switzerland.

CECS-146, 2003. Technical Specification for Strengthening Concrete Structures with Carbon Fiber Reinforced Polymer Laminates, Code of Federal Regulations (CFR).

Chaallal, O., Shahawy, M., 2000. Performance of fiber-reinforced polymer-wrapped reinforced concrete column under combined axial-flexural loading. ACI Struct. J. 97 (4), 659–668.

Chajes, M., Januszka, T.F., Mertz, D.R., Thomson, T.A., Finch, W.W., 1995. Shear strengthening of reinforced concrete beams using externally applied composite fabrics. Struct. J. ACI. 92 (3), 295–303.

Chen, J.F., Yuan, H., Teng, J.G., 2007. Debonding failure along a softening FRP-to-concrete interface between two adjacent cracks in concrete members. J. Eng. Struct. 29 (2), 259–270.

Choi, H.T., West, J.S., Soudki, K.A., 2008. Analysis of the flexural behavior of partially bonded FRP strengthened concrete beams. J. Compos. Constr. July/August, 375–386.

Chu, W., Karbhari, V.M., Wu, L., 2004. Durability evaluation of moderate temperature cured E-glass/vinylester systems. Compos. Struct. 66, 367–376.

CNR-DT 200/2004, 2004. Guide for the Design and Construction of Externally Bonded FRP Systems for Strengthening Existing Structures.

Co Mite EURO-International Du Beton, 1993. CEB-FIP Model Code 1990. Thomas Telford, London.

Concrete Society Technical Report 54, 2000. Diagnosis of deterioration in concrete structures. The Concrete Society, Crowthorne, UK.

Concrete Society Technical Report 55, 2000. Design guidance for strengthening concrete structures using fibre composite materials. The Concrete Society, Crowthorne, UK.

Cox, B.N., Dadkhah, M.S., Inman, R.V., Morris, W.L., 1992. Compressive failure mechanisms in 3D composites. Acta Metall. Mater. 40, 3285–3298.

Cox, B.N., Dadkhah, M.S., Morris, W.L., Flintoff, J.G., 1994. Failure mechanisms of 3D woven composites in tension, compression, and bending. Acta Metall. Mater. 42, 3967–3984.

Cox, B.N., Dadkhah, M.S., Morris, W.L., 1996. On the tensile failure of textile composites. Composites, Part A. 27 (6), 447–458.

Cross, B., et al., 2009. Analytical and experimental investigation of bridge girder shear distribution factors. J. Bridge Eng. 14 (3), 154–163.

Cuninghame, J.R., Jordan, R.W., Assejev, A., 1999. Fibre reitiforced plastic strengthening of bridge supports to resist vehicle impact. Unpublished Project Report. Transport Research Laboratory, Crowthome.

Darlow, M.S., Bettigole, N.H., 1989. Instrumentation and testing of bridge rehabilitated with exodermic deck. J. Struct. Eng. N. Y. 115 (10), 2461–2480.

Davalos, J.F., et al., 2012. Comprehensive study on using externally bonded FRP composites for the rehabilitation of reinforced concrete T-beam bridges. J. Infrastruct. Syst. 18 (2).

De Lorenzis, L., Tepfers, R., 2003. Comparative study of models on confinement of concrete cylinders with fiber-reinforced polymer composites. J. Compos. Constr. ASCE. 7 (3), 219–237.

De Lorenzis, L., Lundgren, K., Rizzo, A., 2004. Anchorage length of near-surface-mounted FRP bars for concrete strengthening-experimental investigation and numerical modeling. ACI Struct. J. 101 (2), 269–278.

Demers, M., Neale, K., 1999. Confinement of reinforced concrete columns with fibre reinforced composites sheets—an experimental study. Can. J. Civil Eng. 26, 226−241.
Deniaud, C., Cheng, J.J.R., 2001. Shear behavior of reinforced concrete T-beams with externally bonded fiber-reinforced polymer sheets. ACI Struct. J. 98 (3), 386−394.
Deniaud, C., Cheng, J.J.R., 2003. Reinforced concrete T-beams strengthened in shear with fiber reinforced polymer sheets. J. Compos. Constr. ASCE. 7 (4), 302−310.
Denton, S.R., Christie, T.J.C., Powell, S.M., 2000. The development of design charts for column strengthening using FRP in bridge management: inspection, maintenance, assessment and repair. In: Ryall, M.J., Parke, G.A.R., Harding, J.E. (Eds.), Proceedings of Fourth International Conference, University of Surrey. Thomas Telford, UK.
Desayi, P., Krishnan, S., 1964. Equation for the stress−strain curve of concrete. J. Am. Concr. Inst. 61 (3), 345−350.
Dicleli, M., Erhan, S., 2009. Live load distribution formulas for single-span prestressed concrete integral abutment bridge girders. J. Bridge Eng. 14 (6), 472−486.
Dutta, P.K., 1989. A theory of strength degradation of unidirectional fiber composites at low temperature. In: Smith, F.W. (Ed.), Proceedings of Advanced Materials Conference, Golden, CO. pp. 647−662.
Dutta, P.K., 1992. Low temperature compressive strength of glass-fiber reinforced polymer composites. In: Proceedings of the 11th International Conference on Off-Shore Mechanics and Arctic Engineering, Calgary, Canada.
Dutta, P.K., 1998. Structural fiber composite materials for cold regions. J. Cold Regions Eng. 3 (2), 124−132.
Dutta, P.K., Hui, D., 1996. Low temperature and freeze-thaw durability of thick composites. Compos. B: Eng. 27 (3-4), 371−379.
Eamon, C., Nowak, A.S., 2002. Effects of edge-stiffening elements and diaphragms on bridgeresistance and load distribution. J. Bridge Eng. 7 (5), 258−266.
Eamon, C., Jensen, E., Grace, N., Shi, X., 2012. Life cycle cost analysis of alternative bridge reinforcement materials for bridge superstructures considering cost and maintenance uncertainties. ASCE J. Mater. Civil Eng.
Ebeido, T., Kennedy, J.B., 1996. Girder moments in continuous skew composite bridges. J. Bridge Eng. 1 (1), 37−45.
Elarbi, A., 2011. Durability Performance of FRP Strengthened Concrete Beams and Columns Exposed to Hygrothermal Environment, PhD Dissertation. Department of Civil and Environmental Engineering, Wayne State University, Detroit, MI.
El-Maaddawy, T., Chahrour, A., Soudki, K.A., 2006. Effect of FRP-Wraps on Corrosion Activity and Concrete Cracking in Chloride-Contaminated Concrete Cylinders.
Elnabelsy, G., Saatcioglu, M., 2004. Seismic Retrofit of Circular and Square Bridge Columns with CFRP Jackets. Advanced Composite Materials in Bridges and Structures, Calgary, AB, Canada, 8 pp. (CD-ROM).
El-Tawil, S., Ogunc, C., Okeil, A.M., Shahawy, M., 2001. "Static and fatigue analyses of RC beams strengthened with CFRP laminates". J. Compos. Constr. 5 (4), 258−267.
Eom, J., Nowak, A.S., 2001. Live load distribution for steel girder bridges. J. Bridge Eng. 6 (6), 489−497.
Faber, M.H., Val, D.V., Stewart, M.G., 2000. Proof load testing for bridge assessment and ungrading. Eng. Struct. 22 (12), 1677−1689.
Fanous, F., May, J., Wipf, T., 2011. Development of live-load distribution factors for glued-laminated timber girder bridges. J. Bridge Eng. 16 (2), 179−187.
Fardis, M.N., Khalili, H.H., 1982. FRP-encased concrete as a structural material. Mag. Concr. Res. 34 (121), 191−201.

FIB Technical Report Bulletin 14, 2001. Externally Bonded FRP Reinforcement for RC Structures, published in Europe (FIB, CEB-FIP).

Fu, G., Tang, J., 1995. Risk-based proof-load requirements for bridge evaluation. J. Struct. Eng. ASCE. 121 (3), 542−556.

Funakawa, I., Shimono, K., Watanabe, T., Asada, S., Ushijima, S., 1997. Experimental study on shear strengthening with continuous fiber reinforcement sheet and methyl methacrylate resion, Third International Symposiiun on Non-Metallic (FRP) Reinforcement for Concrete Structures (FRPRCS-3), vol. 1. Japan Concrete Institute, Tokyo, Japan, pp. 475−482.

Galati, N., Nanni, A., Dharani, L.R., Focacci, F., Aiello, M.A., 2006. Thermal effects on bond between FRP rebars and concrete. Compos. A. 37 (8), 1223−1230.

GangaRao, H.V.S., Vijay, P.V., 1998. Bending behavior of concrete beams wrapped with carbon fabric. J. Struct. Eng. 124 (1), 3−10.

Garden, H.N., 1997. The Strengthening of Reinforced Concrete Members Using Externally Bonded Composite Materials. Doctoral Thesis, University of Surrey.

Gibson, R.F., 1994. Principles of Composite Material Mechanics. Mc-Graw-Hill Press.

Gibson, R.F., 2000. Modal vibration response measurements for characterization of composite materials and structures. Compos. Sci. Technol. 60, 2769−2780.

Green, M., Bisby, L., Beaudoin, Y., Labossiere, P., 1998. Effects of freeze−thaw action on the bond of FRP sheets to concrete. In: Proceedings of the First International Conference on Durability of Composites for Construction, Sherbrooke, QC, Canada, October, pp. 179−190.

Hamada, H., Maekawa, Z., Morii, T., Tanimoto, T., Yokoyama, A., 1996. Damage mechanics on hydrothermal aged fiber reinforced plastics. In: Deo, R.B., Saff, C.R. (Eds.), Composite Materials: Testing and Design (Twelfth Volume), ASTM STP 1274. American Society for Testing and Materials, Conshohocken, PA, pp. 88−102.

Haramis, J., 2003. Freeze−Thaw Durability of Polymeric Composite Materials for Use in Civil Infrastructure, Ph.D. Dissertation. Dept. of Civil Engineering, Virginia Polytechnic Institute and State University.

Harichandran, R.S., Baiyasi, M.I., 2000. Repair of Corrosion-Damaged Columns using FRP Wraps. MDOT Research Report RC-1386.

Harries, K.A., Carey, S.A., 2003. Shape and 'gap' effects on the behavior of variably confined concrete. Cem. Concr. Res. 33 (6), 881−890.

Harris, H.H., Somboonsong, W., Ko, F.K., 1998. New ductile hybrid FRP reinforcing bar for concrete structures. J. Compos. Constr. 2 (1), 28−37.

Harris, D.K., 2010. Assessment of flexural lateral load distribution methodologies for stringer bridges. Eng. Struct. 32 (11), 3443−3451.

Hassan, T., Rizkalla, S., 2003. Investigation of bond in concrete structures strengthened with near surface mounted CFRP strips. J. Compos. Constr. ASCE. 7 (3), 248−257.

Haynes, L., 1997. An Investigation of Bond Between Concrete and Externally Bonded Carbon Fiber Reinforced Plastic Plates. M.S. Special Report Submitted to the Faculty of the School of Civil Engineering in Partial Fulfillment of the Requirements of the Degree of Master of Science in Civil Engineering, Georgia Institute of Technology, Atlanta, Georgia.

Helbling, C., Abanilla, M., Lee, L., Karbhari, V.M., 2006. Issues of variability and durability under synergistic exposure conditions related to advanced polymer composites in the civil infrastructure. Compos. A. 37 (8), 1102−1110.

HITEC, 2001. Evaluation Plan for FRP Composite Systems for Concrete Structure Repair and Strengthening. Final Report. Highway Innovative Technology Evaluation Center, Washington, DC.

Hollaway, L.C., Head, P.R., 2001. Advanced Polymer Composites and Polymer in the Civil Infrastrucure. Elsevier Press, Oxford, UK.

Holzenkämpfer, P., 1994. (in German). Ingenieurmodelle des verbundes geklebter bewehrung für betonbauteile. Dissertation. TU Braunschweig.

Hong, S., Harichandran, R., 2005. Sensors to monitor CFRP/concrete bond in beams using electrochemical impedance spectroscopy. J. Compos. Constr. 9 (6).

Hoppel, C.P.R., Bogetti, T.A., Gillespie, J.W., 1997. Design and analysis of composite wraps for concrete columns. J. Reinforced Plast. Compos. 16 (7), 588–602.

Hormann, M., Seible, F., Karbhari, V., Seim, W., 1998. Preliminary Structural Tests for Strengthening of Concrete Slabs Using FRP Composites, Report No. TR-98/13, University of California at San Diego.

Howie, I., Karbhari, V.M., 1995. Effect of tow sheet composite wrap architecture on strengthening of concrete due to confinement: I—experimental studies. J. Reinforced Plast. Compos. 14 (9), 1008–1030.

Hughs, E., 2006. Live-load distribution factors for prestressed concrete, spread box-girder bridge. J. Bridge Eng. 11 (5), 573–581.

Iacobucci, R., Sheikh, S., Bayrak, O., 2003. Retrofit of square concrete columns with carbon fiber-reinforced polymer for seismic resistance. ACI Struct. J. 100 (6), 785–794.

Ibrahim, A.M., Mahmood, M.S., 2009. Finite element modeling of reinforced concrete beams strengthened with FRP laminates. Eur. J. Sci. Res. 30 (4), 526–541.

ICRI 03733, 2009. (International Concrete Repair Institute), Guide for Selecting and Specifying Materials for Repairs of Concrete Surfaces.

International Concrete Repair Institute (ICRI) 03730, 2008. Guide for Surface Preparation for the Repair of Deteriorated Concrete Resulting from Reinforcing Steel Corrosion.

ISIS, 2008. FRP Rehabilitation of Reinforced Concrete Structures, Design Manual 4 Version 2.

ISIS Canada, 2002. In: Neale, K.W. (Ed.), Strengthening Reinforced Concrete Structures with Externally-Bonded Fibre Reinforced Polymers (FRPs), Manual No. 4. ISIS Canada, Université de Sherbrooke, Sherbrooke, Canada.

Institution of Structural Engineers, 1996. Appraisal of Existing Structures. London, UK.

ISO (TC71/SC6N), 2003. Non-Conventional Strengthening of Concrete—Test Methods-Part 1: Fiber Strengthened Polymer (FRP) Bars and Grids.

JCI, 1998. Continuous Fiber Reinforced Concrete, Technical Report TC952. Japan Concrete Institute, Tokyo, Japan.

Jones, R., Swamy, R.N., Charif, A., 1998. Plate separation and anchorage of reinforced concrete beams strengthened with epoxy-bonded steel plates. Struct. Eng. 66 (5), 85–94.

Jones, R.M., 1999. Mechanics of Composite Materials. 2nd ed Taylor & Francis, Philadelphia, PA.

JSCE, 1997. Recommendation for Design and Construction of Concrete Structures Using Continuous Fiber Reinforcing Materials, Concrete Engineering Series, No. 23. Japan Society of Civil Engineers, Tokyo, Japan, 325 pp.

JSCE, 2000. Test Method for Continuous Fiber Sheets. Japan Society of Civil Engineers, Tokyo, Japan.

JSCE, 2001. Recommendations for Upgrading of Concrete Structures with Use of Continuous Fiber Sheets. Japan Society of Civil Engineers, Tokyo, Japan.

JSCE-E 546, 2000. Test method for tensile fatigue of continuous fiber sheets. Japan Society of Civil Engineers. Tokyo, Japan.

JSCE-E 531, 1995. Test Method for Tensile Properties of Continuous Fiber Reinforcement Materials. Japan Society of Civil Engineers, Tokyo, Japan.

JSCE-E 542, 2000. Test Method for Overlap Splice Strength of Continuous Fiber sheets. Japan Society of Civil Engineers, Tokyo, Japan.

Karbhari, V., Howie, I., 1997. Effect of composite wrap architecture on strengthening of concrete due to confinement: II-strain and damage effects. J. Reinforced Plast. Compos. 16 (II), 1039–1063.

Karbhari, V.M., 2002. Response of FRP confined concrete exposed to freeze-thaw regimes. ASCE J. Compos. Constr. 6 (1), 35–40.

Karbhari, V.M., 2004. E-glass/Vinylester composite in aqueous environments: effects on short-beam shear strength. J. Compos. Constr. ASCE. 8 (2), 148–156.

Karbhari, V.M., Pope, G., 1994. Impact and flexure properties of glass/vinyl ester composites in cold regions. J. Cold Region Eng. ASCE. 8 (1), 1–20.

Karbhari, V.M., Eckel, D.A., Tunis, G.C., 1993. Strengthening of concrete column stubs through resin infused composite wraps. J. Thermoplast. Compos. Mater. 6, 92–107.

Karbhari, V.M., Rivera, J., Dutta, P.K., 2000. Effect of short-term freeze–thaw cycling on composite confined concrete. J. Compos. Constr. ASCE. 4 (4), 191–197.

Karbhari, V.M., Rivera, J., Zhang, J., 2002. Low-temperature hygrothermal degradation of ambient cured E-glass/vinyl ester composites. J. Appl. Polym. Sci. 86, 2255–2260.

Karbhari, V.M., Chin, J.W., Hunston, D., Benmokrane, B., Juska, T., Morgan, R., et al., 2003. Durability gap analysis for fiber-reinforced polymer composites in civil infrastructure. J. Compos. Constr. ASCE. 7 (3), 238–247.

Katz, A., Berman, N., Bank, L.C., 1999. Effect of high temperature on the bond strength of FRP rebars. ASCE J. Compos. Constr. 3 (2), 73–81.

Khalifa, A., Alkhrdaji, T., Nanni, A., Lansburg, S., 1999. Anchorage of surface-mounted FRP reinforcement. Concr. Int. 21 (10), 49–54.

Khan, M., 2010. Bridge and Highway Structure Rehabilitation and Repair. ISBN: 978-0071545921.

Ko, F.K., 1989. Three dimensional fabrics for composites. In: Chou, T.W., Ko, F.K. (Eds.), Textile Structural Composites: Series 3. Elsevier, New York, p. 1989.

Kotynia, R., 2005. Strain Efficiency of Near-Surface Mounted CFRP-Strengthened Reinforced Concrete Beams. International Conference on Composites in Construction, Lyon, July 11–13, 2005.

Kulkarni, A., Gibson, R.F., 2003. Nondestructive characterization of effects of temperature and moisture on elastic moduli of vinyl ester resin and E-glass/vinyl ester composite. CD Proceeding of The American Society for Composites 18th Annual Conference. CRC Press.

Labossiere, P., Neale, K.W., Demers, M., Picher, F., 1995. Repair of reinforced concrete columns with advanced composite materials confinement. In: Toutanji, H.T. (Ed.), Repair and Rehabilitation of the Infrastructure of the Americas. University of Puerto Rico, Puerto Rico, pp. 153–165.

Lam, L., Teng, J., 2003a. Design-oriented stress–strain model for FRP-confined concrete. Constr. Build. Mater. 17, 471–489.

Lam, L., Teng, J., 2003b. Design-oriented stress–strain model for FRP-confined concrete in rectangular columns. J. Reinforced Plastics Compos. 22 (13), 1149–1186.

Leung, C.K.Y., Tung, W.K., 2006. Three-parameter model for debonding of FRP plate from concrete substrate. J. Eng. Mech. 132 (5), 509–518.

Lichtenstein, A.G., 1993. Bridge Rating Through Nondestructive Load Testing. NCHRP Report 12-28(13) A. Transportation Research Board, Washington, DC.

Lichtenstein, A.G., 1998. Manual for bridge rating through load testing. Research Results Digest. National Cooperative Highway Research Program, No. 234.

Lillis tone, D., 2000. Non-Ferrous Compositely Reitiforced Concrete Columns, PhD Thesis Submitted to the University of Southampton.

Lillis tone, D., Jolly, C.K., 2000. An innovative form of reinforcement for concrete columns using advanced composites. Struct. Eng. 78 (23/24).

Lopez, M.M., Naaman A.E., 2003. Concrete Cover Failure or Tooth Type Failure on RC Beams Strengthened with FRP Laminates. In: Proceedings of the Sixth International Symposium on Fiber Reinforced Polymer (FRP) for Reinforced Concrete Structures (FRPRCS-6). pp. 317−326.

Lord, H.W., Dutta, P.K., 1988. On the design of polymeric composite structures for cold regions applications. J. Reinforced Plastics Compos. 7 (5), 435−458.

Ludovico, D., Nanni, A., Prota, A., Cosenza, E., 2005. Repair of bridge girders with composites: experimental and analytical validation. ACI Struct. J. 102 (5), 639−648.

Maeda, T., et al., 1997. A study on bond mechanism of carbon fibre sheet, Proceedings of the Third Symposium on Non-Metallic (FRP) Reiriforcement for Concrete Structures, 1. Japan Concrete Institute, Tokyo, Japan, pp. 279−286.

Malek, A., Saadatmanesh, H., Ehsani, M., 1998. Prediction of failure load of R/C beams strengthened with FRP plate due to stress concentrations at the plate end. ACI Struct. J. 95 (1), 142−152.

Mallick, P., 2007. Fiber-Reinforced Composites-Materials, Manufacturing, and Design, third ed., ISBN: 0849342058.

Malvar, L., 1998. Durability of Composites in Reinforced Concrete. In: Proceedings of the First International Conference on Durability of Composites for Construction, August, Sherbrooke, Canada, pp. 361−372.

Malvar, L., Warren, G., Inaba, C., 1995. Rehabilitation of Navy Pier Beams with Composite Sheets. In: Second FRP International Symposium on Non-Metallic (FRP) Reinforcement for Concrete Structures, Ghent, Belgium, August, pp. 533−540.

Mander, J.B., Priestly, M.J.N., Park, R., 1998. Theoretical stress−strain model for confined concrete. ASCE J. Struct. Eng. 114 (8), 1804−1826.

Matthews, F.L., Rawlings, R., 1994. Composite Materials: Engineering and Science. Chapman and Hall, London.

Matthys, S., Triantafillou, T., 2001. Shear and torsion strengthening with externally bonded FRP reinforcement. Compos. Constr.203−212.

Meier, U., 1987. Bridge repair with high performance composite materials. Mater. Technik. 4, 125.

Meier, U., 1995. Strengthening of structures using carbon fiber/epoxy composites. Constr. Build. Mater. 9 (6), 341−351.

Meier, U., Kaiser, H., 1991. Strengthening of Structures with CFRP Laminates. Advanced Composite Materials in Civil Engineering Structures, ASCE Specialty Conference, pp. 224−232.

Memmott, J., 2007. Highway Bridges in the United States—An Overview. Special Report, USDOT, Bureau of Transportation Statistics (BTS), Research and Innovative Technology Administration (RITA).

Memon, M., Sheikh, S., 2005. Seismic Resistance of Square Concrete Columns Retrofitted with Glass Fiber-reinforced polymers. ACI Struct. J. 102 (5), 774−783.

Mertz, D., Chajes, M., Gillespie, J., Kukich, D., Sabol, S., Hawkins, N., et al., 2003. Application of Fiber Reinforced Polymer Composites to the Highway Infrastructure, NCHRP Report 503. Transportation Research Board, Washington, DC.

Mertz, D.R., Gillespie Jr., J.W., 1996. Rehabilitation of Steel Bridge Girders Through the Application of Advanced Composite Materials. Transportation Research Board, Washington, DC.

Mikami, C., Wu, H.C., Elarbi, A., 2015. Effect of hot temperature on bond strength of FRP bonded concrete. Constr. Build. Mater. 91, 180–186.

Miller, R.A., Castrodale, R., Mirmiran, A., Hastak, M., 2004. Connection of simple-span precast concrete girders for continuity. NCHRP Report 519. Transportation Research Board, Washington, DC.

Miller, T.C., Chajes, M.J., Mertz, D.R., Hastings, J.N., 2001. Strengthening of a steel bridge girder using CFRP plates. J. Bridge Eng. 6 (6), 514–522.

Mirmiran, A., Shahawy, M., Samaan, M., El Echary, H., Mastrapa, J.C., Pico, O., 1998. Effect of column parameters on FRP-confined concrete. J. Compos. Constr. ASCE. 2 (4), 175–185.

Mirmiran, A., Shahawy, M., Nammi, A., Karbhari, V., 2004. Bonded Repair and Retrofit of Concrete Structures Using FRP Composites, NCHRP Report 514. Transportation Research Board, Washington, DC.

Mo, Y.L., Yeh, Y.-K., Hsieh, D.M., 2004. Seismic retrofit of hollow rectangular bridge columns. J. Compos. Constr. 8 (1), 43–51.

Mosallam, A., Chakrabarti, R., Sim, S., Elasnadedy, H., 2000. Seismic response of reinforced concrete moment connections repaired and upgraded with FRP composites. Innovative Systems for Seismic Repair and Rehabilitation of Structures. In: Mosallam, A., (Ed.), Proceedings, SRRS2 Conference, Fullerton, CA, March 20–21, pp. 59–72.

Mu, B., Wu, H.C., Yan, A., Warnemuende, K., Fu, G., Gibson, R.F., et al., 2006. FEA of complex bridge system with FRP composite deck. J. Compos. Constr. 10 (1), 79–86.

Naaman, A.E., Lopez, M., 1999. Repair and Strengthening of Reinforced Concrete Beams Using CFRP Laminates. Michigan Department of Transportation, Report No. RC-1372, April

Nakai, A., Masui, M., Hamada, H., 1997. Fabrication of large-scale braided composite with I-shaped structure. Proceedings of the 11th International Conference on Composite Materials (ICCM-11), Gold Coast, Queensland, Australia. Australian Composites Structures Society and Woodhead Publishing, Queensland, Australia, pp. 3830–3837.

Nanni, A., 1999. Composites: coming on strong. Concr. Constr. 44, 120.

Nanni, A., 2000. FRP reinforcement for bridge structures. Proceedings, Structural Engineering Conference. The University of Kansas, Lawrence, KS.

Nanni, A., 2004. Strengthening of impact-damaged PC girder. Concr. Repair Bull. 17 (3), 16–20.

Nanni, A., Bradford, N., 1995. FRP jacketed concrete under uniaxial compression. Constr. Build. Mater. 9 (2), 115–124.

Nanni, A., Gold, W., 1998. Strength assessment of external FRP reinforcement. Concr. Int. 20 (6), 39–42.

Nanni, A., Norris, M.S., Bradford, N.M., 1992. Lateral Confinement of Concrete Using FRP Reinforcement. ACI SP 138, Fiber Reinforced Plastic Reinforcement for Concrete Structures, pp. 193–209.

Nanni, A., Bakis, C.E., Boothby, T.E., Frigo, E.L., Lee, Y.-J., 1997. Tensile reinforcement by FRP sheets applied to RC. Proc. Intl. Composites Expo '97. Soc. Plastics Engineers, New York.

NCHRP Report 609, 2008. Recommended Construction Specifications and Process Control Manual for Repair and Retrofit of Concrete Structures Using Bonded FRP Composites. Transportation Research Board, Washington, DC.

Neubauer, U., Rostasy, F.S., 1997. Design Aspects of Concrete Structures Strengthened with Externally Bonded CFRP Plates. ECS Publications, Concrete and Composites, Proceedings of 7th International Conference on Structural Faults and Repair, Edinburgh, vol. 2, pp. 109–118.

Nguyen, T., Byrd, E., Alshed, D., Aouadi, K., Chin, J., 1998. Water at the polymer/substrate interface and its role in the durability of polymer/glass fiber composites, In: Benmokrane, B., Rahman, H., (Eds.), Durability of FRP Composits for Construction, 1st International Conference, August 1998, Canada, pp. 451–462.

Niu, H., Wu, Z.S., 1990. Analytical modeling on debonding failure of FRP-strengthened RC flexural structures. In: The Third International Conference on Composites in Infrastructures (CD-ROM).

Nosho, K.J., 1996. Retrofit of Rectangular Reinforced Concrete Columns using Carbon Fiber, MS thesis. University of Washington, Seattle, WA, 194 pp.

Nowak, A.S., 1999. Calibration of LRFD Bridge Design Code. NCHRP 368. Transportation Research Board, Washington, DC.

Nowak, A.S., Eom, J., 2001. Verification of girder distribution factors for steel girder bridges. MDOT Research Report RC-1393. Michigan Department of Transportation, Lansing, MI.

Nowak, A.S., Saraf, V., 1996. Load Testing of Bridges. Michigan Department of Transportation Report 1347.

Nowak, A.S., Szerszen, M.M., 2003. Calibration of design code for buildings (ACI 318): Part I-statistical models for resistance. ACI Struct. J. 100 (3), 377–382.

Nowak, A.S., Sanli, A., Kim, S., Eamon, C., Eom, J., 1998. Development of a Guide for Evaluation of Existing Bridges, Part II. Report UMCEE 98-13 for MDOT, University of Michigan.

Obaidat, Y.T., Heyden, S., Dahlblom, O., 2010. The effect of CFRP and CFRP/concrete interface models when modeling retrofitted RC beams with FEM. Compos. Struct. 92, 1391–1398.

Oehlers, D.J., Seracino, R., 2004. Design of FRP and steel plated RC structures. Elsevier Science, Oxford, UK.

Oesterle, R., Mehrabi, A.B., Tabatabai, H., Scanlon, A., Ligozio, C.A., 2004. Continuity considerations in prestressed concrete jointless bridges. In: Proceedings, 2004 Structures Congress, pp. 227–234.

Ogin, S.L., 2000. Textile reinforced composite materials. In: Horrocks, A.R., Anand, S.C. (Eds.), Handbook of Technical Textiles. Woodhead Publishing, Cambridge, UK.

Okeil, A., Elsafty, A., 2005. Partial continuity in bridge girders with jointless decks. Practice Periodical Struct. Des. Constr. 10 (4), 229–238.

Okeil, A.M., Bingol, Y., Alkhrdaji, T., 2007. Analyzing model uncertainties for concrete beams flexurally strengthened with FRP laminates. In: Proceedings of the Transportation Research Board 86th Annual Meeting, January 21–25, Washington, DC, 15 pp. (CD-ROM).

Ouyang, Z., Wan, B., 2006. Numerical Simulation of Bond Deterioration between CFRP Plate and Concrete in Moisture Environment. In: Proc. 3rd Inter. Conf on FRP Composites in Civil Engineering, Miami, pp. 395–398.

Pellegrino, C., Modena, C., 2002. Fiber reinforced polymer shear strengthening of reinforced concrete beams with transverse steel reinforcement. J. Compos. Constr. ASCE. 6 (2), 104–111.

Pesic, N., Pilakoutas, K., 2003. Concrete beams with externally bonded flexural FRP-reinforcement: analytical investigation of debonding failure. Compos. B: Eng. 34 (4).

Pessild, S., Harries, K.A., Kestner, J., Sause, R., Ricles, J.M., 2001. The axial behavior of concrete confined with fiber reinforced composite jackets. J. Compos. Constr. ASCE. 5 (4), 237–245.

Picher, F., Rochette, P., Labossiere, P., 1996. Confinement of cylinders and short concrete columns with ACM. In: Saadatmanesh, H., Ehsani, M.R. (Eds.), Proceedings of the First International Conference on Composite Infrastructures. University of Tucson, Arizona, USA, pp. 829–841.

Priestley, M., Seible, F., Calvi, G., 1996. Seismic Design and Retrofit of Bridges. John Wiley and Sons, New York, 704 pp.

Puckett, J.A., Sharon, X.H., Jabllin, M., Mertz, D.R., 2012. Framework for simplified live load distribution-factor computations. J. Bridge Eng. 16 (6), 777–791.

Ramakrishna, S., 1997. Characterization and modeling of the tensile properties of plain weft-knit fabric reinforced composites. Compos. Sci. Technol. 57, 1–22.

Reed, C.E., Peterman, R.J., Rasheed, H.A., 2005. Evaluating FRP repair method for cracked prestressed concrete bridge members subjected to repeated loadings (Phase l), KTRAN Report No. K-TRAN: KSU-01-2. Kansas Department of Transportation, Topeka, KS, 106 pp.

Richart, F.E., Brandtzaeg, A., Brown, R.L., 1928. A Study of the Failure of Concrete Under Combined Compressive Stresses. Technical Report Bulletin No. 185. Engineering Experiment Station, University of Illinois, Urbana.

Ritchie, P., Thomas, D., Lu, L., Conneley, G., 1991. External reinforcement of concrete beams using fiber reinforced plastics. ACI Struct. J. 88 (4), 490–500.

Ritter, W., 1899. Die Bauweise Hennebique. Schweizerische, Bauzeitung. 33 (7), 59–61.

Rivera, J., Karbhari, V.M., 2002. Cold-temperature and simultaneous aqueous environment related degradation of carbon/vinylester composites. Compos. B. 33 (1), 17–24.

Rizkalla, S., Dawood, M., David Schnerch, D., 2008. Development of a carbon fiber reinforced polymer system for strengthening steel structures. Compos. A. 39, 388–397.

Roberts, T.M., 1989. Approximate analysis of shear and normal stress concentrations in the adhesive layer of plated RC beams. Struct. Eng. 67 (12/20), 229–233.

Rocca, S., Galati, N., Nanni, A., 2006. Experimental Evaluation of FRP Strengthening of Large-Size Reinforced Concrete Columns. Report No. UTC-142, University of Missouri-Rolla, MO.

Rocca, S., Galati, N., Nanni, A., 2008. Review of design guidelines for FRP confinement of reinforced concrete columns of noncircular cross sections. J. Compos. Constr. ASCE. 12 (1), 80–92.

Rosenboom, O.A., Rizkalla, S.H., 2006. Behavior of prestressed concrete strengthened with various CFRP systems subjected to fatigue loading. J. Compos. Constr. ASCE.

Saadatmanesh, H., Ehsani, M.R., Li, M.W., 1994. Strength and ductility of concrete columns externally reinforced with fiber composite straps. ACI Struct. J. 91 (4), 434–447.

Saadatmanesh, H., Ehsani, M.R., Jin, L., 1996. Seismic strengthening of circular bridge pier models with fiber composites. ACI Struct. J. 93 (6), 639–647.

Saafi, M., Houssam, A., Toutanji, Zongjin, L., 1999. Behaviour of concrete columns confined with fibre reinforced polymer tubes. ACI Mater. J. 96 (4), 500–509.

Samaan, M., Mirmiran, A., Shaha Wy, M., 1998. Model of concrete confined by fibre composites. ASCE J. Struct. Eng. 24 (9), 1025–1031.

Sato, Y., Ueda, T., Kakuta, Y., Tanaka, T., 1996. Shear reinforcing effect of carbon fiber sheet attached to side of reinforced concrete beams. In: El-Badry, M.M., (Ed.), Advanced Composite Materials in Bridges and Structures, pp. 621–627.

Sause, R., Harries, K.A., Walkup, S.L., Pessiki, S., Rides, J.M., 2004. Flexural behavior of concrete columns with carbon fiber composite jackets. ACI Struct. J. 101 (5), 708–716.

Seible, F., Priestley, M.J.N., Hegemier, G.A., Innamorato, D., 1997. Seismic retrofit of RC columns with continuous carbon fiber jackets. J. Compos. Constr. 1 (2), 52–62.

Senne, J.L., Lesko, J.J., Case, S.W., Cousins, T., 2000. Life prediction methodology for fatigue loading of FRP hybrid beams. Proc. 14th Engineering Mechanics Conference. ASCE, Austin, TX.

Shahawy, M., Beitelman, T.E., 1999. Static and fatigue performance of RC beams strengthened with CFRP laminates. J. Struct. Eng. 125 (6), 613–621.

Shahawy, M., Beitelman, T.E., 2000. Static and fatigue performance of RC beams strengthened with CFRP laminates. Report, Structural Research Center, Florida Department of Transportation, 2007 East Dirac Drive, Tallahassee, FL.

Sharaf, M.H., Soudki, K.A., Van Dusen, M., 2006. CFRP strengthening for punching shear of interior slab-column connections. J. Compos. Constr. ASCE. 10 (5), 410–418.

Sharif, A., Al-Sulaimani, G., Basunbul, I., Baluch, M., Ghaleb, B., 1994. Strengthening of initially loaded reinforced concrete beams using FRP plates. ACI Struct. J. 91 (2), 160–168.

Sheikh, S., Yau, G., 2002. Seismic behavior of concrete columns confined with steel and fiber-reinforced polymers. ACI Struct. J. 99 (1), 72–80.

Shepherd, R., Sidwell, G.K., 1973. Composite road bridges. Highways Road Constr. 41 (1767), 20–25.

Somboonsong, W., Ko, F.K., Harris, H.G., 1998. Ductile hybrid fiber reinforced plastic (FRP) rebar for concrete structures: design methodology. ACI Mater. J. 95 (6), 655–666.

Stallings, J.M., Yoo, C.H., 1993. Tests and ratings of short span bridges. J. Struct. Eng. 19 (7), 2150–2168.

Staton, J., Knauff, J., 2007. Performance of Michigan's Concrete Barriers. Research Report R-1498, MDOT, Materials Section, Construction and Technology Division.

Suarez, S.A., Gibson, R.F., 1987. Improved impulse-frequency response technique for measurement of dynamic mechanical properties of composite materials. J. Test. Eval. 15 (2), 114–121.

Suarez, S.A., Gibson, R.F., Deobald, L.R., 1984. Random and impulse techniques for measurement of damping in composite materials. Exp. Techniq. 8 (10), 19–24.

Szerszen, M.M., Nowak, A.S., 2003. Calibration of design code for buildings (ACI 318): Part 2—Reliability analysis and resistance factors. ACI Struct. J. 100 (3), 383–391.

Tabatabai, H., et al., 2005. Rehabilitation techniques for concrete bridges. Technical Report, Wisconsin Highway Research Program, Wisconsin DOT.

Taljsten, B., 1996. Strengthening of concrete prisms using the plate-bonding technique. Int. J. Fract. 82 (3), 253–266.

Tavakkolizadeh, M., Saadatmanesh, H., 2003. Strengthening of steel–concrete composite girders using carbon fiber reinforced polymer sheets. J. Struct. Eng. 129 (1), 30–40.

TCS, 2000. Design Guidance for Strengthening Concrete Structures Using Fiber Composite Materials, Technical Report TR-55, the Concrete Society, Berkshire, United Kingdom.

Telang, N., Dumlao, C., Mehrabi, A., Ciolko, A., Gutierrez, J., 2006. Field Inspection of In-Service FRP Bridge Decks, NCHRP Report 564. Transportation Research Board, Washington, DC.

Teng, J.G., Smith, S.T., Yao, J., Chen, J.F., 2001. Intermediate crack induced debonding in RC beams and slabs. Constr. Build. Mater. 17 (6-7), 447–462.

Teng, J.G., Chen, J.F., Smith, S.T., Lam, L., 2002. FRP Strengthened RC Structures. John Wiley & Sons, Ltd, Chichester, UK.

Teng, J.G., Lu, X.Z., Ye, L.P., Jiang, J.J., 2004. Recent research on intermediate crack induced debonding in FRP strengthened beams. In: Proceedings of the 4th International Conference on Advanced Composite Materials for Bridges and Structures, Calgary, AB, Canada.

Thériault, M., Neale, K.W., 2000. Design equations for axially loaded reinforced concrete columns strengthened with fibre reinforced polymer wraps. Can. J. Civil Eng. 27 (5), 1011–1020.

Thomsen, H., Spacone, E., Limkatanyu, S., Camata, G., 2004. Failure mode analyses of reinforced concrete beams strengthened in flexure with externally bonded fiber-reinforced polymers. J. Compos. Constr. 8, 123–131.

Timoshenko, S., Woinowsky-Krieger, S., 1959. Theory of Plates and Shells. McGraw-Hill, New York.

Todeschini, C.E., Bianchini, A.C., Kesler, C.E., 1964. Behavior of concrete columns reinforced with high strength steels. ACI J. 61 (6), 701–716.

Toutanji, H., 1999. Stress–strain characteristics of concrete columns externally confined with advanced fiber composite sheets. ACI Mater. J. 96 (3), 397–404.

Toutanji, H.A., Balaguru, P., 1999. Effects of freeze–thaw exposure on performance of concrete columns strengthened with advanced composites. ACI Mater. J. 96 (5), 605–610.

Triantafillou, T.C., 1998. Shear strengthening of reinforced concrete beams using epoxy-bonded FRP composites. ACI Struct. J. 95 (2), 107–115.

Tsai, S., 1988. Composite Design. fourth ed Think Composites, Dayton, OH.

USDOT FHWA, 2001. National Bridge Inspection Standards. 23 CFR part 650, FHWA Docket No. FHWA 2001-8954, Federal Highway Administration, Washington, DC.

USDOT-FHWA, 2004. National Bridge Inspection Standards (NBIS), Federal Register, 69, 239

USDOT, FHWA, 2010. 2010 Status of the Nation's Highways, Bridges, and Transit: Conditions and Performance. Federal Highway Administration, Washington, DC.

Val, D., 2003. Reliability of fiber-reinforced polymer-confined reinforced concrete columns. J. Struct. Eng. ASCE. 129 (8), 1122–1130.

Vija, P.V., Kumar, S., Gangarao, H.V.S., 1996. Design of carbon sheet wrapped concrete beams. West Virginia University.

Walker, R., Karbhari, V.M., 2006. Durability based design of FRP jackets for seismic retrofit. Compos. Polycon 2006. American Composites Manufacturers Association, St. Louis, MO.

Wan, B., Petrou, M.F., Harries, K.A., 2006. Effect of the presence of water on the durability of bond between CFRP and concrete. J. Reinforced Plastics Compos. 25 (8), 875–890.

Wang, Y.C., Restrepo, J.I., 2001. Investigation of concentrically loaded reinforced concrete columns confined with glass fiber-reinforced polymer jackets. ACI Struct. J. 98 (3), 377–385.

Williams, B.K., Bisby, L.A., Kodur, V.K.R., Green, M.F., Chowdhury, E., 2006. Fire insulation schemes for FRP-strengthened concrete slabs. Compos. A. 37, 1151–1160.

Wipf et al., 2003. Evaluation of Appropriate Maintenance, Repair and Rehabilitation Methods for Iowa Bridges. Final Report, Iowa DOT Project TR-429.

Wu, H.C., 1992. Energy approach for rope strength prediction. J. Text. Inst. 83 (4), 542–549.

Wu, H.C., 1993. Frictional constraint of rope strands. J. Text. Inst. 84 (2), 199–213.

Wu, H.C., Seo, M.H., Backer, S., Mandell, J.F., 1995. Structural modeling of double-braided synthetic fiber ropes. Text. Res. J. 65 (11), 619–631.

Wu, H.C., Warnemuende, K., 2002. Nonlinear active wave modulation approach for evaluating bond conditions between adhesively bonded frp sheet/concrete substrate. In: Kundu, T., (Ed.), Proc. SPIE's 7th International Symposium on Advanced NDE for Structural and Biological Health Monitoring, pp. 222–230, San Diego, CA.

Wu, H.C., Yan, A., 2011. Time-dependent deterioration of FRP bridge deck under freeze/thaw conditions. Compos. B. 42, 1226–1232.

Wu, H.C., Yan, A., 2013. Durability simulation of FRP bridge decks subject to weathering. Compos. B: Eng. 51, 162–168.

Wu, H.C., Fu, G., Yan, A., Warnemuende, K., Gibson, R.F., 2004. Gobal-local FE analysis of FRP sandwich deck. In: CD Proceeding of 4nd International Conference on Advanced Composite Materials in Bridges and Structures.

Wu, H.C., Fu, G., Gibson, R.F., Yan, A., Warnemuende, K., Anumandla, V., 2006a. Durability of FRP composite bridge deck materials under freeze–thaw and low temperature conditions. J. Bridge Eng. 11 (4), 443–451.

Wu, H.C., Fu, G., Gibson, R.F., Warnemuende, K., Yan, A., Anumandla, V., 2006b. Durability testing of FRP material in low temperature weathering condition. CD Proc. 21st Annual Technical Conference. American Society of Composites, Dearborn, MI.

Yamaguchi, T., Kato, Y., Nishimura, T., Uomoto, T., 1997. Creep rupture of FRP rods made of aramid, carbon and glass fibers, Third International Symposium on Non-Metallic (FRP) Reinforcement for Concrete Structures (FRPRCS-3), 2. Japan Concrete Institute, Tokyo, Japan, pp. 179–186.

Yan, A., 2005. Durability of glass fiber/vinyl ester composites as bridge deck subject to low temperature weathering conditions. Ph.D. Dissertation. Department of Civil and Environmental Engineering, Wayne State University, Detroit, MI.

Yang, J.-M., Chou, T.-W., 1987. Performance maps of textiles structural composites. In: Matthews, F.L., Buskell, N.C.R., Hodgkinson, J.M., Morton, J. (Eds.), Proceedings of Sixth International Conference on Composite Materials and Second European Conference on Composite Materials (ICCM6/ECCM2). Elsevier, London, pp. 5579–5588.

Yao, J., 2004. Debonding failures in RC beams and slabs strengthened with FRP plates, PhD. Thesis. The Hong Kong Polytechnic University, Hung Hom, Kowloon, Hong Kong.

Youssef, M.N., 2003. Stress Strain Model for Concrete Confined by FRP Composites, PhD dissertation. University of California-Irvine, Irvine, CA, 310 pp.

Yousif, Z., Hindi, R., 2007. AASHTO-LRFD live load distribution for beam-and-slab bridges: Limitations and applicability. J. Bridge Eng. 12 (6), 765–773.

Zia, P., Caner, A., El-Safty, A.K., 1995. Jointless Bridge Decks. Final Report. Department of Transportation, North Carolina.

Zokaie, T., Imbsen, R.A., 1992. Distribution of Wheel Loads on Highway Bridges. NCHRP 12-26. National Cooperative Highway Research Program, Washington, DC.

Zureick, A.-H., Ellingwood, B., Nowak, A., Mertz, D., Triantafillou, T., 2010. Recommended Guide Specification for the Design of Externally Bonded FRP Systems for Repair Strengthening of Concrete Bridge Elements, NCHRP Report 655. Transportation Research Board, Washington, DC.

This page intentionally left blank

Index

Note: Page numbers followed by "*f*" and "*t*" refer to figures and tables, respectively.

This book presents guidelines for the strengthening of concrete structures using fiber reinforced polymer (FRP) composites.

Strengthening of Concrete Structures Using Fiber Reinforced Polymers (FRP) briefly covers the basic concepts of FRP materials and composite mechanics while focusing on practical design and construction issues, including inspection and quality control. Special attention is given to the different approaches and recommendations found in a selection of international FRP design standards.

This book provides a review and comparison of the provisions found in a selection of the existing guidelines, and then suggests design, installation, inspection, quality control, and maintenance activities for best practice.

This book aims to fill a significant gap in the available strengthening guides and might serve as a resource for engineers, architects, academics, and students interested in FRP materials and their structural applications.

Hwai-Chung Wu is an Associate Professor of Structural Engineering and Materials at Wayne State University. He received his doctorate in 1990 in Polymer Composites from the Department of Materials Science and Engineering, Massachusetts Institute of Technology. Dr. Wu specializes in advanced construction materials and Fiber Reinforced Plastics Composites for infrastructural applications. He has been involved in the design/analysis and durability of FRP materials since 2000 and has co-authored numerous technical papers on these subjects as well as several project reports.

Christopher D. Eamon is an Associate Professor of Structural Engineering at Wayne State University. Prior to joining WSU, he was a faculty member at Lawrence Technological University and Mississippi State University. He received B.S. (1993) and M.Arch (1995) degrees from the Universities of Wisconsin (Milwaukee) and Michigan (Ann Arbor), respectively, and M.S.E. (1996) and Ph.D. (2000) degrees in Civil Engineering from the University of Michigan (Ann Arbor). His research interests include structural reliability and probabilistic design, computational methods, and fiber reinforced polymers.

ENGINEERING

ISBN 978-0-08-100636-8

9 780081 006368

ELSEVIER

WP
WOODHEAD PUBLISHING
An imprint of Elsevier
elsevier.com/books-and-journals